Nouveaux modèles d'éléments finis de poutres enrichies

Mohammed Khalil Ferradi

UNIVERSITÉ PARIS-EST

Thèse présentée pour l'obtention du grade de Docteur de L'Université Paris-Est

Spécialité : Mécanique des Structures

Par

Mohammed-Khalil Ferradi

NOUVEAUX MODELES D'ELEMENTS FINIS DE POUTRES ENRICHIS

Composition du jury de thèse :

M. Patrice Cartraud	Professeur, Centrale Nantes	Rapporteur
M. David Ryckelynck	Professeur, Mines Paris-Tech	Rapporteur
M. Mohammed Hjiaj	Professeur, INSA Rennes	Examinateur
M. Vincent de Ville de Goyet	Directeur, Greisch	Examinateur
M. Arthur Lebée	Chercheur, ENPC	Examinateur
M. Xavier Cespedes	Président, Strains	Examinateur
M. Karam Sab	Professeur, ENPC	Directeur de thèse

Remerciements :

Je remercie particulièrement Xavier Cespedes, CEO de STRAINS, pour m’avoir soutenu dans ce projet dès le début.

Je remercie également mon directeur de thèse Karam Sab et Arthur Lebée du laboratoire Navier pour avoir tout de suite été enthousiastes à ce projet, et de m’avoir procuré les conseils nécessaires pour sa réalisation.

Je remercie tous mes collègues et amis de STRAINS pour leurs remarques constructives et leurs soutien moral constant durant tout ce travail.

Table des matières :

Article 1 : A higher order beam element with warping eigenmodes. Engineering Structures, 46, 748-762.

Article 2 : A new beam element with transversal and warping eignemodes. Computers & Structures, 131, 12-33.

Article 3 : A model reduction technique for beam analysis with the asymptotic expansion method. Submitted to Computers & Structures.

Préambule:

La présente thèse, commencée en septembre 2014 dans le cadre d'une thèse sur travaux au laboratoire Navier, est en fait la continuité d'un travail commencé en septembre 2009 lors d'un stage de fin d'étude chez SETEC-TPI, dont le titre était « Etude du Gauchissement des Sections Soumises aux Cisaillements » [6]. Ce travail a été poursuivi d'abord au sein de SETEC-TPI, puis chez STRAINS en collaboration avec le laboratoire Navier. Après les résultats encourageants obtenus et la publication de deux articles scientifiques dans des journaux à comité lecture, la décision de valoriser le travail effectué par une thèse sur travaux a été prise naturellement, et c'est dans cet objectif que la collaboration entre STRAINS le laboratoire Navier a été entamée.

1 Introduction :

Les poutres sont certainement les modèles mathématiques les plus utilisés par les ingénieurs structures dans leurs différents projets. Ceci est principalement dû à leur simplicité d'utilisation, que ce soit pour modéliser un ouvrage de pont, une charpente métallique ou un immeuble d'habitation. Elles permettent à l'ingénieur d'avoir accès au comportement global de ce type de structure d'une manière simple, fiable et rapide. Ainsi, les ponts les plus modernes construits actuellement dans le monde ont été modélisés avec des éléments de poutres. Cette modélisation simplifiée n'empêchant pas dans une deuxième phase, de construire des modèles auxiliaires plus riches, en utilisant des éléments de coques ou volumiques, pour étudier les phénomènes locaux apparaissant dans la structure. On peut donner comme exemple le viaduc de Millau, dont le tablier large de 32m (Fig.1), a été étudié avec un modèle constitué principalement d'éléments finis de poutres. Mais si le modèle représentant la réalité physique de l'ouvrage est ainsi très simplifié, il doit permettre néanmoins d'effectuer plusieurs calculs, nécessaires pour une étude complète de l'ouvrage, tels que la prise en compte du phasage de construction, des non linéarités géométriques, du fluage/retrait du béton….

Figure 1 : le viaduc de Millau en construction. Crédit photo : groupe Eiffage.

Cependant, si le modèle de poutre a pour principal avantage sa simplicité, il est, comme tout modèle mathématique, basé sur certaines hypothèses simplificatrices, dont il est nécessaire, pour tout

ingénieur faisant usage de ces éléments, de connaître les implications, pour pouvoir préciser la pertinence et les limitations de son modèle.

Après la définition des notations, on détaille dans la partie suivante quelques théories de poutres classiques, pour donner après un résumé des trois articles qui composent le présent manuscrit.

Notations :

- Une poutre est un objet 3D prismatique, occupant un volume *V* dans l'espace. Elle est paramétrée par une courbe continue et différentiable, pour qui à chaque abscisse, on associe une section droite *S*. En général cette courbe représente la ligne moyenne, qui est par définition la courbe reliant les centres de gravité de toutes les sections.

- La position d'un point quelconque du volume *V* peut être représentée par :$\boldsymbol{X} \coloneqq (x_1, x_2, x_3)$. Avec x_3 représentant la position du point dans la ligne moyenne et $\boldsymbol{x} \coloneqq (x_1, x_2)$ la position dans la section.

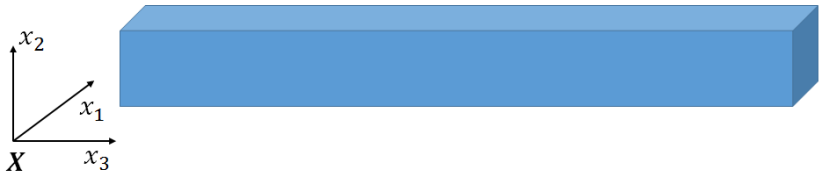

Figure 2 : une poutre droite rectangulaire avec son repère

- Les lettres écrites en gras représentent des vecteurs ou des tenseurs.

- La convention de sommation pour des indices répétés dans une même équation sera toujours utilisée, sauf pour certains cas où le contraire sera clairement exprimé. Si les indices sont des lettres de l'alphabet latin, alors elles prennent des valeurs allant de 1 à 3, et si ce sont des lettres de l'alphabet grec, elles prennent des valeurs allant de 1 à 2 :

$$a_i b_i \coloneqq \sum_{i=1}^{3} a_i b_i \quad , \quad a_\alpha b_\alpha \coloneqq \sum_{\alpha=1}^{2} a_\alpha b_\alpha$$

- Pour les dérivées on utilise les notations suivantes :

$$a_{,1} \coloneqq \frac{\partial a}{\partial x_1} \quad , \quad a_{,2} \coloneqq \frac{\partial a}{\partial x_2} \quad , \quad a_{,3} \coloneqq \frac{\partial a}{\partial x_3} \quad , \quad a_{,i} \coloneqq \frac{\partial a}{\partial x_i}$$

2 Les théories de poutres les plus courantes et leur domaine de pertinence :

La théorie des poutres a aujourd'hui plusieurs siècles derrière elle. Certaines sources font remonter les premières avancées dans ce domaine à Leonard De Vinci et Galilée [2]. Dans cette partie on expose quelques-unes des théories de poutres les plus couramment utilisées, où on se limite au cas élastique linéaire, et en utilisant les approximations des petits déplacements/rotations et des petites déformations.

2.1 Poutre d'Euler-Bernoulli :

La théorie d'Euler-Bernoulli est probablement une des plus anciennes théories de poutres connues. Elle est basée sur les trois hypothèses suivantes :

- Les sections droites restent perpendiculaires à la ligne moyenne après déformation. H1
- Les sections planes restent planes après déformation. H2
- Les sections sont indéformables dans leurs plans. H3

Les hypothèses ci-dessus permettront de définir la cinématique de la poutre, qui définit la forme générale du déplacement de la poutre, quel que soit le chargement auquel elle sera soumise. On analyse donc l'effet de chacune de ces hypothèses sur le comportement de la poutre, mais pour cela il est nécessaire de définir au préalable deux notions importantes qui seront utilisées/analysées dans tout ce qui suit, le gauchissement et la déformation transversale (distorsion) des sections.

Définition 1 : on appelle gauchissement d'une section droite, tout déplacement dans le sens longitudinal de la poutre (hors plan de la section), autre que les mouvements rigides longitudinaux, de déplacement uniforme et de rotation de flexion.

Définition 2 : on appelle déformation transversale d'une section droite, tout déplacement de la section dans son plan, autre que les mouvements de corps rigide (déplacement vertical/horizontal et rotation de torsion).

Les hypothèses H2 et H3 impliquent donc que la poutre ne subira ni gauchissement ni déformation transversale. Quant à l'hypothèse H1, elle implique que la rotation de flexion de la section est proportionnelle à la dérivée de la déformée de la poutre.

Ces hypothèses sont traduites par la cinématique suivante :

$$\boldsymbol{d} \coloneqq \begin{Bmatrix} u_1(x_3) \\ u_2(x_3) \\ u_3(x_3) - x_\alpha \theta_\alpha(x_3) \end{Bmatrix} \tag{1}$$

Avec, selon l'hypothèse H1 : $\theta_\alpha(x_3) = \frac{du_\alpha(x_3)}{dx_3}$

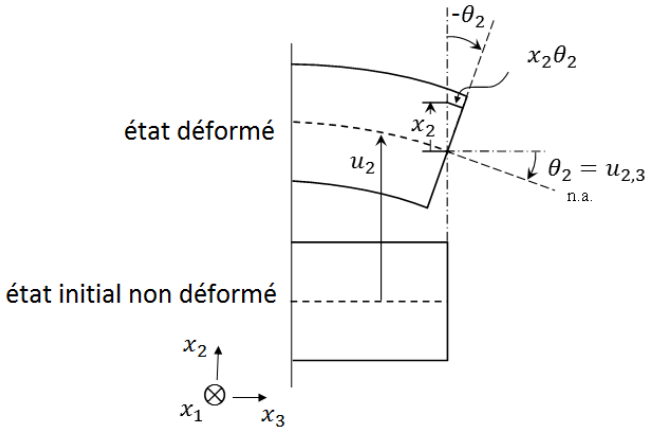

Figure 3: une poutre avec une cinématique d'Euler-Bernoulli

La cinématique d'une poutre d'Euler-Bernoulli (en flexion uniquement Eq.1) contient donc trois paramètres indépendants (ou degrés de libertés d.d.l.) variant le long de la poutre. Les équations d'équilibre permettent le calcul de ces d.d.l., pour un chargement donné appliqué à la poutre.

Pour ce qui suit, on se pose dans le cas où les axes de définition de la section sont les axes principaux d'inertie, centrés au centre de gravité de la section. Les coordonnées des points dans la section vérifient donc par définition les équations suivantes :

$$\int_S x_\alpha dS = 0 \quad , \quad \int_S x_1 x_2 dS = 0 \tag{2}$$

De la cinématique dans Eq.1, le tenseur des déformations est déduit :

$$\boldsymbol{\varepsilon} \coloneqq \frac{1}{2}(\boldsymbol{\nabla_X d} + (\boldsymbol{\nabla_X d})^T) = \begin{bmatrix} 0 & 0 & 0 \\ & 0 & 0 \\ \text{sym} & & u_{3,3} - x_\alpha u_{\alpha,33} \end{bmatrix} \tag{3}$$

Avec $\boldsymbol{\nabla_X}$ l'opérateur gradient par rapport à $\boldsymbol{X}$.

Dans la théorie classique de la poutre d'Euler-Bernoulli, le tenseur des contraintes s'expriment de la manière suivante (hypothèse des contraintes planes):

$$\boldsymbol{\sigma} = \begin{bmatrix} 0 & 0 & 0 \\ & 0 & 0 \\ \text{sym} & & E\left(u_{3,3} - x_\alpha u_{\alpha,33}\right) \end{bmatrix} \tag{4}$$

Avec *E* le module d'Young.

Or, on constate que le tenseur exprimé dans Eq.4 ne vérifie pas la vrai loi de comportement pour un matériau élastique isotrope (sauf dans le cas d'un coefficient de Poisson nul), et qui s'exprime

par : $\boldsymbol{\sigma} \coloneqq \boldsymbol{C} : \boldsymbol{\varepsilon} = 2\mu\boldsymbol{\varepsilon} + \lambda \mathrm{tr}(\boldsymbol{\varepsilon})$. L'erreur vient du fait qu'à cause de l'effet Poisson, on ne peut pas avoir des états plans de contraintes et de déformations en même temps.

Pour ré-exprimer les déformations et les contraintes d'une manière rigoureuse, on suppose uniquement un état plan de contrainte où le tenseur des contraintes est toujours donné par Eq.4. En utilisant la loi de comportement, le tenseur des déformations sera ainsi donné par :

$$\boldsymbol{\varepsilon} \coloneqq \boldsymbol{C}^{-1} : \boldsymbol{\sigma} = \begin{bmatrix} -\nu\left(u_{3,3} - x_\alpha u_{\alpha,33}\right) & 0 & 0 \\ & -\nu\left(u_{3,3} - x_\alpha u_{\alpha,33}\right) & 0 \\ \text{sym} & & u_{3,3} - x_\alpha u_{\alpha,33} \end{bmatrix} \tag{5}$$

De la relation ci-dessus on voit bien que $\varepsilon_{11} = \varepsilon_{22} = -\nu\varepsilon_{33} \neq 0$ (pour $\nu \neq 0$). Pour respecter la condition de compatibilité, l'intégration des deux composantes de déformations $(\varepsilon_{11}, \varepsilon_{22})$ donnera une contribution au déplacement transversal de la poutre. Cette contribution sera négligeable devant les autres mouvements de corps rigide, puisque les dimensions de la section sont petites devant la longueur de la poutre. Elle ne sera donc pas présente dans la cinématique exprimée dans Eq.1, respectant toujours ainsi l'hypothèse H3.

De l'expression des déformations dans Eq.5, on observe un des aspects importants de la théorie d'Euler-Bernoulli. Les déformations de cisaillements sont nulles. Pour des poutres très élancées, les cisaillements d'efforts tranchants peuvent être négligés, dans ce cas la théorie d'Euler-Bernoulli est pertinente, mais pour des poutres avec un faible élancement, négliger les déformations de cisaillements mène à des erreurs non négligeables dans le calcul de la réponse de la poutre. On verra que le modèle de Timoshenko tente de pallier à ce manquement.

Pour écrire les équations d'équilibre de la poutre d'Euler-Bernoulli, on utilise le principe des travaux virtuels (PTV). Pour ce faire on commence par exprimer le travail virtuel interne :

$$\delta W_{int} \coloneqq \int_V \boldsymbol{\sigma} : \delta\boldsymbol{\varepsilon}\, dV \tag{6}$$

$$\delta W_{int} = \int_V \sigma_{33}\left(\delta u_{3,3} - x_\alpha \delta u_{\alpha,33}\right) dV \tag{7}$$

L'expression ci-dessus est intégrée sur la section pour obtenir :

$$\delta W_{int} = \int_0^L \left(N\delta u_{3,3} + M_\alpha \delta u_{\alpha,33}\right) dx_3 \tag{8}$$

Avec L la longueur de la poutre et:

$$N \coloneqq \int_S \sigma_{33} dS = ES u_{3,3} \tag{9}$$

$$M_\alpha \coloneqq -\int_S x_\alpha \sigma_{33} dS = EI_\alpha u_{\alpha,33} \text{ (pas de somme sur α)} \quad , \quad I_\alpha = \int_S x_\alpha^2 dS \tag{10}$$

En intégrant par partie l'équation Eq.8 on obtient:

$$\delta W_{int} = \int_L \left(-N_{,3}\delta u_3 + M_{\alpha,33}\delta u_\alpha\right) dx_3 + \underbrace{\left[N\delta u_3 + M_\alpha \delta u_{\alpha,3} - M_{\alpha,3}\delta u_\alpha\right]_0^L}_{\delta W_{ext}} \tag{11}$$

Du principe des travaux virtuels, on a :

$$\delta W_{int} - \delta W_{ext} = 0 \tag{12}$$

Et donc :

$$\int_L \left(-N_{,3}\delta u_3 + M_{\alpha,33}\delta u_\alpha\right) dx_3 = 0 \tag{13}$$

L'expression ci-dessus étant vérifiée pour tout champ de déplacement virtuel admissible (δu_i), on déduit les équations d'équilibre de la poutre :

$$N_{,3} = 0 \quad , \quad M_{\alpha,33} = 0 \tag{14}$$

L'équilibre est donc obtenu avec trois équations au total, ce qui est en concordance avec le fait qu'il y a trois inconnues (d.d.l.) à déterminer le long de la poutre.

En utilisant dans les équations d'équilibre l'expression des efforts généralisés, on obtient les équations suivantes:

$$u_{3,33} = 0 \quad , \quad u_{\alpha,3333} = 0 \tag{15}$$

En introduisant les conditions aux limites, on peut déterminer les constantes d'intégration des équations ci-dessus, et donc en obtenir une solution unique.

La poutre d'Euler-Bernoulli reste un modèle très simple pour l'étude des poutres. Elle est plus adaptée à l'étude d'éléments en flexion très élancés, où l'hypothèse des déformations de cisaillements négligeables sur la section est valide. Néanmoins en pratique l'ingénieur a besoin d'avoir accès à la distribution du cisaillement transversal dans la section, pour ce faire l'effort tranchant est d'abord déterminé comme étant la dérivée du moment de flexion, puis en utilisant la formule de Jouravsky Eq.16 & Fig.4, la distribution des contraintes de cisaillements est obtenue.

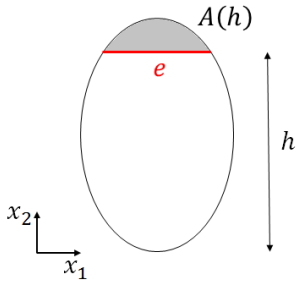

Figure 4: coupe droite d'une section

$$\tau(h) = \frac{T}{Ie(h)} m(h) = \frac{T}{Ie(h)} \int_{A(h)} x_2 \, dA \tag{16}$$

Avec τ les contraintes tangentielles à l'endroit de la coupe, *T* l'effort tranchant, *e* l'épaisseur à l'endroit de la coupe, *I* l'inertie de flexion et *m(h)* le moment statique.

2.2 Poutre de Timoshenko :

La poutre de Timoshenko représente une évolution par rapport à la poutre de Bernoulli, en permettant d'obtenir une moyenne des déformations d'effort tranchant dans la section. Pour cela, on s'affranchit de l'hypothèse H1, en considérant les deux rotations de flexions comme des paramètres indépendants de la déformée. Les deux hypothèses H2 & H3 restent valides pour ce modèle. La cinématique d'une poutre de Timoshenko s'écrit donc exactement de la même manière que pour celle d'Euler-Bernoulli, à la différence que maintenant $\theta_\alpha \neq u_{\alpha,3}$.

De la nouvelle cinématique, on déduit les nouveaux tenseurs des déformations et des contraintes, toujours dans le cadre de l'hypothèse de contraintes planes :

$$\boldsymbol{\sigma} = \begin{bmatrix} 0 & 0 & G(u_{1,3} - \theta_1) \\ & 0 & G(u_{2,3} - \theta_2) \\ \text{sym} & & E(u_{3,3} - x_\alpha \theta_{\alpha,3}) \end{bmatrix} \tag{17}$$

$$\boldsymbol{\varepsilon} = \begin{bmatrix} -\nu(u_{3,3} - x_\alpha \theta_{\alpha,3}) & 0 & \frac{1}{2}(u_{1,3} - \theta_1) \\ & -\nu(u_{3,3} - x_\alpha \theta_{\alpha,3}) & \frac{1}{2}(u_{2,3} - \theta_2) \\ \text{sym} & & u_{3,3} - x_\alpha \theta_{\alpha,3} \end{bmatrix} \tag{18}$$

Dans ce modèle, les contraintes de cisaillements s'écrivent sous la forme suivante :

$$\sigma_{\alpha 3} = G(u_{\alpha,3} - \theta_\alpha) \tag{19}$$

Ces contraintes sont constantes dans la section, puisque l'expression ci-dessus ne dépend que de x_3. Or du théorème de Cauchy, si la surface extérieure de la poutre n'est pas chargée, la composante normale au bord de la section des contraintes de cisaillements doit être nulle :

$$\sigma_{\alpha 3} n_\alpha = 0 \tag{20}$$

Avec $\boldsymbol{n} = (n_1, n_2)$ le vecteur normal au bord de la section.

Ce qui pose un problème de compatibilité, puisqu'imposer cette condition serait revenir au modèle d'Euler-Bernoulli, où tout simplement les contraintes de cisaillements sont nulles partout dans la section. La poutre de Timoshenko a donc aussi ses limitations, mais à défaut d'une représentation réaliste du comportement de la poutre, elle permet néanmoins de prendre en compte les déformations d'effort tranchant d'une manière approximative.

En utilisant maintenant le PTV de la même manière que pour la poutre d'Euler-Bernoulli, on obtient les équations d'équilibre suivantes :

$$u_{3,33} = 0 \quad , \quad u_{\alpha,33} - \theta_{\alpha,3} = 0 \quad , \quad \theta_{\alpha,333} = 0 \tag{21}$$

Ces équations peuvent être résolues aisément en utilisant les conditions aux limites pour obtenir les constantes d'intégration. En intégrant la loi de comportement sur la section, on obtient la relation liant les efforts généralisés et les déformations:

$$\begin{Bmatrix} N \\ T_1 \\ T_2 \\ M_1 \\ M_2 \end{Bmatrix} = \begin{bmatrix} ES & & & & \\ & GS & & & 0 \\ & & GS & & \\ & & & EI_1 & \\ & 0 & & & EI_2 \end{bmatrix} \begin{Bmatrix} u_{3,3} \\ u_{1,3} - \theta_1 \\ u_{2,3} - \theta_2 \\ \theta_{1,3} \\ \theta_{2,3} \end{Bmatrix} \tag{22}$$

La poutre de Timoshenko est très utilisée par les ingénieurs pour la modélisation de leurs structures, cependant en pratique la version qu'on trouve généralement dans les logiciels de calcul, ne respecte pas parfaitement la relation dans Eq.22, puisque la raideur à l'effort tranchant GS est remplacé par GS_r, où S_r est la section réduite à l'effort tranchant.

2.3 Poutre de Vlassov :

2.3.1 Gauchissement uniforme :

Le gauchissement des sections d'une poutre soumise à de la torsion a été mis en évidence expérimentalement par Duleau (1820) puis Saint-Venant (voir figure ci-dessous).

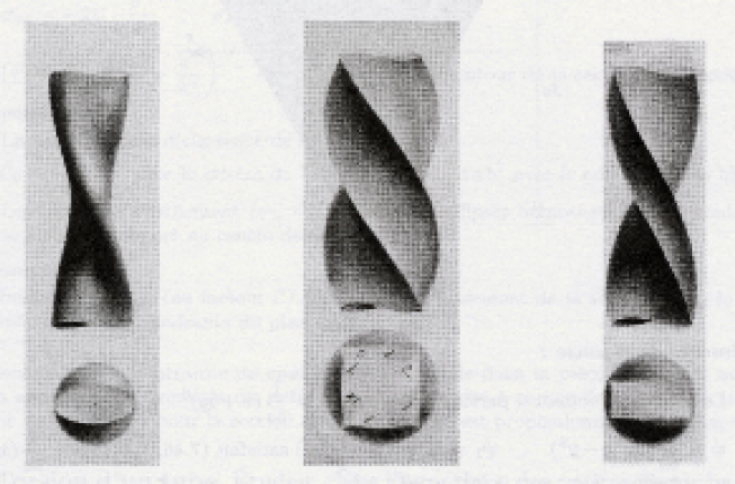

Figure 5: Dessin originaux de Saint-Venant de torsion barres à section elliptique, carré et rectangulaire. Crédit photo :Adhémar Barré de Saint Venant.

Une analyse extensive de la torsion et son effet sur l'instabilité des structures (flambement par torsion, déversement) est donnée dans [10]. Dans l'étude suivante, on commence par le cas le plus simple où la poutre est soumise à un couple de torsion uniforme et où les sections sont libres de se gauchir. Dans ce cas, le gauchissement est uniforme et n'induit pas de changement dans les longueurs des fibres longitudinales composant la poutre, ce qui se traduit par l'équation suivante :

$$\theta_{3,33} = 0 \tag{23}$$

Avec $\theta_3(x_3)$ la fonction représentant l'angle de torsion le long de la poutre.

Pour ce cas d'étude particulier, on souhaite déterminer la fonction variant sur la section et représentant le gauchissement dû à la torsion. Pour ce faire et puisqu'on s'intéresse seulement à la torsion, on écrit ici la cinématique représentant uniquement ce type de mouvement :

$$\boldsymbol{d} \coloneqq \begin{Bmatrix} -x_2\theta_3 \\ x_1\theta_3 \\ \Omega(\boldsymbol{x}) \end{Bmatrix} \tag{24}$$

Avec $\Omega(\boldsymbol{x})$ une fonction représentant le déplacement longitudinal (gauchissement) de la section dû à la torsion et qui a une forme inconnue pour le moment.

Les tenseurs des déformations et des contraintes calculés à partir de la cinématique Eq.24 tout en utilisant la condition dans Eq.23, s'expriment par :

$$\boldsymbol{\varepsilon} = \begin{bmatrix} 0 & 0 & \frac{1}{2}\left(\Omega_{,1} - x_2\theta_{3,3}\right) \\ & 0 & \frac{1}{2}\left(\Omega_{,2} + x_1\theta_{3,3}\right) \\ \text{sym} & & 0 \end{bmatrix} \quad , \quad \boldsymbol{\sigma} = \begin{bmatrix} 0 & 0 & G\left(\Omega_{,1} - x_2\theta_{3,3}\right) \\ & 0 & G\left(\Omega_{,2} + x_1\theta_{3,3}\right) \\ \text{sym} & & 0 \end{bmatrix} \tag{25}$$

Pour déterminer la fonction $\Omega(\boldsymbol{x})$, on utilise l'équation d'équilibre locale de la poutre:

$$\sigma_{3i,i} = 0 \tag{26}$$

$$\Rightarrow \quad \Delta_{\boldsymbol{x}}\Omega = 0 \tag{27}$$

Avec $\Delta_{\boldsymbol{x}} \coloneqq \frac{\partial^2}{\partial x_1^2} + \frac{\partial^2}{\partial x_2^2}$ l'opérateur de Laplace sur la section.

On écrit ensuite la condition aux limites, exprimant le fait que le cisaillement normal au bord de la section doit être nul :

$$\sigma_{3\alpha} n_\alpha = 0 \tag{28}$$

$$\Rightarrow \quad \boldsymbol{\nabla}_{\boldsymbol{x}}\Omega \cdot \boldsymbol{n} = \theta_{3,3}(x_2 n_1 - x_1 n_2) \tag{29}$$

Avec : $\boldsymbol{\nabla}_{\boldsymbol{x}} \coloneqq \left(\frac{\partial}{\partial x_1}, \frac{\partial}{\partial x_2}\right)$ l'opérateur gradient sur la section.

La fonction $\Omega(x_1, x_2)$ est donc déterminée à partir de Eq.27 et Eq.29, formant le problème à dérivés partielles (PDP) suivant :

$$\begin{cases} \Delta_{\boldsymbol{x}}\Omega = 0 & \text{sur } S \\ \boldsymbol{\nabla}_{\boldsymbol{x}}\Omega \cdot \boldsymbol{n} = x_2 n_1 - x_1 n_2 & \text{sur } \Gamma_s \end{cases} \tag{30}$$

La résolution sur la section du (PDP) ci-dessus permet de déterminer la fonction $\Omega(\boldsymbol{x})$ à une condition additive près. Cette résolution est effectuée à l'aide d'une des nombreuses méthodes numériques disponibles, tels que la méthode des éléments finis.

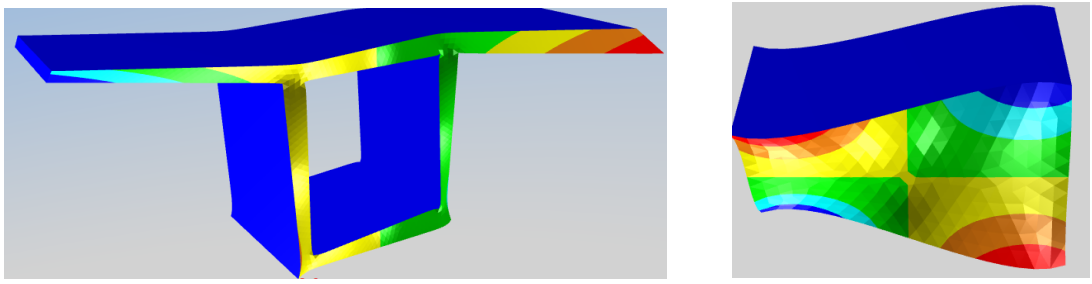

Figure 6: exemple de mode de gauchissement de torsion pour des sections en forme de caisson et rectangulaire.

2.3.2 Modèle de Vlassov :

Vlassov [18] a proposé un modèle de poutre où le gauchissement des sections soumises à de la torsion est pris en compte. Dans ce modèle, le gauchissement est représenté par la même fonction obtenue dans Eq.30, même si cette fonction a été déterminée en utilisant la condition de gauchissement

uniforme, qui n'est pas forcément vérifiée ici (voir [10]). Pour ce modèle, la cinématique de la poutre en torsion s'exprime donc par :

$$\boldsymbol{d} \coloneqq \begin{Bmatrix} -x_2\theta_3 \\ x_1\theta_3 \\ \Omega\,\theta_{3,3} \end{Bmatrix} \tag{31}$$

Les tenseurs des déformations et des contraintes, dans l'hypothèse des contraintes planes, sont donnés par :

$$\boldsymbol{\sigma} = \begin{bmatrix} 0 & 0 & G\big(\Omega_{,1} - x_2\big)\theta_{3,3} \\ & 0 & G\big(\Omega_{,2} + x_1\big)\theta_{3,3} \\ \text{sym} & & E\Omega\theta_{3,33} \end{bmatrix} \quad , \quad \boldsymbol{\varepsilon} = \begin{bmatrix} -\nu\Omega\theta_{3,33} & 0 & \frac{1}{2}\big(\Omega_{,1} - x_2\big)\theta_{3,3} \\ & -\nu\Omega\theta_{3,33} & \frac{1}{2}\big(\Omega_{,2} + x_1\big)\theta_{3,3} \\ \text{sym} & & \Omega\theta_{3,33} \end{bmatrix} \tag{32}$$

Des expressions des tenseurs déformations et contraintes ci-dessus, le travail virtuel interne est ainsi exprimé sous la forme suivante:

$$\delta W_{int} = \int_V \Big(\Omega\,\sigma_{33}\delta\theta_{3,33} + \Big(\sigma_{13}\big(\Omega_{,1} - x_2\big) + \sigma_{23}\big(\Omega_{,2} + x_1\big)\Big)\,\delta\theta_{3,3}\Big)\,dV \tag{33}$$

Après intégration sur la section de l'expression ci-dessus, elle devient:

$$\delta W_{int} = \int_0^L \big(B\delta\theta_{3,33} + (M_3 + \varphi)\delta\theta_{3,3}\big)dx_3 \tag{34}$$

Où les efforts généralisés ci-dessus sont exprimés par:

$$B \coloneqq \int_S \Omega\sigma_{33}dS = EK\theta_{3,33} \qquad \text{avec} \quad K \coloneqq \int_S \Omega^2 dS \tag{35}$$

$$M_3 \coloneqq \int_S \psi_\alpha^{\text{tor}}\sigma_{\alpha 3}dS = GJ\theta_{3,3} \qquad \text{avec} \quad J \coloneqq \int_S \psi_\alpha^{\text{tor}}\big(\Omega_{,\alpha} + \psi_\alpha^{\text{tor}}\big)dS \tag{36}$$

$$\varphi \coloneqq \int_S \Omega_{,\alpha}\sigma_{3\alpha}dS = GP\theta_{3,3} \qquad \text{avec} \quad P \coloneqq \int_S \Omega_{,\alpha}\big(\Omega_{,\alpha} + \psi_\alpha^{\text{tor}}\big)dS \tag{37}$$

Où $\boldsymbol{\psi}^{\text{tor}}$ est le mode de corps rigide de torsion sous forme vectorielle:

$$\boldsymbol{\psi}^{\mathrm{tor}} = (-x_2, x_1) \tag{38}$$

B le bi-moment, *J* la constante de torsion et *K* la constante de gauchissement. Le calcul de la constante *J* fait intervenir la fonction Ω, une attention particulière doit donc être apportée à la manière dont cette constante est déterminée dans les différents codes de calculs commerciaux.

La constante *P* est en fait égal à zéro. Pour pouvoir démontrer cette affirmation, on intègre par parties l'expression intégrale de la constante dans Eq.37 :

$$P = -\int_S \Omega\,(\Delta_{\boldsymbol{x}}\Omega + \mathrm{div}_{\boldsymbol{x}}\boldsymbol{\psi}^{\mathrm{tor}})\,dS + \int_{\Gamma_s} \Omega\,(\boldsymbol{\nabla}_{\boldsymbol{x}}\Omega + \boldsymbol{\psi}^{\mathrm{tor}}) \cdot \boldsymbol{n}\,d\Gamma_s \tag{39}$$

Les fonctions Ω et $\boldsymbol{\psi}^{\mathrm{tor}}$ vérifient par construction les équations suivantes :

$$\begin{cases} \Delta_{\boldsymbol{x}}\Omega = 0 & \text{sur } S \\ \boldsymbol{\nabla}_{\boldsymbol{x}}\Omega \cdot \boldsymbol{n} = -\boldsymbol{\psi}^{\mathrm{tor}} \cdot \boldsymbol{n} & \text{sur } \Gamma_s \end{cases}, \quad \mathrm{div}_{\boldsymbol{x}}\boldsymbol{\psi}^{\mathrm{tor}} = 0 \tag{40}$$

Et donc en remplaçant les équations ci-dessus dans Eq.39, on obtient le résultat recherché suivant:

$$P = 0 \tag{41}$$

En intégrant par partie l'expression du travail virtuel interne dans Eq.34 et en utilisant le résultat ci-dessus, on obtient :

$$\delta W_{int} = \int_0^L \left(B_{,33} - M_{3,3}\right)\delta\theta_3 dx_3 + \underbrace{\left[B\delta\theta_{3,3} + \left(M_3 - B_{,3}\right)\delta\theta_3\right]_0^L}_{\delta W_{ext}} \tag{42}$$

$$\int_0^L \left(B_{,33} - M_{3,3}\right)\delta\theta_3 dx_3 = 0 \tag{43}$$

$$\Longrightarrow \quad B_{,33} - M_{3,3} = 0 \tag{44}$$

Si on remplace par les expressions des efforts généralisés dans l'équation d'équilibre ci-dessus, on obtient :

$$EK\theta_{3,3333} - GJ\theta_{3,33} = 0 \tag{45}$$

$$\theta_{3,3333} - \omega^2\theta_{3,33} = 0 \tag{46}$$

Avec : $\omega^2 \coloneqq \frac{GJ}{EK}$

La solution de Eq.46 s'exprime par :

$$\theta_3(x_3) = ae^{\omega x_3} + be^{-\omega x_3} + cx_3 + d \tag{47}$$

Les constantes d'intégrations seront déterminées en utilisant les conditions aux limites sur la rotation de torsion et le gauchissement des deux sections d'extrémités.

2.4 Poutre de Benscoter :

Une modification proposée par Benscoter [3-10] pour améliorer le modèle de Vlassov dans le cas de la torsion non uniforme, consiste à introduire un nouveau degré de liberté lié au gauchissement de torsion, indépendant de la dérivée de l'angle de torsion. Dans ce cas, la nouvelle cinématique pour la torsion s'exprime par :

$$\boldsymbol{d} \coloneqq \begin{Bmatrix} -x_2\theta_3 \\ x_1\theta_3 \\ \Omega\,\xi \end{Bmatrix} \tag{48}$$

Avec $\xi(x_3)$ le nouveau degré de liberté associé au gauchissement. Par contre, on note que la fonction Ω est celle calculée précédemment en résolvant le problème dans Eq.30.

Remarque : Cette modification peut être vue comme étant analogue à celle apportée par le modèle de Timoshenko au modèle d'Euler-Bernoulli, où l'angle de flexion n'est plus exprimé comme étant la dérivée de la déformée mais en lui attribuant un nouveau paramètre indépendant.

En utilisant le PTV exactement de la même manière que pour le modèle de Vlassov, on obtient les équations d'équilibre suivantes :

$$B_{,33} - \varphi_{,3} = 0 \qquad , \qquad M_{3,3} = 0 \tag{49}$$

Avec les nouvelles expressions des efforts généralisés s'écrivant sous les formes suivantes:

$$M_3 = G\left(I_0\theta_{3,3} + L\xi\right) \qquad \text{avec} \quad L \coloneqq \int_S \boldsymbol{\nabla_x}\Omega \cdot \boldsymbol{\psi}^{\text{tor}}\, dS = J - I_0 \tag{50}$$

$$B = EK\xi_{,3} \qquad \text{avec} \quad K \coloneqq \int_S \Omega^2\, dS \tag{51}$$

$$\varphi = G\left(Q\xi + L\theta_{3,3}\right) \qquad \text{avec} \quad Q \coloneqq \int_S \boldsymbol{\nabla_x}\Omega \cdot \boldsymbol{\nabla_x}\Omega\, dS \tag{52}$$

Avec $I_0 \coloneqq I_1 + I_2$ l'inertie polaire de la section.

En remplaçant les expressions ci-dessus dans Eq.49, on obtient :

$$EK\xi_{,333} - G\left(Q\xi_{,3} + L\theta_{3,33}\right) = 0 \quad , \quad I_0\theta_{3,33} + L\xi_{,3} = 0 \tag{53}$$

$$\Longrightarrow \quad \xi_{,333} - \omega^2\xi_{,3} = 0 \quad , \quad \theta_{3,33} = -\frac{L}{I_0}\xi_{,3} \tag{54}$$

Avec : $\omega^2 \coloneqq \frac{G}{EK}\left(Q - \frac{L^2}{I_0}\right) = -\frac{GLJ}{EKI_0}$

La forme de la solution des équations d'équilibre ci-dessus peut être exprimée de la manière suivante :

$$\xi = ae^{\omega x_3} + be^{-\omega x_3} + c \quad , \quad \theta_3 = -\frac{L}{I_0\omega}(ae^{\omega x_3} - be^{-\omega x_3}) + dx_3 + e \tag{55}$$

Les constantes d'intégration dans les expressions ci-dessus sont obtenues en fonction des conditions aux limites de chaque cas.

Quelques éditeurs de logiciels de calcul de structure proposent des poutres à 7 d.d.l. en incluant le gauchissement dû à la torsion. Cependant, l'ingénieur qui souhaite utiliser ces éléments, plus riches que le modèle de poutre classique de Timoshenko, doit vérifier si l'élément utilise le modèle de Vlassov ou celui de Benscoter. En effet, ils donnent des résultats différents dans le cas d'un gauchissement gêné ou d'une torsion non uniforme, qui représentent des cas usuels dans une structure soumise à de la torsion.

3 Résumé de l'article 1 [7]:

Dans les théories de poutres classiques d'Euler-Bernoulli ou de Timoshenko, on fait l'hypothèse que les sections droites restent toujours planes (pas de gauchissement). Des théories plus avancées telles que celles de Vlassov ou Benscoter, permettent une nette amélioration pour l'étude de la torsion, en prenant en compte le gauchissement dû à ce mouvement. Néanmoins ces modèles sont toujours insuffisants pour représenter un gauchissement quelconque d'une section, puisque la torsion n'est pas la seule à provoquer un gauchissement des sections, il y a aussi les efforts tranchants, ayant pour effet de faire apparaître ce qui est communément appelé le traînage de cisaillement (shear lag) [6,14].

Le traînage de cisaillement est un phénomène connu dans les poutres de largeur importante. Il a comme conséquence défavorable une surconcentration des contraintes normales à certains endroits de la section. L'Eurocode 3 permet de prendre en compte ce phénomène pour des poutres métalliques, en considérant une largeur effective (ou réduite) au lieu de la largeur totale, voir fig.7.

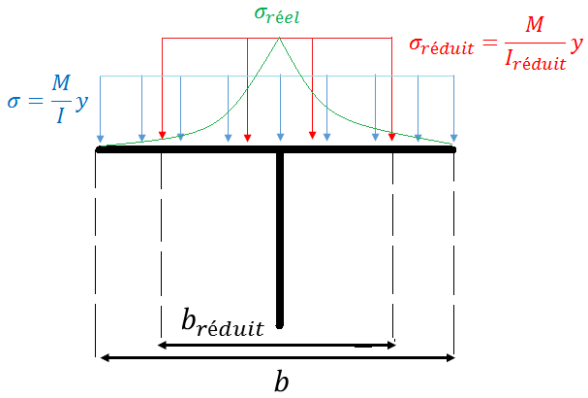

Figure 7 : trainage de cisaillement dans une section en T d'une poutre en flexion

Dans cette partie, on résume le travail développé dans l'article 1 de cette thèse. On considère toujours l'hypothèse H3 (section indéformable dans son plan) comme valide. On s'intéresse donc au gauchissement des sections, soumises au seul mouvement transversal de corps rigide, c.à.d. soumises à des efforts tranchants plus la torsion.

Notre objectif est de construire une base de fonctions, où le gauchissement quelconque (sous l'hypothèse H3) des sections sera décomposé. On appellera ces fonctions des 'modes de gauchissement' qui ne dépendront que de la géométrie de la section. Dans un premier temps des modes de 1er ordre seront déterminés, en utilisant l'hypothèse de gauchissement uniforme le long de la poutre. Vu que cette hypothèse est rarement vérifiée dans un cas réel, des modes d'ordres supérieurs seront déterminés pour représenter le cas plus général de gauchissement non uniforme.

3.1 Détermination des modes de gauchissement de 1er ordre :

Le mode de gauchissement de 1er ordre pour la torsion a déjà été déterminé pour le modèle de Vlassov. On détaille ici uniquement la détermination des deux modes de 1er ordre pour des efforts tranchants dans les deux sens horizontal et vertical, sachant que la méthode est la même manière pour les deux sens.

Soit donc une poutre libre de se gauchir, soumise à un effort tranchant T_1 *constant*. On considère ici la cinématique d'Euler-Bernoulli représentant la flexion dans le sens vertical à laquelle ait ajouté un mode de gauchissement (la flexion dans l'autre sens a été omise par souci de simplification, puisque son traitement se fera de la même manière) :

$$\boldsymbol{d} \coloneqq \begin{Bmatrix} u_1(x_3) \\ 0 \\ -x_1 \dfrac{du_1}{dx_3} + \Omega_1(\boldsymbol{x}) \end{Bmatrix} \tag{56}$$

Avec $\Omega^1(\boldsymbol{x})$ représentant le gauchissement (de 1er ordre) de la section (uniforme le long de la poutre) dû à l'effort tranchant, et dont on souhaite déterminer l'expression.

De la cinématique on déduit les expressions des tenseurs des déformations et des contraintes toujours sous l'hypothèse de contraintes planes:

$$\boldsymbol{\sigma} = \begin{bmatrix} 0 & 0 & G\Omega_{1,1} \\ & 0 & G\Omega_{1,2} \\ \text{sym} & & -Ex_1u_{1,33} \end{bmatrix} \quad , \quad \boldsymbol{\varepsilon} = \begin{bmatrix} \nu x_1 u_{1,33} & 0 & \frac{1}{2}\Omega_{1,1} \\ & \nu x_1 u_{1,33} & \frac{1}{2}\Omega_{1,2} \\ \text{sym} & & -x_1u_{1,33} \end{bmatrix} \tag{57}$$

On écrit l'équation d'équilibre locale :

$$\sigma_{3i,i} = 0 \tag{58}$$

$$\Longrightarrow \quad \sigma_{33,3} + G\Delta_{\boldsymbol{x}}\Omega_1 = 0 \tag{59}$$

Or pour une poutre soumise à un effort tranchant, l'expression des contraintes normales est donnée par:

$$\sigma_{33} = \frac{M_1}{I_1}x_1 \quad \Longrightarrow \quad \sigma_{33,3} = -\frac{T_1}{I_1}x_1 \tag{60}$$

L'expression ci-dessus est remplacée dans Eq.59 pour obtenir:

$$\Delta_{\boldsymbol{x}}\Omega_1 = \frac{T_1}{GI_1}x_1 \tag{61}$$

On écrit la condition aux limites, exprimant le fait que le cisaillement normal au bord de la section doit être nul :

$$\sigma_{3\alpha}n_\alpha = 0 \quad \Longrightarrow \quad \boldsymbol{\nabla_x}\Omega_1 \cdot \boldsymbol{n} = 0 \tag{62}$$

Le problème à dérivées partielles, permettant de déterminer le mode de 1[er] ordre dû à un effort tranchant horizontal, s'exprime donc par :

$$\begin{cases} \Delta_{\boldsymbol{x}}\Omega_1 = x_1 & \text{sur S} \\ \boldsymbol{\nabla_x}\Omega_1 \cdot \boldsymbol{n} = 0 & \text{sur } \Gamma_s \end{cases} \tag{63}$$

Le terme constant $\frac{T_1}{GI_1}$ a été supprimé de l'équation au laplacien Eq.61, car ce qui nous intéresse ici est d'obtenir la forme du mode de gauchissement, et donc de le déterminer à une constante multiplicative près.

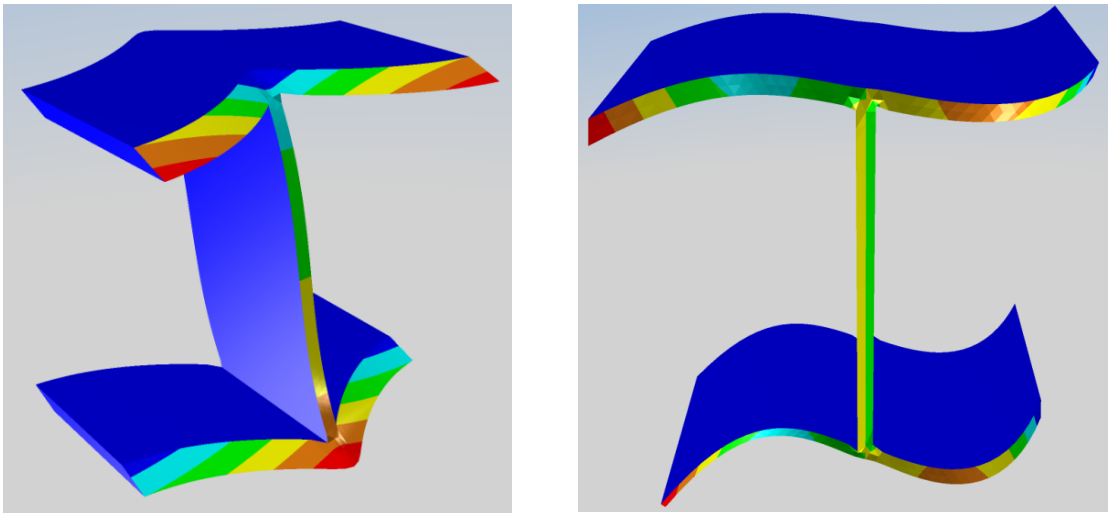

Figure 8: exemple des modes gauchissements de 1er ordre d'une section en I, pour un effort tranchant vertical et horizontal.

3.2 Détermination des modes de gauchissement d'ordre supérieur :

Dans ce qui précède, les modes de 1er ordre, pour des efforts tranchants dans les directions 1 et 2, ont été déterminé en faisant l'hypothèse que l'effort tranchant était uniforme le long de la poutre et que le gauchissement est non gêné, donc uniforme le long de la poutre. Ceci bien sûr représente rarement un cas réel où le gauchissement est généralement non uniforme (variable le long de la poutre).

Dans le cas de l'effort tranchant, on a déterminé le gauchissement de 1er ordre en équilibrant les contraintes normales dues à la flexion par des contraintes de cisaillements dues au gauchissement. Or ce mode créera à son tour des contraintes normales dans le cas d'un gauchissement non uniforme, qui seront par construction du modèle non équilibrées. D'ici vient l'idée de restaurer l'équilibre, à un ordre plus élevé, en déterminant un nouveau mode de gauchissement, dont les contraintes de cisaillements associées, équilibreront précisément ces contraintes normales non-équilibrées du mode précédent. Cette procédure peut être vue comme le point de départ d'un processus itératif, permettant de déterminer des modes de gauchissement d'ordre supérieur pour représenter le gauchissement non uniforme de la poutre.

Pour exprimer ce processus itératif, on suppose que le mode de gauchissement d'un certain ordre *n* est connu, et qu'on souhaite de déterminer le mode d'ordre *n+1*. Pour ce faire on écrit l'équation exprimant la restauration de l'équilibre à l'aide du nouveau mode :

$$\sigma_{33,3}^{n} + \sigma_{3\alpha,\alpha}^{n+1} = 0 \tag{64}$$

Avec : $\sigma_{33}^{n} = E\xi_{n,3}\Omega_n$, $\sigma_{3\alpha}^{n+1} = G\xi_{n+1}\Omega_{n+1,\alpha}$, et ξ_n, ξ_{n+1} étant les d.d.l. associés aux modes de gauchissement d'ordre *n* et *n+1*, respectivement.

On remplace par les expressions des contraintes dans Eq.64 :

$$E\xi_{n,3}\Omega_n + G\xi_{n+1}\Delta_x\Omega_{n+1} = 0 \tag{65}$$

De même que pour les modes de 1[er] ordre, pour les ordres supérieurs aussi on ne s'intéresse qu'à la forme des fonctions de gauchissement pour construire la base des modes. Donc de Eq.65, on déduit le PDP menant à la détermination du nouveau mode :

$$\begin{cases} \Delta_{\boldsymbol{x}}\Omega_{n+1} = \Omega_n & \text{sur S} \\ \boldsymbol{\nabla}_{\boldsymbol{x}}\Omega_{n+1} \cdot \boldsymbol{n} = 0 & \text{sur } \Gamma_s \end{cases} \tag{66}$$

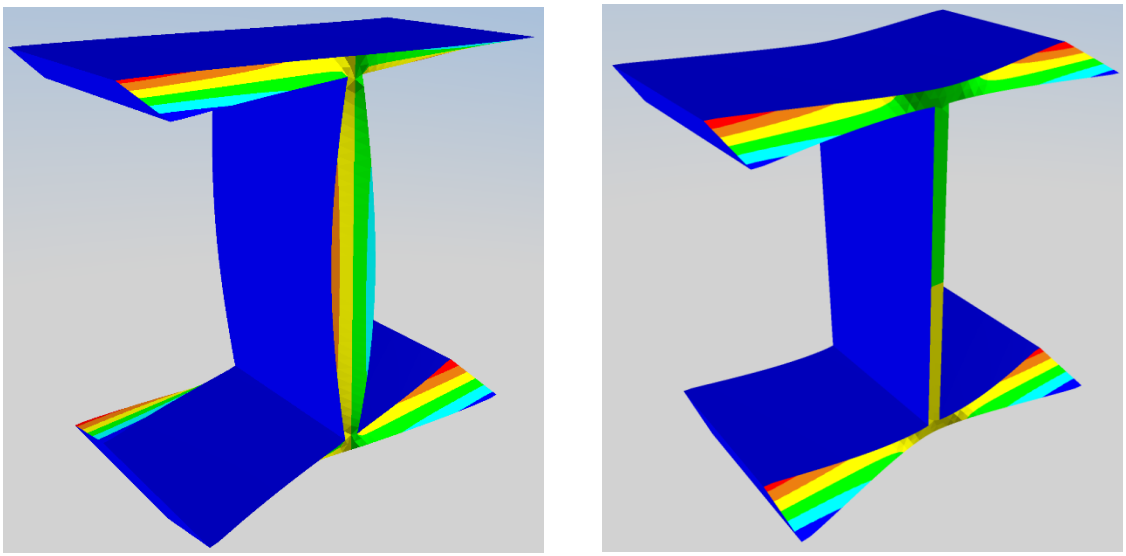

Figure 9: modes de gauchissements d'ordre supérieur dû aux efforts tranchants pour une section en I

Maintenant que les modes de gauchissement sont déterminés, la forme générale pour la cinématique de la poutre dans ce cas, s'exprime par :

$$\boldsymbol{d} \coloneqq \begin{Bmatrix} u_1 - x_2\theta_3 \\ u_2 + x_1\theta_3 \\ u_3 - x_\alpha u_{\alpha,3} + \sum_j \Omega_j(\boldsymbol{x})\xi_j(x_3) \end{Bmatrix} \tag{67}$$

Où tous les modes de gauchissement sont mis dans la somme ci-dessus, indistinctement du fait qu'ils soient déterminés pour la torsion ou un effort tranchant.

A partir de la cinématique ci-dessus, les équations d'équilibre peuvent être déduites à partir du PTV et résolues exactement pour construire la matrice de raideur de l'élément de poutre. Dans ce nouvel élément, il y a aura autant de nouveaux d.d.l. que de modes de gauchissement introduits dans la cinématique.

4 Résumé de l'article 2 [8]:

Le travail effectué dans le 2ième article est une généralisation de celui du 1er, où seul le mouvement transversal de corps rigide avait été considéré (hypothèse H3). Dans cette partie, on abandonnera cette dernière hypothèse, pour considérer une poutre capable de se déformer d'une manière quelconque. Pour cela, il nous faut construire une base de modes transversaux, sur laquelle le déplacement transversal de la section sera projeté.

La méthode proposée dans l'article 2 pour la détermination de cette base, est basée sur une analyse aux valeurs propres d'un modèle mécanique de la section. La section est maillée à l'aide d'éléments triangulaires, auxquels on associe une matrice de raideur (hypothèse de déformations planes). De la même manière que pour une structure 2D, ces matrices sont assemblées pour obtenir la matrice de raideur globale de la section $\boldsymbol{K}_s$. Une analyse aux valeurs propres sur cette matrice, permet de déterminer les couples $(\lambda, \boldsymbol{\psi})$ vérifiant :

$$\boldsymbol{K}_s\boldsymbol{\psi} = \lambda\boldsymbol{\psi} \quad , \quad \boldsymbol{\psi} \neq \mathbf{0} \tag{68}$$

La base des vecteurs propres, est par construction, une base de l'espace des déformations transversales. Une méthode analogue a été utilisée par Kreutz [13] pour la détermination de cette base pour des sections épaisses, alors que Jang et al [12] analysent des sections minces en utilisant des poutres 3D pour mailler la section, obtenant ainsi, après une analyse aux valeurs propres, la base des modes transversaux en même temps que la base des gauchissements.

Un des inconvénients de la méthode est que la base des vecteurs propres peut être composée de plusieurs milliers d'éléments. On ne peut/veut donc pas utiliser tous les vecteurs de cette base pour enrichir la cinématique de la poutre. Un critère de choix entre ces modes est donc nécessaire, et on choisit de prendre les vecteurs propres ayant les plus faibles valeurs propres. Pour comprendre ce qui motive ce choix, considérant un vecteur propre $\boldsymbol{\psi}$ avec λ la valeur propre qui lui est associée. L'énergie de déformation élastique U associée à ce mode est donnée par :

$$2\mathrm{U} = \boldsymbol{\psi}^T \boldsymbol{K}_s\boldsymbol{\psi} = \lambda \tag{69}$$

Les trois modes de corps rigide auront une valeur propre nulle, ce sont les modes prépondérants présents dans toutes les cinématiques de poutre. On peut poursuivre la sélection de modes avec ceux ayant les plus petites valeurs propres, puisque de la relation ci-dessus on peut déduire qu'un mode avec une plus faible valeur propre mobilise moins d'énergie, et donc a plus de chance d'apparaître lors de la déformation de la poutre. Cet argument n'étant qu'heuristique, il ne suffit donc pas pour assurer que le mode ait une participation non nulle à la réponse de la poutre. Mais c'est le seul critère de choix entre modes utilisé dans cet article.

Les modes transversaux ainsi déterminés, on souhaite maintenant obtenir la base des modes de gauchissement. On va donc, d'une manière similaire à l'article 1, déterminer des modes de gauchissement de 1er ordre, associé à chaque mode transversal dans le cadre de l'hypothèse d'un gauchissement uniforme, puis des modes d'ordre supérieurs pour représenter le cas général de gauchissement non uniforme avec le même processus d'équilibre itératif.

Pour comprendre cette procédure, on peut assimiler les trois modes de corps rigide à des modes transversaux. Le mode de gauchissement de 1er ordre associé à un déplacement vertical serait la

flexion par rapport à l'axe horizontal. Pour la torsion, le mode de gauchissement de 1er ordre serait le mode Vlassov donné par Eq.30. Notre but est donc, d'une manière tout à fait analogue, d'étendre cette procédure à tous les modes transversaux.

Soit donc une cinématique avec un mode transversal quelconque $\boldsymbol{\psi}(\boldsymbol{x}) = \big(\psi_1(\boldsymbol{x})\,,\ \psi_2(\boldsymbol{x})\big)$:

$$\boldsymbol{d} \coloneqq \begin{Bmatrix} \psi_1(\boldsymbol{x})\,\zeta(x_3) \\ \psi_2(\boldsymbol{x})\,\zeta(x_3) \\ \Omega(\boldsymbol{x}) \end{Bmatrix} \tag{70}$$

Avec $\zeta(x_3)$ le d.d.l. associé au mode transversal considéré, et $\Omega(\boldsymbol{x})$ représentant le gauchissement uniforme dans la poutre dû à $\boldsymbol{\psi}(\boldsymbol{x})$, et dont on souhaite déterminer la forme dans ce qui suit.

Pour cela on utilise l'équation d'équilibre locale s'exprimant de la manière suivante :

$$\sigma_{33,3} + \mathrm{div}_{\boldsymbol{x}}\boldsymbol{\tau} = 0 \tag{71}$$

Avec : $\boldsymbol{\tau} \coloneqq (\sigma_{13}, \sigma_{23}) = G\big(\boldsymbol{\nabla}_{\boldsymbol{x}}\Omega + \boldsymbol{\psi}\,\zeta_{,3}\big)$ le vecteur des contraintes de cisaillements dans la section et $\sigma_{33,3} = 0$ d'après la condition de gauchissement uniforme.

L'équation d'équilibre Eq.71 devient donc :

$$\Delta_{\boldsymbol{x}}\Omega = -\zeta_{,3}\ \mathrm{div}_{\boldsymbol{x}}\,\boldsymbol{\psi} \tag{72}$$

Pour former le PDP qui permet d'obtenir la fonction $\Omega(\boldsymbol{x})$, on a besoin des conditions aux limites :

$$\boldsymbol{\tau}\cdot\boldsymbol{n} = 0 \tag{73}$$

$$\Longrightarrow \quad \boldsymbol{\nabla}_{\boldsymbol{x}}\Omega\cdot\boldsymbol{n} = -\zeta_{,3}\,\boldsymbol{\psi}\cdot\boldsymbol{n} \tag{74}$$

On obtient ainsi le PDP permettant de déterminer le mode de gauchissement de 1er ordre pour un mode transversal quelconque donné :

$$\begin{cases} \Delta_{\boldsymbol{x}}\Omega = \mathrm{div}_{\boldsymbol{x}}\,\boldsymbol{\psi} & \text{sur S} \\ \boldsymbol{\nabla}_{\boldsymbol{x}}\Omega\cdot\boldsymbol{n} = \boldsymbol{\psi}\cdot\boldsymbol{n} & \text{sur } \Gamma_s \end{cases} \tag{75}$$

Ici aussi on a laissé tomber le terme $\zeta_{,3}$, vu qu'on est uniquement intéressé par la forme de Ω dans la section.

La détermination des modes d'ordres supérieurs ne sera pas détaillée ici, puisqu'une fois le mode de 1er ordre déterminé, on suit exactement la même procédure décrite dans l'article 1 et déjà présentée à la partie précédente, pour la détermination des modes d'ordres supérieurs.

4.1 Equations d'équilibre :

On suppose que la cinématique de la poutre a été construite et s'écrit sous la forme générale suivante :

$$\boldsymbol{d} = \begin{Bmatrix} \sum_i \psi_1^i(\boldsymbol{x})\zeta^i(x_3) \\ \sum_i \psi_2^i(\boldsymbol{x})\zeta^i(x_3) \\ \sum_j \Omega_j(\boldsymbol{x})\xi_j(x_3) \end{Bmatrix} \tag{76}$$

Dans la cinématique ci-dessus, la base des modes de gauchissement et la base des modes transversaux, doivent être libres, une condition nécessaire pour ne pas avoir plus tard de singularité dans la matrice de raideur de l'élément de poutre. Les fonctions formant les deux bases doivent être continues et dérivables. Sinon, pour ce qui suit, il n'y a aucune autre condition devant être satisfaite par la cinématique, les modes ainsi présents dans Eq.76 peuvent être quelconques, obtenus par la méthode qui nous paraît la plus judicieuse, d'ailleurs dans l'article 3 une nouvelle méthode sera proposée pour la construction de la cinématique, tout en utilisant la formulation de l'élément de poutre développée dans l'article 2, basée sur une résolution exacte des équations d'équilibre.

Pour simplifier l'écriture des équations, on va dans cette partie et uniquement dans cette partie, autoriser à ce que les lettres latines '*j*' et '*k*' prennent des valeurs allant de 1 au nombre total des modes de gauchissement présents dans la cinématique, et que les lettres latines '*i*' et '*l*' varient de 1 au nombre total de modes transversaux utilisés dans la cinématique.

De la cinématique Eq.76, on détermine les expressions des tenseurs des déformations et des contraintes :

$$\boldsymbol{\varepsilon} \coloneqq \frac{1}{2}(\boldsymbol{\nabla_X d} + (\boldsymbol{\nabla_X d})^T) = \begin{bmatrix} \psi_{1,1}^i\zeta^i & \frac{1}{2}(\psi_{1,2}^i + \psi_{2,1}^i)\zeta^i & \frac{1}{2}(\Omega_{j,1}\xi_j + \psi_1^i\zeta_{,3}^i) \\ & \psi_{2,2}^i\zeta^i & \frac{1}{2}(\Omega_{j,2}\xi_j + \psi_2^i\zeta_{,3}^i) \\ \text{sym} & & \Omega_j\xi_{j,3} \end{bmatrix} \tag{77}$$

$$\boldsymbol{\sigma} \coloneqq \boldsymbol{C} : \boldsymbol{\varepsilon} = \begin{bmatrix} 2\mu\psi_{1,1}^i\zeta^i + \sigma_r & \mu(\psi_{1,2}^i + \psi_{2,1}^i)\zeta^i & \mu(\Omega_{j,1}\xi_j + \psi_1^i\zeta_{,3}^i) \\ & 2\mu\psi_{2,2}^i\zeta^i + \sigma_r & \mu(\Omega_{j,2}\xi_j + \psi_2^i\zeta_{,3}^i) \\ \text{sym} & & 2\mu\Omega_j\xi_{j,3} + \sigma_r \end{bmatrix} \tag{78}$$

Avec : $\sigma_r \coloneqq \lambda\,\mathrm{tr}\boldsymbol{\varepsilon} = \lambda(\zeta^i \mathrm{div}_{\boldsymbol{x}}\boldsymbol{\psi}^i + \Omega_j\xi_{j,3})$.

On note ici que pour un matériau quasi-incompressible ($\nu \mapsto 0.5 \implies \lambda \mapsto +\infty$), il faut être capable de représenter la condition $\mathrm{tr}\boldsymbol{\varepsilon} = 0$ sinon $\sigma_r \mapsto +\infty$, ayant pour conséquence de provoquer un 'verrouillage incompressible' (incompressible locking). Pour pouvoir être capable de vérifier cette condition, il faut que des 'modes de déformations transversales incompressibles' sont inclus dans la cinématique. Par exemple pour un mode de gauchissement quelconque Ω, le mode transversal incompressible correspondant doit vérifier $\mathrm{div}_{\boldsymbol{x}}\boldsymbol{\psi} = \Omega$. À cause de ce problème de verrouillage, les

exemples présentés dans l'article 2 ont été réalisé pour $\nu = 0$, sachant que ce problème sera résolu plus tard dans l'article 3 avec la méthode des développements asymptotiques.

Pour la détermination des équations d'équilibre on va utiliser comme précédemment le PTV. On commence par écrire le travail virtuel interne :

$$\delta W_{int} \coloneqq \int_V \boldsymbol{\sigma} : \delta\boldsymbol{\varepsilon}\, dV = \int_V \left(\sigma_{33}\,\Omega_j\,\delta\xi_{j,3} + \sigma_{3\alpha}\Omega_{j,\alpha}\delta\xi_j + \sigma_{3\alpha}\psi^i_\alpha\delta\zeta^i_{,3} + \sigma_{\alpha\beta}\psi^i_{\alpha,\beta}\delta\zeta^i\right)dV \tag{79}$$

En intégrant sur la section, l'équation ci-dessus devient :

$$\delta W_{int} = \int_0^L \left(M_j\delta\xi_{j,3} + T_j\delta\xi_j + \Lambda^i\delta\zeta^i_{,3} + \Phi^i\delta\zeta^i\right)dx_3 \tag{80}$$

Avec les expressions des efforts généralisés sont données par :

$$M_j = \int_S \sigma_{33}\Omega_j\, dS = K_{jk}\xi_{k,3} + Q^i_j\zeta^i \tag{81}$$

$$T_j = \int_S \sigma_{3\alpha}\Omega_{j,\alpha}dS = J_{jk}\xi_k + D^i_j\zeta^i_{,3} \tag{82}$$

$$\Lambda^i = \int_S \sigma_{3\alpha}\psi^i_\alpha\, dS = D^i_j\xi_j + C^{il}\zeta^l_{,3} \tag{83}$$

$$\Phi^i = \int_S \sigma_{\alpha\beta}\psi^i_{\alpha,\beta}dS = Q^i_j\xi_{j,3} + H^{il}\zeta^l \tag{84}$$

Et les différents coefficients :

$$K_{jk} = \int_S (2\mu+\lambda)\Omega_j\Omega_k\, dS \quad , \quad J_{jk} = \int_S \mu\,\Omega_{j,\alpha}\Omega_{k,\alpha}\, dS \quad , \quad D^i_j = \int_S \mu\,\psi^i_\alpha\Omega_{j,\alpha}\, dS \tag{85}$$

$$Q^i_j = \int_S \lambda\,\Omega_j\psi^i_{\alpha,\alpha}dS \quad , \quad C^{il} = \int_S \mu\,\psi^i_\alpha\psi^l_\alpha\, dS \quad , \quad H^{il} = \int_S \left(\mu\psi^i_{\alpha,\beta}\psi^l_{\alpha,\beta} + \lambda\psi^i_{\alpha,\alpha}\psi^l_{\beta,\beta}\right)dS \tag{86}$$

Après intégration par partie de Eq.80 et en utilisant le PTV, on obtient les équations d'équilibre:

$$\int_0^L \left(\left(M_{j,3} - T_j\right)\delta\xi_j + \left(\Lambda^i_{,3} - \Phi^i\right)\delta\zeta^i\right)\, dx_3 = 0 \tag{87}$$

$$\Longrightarrow \quad M_{j,3} - T_j = 0 \qquad , \qquad \Lambda^i_{,3} - \Phi^i = 0 \tag{88}$$

En remplaçant par les expressions des efforts généralisés dans les équations d'équilibre ci-dessus, le système d'équations différentielles suivant est obtenu :

$$\begin{cases} K_{jk}\xi_{k,33} + \left(Q^i_j - D^i_j\right)\zeta^i_{,3} - J_{jk}\xi_k = 0 \\ C^{il}\zeta^l_{,33} - \left(Q^i_j - D^i_j\right)\xi_{j,3} - H^{il}\zeta^l = 0 \end{cases} \tag{89}$$

Pouvant aussi être exprimé sous la forme matricielle suivante :

$$\boldsymbol{M}\boldsymbol{u}'' + \boldsymbol{C}\boldsymbol{u}' - \boldsymbol{K}\boldsymbol{u} = \boldsymbol{0} \tag{90}$$

Avec :

$$\boldsymbol{u} = \begin{Bmatrix} \xi_j \\ \zeta^i \end{Bmatrix} \quad , \quad \boldsymbol{M} = \begin{bmatrix} K_{jk} & 0 \\ 0 & C^{il} \end{bmatrix} \quad , \quad \boldsymbol{C} = \begin{bmatrix} 0 & Q^i_j - D^i_j \\ D^i_j - Q^i_j & 0 \end{bmatrix} \quad , \quad \boldsymbol{K} = \begin{bmatrix} J_{jk} & 0 \\ 0 & H^{il} \end{bmatrix} \tag{91}$$

Dans l'équation Eq.90, les notations matricielles ont été choisies de manière à faire sortir l'analogie avec l'équation de la dynamique. Ce système est résolu d'une manière exacte en le transformant en un problème à valeurs propres quadratiques [17]. La matrice de raideur de l'élément sera assemblée à partir de cette solution. Les détails de la procédure sont donnés dans l'article 2.

5 Résumé de l'article 3 [9] :

5.1 Exemple d'introduction à la méthode des développements asymptotiques:

La méthode des développements asymptotiques (AEM : asymptotic expansion method) est une méthode générale pour la résolution d'équations différentielles. Pour introduire la méthode, on considère l'exemple suivant d'une équation différentielle très simple, qu'on souhaite résoudre en utilisant la AEM :

$$u'(x) - \eta u(x) = 0 \tag{92}$$

Avec $\eta \neq 0$ une constante réelle non nulle.

On cherche la solution de l'équation ci-dessus à l'aide de la AEM. Le principe de la méthode est d'exprimer la solution, qui dépend du paramètre η, sous forme d'une série entière de η :

$$u(x) \coloneqq u_0(x) + \eta u_1(x) + \eta^2 u_2(x) + \cdots \tag{93}$$

Cette série est remplacée dans Eq.92, pour ensuite identifier les termes associés à la même puissance de η :

$$(u_0' + \eta u_1' + \cdots) - \eta(u_0 + \eta u_1 + \cdots) = 0 \tag{94}$$

$$u_0' + \sum_{p\geq 1} \eta^p \left(u_p' - u_{p-1}\right) = 0 \tag{95}$$

Les termes associés à chaque puissance de η dans l'équation ci-dessus seront nuls, ce qui mène à la suite d'équations suivante :

$$\begin{cases} u_0' = 0 \\ u_p' - u_{p-1} = 0 \quad , \quad p \geq 1 \end{cases} \tag{96}$$

Ces équations sont résolues itérativement pour obtenir :

$$u_p = c\frac{x^p}{p!} \quad , \quad p \in \mathbb{N} \ , \ c \in \mathbb{R} \tag{97}$$

Avec $u_0 = c$.

En remplaçant les expressions ci-dessus dans Eq.93, on obtient la forme générale de la solution :

$$u(x) = c\left(1 + \eta x + \eta^2 \frac{x^2}{2!} + \eta^3 \frac{x^3}{3!} + \cdots\right) \tag{98}$$

$$u(x) = ce^{\eta x} \tag{99}$$

On retrouve donc bien avec la AEM, la solution classique d'une équation différentielle du type Eq.92.

5.2 Problème d'une poutre 3D :

Malgré les bons résultats de la méthode proposée dans l'article 2 pour enrichir la cinématique de la poutre, elle comporte deux points faibles. Le premier étant que le choix des modes transversaux se fait d'une manière heuristique, et donc ne forment pas une base optimale pour la description de la déformation de la poutre. Et le deuxième concerne le problème de verrouillage incompressible déjà mentionné.
Dans cette partie, on utilise la AEM pour décrire une nouvelle méthode pour l'obtention d'une base de modes transversaux et de gauchissements, plus optimale, pour enrichir la cinématique. La AEM va être appliquée, de la même manière que pour l'exemple d'introduction, à la forme forte du système d'équations d'équilibre mécanique d'une poutre 3D en élasticité linéaire, qui s'écrit sous la forme générale suivante :

$$\begin{cases} \mathrm{div}_{\boldsymbol{X}}(\boldsymbol{\sigma}) + \bar{\boldsymbol{b}} = \boldsymbol{0} & \text{sur } V \\ \boldsymbol{\varepsilon} = \boldsymbol{\nabla}_{\boldsymbol{X}}^{s}\boldsymbol{d} & \\ \boldsymbol{\sigma} = \boldsymbol{C} : \boldsymbol{\varepsilon} & \\ \boldsymbol{\sigma} \cdot \boldsymbol{n} = \bar{\boldsymbol{t}} & \text{sur } \Gamma \end{cases} \tag{100}$$

Avec $\boldsymbol{\nabla}_{\boldsymbol{X}}^{s} \coloneqq \frac{1}{2}(\boldsymbol{\nabla}_{\boldsymbol{X}} + (\boldsymbol{\nabla}_{\boldsymbol{X}})^{T})$ l'opérateur gradient symétrique, $\bar{\boldsymbol{b}}$ les forces volumiques et $\bar{\boldsymbol{t}}$ les forces surfacique. Les inconnues de ce système sont $\boldsymbol{d}$, $\boldsymbol{\varepsilon}$ et $\boldsymbol{\sigma}$, respectivement, le vecteur déplacement et les tenseurs des déformations et des contraintes.

Avant d'écrire le développement asymptotique des différentes grandeurs du système précédent. On effectue le changement de variable suivant, nécessaire pour séparer les variables transversales de la variable longitudinale :

$$(x_1, x_2, x_3) \coloneqq (hy_1, hy_2, Ly_3) \tag{101}$$

Avec *h* une dimension de la section et *L* la longueur de la poutre.

Ce changement de variable est appliqué aux opérateurs différentiels présents dans le système Eq.100 :

$$\begin{cases} \boldsymbol{\nabla}_{\boldsymbol{X}}^{s} = \dfrac{1}{L}\left(\boldsymbol{\nabla}_{y_3}^{s} + \dfrac{1}{\eta}\boldsymbol{\nabla}_{\boldsymbol{y}}^{s}\right) \\ \mathrm{div}_{\boldsymbol{X}} = \dfrac{1}{L}\left(\mathrm{div}_{y_3} + \dfrac{1}{\eta}\mathrm{div}_{\boldsymbol{y}}\right) \end{cases} \tag{102}$$

Avec $\boldsymbol{y} \coloneqq (y_1, y_2)$ et $\eta \coloneqq \frac{h}{L}$ ce qu'on appellera le paramètre de "scaling", qui sera utilisé pour écrire toutes les données et les inconnues du système dans Eq.100 sous forme de série entière.

Exactement de la même manière que pour l'exemple d'introduction, on exprime sous forme de série entière de η, les inconnues du problème que sont les déplacements, les déformations et les contraintes :

$$\boldsymbol{d} \coloneqq L\left(\frac{1}{\eta}\boldsymbol{d}^{-1} + \boldsymbol{d}^{0} + \eta\,\boldsymbol{d}^{1} + \eta^{2}\boldsymbol{d}^{2} + \cdots\right) \tag{103}$$

$$\boldsymbol{\sigma} \coloneqq \boldsymbol{\sigma}^{0} + \eta\,\boldsymbol{\sigma}^{1} + \eta^{2}\boldsymbol{\sigma}^{2} + \cdots \tag{104}$$

$$\boldsymbol{\varepsilon} \coloneqq \boldsymbol{\varepsilon}^{0} + \eta\,\boldsymbol{\varepsilon}^{1} + \eta^{2}\boldsymbol{\varepsilon}^{2} + \cdots \tag{105}$$

Les efforts dans le système Eq.100 doivent aussi être développés asymptotiquement. Ils seront introduits à des ordres bien définis (c.à.d. à des puissances définies de η), de la même manière que Buannic & Cartraud [4] et Lebée & Sab [15]:

$$\overline{b_\alpha} \coloneqq \frac{1}{h}\,\eta^{2}\,b_\alpha(\boldsymbol{y})\,f(y_3) \quad , \quad \overline{t_\alpha} \coloneqq \eta^{2}\,t_\alpha(\boldsymbol{y})\,f(y_3) \tag{106}$$

$$\overline{b_3} \coloneqq \frac{1}{h}\,\eta\,b_3(\boldsymbol{y})\,f(y_3) \quad , \quad \overline{t_3} \coloneqq \eta\,t_3(\boldsymbol{y})\,f(y_3) \tag{107}$$

Avec $f(y_3)$ une fonction de classe C^{∞}.

Dans les équations ci-dessus on a supposé une séparation des variables pour les différends efforts externes. Cette hypothèse aura pour conséquence une séparation des variables dans l'expression du déplacement, permettant ainsi d'obtenir des modes de déformations transversales ou de

gauchissements ne dépendant que de la géométrie de la section, ayant des variables (d.d.l.) qui leurs sont associés, représentant leurs variations le long de la poutre.

On introduit toutes ces expressions dans les différentes équations du système Eq.100. Pour illustrer la procédure on considère l'équation de compatibilité :

$$\boldsymbol{\varepsilon} = \left(\boldsymbol{\nabla}^s_{y_3} + \frac{1}{\eta}\boldsymbol{\nabla}^s_{\boldsymbol{y}}\right)\left(\frac{1}{\eta}\boldsymbol{d}^{-1} + \boldsymbol{d}^0 + \eta\,\boldsymbol{d}^1 + \cdots\right) \tag{108}$$

$$\boldsymbol{\varepsilon} = \eta^{-2}\boldsymbol{\nabla}^s_{\boldsymbol{y}}\boldsymbol{d}^{-1} + \eta^{-1}\left(\boldsymbol{\nabla}^s_{\boldsymbol{y}}\boldsymbol{d}^0 + \boldsymbol{\nabla}^s_{y_3}\boldsymbol{d}^{-1}\right) + \left(\boldsymbol{\nabla}^s_{\boldsymbol{y}}\boldsymbol{d}^1 + \boldsymbol{\nabla}^s_{y_3}\boldsymbol{d}^0\right) + \cdots \tag{109}$$

En comparant les deux expressions du tenseur des déformations dans Eq.109 et Eq.105, on obtient les relations suivantes en identifiant les termes correspondant au même ordre :

$$\boldsymbol{\varepsilon}^{-2} = \boldsymbol{\nabla}^s_{\boldsymbol{y}}\boldsymbol{d}^{-1} = \boldsymbol{0} \quad , \quad \boldsymbol{\varepsilon}^{-1} = \boldsymbol{\nabla}^s_{\boldsymbol{y}}\boldsymbol{d}^0 + \boldsymbol{\nabla}^s_{y_3}\boldsymbol{d}^{-1} = \boldsymbol{0} \tag{110}$$

$$\boldsymbol{\varepsilon}^p = \boldsymbol{\nabla}^s_{\boldsymbol{y}}\boldsymbol{d}^{p+1} + \boldsymbol{\nabla}^s_{y_3}\boldsymbol{d}^p \quad \text{pour} \quad p \in \mathbb{N} \tag{111}$$

Les deux équations présentes dans Eq.110 sont des équations différentielles résolues indépendamment de l'équilibre de la poutre, obtenant ainsi la forme des vecteurs déplacements $\boldsymbol{d}^{-1}$ et $\boldsymbol{d}^0$:

$$\boldsymbol{d}^{-1} = \begin{Bmatrix} U_1^{-1}(y_3) \\ U_2^{-1}(y_3) \\ 0 \end{Bmatrix} \quad , \quad \boldsymbol{d}^0 = \begin{Bmatrix} U_1^0(y_3) - y_2\theta^0(y_3) \\ U_2^0(y_3) + y_1\theta^0(y_3) \\ U_3^0(y_3) - y_\alpha U_\alpha^{-1}(y_3) \end{Bmatrix} \tag{112}$$

L'expression du déplacement à l'ordre 0 ci-dessus, ne contient que les mouvements de corps rigide, plus les rotations de flexions.

De même que pour l'équation de compatibilité, le changement de variable et les expressions des développements asymptotiques des différentes grandeurs seront utilisés dans les équations restantes du système Eq.100. On obtiendra ainsi pour chaque ordre (puissance de η) un problème à résoudre. On donne ci-dessous l'expression, sous forme indicielle, de ces différents problèmes pour les différents ordres. Pour plus de détails sur la procédure menant à leur obtention voir article 3.

- Problème P^1 :

$$\begin{cases} \sigma^0_{\alpha\beta,\beta} = 0 & (a) \\ \sigma^0_{3\beta,\beta} = 0 & (b) \\ \varepsilon^0_{\alpha\beta} = \frac{1}{2}\left(d^1_{\alpha,\beta} + d^1_{\beta,\alpha}\right) \quad , \quad \varepsilon^0_{\alpha 3} = \frac{1}{2}\left(d^1_{3,\alpha} + d^0_{\alpha,3}\right) \quad , \quad \varepsilon^0_{33} = d^0_{3,3} & \\ \sigma^0_{ij} = 2\mu\varepsilon^0_{ij} + \lambda\varepsilon^0_{kk}\delta_{ij} & \\ \sigma^0_{ij}n_j = 0 & \end{cases} \tag{113}$$

Avec $\mu \coloneqq \frac{E}{2(1+\nu)}$, $\lambda \coloneqq \frac{\nu E}{2(1+\nu)(1-2\nu)}$ les deux coefficients de Lamé.

On remarque qu'à cet ordre l'inconnue est le vecteur déplacement $\boldsymbol{d}^1$, alors que $\boldsymbol{d}^0$, dont la forme est connue, sert en quelque sorte de chargement au problème. On note aussi que les chargements externes qui varient selon la fonction *f*, n'apparaissent pas encore.

- Problème P^2 :

$$\begin{cases} \sigma^1_{\alpha\beta,\beta} + \sigma^0_{\alpha 3,3} = 0 \\ \sigma^1_{3\beta,\beta} + \sigma^0_{33,3} + b_3 f = 0 \\ \varepsilon^1_{\alpha\beta} = \frac{1}{2}\left(d^2_{\alpha,\beta} + d^2_{\beta,\alpha}\right) \quad , \quad \varepsilon^1_{\alpha 3} = \frac{1}{2}\left(d^2_{3,\alpha} + d^1_{\alpha,3}\right) \quad , \quad \varepsilon^1_{33} = d^1_{3,3} \\ \sigma^1_{ij} = 2\mu\varepsilon^1_{ij} + \lambda\varepsilon^1_{kk}\delta_{ij} \\ \sigma^1_{\alpha j} n_j = 0 \ , \ \sigma^1_{3j} n_j = t_3 f \end{cases} \tag{114}$$

À cet ordre les forces externes longitudinales, volumiques et surfaciques, apparaissent. Ils mèneront à la détermination d'un mode de gauchissement spécifique, qui dépendra donc de la répartition transversale $\left(b_3(\boldsymbol{y}), t_3(\boldsymbol{y})\right)$ des forces longitudinales.

- Problème P^3 :

$$\begin{cases} \sigma^2_{\alpha\beta,\beta} + \sigma^1_{\alpha 3,3} + b_\alpha f = 0 \\ \sigma^2_{3\beta,\beta} + \sigma^1_{33,3} = 0 \\ \varepsilon^2_{\alpha\beta} = \frac{1}{2}\left(d^3_{\alpha,\beta} + d^3_{\beta,\alpha}\right) \quad , \quad \varepsilon^2_{\alpha 3} = \frac{1}{2}\left(d^3_{3,\alpha} + d^2_{\alpha,3}\right) \quad , \quad \varepsilon^2_{33} = d^2_{3,3} \\ \sigma^2_{ij} = 2\mu\varepsilon^2_{ij} + \lambda\varepsilon^2_{kk}\delta_{ij} \\ \sigma^2_{\alpha j} n_j = t_\alpha f \quad , \quad \sigma^2_{3j} n_j = 0 \end{cases} \tag{115}$$

Dans le problème P^3, c'est au tour des forces externes transversales d'apparaître (b_α, t_α), pour lesquelles un mode transversal spécifique sera déterminé. Dans P^2 un mode de gauchissement associé au chargement sera déterminé, désigné par la fonction $\Omega^{2.3}$, apparaissant donc dans la composante longitudinale du vecteur déplacement $\boldsymbol{d}^2$ de la manière suivante:

$$d^2_3 = \cdots + \Omega^{2.3} f \tag{116}$$

L'expression de la déformation longitudinale ε^2_{33} dans P^3 fera donc intervenir la dérivée de *f* dans le problème, ce qui aura pour effet la détermination à cet ordre d'un mode transversal associé à f'.

- Problème P^p pour $p \geq 4$:

$$\begin{cases} \sigma^p_{i\beta,\beta} + \sigma^{p-1}_{i3,3} = 0 \\ \varepsilon^p_{\alpha\beta} = \frac{1}{2}\left(d^{p+1}_{\alpha,\beta} + d^{p+1}_{\beta,\alpha}\right) \quad , \quad \varepsilon^p_{\alpha 3} = \frac{1}{2}\left(d^{p+1}_{3,\alpha} + d^p_{\alpha,3}\right) \quad , \quad \varepsilon^p_{33} = d^p_{3,3} \\ \sigma^p_{ij} = 2\mu\varepsilon^p_{ij} + \lambda\varepsilon^p_{kk}\delta_{ij} \\ \sigma^p_{ij} n_j = 0 \end{cases} \tag{117}$$

Pour les ordres supérieurs p ≥ 4, le seul chargement viendra de la variation longitudinale du déplacement de l'ordre précédent exprimée par sa dérivée $\boldsymbol{d}^{p}_{,3}$. On déterminera ainsi des modes de gauchissements et/ou de déformations transversales d'ordre supérieur, à l'aide d'une relation de récurrence, où les nouveaux modes à déterminer s'expriment en fonction de ceux des ordres précédents.

Le problème initial dans Eq.100, de l'équilibre mécanique d'une poutre occupant un volume *V*, a été transformé en une série de problèmes à résoudre. À chaque ordre, le problème correspondant donne la forme du vecteur déplacement pour l'ordre considéré. En remplaçant toutes ces expressions dans Eq.103, on obtiendrait au final la forme générale du déplacement. Mais ici la résolution du problème ne sera pas poussée jusqu'à l'obtention de la variation des différents degrés de libertés. On applique la AEM uniquement pour déterminer la forme de la cinématique, l'équilibre sera ensuite résolu par la méthode de l'article 2. On ne s'intéresse donc pas ici aux différentes conditions d'appuis de la poutre, ni à comment elles sont traduites dans le cadre de la AEM, à l'inverse de la procédure proposée dans [5] et [11].

5.3 Solution du problème et forme du déplacement :

Les détails de la solution des différents problèmes exprimés ci-dessus seront donnés dans l'article 3. Ici on exprime puis on analyse la forme finale du déplacement après la solution des différents problèmes :

$$d_\alpha = U_\alpha + \psi_\alpha^{\mathrm{tor}}\theta + \eta\,\psi_\alpha^{1.3}U_{3,3} + \eta^2\psi_\alpha^{1.\beta}U_{\beta,33} + \sum_{p\geq 3\ impair} \eta^p\left(\psi_\alpha^{p.1}f^{(p-3)} + \psi_\alpha^{p.2}f^{(p-2)}\right) \tag{118}$$

$$d_3 = U_3 + \eta\left(-x_\alpha U_{\alpha,3} + \Omega^{1.1}\theta_{,3}\right) + \eta^2\Omega^{2.\alpha}T_\alpha + \eta^2\Omega^{2.3}f + \sum_{p\geq 4\ pair} \eta^p\left(\Omega^{p.1}f^{(p-3)} + \Omega^{p.2}f^{(p-2)}\right) \tag{119}$$

Avec $f^{(p)} := \frac{d^p f}{dx_3^p}$ exprimant la p[ième] dérivées de f par rapport à x_3. $U_i(x_3)$ et $\theta(x_3)$ des fonctions variant le long de la poutre représentant les mouvements de corps rigide et T_α les deux composantes de l'effort tranchant dans la section. On rappelle que $\boldsymbol{\psi}^{\mathrm{tor}} := (-x_2, x_1)$ représente le mode de torsion, les fonctions qui sont désignées par $\Omega^{p.i}(\boldsymbol{x})$ des modes de gauchissements et les fonctions $\boldsymbol{\psi}^{p.i}(\boldsymbol{x}) = \left(\psi_1^{p.i}(\boldsymbol{x}), \psi_2^{p.i}(\boldsymbol{x})\right)$ des modes transversaux, avec *p* l'ordre auquel ils ont été déterminés et *i* leurs numéros dans l'ordre.

Les termes encadrés en bleu représentent la cinématique classique d'une poutre d'Euler-Bernoulli. Les termes encadrés en rouge sont quant à eux obtenus dans la solution de Saint-Venant du problème de l'équilibre d'une poutre. Ces termes ne dépendent pas du chargement extérieur sur la poutre, mais seulement des conditions aux extrémités sur les déplacements. La contribution du chargement extérieur à la cinématique sera donnée par les termes encadrés en vert, qui sont tous associés à *f* ou à une de ses dérivées.

Pour illustrer les modes de déformations transversales et de gauchissements introduits dans la cinématique Eq.118-119, on considère l'exemple d'une section rectangulaire :

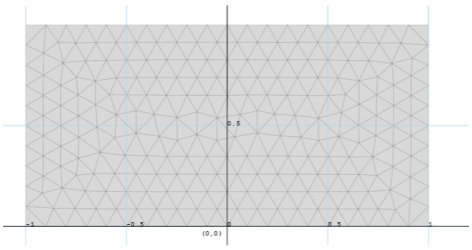

Figure 10: la section et son maillage avec des éléments triangulaires quadratiques.

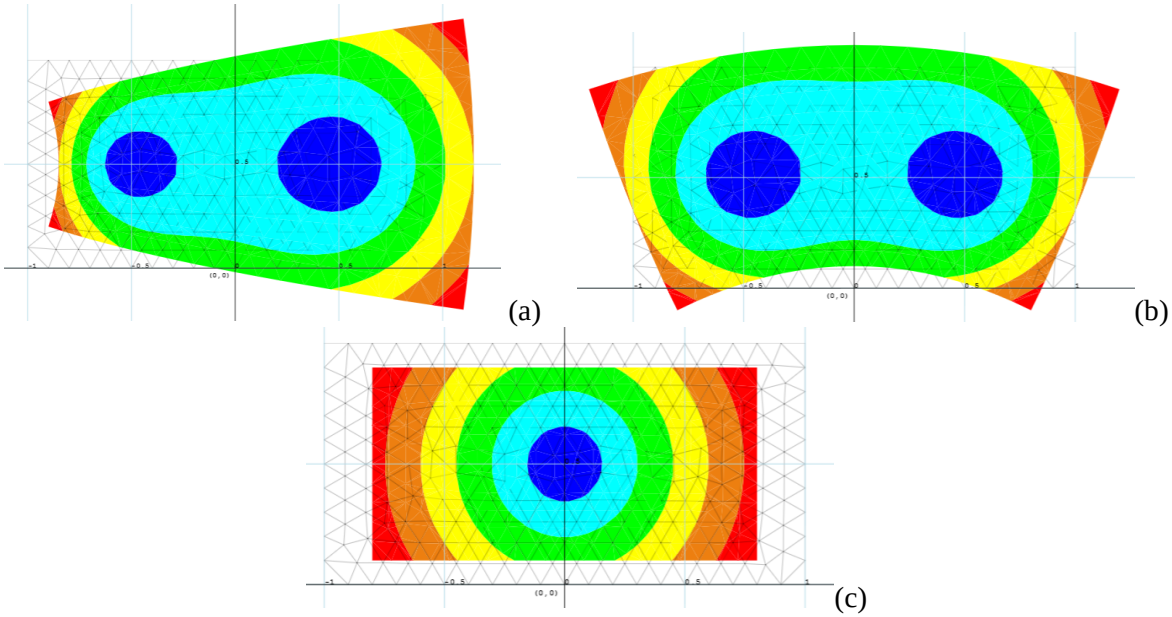

Figure 11: (a) mode $\boldsymbol{\psi}^{1.1}$ (b) mode $\boldsymbol{\psi}^{1.2}$ (c) mode $\boldsymbol{\psi}^{1.3}$

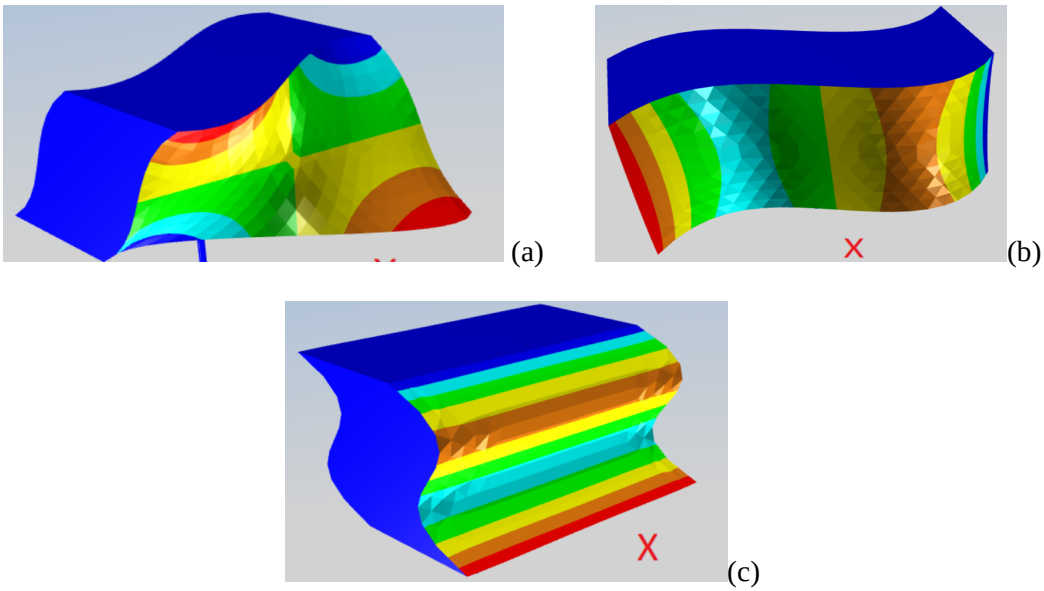

Figure 12: (a) mode $\Omega^{1.1}$ (b) mode $\Omega^{2.1}$ (c) mode $\Omega^{2.2}$

Dans le cas particulier d'une section à matériau homogène, l'expression analytique des modes $\boldsymbol{\psi}^{1.i}$ peut être donnée :

$$\begin{cases}\psi_1^{1.1} = \dfrac{\nu}{2}(x_1^2 - x_2^2) \\ \psi_2^{1.1} = \nu\, x_1 x_2\end{cases} \quad , \quad \begin{cases}\psi_1^{1.2} = \nu\, x_1 x_2 \\ \psi_2^{1.2} = \dfrac{\nu}{2}(x_2^2 - x_1^2)\end{cases} \quad , \quad \begin{cases}\psi_1^{1.3} = -\nu\, x_1 \\ \psi_2^{1.3} = -\nu\, x_2\end{cases} \tag{120}$$

Avec ν le coefficient de Poisson.

Pour illustrer les modes dus aux forces, on considère une section en forme de caisson, une géométrie très utilisée dans des projets réels. Les modes représentés ci-dessous sont tous déterminés pour la force verticale, répartie sur le hourdis supérieur :

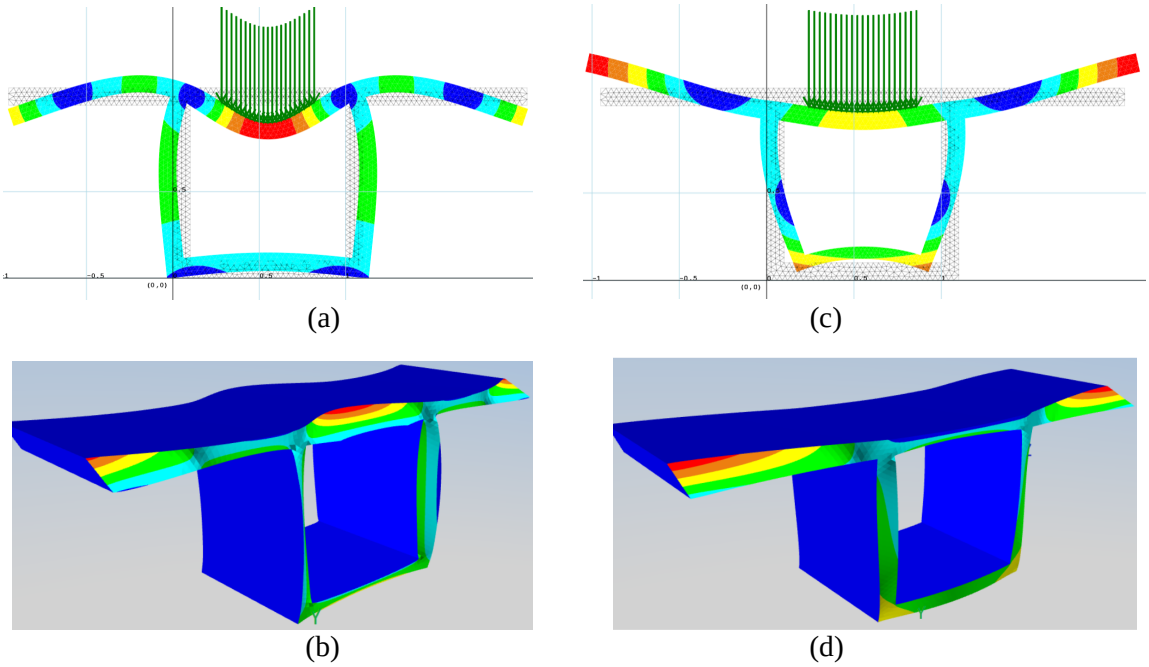

Figure 13: (a) mode transversal $\boldsymbol{\psi}^{3.1}$ (b) mode de gauchissement $\Omega^{4.1}$
(c) mode transversal $\boldsymbol{\psi}^{5.1}$ (d) mode de gauchissement $\Omega^{6.1}$

De l'analyse de la cinématique écrite dans Eq.118-119, plusieurs remarques peuvent être faites:

Rq.1 : La méthode des développements asymptotiques permet de retrouver (ou justifier) d'une manière rigoureuse des modèles de poutres existants, tels que les modèles d'Euler-Bernoulli, Vlassov ou Saint-Venant.

Rq.2 : Le gauchissement de Vlassov (terme en $\Omega^{1.1}$) est du 1er ordre (même ordre que la flexion), ce qui confirme l'importance de ce terme pour le comportement des poutres en torsion.

Rq.3 : En l'absence de force extérieure, la solution déterminée par la AEM correspond en fait à la solution de Saint-Venant pour les poutres.

Rq.4 : La cinématique ne prend pas en compte les effets de bords aux extrémités de la poutre. Ceci revient à avoir considéré une poutre infinie où ces effets peuvent être négligés.

Rq.5 : Lorsque la fonction *f*, représentant la variation longitudinale des efforts, a une forme polynomiale, la forme exacte du déplacement (pour une poutre infinie) est obtenue en tronquant les deux sommes infinies à l'ordre du polynôme.

Rq.6 : Chacun des modes d'ordres supérieurs associés aux efforts extérieurs, varient selon une dérivée de *f*. Dans le cas où cette fonction n'est pas de classe C^{∞} (cas d'une force ponctuelle), la cinématique déterminée par la AEM donnera quand même d'excellents résultats (loin des extrémités) avec très peu de modes.

6 Discussion générale et analyse des résultats :

Dans les trois articles présentés ici, la construction du modèle de poutre enrichi est effectuée en deux étapes principales. La première est la détermination de la cinématique qui va régir le mouvement de la poutre. Cette étape est importante puisque quelles que soient les charges auxquelles sera soumise la poutre plus tard (forces, poids propre, fluage…), elle ne pourra se déformer que selon la cinématique adoptée initialement. Le choix de cette dernière doit se faire donc en fonction des chargements que va subir la poutre, pour qu'il soit le plus optimal possible. La deuxième étape est l'obtention et la résolution des équations d'équilibre pour construire la matrice de raideur de l'élément. Deux choix s'offrent à nous dans cette étape, le premier consiste à utiliser des fonctions d'interpolations (polynômes de Lagrange, Spline…) pour l'approximation des degrés de libertés, le deuxième consiste à résoudre les équations d'équilibre d'une manière exacte. C'est ce second choix qui a été adopté dans ce travail. Cependant la solution exacte ne peut être obtenue (du moins à notre connaissance) que pour le cas linéaire élastique avec des sections constantes, un cas plus général complique considérablement les équations d'équilibres pour qu'elles puissent encore être résolues d'une manière exacte. Dans ces cas, l'utilisation des fonctions d'interpolations s'impose. La solution exacte est relativement facile à obtenir dans l'article 1 (section infiniment rigide dans leur plan mais pouvant gauchir), mais pour le cas général de l'article 2 et 3 (section pouvant se déformer dans son plan et gauchir) elle n'est atteinte qu'après un long processus de résolution des équations d'équilibre. La solution exacte permet de s'affranchir d'un maillage trop fin et des problèmes de verrouillage numérique pouvant apparaître. Ce qui en fait, malgré sa difficulté, une approche élégante, qui doit toujours être adoptée quand elle est possible.

La méthode des développements asymptotiques (AEM) offre une approche efficace et générale pour déterminer une base réduite adaptée pour enrichir la cinématique de la poutre. Elle peut être considéré comme une approche plus simple que les méthodes de réduction de modèle, tels que la PGD (proper generalized decompostion) ou la POD (proper orthogonal decompostion), voir Ryckelynck & al [16]. Ces approches ont pour point de départ les équations d'équilibre 3D de la poutre, seulement pour la AEM seule une pré-analyse de la section est nécessaire pour déterminer les modes de déformations, au lieu d'un calcul 3D global de la poutre pour les autres approches.

La AEM suppose que la poutre est infiniment longue, et utilise une séparation de variables pour les efforts, variant longitudinalement selon une fonction infiniment dérivable. En considérant toutes ces hypothèses, la forme générale du déplacement de la structure est obtenue.

Pour l'usage qu'on fait de la AEM, l'expression exacte de la fonction représentant la variation longitudinale des efforts ne nous intéresse pas, puisque la AEM nous sert seulement à déterminer des modes de déformations associés à chacune des dérivées de ladite fonction. Cependant, parmi les cas de charges usuels qui se présentent à l'ingénieur, certains sont ponctuels (fonction delta de Dirac) ou bien répartis sur une longueur réduite de la poutre (fonction porte). On serait donc en droit de supposer, que pour ces types de fonctions, il faut pousser le développement asymptotique à un ordre très élevé pour

obtenir de bons résultats. Cependant dans tous les cas tests proposés dans l'article 3 où le chargement est ponctuel, on obtient de très bon résultats en comparaison avec ceux obtenus avec des modèles de référence en éléments de coques ou volumiques, et cela en s'arrêtant aux modes liés à la dérivée cinquième de la fonction de répartition longitudinale des efforts. On a donc, même pour le cas de comparaison extrême d'une force ponctuelle, de très bons résultats avec très peu de modes.

Il faut noter ici un point de différence important entre les résultats des deux premiers articles avec ceux du dernier. Dans les exemples proposés dans les deux premiers articles, la comparaison est faite sur la distribution des contraintes normales ou tangentielles au voisinage de l'encastrement des poutres, qui représente la zone de perturbation. Les résultats sont comparés à des modèles de références, et montrent une très bonne concordance. Ces résultats ne peuvent pas être reproduits en utilisant les modes provenant de la AEM, puisque une des hypothèses de la méthode est qu'on est dans une poutre infinie (et donc très loin des zones de perturbations). Malheureusement ici pas de miracle, les résultats concernant les contraintes deviennent médiocres en s'approchant des appuis. Ces résultats peuvent néanmoins être améliorés en incorporant les modes de gauchissement obtenus par la méthode développée dans l'article 1, ce qui peut être observé dans la figure 11 de l'article 3.

Une remarque dans l'article 2 précisait que l'effet Poisson allait être négligé à cause de l'apparition du verrouillage incompressible, et que par conséquent dans tous les exemples proposés, un coefficient de Poisson nul a été considéré. Pour résoudre ce problème, il faut, comme expliqué dans la remarque, inclure des modes de déformations d'une manière à compenser (ou représenter) les déformations créées par l'effet Poisson. En utilisant la AEM, l'effet Poisson sera naturellement pris en compte dans les modes qui seront déterminés, ce qui résout le problème du verrouillage incompressible.

De l'AEM on obtient un résultat intéressant concernant la définition du centre de gravité et les axes principaux d'inerties. Pour déterminer la position du centre de gravité et l'orientation des axes principaux, la définition classique est que le système de coordonnées doit vérifier les trois équations suivantes:

$$\int_S E y_\alpha dS = 0 \quad , \quad \int_S E y_1 y_2 dS = 0 \tag{121}$$

Avec $\boldsymbol{y} \coloneqq (y_1, y_2)$ les coordonnées des points de la section et $E(\boldsymbol{y})$ le module d'Young.

Cependant cette définition n'est valable que dans le cas d'une section avec un coefficient de Poisson constant, sinon elle n'a plus aucun sens. Une nouvelle définition peut néanmoins être adoptée, en utilisant les relations dans Eq.96 de l'article 3, et qui s'expriment par :

$$\int_S \mu \left(2 - \mathrm{div}_{\boldsymbol{y}}(\boldsymbol{\psi}^{1.3})\right) y_\alpha dS = 0 \tag{122}$$

$$\int_S \mu \left(2y_1 + \mathrm{div}_{\boldsymbol{y}}(\boldsymbol{\psi}^{1.1})\right) y_2 dS = \int_S \mu \left(2y_2 + \mathrm{div}_{\boldsymbol{y}}(\boldsymbol{\psi}^{1.2})\right) y_1 dS = 0 \tag{123}$$

Avec $\boldsymbol{\psi}^{1.i}$ les trois modes de déformations transversales dus au coefficient de Poisson Eq.. Ces relations définissent le centre de gravité et l'orientation des axes principaux, permettant ainsi un découplage entre l'effort normal et les moments de flexions.

7 Conclusion et perspective future:

En couplant la AEM pour la détermination de la cinématique de la poutre, présentée en détail dans l'article 3, avec la résolution exacte des équations d'équilibres développée dans l'article 2, on obtient une procédure efficace pour la construction d'un modèle de poutre enrichie, basée sur une résolution analytique des équations d'équilibre, capable de rivaliser avec des modèles en éléments de coques ou briques.

Dans l'article 3, la AEM a été utilisée pour déterminer des modes spécifiques aux forces extérieures appliquées à la poutre. La procédure peut être aussi adaptée, sans trop de difficultés, pour déterminer des modes spécifiques à des déformations imposées (gradient thermique, fluage…).

Le modèle présenté dans ce travail ne concerne pour l'instant que des poutres à sections constantes. Pour le cas des sections variables, une solution générale exacte n'est plus possible. Il faut donc utiliser des fonctions d'interpolations (Spline, Nurbs…) pour approximer la géométrie arbitraire de la poutre, ainsi que la variation des différents degrés de libertés pour construire la matrice de raideur de l'élément.

Cependant, pour des poutres à section variable, courbes, biaises, ou plus généralement initialement déformées d'une manière quelconque, la différence avec les poutres à sections constantes ne réside pas seulement dans le fait que la solution exacte n'est plus possible, mais surtout dans le fait que la géométrie initiale quelconque de la poutre, produit des effets non négligeable sur la déformation de la poutre, qui de la même manière que pour le chargement extérieur, nécessitent de déterminer des modes de déformations (gauchissements et transversaux) spécifiques pour pouvoir les représenter.

Le traitement des non linéarités géométriques pour ce type de poutre enrichie est, comme on peut s'y attendre, un sujet complexe. Ici aussi, comme pour la prise en compte de la géométrie initiale, il faudrait imaginer qu'à chaque itération d'un processus de résolution d'équations non-linéaires (Newton-Raphson…), on détermine des modes spécifiques à l'état de déformation atteinte par la poutre. Cette première idée laisse entrevoir la complexité de cette problématique, qui reste un des axes de recherche à poursuivre.

La prise en compte des non linéarités matérielles dans le cadre de la méthode des développements asymptotiques, est tout autant, si ce n'est plus difficile que celle des non linéarités géométriques. Plusieurs pistes sont envisageables, mais pour l'instant ce sujet est encore à l'état embryonnaire, et représente un axe de développement futur en cours.

Des sujets pouvant paraître moins théoriques au premier abord, sont en réalité tout aussi difficiles et importants que les problématiques de non linéarités géométriques et matérielles, puisqu'ils sont essentiels pour l'usage pratique de cet élément de poutre enrichi. On peut notamment citer la question de la prise en compte l'effet des raidisseurs transversaux, présents généralement dans la grande majorité des tabliers de ponts. Celle de savoir comment connecter une poutre venant se raccorder latéralement à une autre poutre (par des boulons, des soudures…) et quel est l'effet de cette connexion sur la cinématique à choisir.

La liste des sujets de développement futurs, détaillée ci-dessus, est loin d'être exhaustive. La résolution de tous les problèmes liés aux poutres enrichies nécessite certainement des années recherches. Mais qui nous le croyons, ouvre la voie à une nouvelle génération des logiciels de calcul de structures, offrant ainsi des outils modernes aux ingénieurs pour une meilleure compréhension du comportement de leurs ouvrages.

Référence :

[1] Alsafadie, R., Hjiaj, M., & Battini, J. M. (2010). Corotational mixed finite element formulation for thin-walled beams with generic cross-section. *Computer Methods in Applied Mechanics and Engineering, 199(49), 3197-3212.*

[2] Ballarini, R. (2006). The Da Vinci-Euler-Bernoulli beam theory ? *Mechanical Engineering The Magazine of ASME (20/10/2012), 35*.

[3] Benscoter, S. U. (1954). A theory of torsion bending for multicell beams. *Journal of Applied Mechanics*, *21*(1), 25-34.

[4] Buannic, N., & Cartraud, P. (2001). Higher-order effective modeling of periodic heterogeneous beams. I. Asymptotic expansion method. *International Journal of Solids and Structures, 38(40), 7139-716.*

[5] Buannic, N., & Cartraud, P. (2001). Higher-order effective modeling of periodic heterogeneous beams. II. Derivation of the proper boundary conditions for the interior asymptotic solution. *International Journal of Solids and Structures, 38(40), 7163-7180.*

[6] Ferradi, M. K. (2009). Etude du gauchissment des sections soumises aux cisaillements. *Rapport de stage de fin d'étude, Setec-Tpi.*

[7]. Ferradi, M. K., Cespedes, X., & Arquier, M. (2013). A higher order beam finite element with warping eigenmodes. *Engineering Structures, 46, 748-762.*

[8] Ferradi, M. K., & Cespedes, X. (2014). A new beam element with transversal and warping eigenmodes. *Computers & Structures, 131, 12-33.*

[9] Ferradi, M. K., Lebée, A., Fliscounakis, A., Cespedes, X., Sab, K. (2015). A model reduction technique for beam analysis with the asymptotic expansion method. *Submitted to Computers & Structures.*

[10] Goyet, V.V. (1989). L'analyse statique non linéaire par la méthode des éléments finis des structures spatiales formées de poutres à section non symétrique. *Thèse de Doctorat de l'Université de Liège.*

[11] Gregory, R. D., & Wan, F. Y. (1984). Decaying states of plane strain in a semi-infinite strip and boundary conditions for plate theory. *Journal of Elasticity,14(1), 27-64.*

[12] Jang, G. W., Kim, M. J., & Kim, Y. Y. (2012). Analysis of Thin-Walled Straight Beams with Generally-Shaped Closed Sections Using Numerically-Determined Sectional Deformation Functions. *Journal of Structural Engineering, 1, 438.*

[13] Kreutz, J. (2013). Augmented Beam Elements Using Unit Deflection Shapes Together with a Finite Element Discretisation of the Cross Section. (*Doctoral dissertation, Technische Universität München).*

[14] Krístek, V., & Bazant, Z. P. (1987). Shear lag effect and uncertainty in concrete box girder creep. *Journal of Structural Engineering, 113(3), 557-574.*

[15] Lebée, A., & Sab, K. (2013). Justification of the Bending-Gradient theory through asymptotic expansions. *In Generalized Continua as Models for Materials (pp. 217-236). Springer Berlin Heidelberg.*

[16] Ryckelynck, D., Chinesta, F., Cueto, E., & Ammar, A. (2006). On the a priori model reduction: Overview and recent developments. *Archives of Computational Methods in Engineering*, *13*(1), 91-128.

[17] Tisseur, F., & Meerbergen, K. (2001). The quadratic eigenvalue problem. *Siam Review*, *43*(2), 235-286.

[18] Vlassov, B. Z., & Vlasov, V. Z. (1962). Pièces longues en voiles minces. *Editions Eyrolles*.

Engineering Structures 46 (2013) 748–762

Contents lists available at SciVerse ScienceDirect

Engineering Structures

journal homepage: www.elsevier.com/locate/engstruct

A higher order beam finite element with warping eigenmodes

Mohammed Khalil Ferradi *, Xavier Cespedes, Mathieu Arquier

SETEC-TPI, 42/52 Quai de la Rapée, 75012 Paris, France

ARTICLE INFO

Article history:
Received 28 November 2011
Revised 26 June 2012
Accepted 31 July 2012
Available online 23 October 2012

Keywords:
Shear lag
Restrained torsion
Warping
Finite element method
Beam

ABSTRACT

In this paper, a new beam finite element is presented, with an accurate representation of normal stresses caused by "shear lag" or restrained torsion. This is achieved using an enriched kinematics, representing cross-section warping as the superposition of "warping modes". Detailed definitions and computational methods are given for these associated "warping functions". The exact solution of the equilibrium equations is given for a user-defined number of warping modes, though elastic results are totally mesh-independent.

1. Introduction

In bridge engineering, it is often needed to analyze the effect of torsional warping and shear lag on the stress distribution of beam cross-sections. This can not be achieved by using a model of classical beam finite element, based on either Bernoulli or Timoshenko theory. Two differents approaches are common: The first is based on shell element models, that can be costly with respect to engineer time or computer time calculation, whereas the second relies on analytical methods, based for example on a Fourier series decomposition of forces (see Fauchart [8]), which is valid only for one-span system, can miss some effect when the section is not bi-symmetric, and can hardly be integrated in finite element programs. The lack of an easy-to-use general method has motivated the present work to develop a new beam finite element able to describe very accurately the non-uniform warping of sections, either caused by non uniform torsion or shear lag.

The problem of warping have been widely treated in the existing literature. In Bauchau [1], a similar approach of the one exposed here is used, consisting in ameliorating the Saint-Venant solution, that considers only the warping modes for a uniform warping, by adding new eigenwarping modes, derived from the principle of minimum potential energy. We propose here a different approach, that has the advantage to separate the determination of the warping modes from the equilibrium solution, and to propose a finite element formulation using this modes. Sapountzakis and Mokos [2] calculate a secondary shear stress, due to a non-uniform torsion warping, this can be considered here as the derivation of the second torsion warping mode, however in many cases this is not sufficient to represent accurately the stress distribution over the beam cross-section.

This paper presents a new kinematics for beams, that describe the out of plane displacements in the case of a non-uniform warping of a non-symmetric section. This is achieved with using "warping functions" defined on the beam cross section. The warping functions are determined iteratively using equilibrium equations along the beam, leading to partials derivatives problems. This can be considered as a generalization of the work of Sapountzakis and Mokos [2,3], where a secondary shear stress is considered, obtained by the equilibrium of the normal stress due to the non-uniform warping. In the present work this secondary shear stress would represent the second warping mode. The idea is therefore to go further, considering that this secondary shear stress will induce a new warping mode with its associated normal stresses, that can be at its turn equilibrated, inducing a third shear stress corresponding to the third warping mode, etc. Iterative equilibrium scheme is continued until a sufficient number of mode is obtained to represent accurately the non-uniform warping effects.

In the second part of this work, the variational principle is used to determine the equilibrium equations, containing the new terms introduced by the warping. Analytical resolution of these equations will lead to results that are completely mesh-independent, and avoid shear locking problem in finite element formulation. The main difficulty to perform the exact solution of equilibrium equations is that the number of unknowns and thus of equations, depend on the number of the warping mode used. The size of the stiffness matrix will be then variable, equal to $12 + 2n$, with n the number of warping modes.

* Corresponding author. Tel.: +33 182516209; fax: +33 619326432.
E-mail address: mohammed-khalil.ferradi@tpi.setec.fr (M.K. Ferradi).

0141-0296/$ - see front matter © 2012 Elsevier Ltd. All rights reserved.
http://dx.doi.org/10.1016/j.engstruct.2012.07.038

Finally, the results are presented for different examples of beams, that will be compared to those obtained using a four noded shell elements (MITC-4) model of the beam.

2. Determination of the warping functions

The beam is described on (x,y,z) axis system, x being the longitudinal axis, and y and z principle inertia axes, centered in the gravity center.

u_q, v_q, w_q are the displacements of a material point q along x,y,z axes.

Where in Fig. 1, A is the cross section area and $\Gamma = \bigcup_{0\leqslant i}\Gamma_i$ the border of the section.

We assume the following displacement field of the beam:

$$u_q(x,y,z) = u(x) - y\theta_z(x) + z\theta_y(x) + \sum_{i=1}^{n}\Omega_i\xi_i(x) \tag{1}$$

$$v_q(x,y,z) = v(x) - z\theta_x(x) \tag{2}$$

$$w_q(x,y,z) = w(x) + y\theta_x(x) \tag{3}$$

where Ω_i are the functions of the warping modes, and ξ_i the generalized coordinate associated to each mode.

Thus the resulting stress field for an homogenous cross section:

$$\sigma = E\left(\frac{du}{dx} - y\frac{d\theta_z}{dx} + z\frac{d\theta_y}{dx} + \sum_{i=1}^{n}\Omega_i\frac{d\xi_i}{dx}\right) \tag{4}$$

$$\tau_{xy} = G\left(\frac{dv}{dx} - \theta_z - z\frac{d\theta_x}{dx} + \sum_{i=1}^{n}\frac{\partial\Omega_i}{\partial y}\xi_i\right) \tag{5}$$

$$\tau_{xz} = G\left(\frac{dw}{dx} + \theta_y + y\frac{d\theta_x}{dx} + \sum_{i=1}^{n}\frac{\partial\Omega_i}{\partial z}\xi_i\right) \tag{6}$$

where E and G are respectively the elasticity and shear modulus.

The following sections will present in details the derivation of the different warping modes, characterized by their Ω functions.

2.1. 1st Modes determination

For the derivation of 1st warping modes, it is necessary to distinguish between those due to shear, and the one related to torsion. This modes correspond to the Saint-Venant warping functions [9].

Let us start with the 1st warping mode for a shear force along y.

In the case where the beam is submitted to a uniform warping along the beam, due only to a bending in the xy plane, ξ will be constant and we take it equal to 1.

The displacement field becomes:

$$u_q = -y\theta_z(x) + \Omega_{1y} \tag{7}$$

$$v_q = v(x) \tag{8}$$

$$w_q = 0 \tag{9}$$

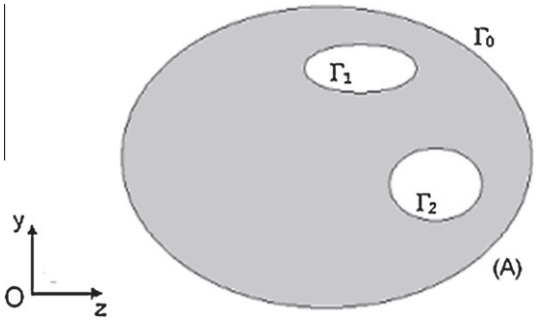

Fig. 1. Cross section of the beam.

Thus the resulting stress field:

$$\sigma = -E\frac{d\theta_z}{dx}y \tag{10}$$

$$\tau_{xy} = G\left(\frac{dv}{dx} - \theta_z + \frac{\partial\Omega_{1y}}{\partial y}\right) \tag{11}$$

$$\tau_{xz} = G\frac{\partial\Omega_{1y}}{\partial z} \tag{12}$$

Assuming no body forces, the equilibrium equation is written as:

$$\frac{\partial\sigma}{\partial x} + \frac{\partial\tau_{xy}}{\partial y} + \frac{\partial\tau_{xz}}{\partial z} = 0 \tag{13}$$

Substituting the stresses with their expressions, it comes:

$$\Delta\Omega_{1y} = \frac{T_y}{GI_z}y \tag{14}$$

With $\Delta = \partial^2/\partial y^2 + \partial^2/\partial z^2$ is the Laplace operator, I_z the moment of inertia and T_y the shear force along y.

The warping must not generate either normal force nor bending moment, which leads to the following orthogonalization equations:

$$\int_A \Omega_{1y}\,dA = 0 \tag{15}$$

$$\int_A y\Omega_{1y}\,dA = 0 \tag{16}$$

$$\int_A z\Omega_{1y}\,dA = 0 \tag{17}$$

With these additional conditions, the solution of (14) will be unique.

Using the same method to derive the 1st warping mode for a shear effort along z, we will have to resolve the following partial derivative problem:

$$\Delta\Omega_{1z} = \frac{T_z}{GI_y}z \tag{18}$$

$$\int_A \Omega_{1z}\,dA = 0 \tag{19}$$

$$\int_A z\Omega_{1z}\,dA = 0 \tag{20}$$

$$\int_A y\Omega_{1z}\,dA = 0 \tag{21}$$

The detail for the derivation of the 1st torsion mode of the Vlassov theory is given in [5] and in [4,6,7] for thin walled section. We give here the stated problem:

$$\Delta\Omega_{1t} = 0 \quad \text{on } A \tag{22}$$

$$\frac{\partial\Omega_{1t}}{\partial n} = yn_z - zn_y \quad \text{on } \Gamma \tag{23}$$

$$\int_A \Omega_{1t}\,dA = 0 \tag{24}$$

All of this partial derivatives problems can be resolved by different methods as finite difference (FDM), finite element (FEM) or boundary element method (BEM).

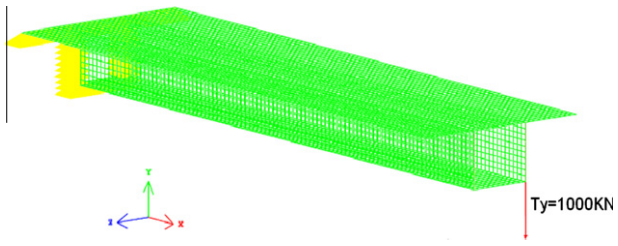

Fig. 2. Shell model of the beam with an external load $T_y = -1000$ kN.

2.2. Determination of the warping function for some modes

In the case of a non-uniform warping, the 1st modes will not be enough to describe the warping of a section, especially in the vicinity of a support section where warping is constrained. This is because the 1st warping modes are calculated by equilibrating the normal stress ($\sigma = \frac{M_z}{I_z} y - \frac{M_y}{I_y} z$ for bending) for a uniform warping (ξ= cst), but in a non uniform case we will have $\frac{d\xi}{dx} \neq 0$, which will lead to the apparition of a warping normal stress $\sigma = E\frac{d\xi}{dx}\Omega$ that are not equilibrated in Eq. (13).

Restoring equilibrium leads to the determination of a secondary shear stress associated to a 2nd warping mode. This reasoning can be considered as an iterative equilibrium schemes, converging to the exact shape of the warping in a section.

We assume that we have determined the nth warping mode, whether for shear or torsion, and we wish to determine the $n+1$th warping mode. The nth warping normal stress σ^n will be equilibrated by the $n+1$th warping shear stress:

$$\frac{\partial \sigma^n}{\partial x} + \frac{\partial \tau_{xy}^{n+1}}{\partial y} + \frac{\partial \tau_{xz}^{n+1}}{\partial z} = 0 \tag{25}$$

where

$$\sigma^n = E\frac{d\xi_n}{dx}\Omega_n; \quad \tau_{xy}^{n+1} = G\xi_{n+1}\frac{\partial \Omega_{n+1}}{\partial y}; \quad \tau_{xz}^{n+1} = G\xi_{n+1}\frac{\partial \Omega_{n+1}}{\partial z}.$$

Thus

$$E\Omega_n \frac{d^2\xi_n}{dx^2} + G\xi_{n+1}\Delta\Omega_{n+1} = 0 \tag{26}$$

The functions Ω_{n+1} and Ω_n depends only of the geometry of the cross section, whereas ξ_{n+1} and ξ_n depends of the abscissa x, so Eq. (26) implies that it necessarily exists two constants γ_{n+1} and β_{n+1}, related to the equilibrium of the beam, verifying: $\Delta\Omega_{n+1} = \gamma_{n+1}\Omega_n$; $\xi_{n+1} = \beta_{n+1}\frac{d^2\xi_n}{dx^2}$.

Our goal is to construct a base of warping functions, where any section warping can be decomposed linearly with the aid of the ξ_i coefficients, that can be seen as the participation rate of the warping modes. In practice we need only to determine the warping functions to a multiplicative constant, and the participation rate for each mode will be obtained by writing the equilibrium of the beam. Thus, only the problem $\Delta\Omega_{n+1} = \Omega_n$ has to be solved. More details on the resolution of this partial derivative problem are given in Appendix B.

Ω_{n+1} has to comply with the orthogonality conditions with respect to the n warping functions of the lower modes, this will assure the uniqueness of the function. To this aim the Gram–Scmidt orthogonalization process can be used:

$$\Omega_{n+1}^{j+1} = \Omega_{n+1}^{j+1} - \frac{\int_A \Omega_{n+1}^j \Omega_j \, dA}{\int_A \Omega_j^2 \, dA}\Omega_j \quad \text{for } j = 1, n$$

At the end of the process we have Ω_{n+1}^{n+1}, which is the researched $n+1$th orthogonalized warping function.

3. Equilibrium equations and their resolutions

3.1. Determination of the equilibrium equations

The internal virtual work may be written as:

$$\delta W_{int} = \int_V \sigma^T \delta\varepsilon \, dV \tag{27}$$

where V is beam's volume $\sigma^T = (\,\sigma_x \quad \tau_{xy} \quad \tau_{xz}\,)$ the stress vector and $\delta\varepsilon^T = (\,\delta\varepsilon_x \quad 2\delta\varepsilon_{xy} \quad 2\delta\varepsilon_{xz}\,)$ the virtual strain vector.

Using the expression of the strain in the internal virtual work:

$$\begin{aligned}\delta W_{int} = \int_V \Bigg(& \sigma_x \frac{d\delta u}{dx} - y\sigma_x \frac{d\delta\theta_z}{dx} + z\sigma_x \frac{d\delta\theta_y}{dx} + \sum_{i=1}^{n} \Omega_i \sigma_x \frac{d\delta\xi_i}{dx} \Bigg) dV \\ & + \int_V \left(\tau_{xy}\left(\frac{d\delta v}{dx} - \delta\theta_z\right) + \tau_{xz}\left(\frac{d\delta w}{dx} + \delta\theta_y\right) \right. \\ & \left. + \frac{d\delta\theta_x}{dx}(y\tau_{xz} - z\tau_{xy}) + \sum_{i=1}^{n} \delta\xi_i \left(\tau_{xy}\frac{\partial\Omega_i}{\partial y} + \tau_{xz}\frac{\partial\Omega_i}{\partial z} \right) \right) dV \end{aligned} \tag{28}$$

After integrating over the whole section, it comes:

$$\begin{aligned}\delta W_{int} = & \int_L \left(N\frac{d\delta u}{dx} + M_z\frac{d\delta\theta_z}{dx} + M_y\frac{d\delta\theta_y}{dx} + \sum_{i=1}^{n} B_i\frac{d\delta\xi_i}{dx} \right) dx \\ & + \int_L \left(T_y\left(\frac{d\delta v}{dx} - \delta\theta_z\right) + T_z\left(\frac{d\delta w}{dx} + \delta\theta_y\right) + M_x\frac{d\delta\theta_x}{dx} + \sum_{i=1}^{n}\varphi_i\delta\xi_i \right) dx \end{aligned} \tag{29}$$

where L is the beam's length.

The expressions of the generalized stresses are:

$$N = \int_A \sigma_x \, dA \tag{30}$$

$$M_z = \int_A -y\sigma_x \, dA = EI_z\frac{d\theta_z}{dx} \tag{31}$$

$$M_y = \int_A z\sigma_x \, dA = EI_y\frac{d\theta_y}{dx} \tag{32}$$

$$B_i = \int_A \Omega_i\sigma_x \, dA = E\sum_{j=1}^{n} K_{i,j}\frac{d\xi_j}{dx} \tag{33}$$

$$T_y = \int_A \tau_{xy} \, dA = G\left(\left(\frac{dv}{dx} - \theta_z\right)A + \sum_{i=1}^{n}\xi_i P_i \right) \tag{34}$$

$$T_z = \int_A \tau_{xz} \, dA = G\left(\left(\frac{dw}{dx} + \theta_y\right)A + \sum_{i=1}^{n}\xi_i Q_i \right) \tag{35}$$

$$M_x = \int_A (y\tau_{xz} - z\tau_{xy}) dA = G\left(I_0\frac{d\theta_x}{dx} + \sum_{i=1}^{n}\xi_i N_i \right) \tag{36}$$

$$\begin{aligned}\varphi_i = & \int_A \left(\tau_{xy}\frac{\partial\Omega_i}{\partial y} + \tau_{xz}\frac{\partial\Omega_i}{\partial z} \right) dA \\ = & G\left(\left(\frac{dv}{dx} - \theta_z\right)P_i + \left(\frac{dw}{dx} + \theta_y\right)Q_i + \frac{d\theta_x}{dx}N_i + \sum_{j=1}^{n}\xi_i M_{j,i} \right) \end{aligned} \tag{37}$$

where $I_0 = I_y + I_z$ is the polar inertia, and the warping-related coefficients are:

$$K_{i,j} = \int_A \Omega_i\Omega_j \, dA; \; P_i = \int_A \frac{\partial\Omega_i}{\partial y} \, dA; \; Q_i = \int_A \frac{\partial\Omega_i}{\partial z} \, dA;$$
$$N_i = \int_A \left(y\frac{\partial\Omega_i}{\partial z} - z\frac{\partial\Omega_i}{\partial y} \right) dA; \; M_{i,j} = \int_A \nabla\Omega_i \cdot \nabla\Omega_j \, dA$$

The efforts due to warping are B_i and φ_i, respectively the bi-moment and the bi-shear, associated to the ith warping mode.

After an integration by parts of the internal virtual work in Eq. (29), one obtains:

$$\begin{aligned}\delta W_{int} = & \int_L \left(\frac{dN}{dx}\delta u + \left(-\frac{dM_z}{dx} - T_y\right)\delta\theta_z + \left(-\frac{dM_y}{dx} + T_z\right)\delta\theta_y \right. \\ & \left. + \sum_{i=1}^{n}\delta\xi_i\left(-\frac{dB_i}{dx} + \varphi_i\right) + \frac{dT_y}{dx}\delta v - \frac{dT_z}{dx}\delta w - \frac{dM_x}{dx}\delta\theta_x \right) d \\ & + \underbrace{\left[N\delta u + T_y\delta v + T_z\delta w + M_x\delta\theta_x + M_y\delta\theta_y + M_z\delta\theta_z + \sum_{i=1}^{n} B_i\delta\xi_i \right]_0^L}_{\delta W_{ext}} \end{aligned} \tag{38}$$

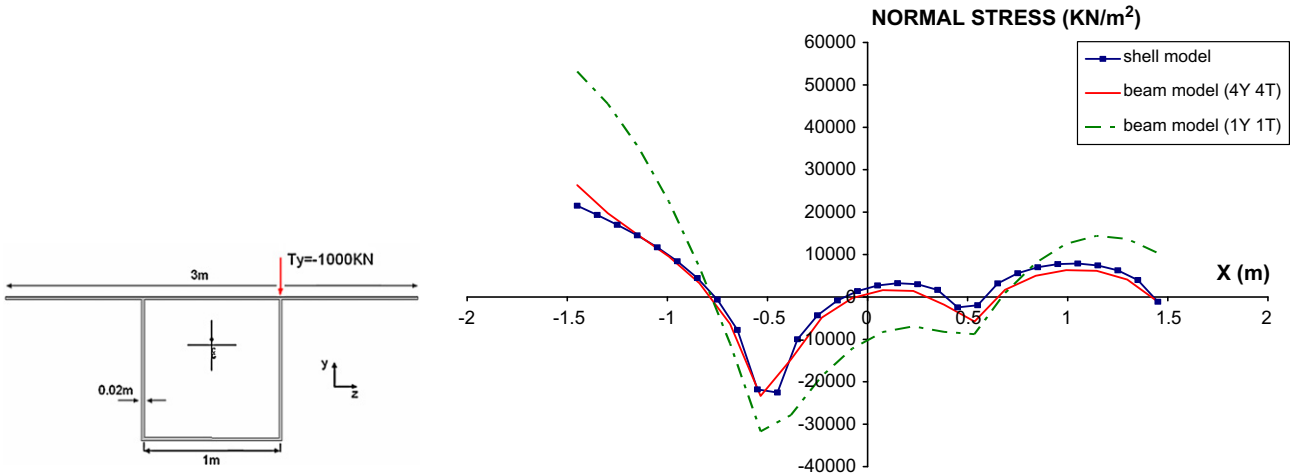

Fig. 3. Comparison of the normal stresses between the shell and the beam model, at $x = 0.05$ m and at mid-depth of the upper slab ($T_y = -1000$ kN).

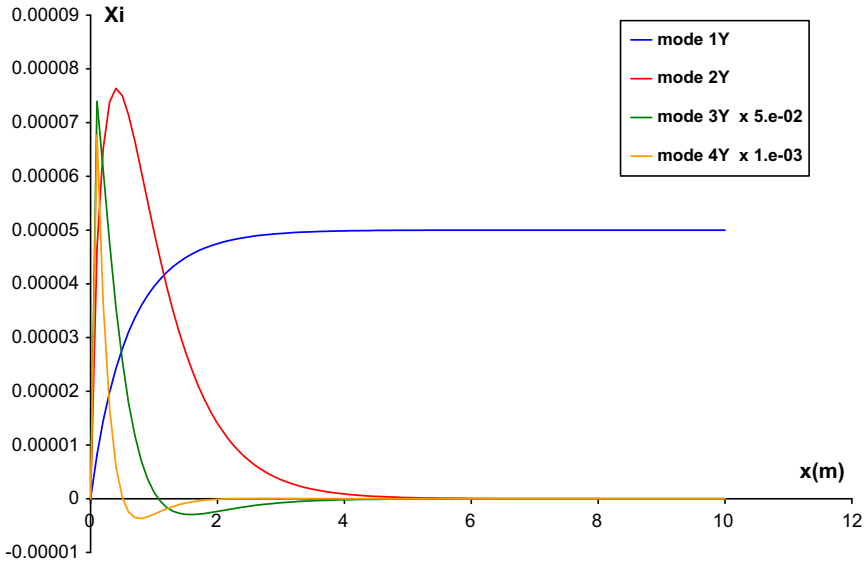

Fig. 4. Shear along y warping d.o.f. along the beam.

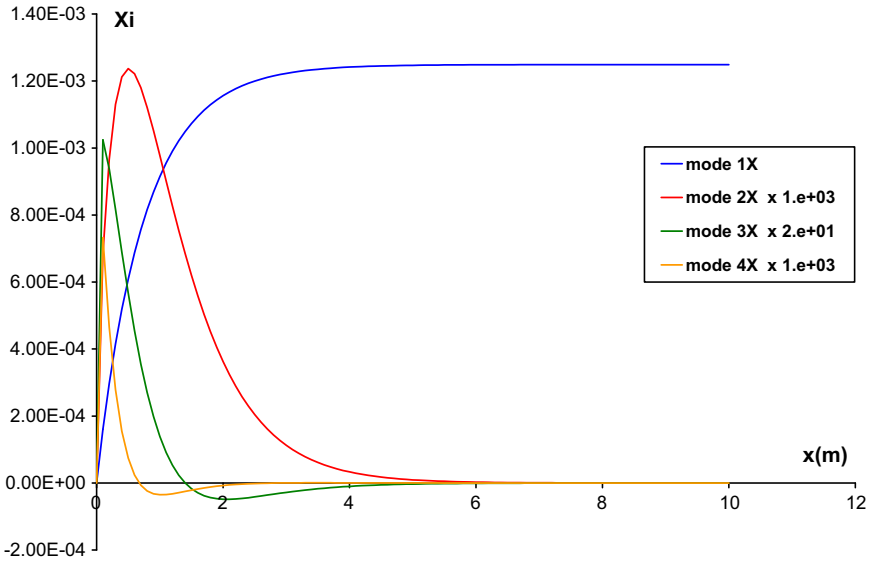

Fig. 5. Torsion warping d.o.f. along the beam.

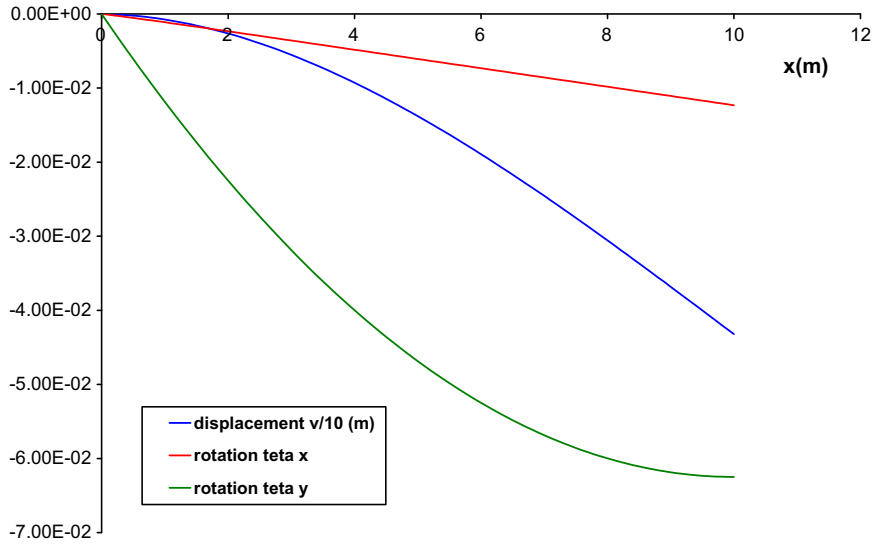

Fig. 6. Displacement and rotations of the beam.

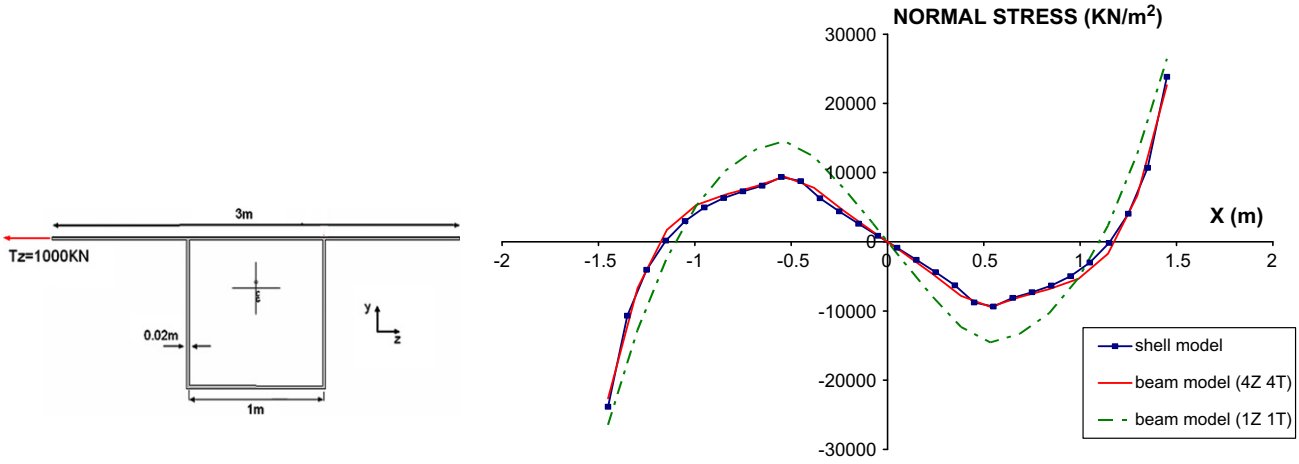

Fig. 7. Comparison of the normal stresses between the shell and the beam model, at $x = 0.05$ m and at mid-depth of the upper slab ($T_z = 1000$ kN).

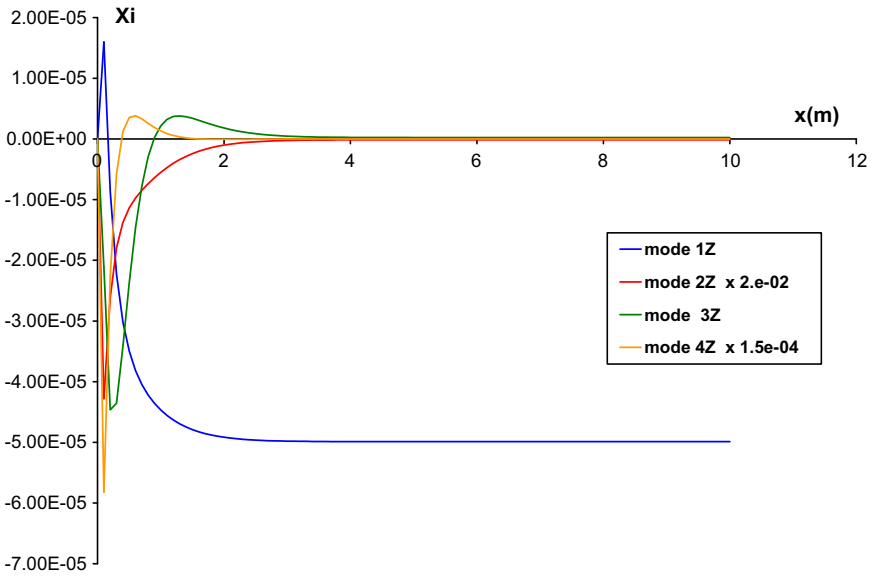

Fig. 8. Shear along z warping d.o.f. along the beam.

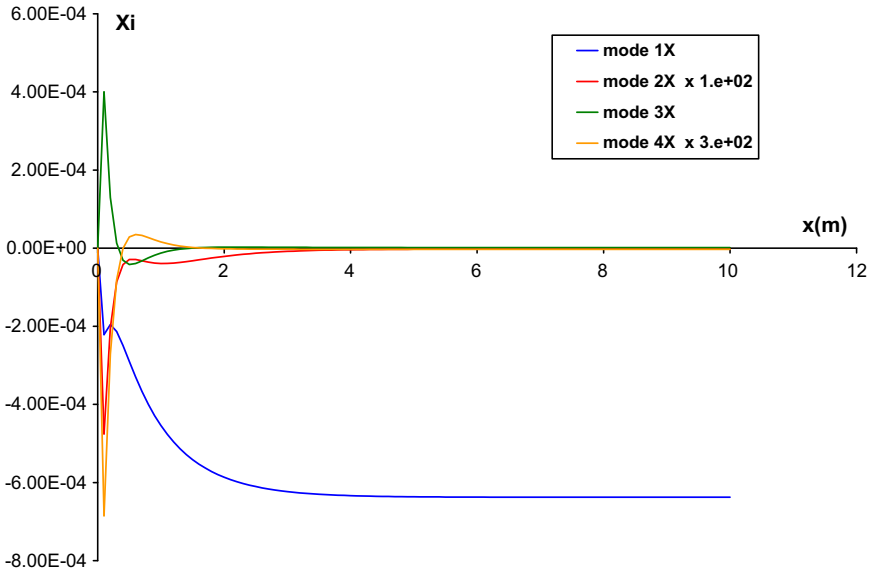

Fig. 9. Torsion warping d.o.f. along the beam.

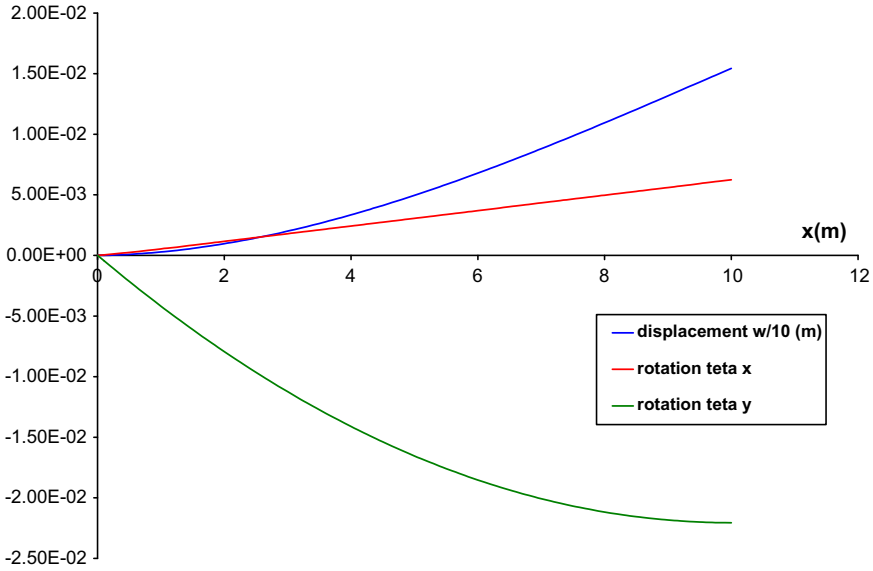

Fig. 10. Displacement and rotations of the beam.

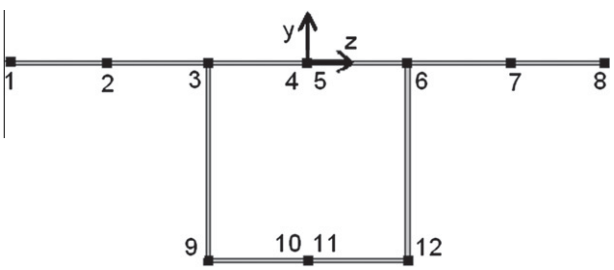

Fig. 11. Measure points in the cross section.

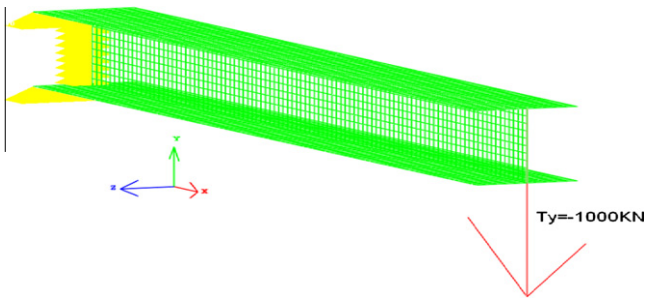

Fig. 12. Shell model of the beam with an external load $T_y = -1000$ kN.

From the principal of virtual work $\delta W_{int} - \delta W_{ext} = 0$, it comes:

$$\int_L \left(\frac{dN}{dx}\delta u + \left(-\frac{dM_z}{dx} - T_y\right)\delta\theta_z + \left(-\frac{dM_y}{dx} + T_z\right)\delta\theta_y + \sum_{i=1}^{n}\delta\xi_i\left(-\frac{dB_i}{dx} + \varphi_i\right) + \left(\frac{dT_y}{dx}\right)\delta v - \left(\frac{dT_z}{dx}\right)\delta w - \left(\frac{dM_x}{dx}\right)\delta\theta_x\right)dx = 0 \quad (39)$$

This relation is valid for any admissible virtual displacements, then all the expressions between brackets have to be zero:

$$\frac{dM_z}{dx} + T_y = 0; \quad \frac{dM_y}{dx} - T_z = 0; \quad \frac{dN}{dx} = 0; \quad \frac{dT_y}{dx} = 0;$$
$$\frac{dT_z}{dx} = 0; \quad \frac{dM_x}{dx} = 0 \quad (40)$$

$$\frac{dB_i}{dx} - \varphi_i = 0 \quad 1 \leqslant i \leqslant n \quad (41)$$

3.2. Eigenmodes of warping

From the expressions of the shear efforts and the torsion moment, we have:

$$\frac{dv}{dx} - \theta_z = \frac{T_y}{AG} - \sum_{i=1}^{n}\xi_i\frac{P_i}{A} \quad (42)$$

$$\frac{dw}{dx} + \theta_y = \frac{T_z}{AG} - \sum_{i=1}^{n}\xi_i\frac{Q_i}{A} \quad (43)$$

$$\frac{d\theta_x}{dx} = \frac{M_x}{GI_0} - \sum_{i=1}^{n}\xi_i\frac{N_i}{I_0} \quad (44)$$

After substituting in the expression of the bi-shear φ_i in Eq. (37), we obtain:

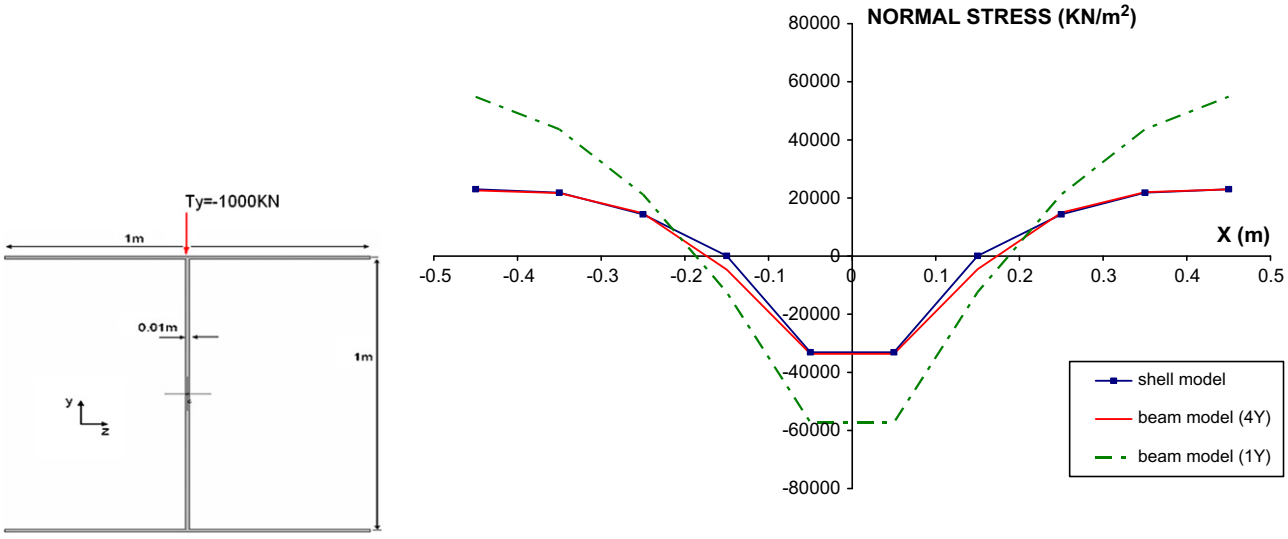

Fig. 13. Comparison of the normal stresses between the shell and the beam model, at $x = 0.05$ m and at mid-depth of the upper slab ($T_y = -1000$ kN).

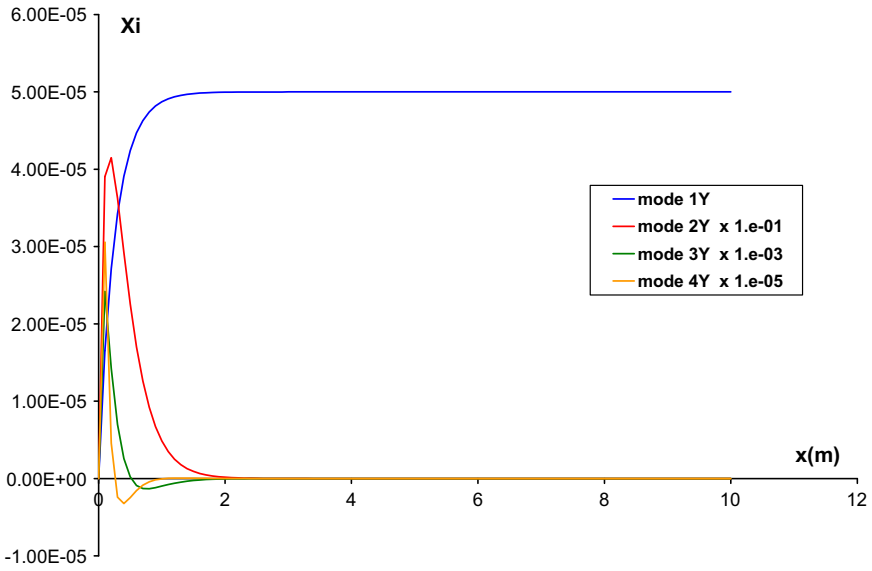

Fig. 14. Shear along y warping d.o.f. along the beam.

$$\varphi_i = \frac{P_i}{A}T_y + \frac{Q_i}{A}T_z + \frac{N_i}{I_0}M_x + G\sum_{j=1}^{n}\xi_j\left(M_{j,i} - \frac{N_iN_j}{I_0} - \frac{Q_iQ_j + P_iP_j}{A}\right) \quad (45)$$

The n equilibrium equations for warping efforts in (41), can now be re-written in a system of differential equations:

$$\begin{Bmatrix}\xi_1''\\ \vdots\\ \xi_n''\end{Bmatrix} = \frac{1}{E}\begin{bmatrix}K_{1,1} & \cdots & K_{1,n}\\ & \ddots & \vdots\\ sym. & & K_{n,n}\end{bmatrix}^{-1}\begin{bmatrix}\frac{P_1}{A} & \frac{Q_1}{A} & \frac{N_1}{I_0}\\ \vdots & \vdots & \vdots\\ \frac{P_n}{A} & \frac{Q_n}{A} & \frac{N_n}{I_0}\end{bmatrix}\begin{Bmatrix}T_y\\ T_z\\ M_x\end{Bmatrix} + \frac{G}{E}\begin{bmatrix}K_{1,1} & \cdots & K_{1,n}\\ & \ddots & \vdots\\ sym. & & K_{n,n}\end{bmatrix}^{-1} \times \begin{bmatrix}M_{1,1} - \frac{N_1^2}{I_0} - \frac{Q_1^2+P_1^2}{A} & \cdots & M_{1,n} - \frac{N_1N_n}{I_0} - \frac{Q_1Q_n+P_1P_n}{A}\\ & \ddots & \vdots\\ sym. & & M_{n,n} - \frac{N_n^2}{I_0} - \frac{Q_n^2+P_n^2}{A}\end{bmatrix} \times \begin{Bmatrix}\xi_1\\ \vdots\\ \xi_n\end{Bmatrix}$$

For what follows, we introduce some notations:

$$\{\xi\} = \begin{Bmatrix}\xi_1\\ \vdots\\ \xi_n\end{Bmatrix};\quad [K] = \begin{bmatrix}K_{1,1} & \cdots & K_{1,n}\\ & \ddots & \vdots\\ sym. & & K_{n,n}\end{bmatrix};$$

$$[P] = \frac{1}{E}[K]^{-1}\begin{bmatrix}\frac{P_1}{A} & \frac{Q_1}{A} & \frac{N_1}{I_0}\\ \vdots & \vdots & \vdots\\ \frac{P_n}{A} & \frac{Q_n}{A} & \frac{N_n}{I_0}\end{bmatrix};\quad \{f\} = \begin{Bmatrix}T_y\\ T_z\\ M_x\end{Bmatrix}$$

$$[M] = \frac{G}{E}[K]^{-1}\begin{bmatrix}M_{1,1} - \frac{N_1^2}{I_0} - \frac{Q_1^2+P_1^2}{A} & \cdots & M_{1,n} - \frac{N_1N_n}{I_0} - \frac{Q_1Q_n+P_1P_n}{A}\\ & \ddots & \vdots\\ sym. & & M_{n,n} - \frac{N_n^2}{I_0} - \frac{Q_n^2+P_n^2}{A}\end{bmatrix}$$

We note that $[K]$ is the Gramian matrix attached to the warping functions, and since all diagonal terms are strictly positive, the matrix will be then positive definite and inversible whatever number of modes considered.

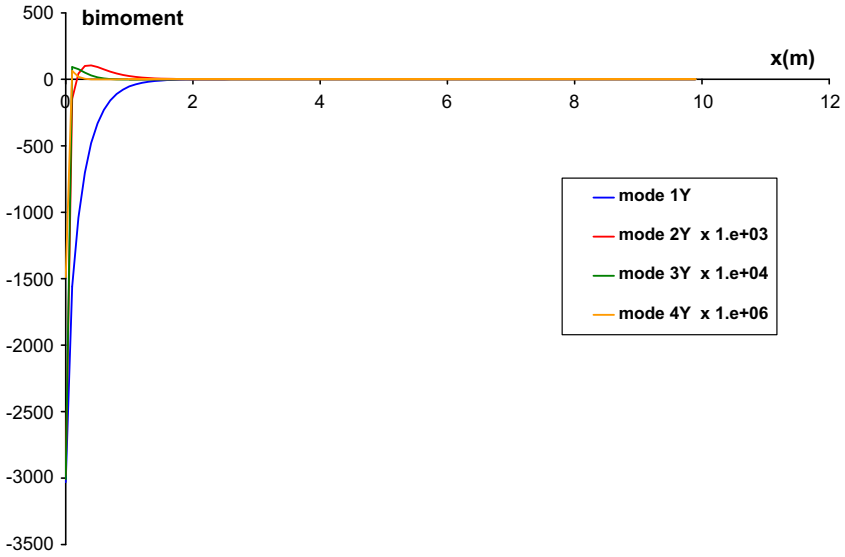

Fig. 15. Bi-moments along the beam.

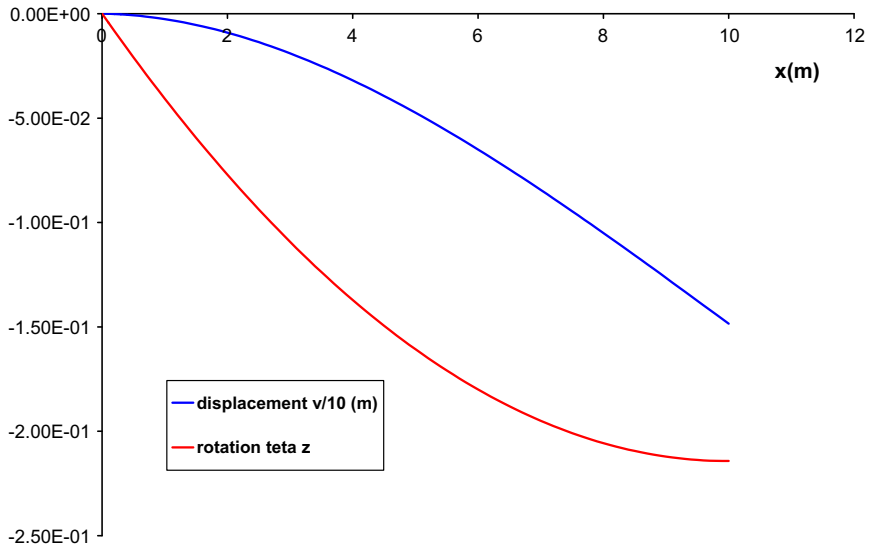

Fig. 16. Displacement and rotation of the beam.

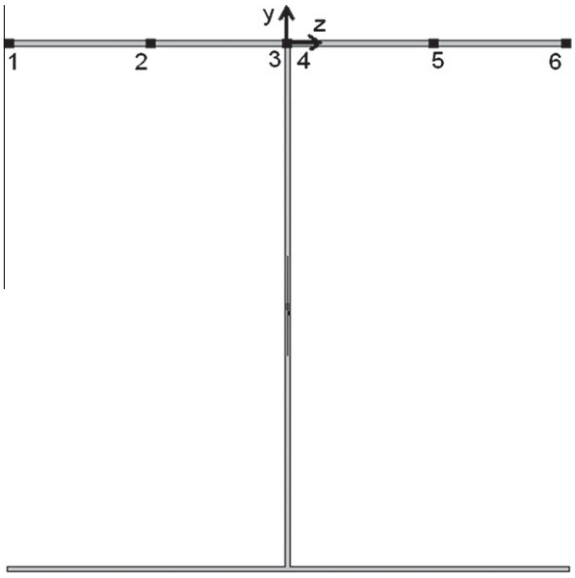

Fig. 17. Measure points in the cross section.

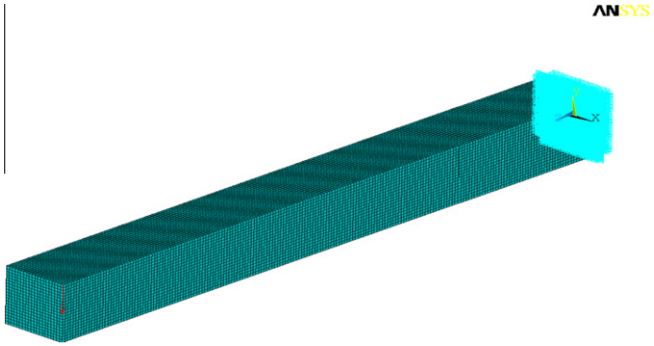

Fig. 18. Brick model of the beam with an external load $T_y = -1000$ kN.

The system of differential equations can now be written in a compact matrix form:

$$\{\xi''\} = [P]\{f\} + [M]\{\xi\} \tag{46}$$

Let: $(\lambda_i)_{1\leqslant i\leqslant n}$ represent the eigenvalues of $[M]$, and $[R]$ the corresponding eingenvectors matrix.

Writing $[\xi] = [R]\{X\}$, we have:

Table 1
Coordinate of the measure points.

	y (m)	z (m)
1	0	−1.45
2	0	−0.95
3	0	−0.45
4	0	−0.05
5	0	0.05
6	0	0.45
7	0	0.95
8	0	1.45
9	−1	−0.45
10	−1	−0.05
11	−1	0.05
12	−1	0.45

$$\begin{aligned}
&[R]\{X''\} = [P]\{f\} + [M][R]\{X\}\\
&\{X''\} = [R]^{-1}[P]\{f\} + [R]^{-1}[M][R]\{X\}\\
&\{X''\} = [R]^{-1}[P]\{f\} + [\lambda]\{X\}
\end{aligned} \tag{47}$$

where $[\lambda]$ is the diagonal matrix containing the eigenvalues.

The system being now uncoupled, it can be solved as :

$$\{X\} = \{z\} - [\lambda]^{-1}[R]^{-1}[P]\{f\} \tag{48}$$

where $z_i = A_i ch(\sqrt{\lambda_i}x) + B_i sh(\sqrt{\lambda_i}x)$ and A_i, B_i integration constants depending on the boundary conditions.

Hence, $\{\xi\}$ is obtained as :

$$\begin{aligned}
&\{\xi\} = [R]\{z\} - [R][\lambda]^{-1}[R]^{-1}[P]\{f\}\\
&\Rightarrow \{\xi\} = [R]\{z\} - \underbrace{[M]^{-1}[P]}_{[H]}\{f\}
\end{aligned} \tag{49}$$

We re-write the solution of the system under the following matrix form :

$$\{\xi\}_x = [R]([ch]_x\{A\} + [sh]_x\{B\}) - [H]\{f\} \tag{50}$$

where $[ch]_x = \begin{bmatrix} ch(\sqrt{\lambda_1}x) & & 0 \\ & \ddots & \\ 0 & & ch(\sqrt{\lambda_n}x) \end{bmatrix}$;

$[sh]_x = \begin{bmatrix} sh(\sqrt{\lambda_1}x) & & 0 \\ & \ddots & \\ 0 & & sh(\sqrt{\lambda_n}x) \end{bmatrix}$; $\{A\} = \begin{Bmatrix} A_1 \\ \vdots \\ A_n \end{Bmatrix}$; $\{B\} = \begin{Bmatrix} B_1 \\ \vdots \\ B_n \end{Bmatrix}$

We will now determine the vectors {A} and {B} in function of the boundary conditions of $\{\xi\}$:

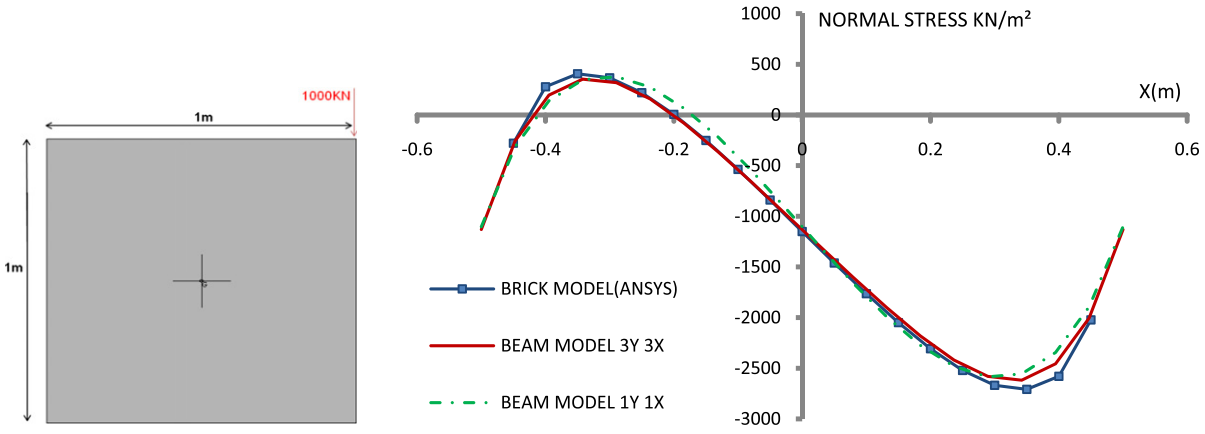

Fig. 19. Comparison of the normal stresses between the brick and the beam model, at $x = 0.05$ m and at the upper fiber of the section ($T_y = -1000$ kN).

$$\{\xi\}_0 = \{\xi_A\} \Rightarrow \{\xi_A\} = [R]\{A\} - [H]\{f\} \quad (51)$$

$$\{\xi\}_L = \{\xi_B\} \Rightarrow \{\xi_B\} = [R]([ch]_L\{A\} + [sh]_L\{B\}) - [H]\{f\} \quad (52)$$

Thus

$$\{A\} = [R]^{-1}(\{\xi_A\} + [H]\{f\}) \quad (53)$$

$$\{B\} = [sh]_L^{-1}[R]^{-1}(\{\xi_B\} + [H]\{f\}) - [th]_L^{-1}[R]^{-1}(\{\xi_A\} + [H]\{f\}) \quad (54)$$

If we note the hyperbolic matrices:

$$[H_1]_x = [R]\left([ch]_x - [sh]_x[th]_L^{-1}\right)[R]^{-1} \quad (55)$$

$$[H_2]_x = [R][sh]_x[sh]_L^{-1}[R]^{-1} \quad (56)$$

We can write $\{\xi\}$ as a function of its end values and the abscissa x in the following form:

$$\{\xi\}_x = [H_1]_x\{\xi_A\} + [H_2]_x\{\xi_B\} + ([H_1]_x + [H_2]_x - I_n)[H]\{f\} \quad (57)$$

3.3. Resolution of the equilibrium equations and determination of the stiffness matrix

In classical beam finite element formulation "arbitrary" interpolation functions are used for the displacements, and then variational principle is used to derive the stiffness matrix. The accuracy of the calculation results obtained with this formulation would be mesh dependent, especially for warping coordinates, which are of hyperbolic form, and we can also have shear locking problem for thin walled beams, due to the fact that we can not assure exactly the constraints of zero shear deformations in every position in the beam.

In the following work a different approach is used to determine the stiffness matrix. From the resolution of the equilibrium equations, we will express the $n + 6$ external generalized forces at each node of the beam, as a function of the $2n + 12$ nodal displacements. With these expressions the stiffness matrix can be assembled. Nevertheless, performing the exact solution has a major difficulty, consisting in that our stiffness matrix has a variable length, depending on the number of warping modes, but must be always derived from the exact solution of the equilibrium equations.

We write the $12 + 2n$ equations from the equilibrium Eqs. (40) and (41) :

$$\frac{dT_y}{dx} = 0 \Rightarrow T_y(x) = T_{yA} \quad \text{in } x = L:$$

$$T_{yA} = T_{yB} \quad (58)$$

$$v(L) = v_B \quad (59)$$

$$\frac{dT_z}{dx} = 0 \Rightarrow T_z(x) = T_{zA} \quad \text{in } x = L:$$

$$T_{zA} = T_{zB} \quad (60)$$

$$w(L) = w_B \quad (61)$$

$$\frac{dM_x}{dx} = 0 \Rightarrow M_x(x) = M_{xA} \quad \text{in } x = L:$$

$$M_{xB} = M_{xA} \quad (62)$$

$$\theta_x(L) = \theta_{xB} \quad (63)$$

$$\frac{dM_z}{dx} + T_y = 0 \Rightarrow M_z(x) = M_{zA} - T_{yA}\cdot x \quad \text{in } x = L: \quad (64)$$

$$M_{zB} = M_{zA} - T_{yA}L$$

$$\theta_z(x) = \theta_{zA} + \frac{M_{zA}}{EI_z}x - \frac{T_{yA}}{2EI_z}x^2 \quad \text{in } x = L: \quad (65)$$

$$\theta_{zB} = \theta_{zA} + \frac{M_{zA}}{EI_z}L - \frac{T_{yA}}{2EI_z}L^2$$

$$\frac{dM_y}{dx} - T_z = 0 \Rightarrow M_y(x) = M_{yA} + T_{zA}x \quad \text{in } x = L: \quad (66)$$

$$M_{yB} = M_{yA} + T_{zA}L$$

$$\theta_y(x) = \theta_{yA} + \frac{M_{yA}}{EI_y}x + \frac{T_{zA}}{2EI_y}x^2 \quad \text{in } x = L: \quad (67)$$

$$\theta_{yB} = \theta_{yA} + \frac{M_{yA}}{EI_y}L + \frac{T_{zA}}{2EI_y}L^2$$

$$\frac{dN}{dx} = 0 \Rightarrow N(x) = N_A \quad \text{in } x = L:$$

$$N_A = N_B \quad (68)$$

$$u(L) = u_B \quad (69)$$

And the additional $2n$ equations for the bi-moment :

$$B_i(0) = B_{iA}; \quad B_i(L) = B_{iB} \quad \text{for } 1 \leqslant i \leqslant n \quad (70)$$

We have then $2n + 12$ equations for 2n + 12 unknowns.

Eqs. (59), (61), (63), (69) and those of biforce (70), need to be developed more explicitly.

For Eq. (59) :

Table 2
Normal stress (kN/m^2) in the measure points for T_y = −1000 kN.

	Measure points											
	1	2	3	4	5	6	7	8	9	10	11	12
Shell (MITC4)	21,516	8431	−22,528	1385	2705	−2452	7737	−1136	12,777	−8483	−8361	13,505
Beam 4Y4T	26,372	7970	−22,026	220	1437	−4940	6103	−1146	7152	−9463	−8571	18,909
Beam 1Y1T	53,175	18,457	−32,755	−11,310	−8744	−9661	11,540	10,363	3144	−9404	−6977	24,986

Table 3
Normal stress (kN/m^2) in the measure points for T_z = 1000 kN.

	Measure points											
	1	2	3	4	5	6	7	8	9	10	11	12
Shell (MITC4)	−23,844	4961	8774	869	−869	−8774	−4961	23,844	−5339	−177	177	5339
Beam 4Z4T	−22,633	5859	9360	958	−965	−9361	−5855	22,640	−7579	−240	243	7581
Beam 1Y1T	−26,451	6856	14,069	1743	−1741	−14,067	−6856	26,449	−10,055	−938	939	10,056

Table 4
Coordinate of the measure points.

	y (m)	z (m)
1	0	−0.45
2	0	−0.25
3	0	−0.05
4	0	0.05
5	0	0.25
6	0	0.45

Table 5
Normal stress (kN/m^2) in the measure points for $T_y = -1000$ kN.

	Measure points					
	1	2	3	4	5	6
Shell (MITC4)	23,022	14,371	−33,110	−33,110	14,371	23,022
Beam 4Y4T	22,630	14,742	−33,668	−33,627	14,986	22,988
Beam 1Y1T	54,827	21,204	−57,258	−57,267	21,206	54,841

Table 6
Coordinate of the measure points.

	y (m)	z (m)
1	−0.5	−0.45
2	−0.5	−0.3
3	−0.5	−0.15
4	−0.5	0
5	−0.5	0.15
6	−0.5	0.3
7	−0.5	0.45

$$\begin{aligned}\frac{dv}{dx} &= \theta_z + \frac{T_y}{AG} - \sum_{i=1}^{n}\xi_i\frac{P_i}{A}\\ \frac{dv}{dx} &= \theta_{zA} + \frac{M_{zA}}{EI_z}x - \frac{T_{yA}}{2EI_z}x^2 + \frac{T_{yA}}{AG} - \frac{1}{A}\{P\}^T\{\xi\}\end{aligned} \tag{71}$$

where $\{P\}^T = \{P_1 \quad \cdots \quad P_n\}$

Integrating (71) from 0 to L:

$$\begin{aligned}&-\frac{M_{zA}}{2EI_z}L^2 + T_{yA}\left(\frac{L^3}{6EI_z} - \frac{L}{GA}\right) + \frac{2}{A}\{P\}^T[T_1][H]\{f\} - \frac{L}{A}\{P\}^T[H]\{f\}\\ &= v_A - v_B + \theta_{zA}L + \frac{1}{A}\{P\}^T[T_1](\{\xi_A\} + \{\xi_B\})\end{aligned} \tag{72}$$

With: $[T_1] = \int_0^L [H_1]_x\,dx = \int_0^L [H_2]_x\,dx = [R]\left[\frac{1}{\sqrt{\lambda_i}}g(\sqrt{\lambda_i}L)\delta_{ij}\right]_{1\leqslant i,j\leqslant n}[R]^{-1}$

and $g(x) = \frac{1}{th(x)} - \frac{1}{sh(x)}$

The same method is applied for Eqs. (61) and (63), leading to the following equations:

$$\begin{aligned}&\frac{M_{yA}}{2EI_y}L^2 + T_{zA}\left(\frac{L^3}{6EI_y} - \frac{L}{GA}\right) + \frac{2}{A}\{Q\}^T[T_1][H]\{f\} - \frac{L}{A}\{Q\}^T[H]\{f\}\\ &= w_A - w_B - \theta_{yA}L + \frac{1}{A}\{Q\}^T[T_1](\{\xi_A\} + \{\xi_B\})\end{aligned} \tag{73}$$

$$\begin{aligned}&-\frac{M_{xA}L}{GI_0} + \frac{2}{I_0}\{N\}^T[T_1][H]\{f\} - \frac{L}{I_0}\{N\}^T[H]\{f\}\\ &= \theta_{xA} - \theta_{xB} + \frac{1}{I_0}\{N\}^T[T_1](\{\xi_A\} + \{\xi_B\})\end{aligned} \tag{74}$$

where $\{Q\}^T = \{Q_1 \quad \cdots \quad Q_n\}$; $\{N\}^T = \{N_1 \quad \cdots \quad N_n\}$.

For the $2n$ equations in (70), related to bi-moment:

$$\{B(0)\} = \{B_A\} \quad \Rightarrow E[K]\{\xi'\}_0 = \{B_A\} \tag{75}$$

$$\{B(L)\} = \{B_B\} \quad \Rightarrow E[K]\{\xi'\}_L = \{B_B\} \tag{76}$$

From the expression of $\{\xi\}$ it comes :

$$\{\xi'\}_0 = [T_2]\{\xi_A\} + [T_3]\{\xi_B\} + ([T_2] + [T_3])[H]\{f\} \tag{77}$$

$$\{\xi'\}_L = -[T_3]\{\xi_A\} - [T_2]\{\xi_B\} - ([T_2] + [T_3])[H]\{f\} \tag{78}$$

where

$$\begin{aligned}[T_2] &= \left(\frac{d}{dx}[H_1]_x\right)_{x=0} = -\left(\frac{d}{dx}[H_2]_x\right)_{x=L}\\ &= [R][\sqrt{\lambda_i}h(\sqrt{\lambda_i}L)\delta_{ij}]_{1\leqslant i,j\leqslant n}[R]^{-1} \quad \text{and } h(x) = \frac{-1}{th(x)}\\ [T_3] &= \left(\frac{d}{dx}[H_2]_x\right)_{x=0} = -\left(\frac{d}{dx}[H_1]_x\right)_{x=L}\\ &= [R][\sqrt{\lambda_i}t(\sqrt{\lambda_i}L)\delta_{ij}]_{1\leqslant i,j\leqslant n}[R]^{-1} \quad \text{and } t(x) = \frac{1}{sh(x)}\end{aligned}$$

Thus we write:

$$\{B_A\} - E[K]([T_2] + [T_3])[H]\{f\} = [T_2]\{\xi_A\} + [T_3]\{\xi_B\} \tag{79}$$

$$\{B_B\} + E[K]([T_2] + [T_3])[H]\{f\} = -[T_3]\{\xi_A\} - [T_2]\{\xi_B\} \tag{80}$$

And finally for Eq. (69):

$$\frac{du}{dx} = \frac{N_A}{EA} \Rightarrow \frac{N_A}{EA}L = u_B - u_A \tag{81}$$

By assembling all of the $2n + 12$ equations, we obtain the following system:

$$[K_F]\{\Psi\} = [K_D]\{d\} \tag{82}$$

where {d} and $\{\Psi\}$ represent, respectively, the displacements and the generalized efforts vector.

We deduce the stiffness matrix $[K_S]$:

$$[K_S] = [K_F]^{-1}[K_D] \tag{83}$$

4. Numerical examples

Three examples are presented below, all being a 10 m-length cantilever beam, Young's modulus $E = 40$ GPa, Poisson's ration $\upsilon = 0$, but with different cross sections. The comparisons will be performed with a finite element model of the cantilever beam using MITC 4 noded shell elements, described in [10], for thin walled profiles, and with brick elements (SOLID186 in Ansys, 20 nodes non-layered structural solid) for the thick walled profile. In exception of the beam model with brick elements, all the comparisons have been performed with Pythagore Software.

Table 7
Normal stress (kN/m^2) in the measure points for $T_y = -1000$ kN.

	Measure points						
	1	2	3	4	5	6	7
Brick (ANSYS)	−279.049	367.0382	−251.6	−1150.67	−2049.74	−2668.38	−2022.29
Beam 3Y3X	−288.801	337.883	−257.383	−1131.33	−2000.44	−2600.65	−1971.92
Beam 1Y1X	−343.017	384.433	−108.373	−1103.42	−2095.53	−2591.74	−1862.76

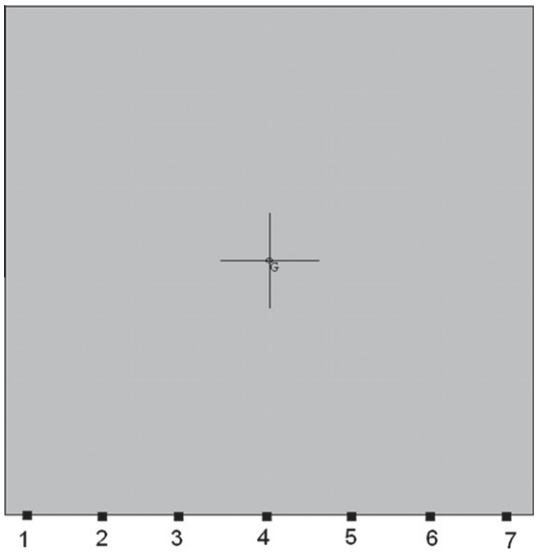

Fig. 20. Measure points in the cross section.

We only compare the normal stress due to warping:

- On the shell or brick finite element model, warping normal stress is obtained by deducing an assumed linear stress state from the actual calculated stress.
- On the beam model, we use the stress calculated by $\sigma = E \sum \Omega_i \frac{d\xi_i}{dx}$.

The boundary conditions of the beam model for this example are:

- Restrained warping at the beam's bearing: $\xi_i = 0$
- No warping restraining at the free end: $\frac{d\xi_i}{dx} = 0$

The comparison of the normal stresses between the different models is carried out at $x = 0.05$ m from the fixed end, sufficiently far from load application point to respect the Saint-Venant principle, and where the restrained-warping effect is important. The higher eigenmodes of warping will not be neglectable and so we can see their effects on the normal stress.

For the following examples, we will mean by 'beam model(*iY jZ kT*)', a model with beam finite element with *i*-warping modes of shear along *y*, *j*-warping modes of shear along *z* and *k*-warping modes of torsion.

4.1. Box girder

The comparison of the normal stresses in the section will be carried out at mid-thickness of the upper slab.

From Figs. 4 and 5, we can clearly see that the effect of the higher warping modes will be non negligible in the fixed end, and disappear when we moves away from it. If we have used interpolation functions, it will have been necessary to use a refined meshing near the fixed end, to obtain the higher order mode with precision, this shows the advantage of using an exact solution of the equilibrium equations to construct the stiffness matrix.

4.2. I-beam

See Figs. 12–17.

4.3. Thick walled section

In Fig. 2, 12 and 18 we illustrate the shell and brick model and the position of the load vector, these models are used for comparison with our beam model. In Figs. 4–6, 8–10, and 14–16 we illustrate the resulting distribution of the displacement, the rotation and the generalized coordinate of the warping mode in the beam length.

5. Conclusion

A new beam element has been derived, allowing an accurate representation of the restrained warping effect. It can be used for shear lag representation or restrained torsion. We note that all the stresses measures performed in the numerical examples and represented in Figs. 3, 7, 13 and 19, were done in the vicinity of the support section at $x = L/200$, the results shows that we can not neglect the effect of the higher warping modes, if we want to obtain an accurate description of warping.

The number of additional d.o.f. is user-determined. The element has shown very precise results with four warping parameters at each node, for torsion and for each shear direction – total 24 additional d.o.f. on the element. The numerical results are presented in Tables 2, 3, 5 and 7, giving the value of the normal stress in different measure points, which coordinates and position are given in Table 1, Table 4 and Table 6 and Figs. 11, 17 and 20.

Longitudinal interpolation is exact for linear-elastic behavior, so that the results are totally mesh-independent. This important feature allows the use of this new element with coarse discretization, in a similar way as Euler–Bernoulli traditional elements.

The formulation used here can be generalized easily to anisotropic materials, the main difference will be in the derivation of the warping functions.

Appendix A

We give here some examples of warping modes for different section.

A.1. Rectangular section

Figs. A.1, A.2, A.3, A.4, A.5, A.6 and A.7.

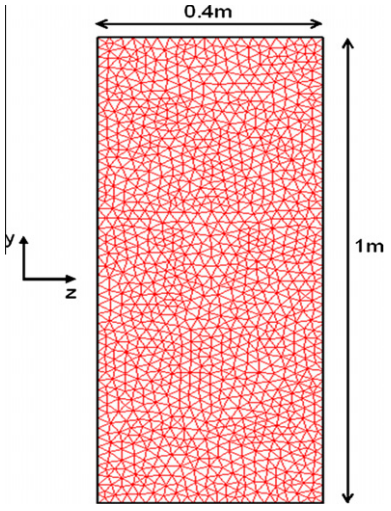

Fig. A.1. Section mesh, 2164 triangular elements and 1151 nodes.

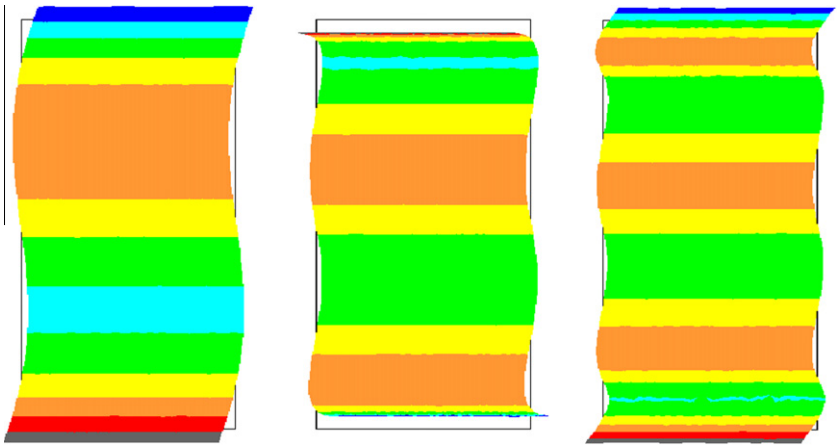

Fig. A.2. 3 first warping modes of shear along y.

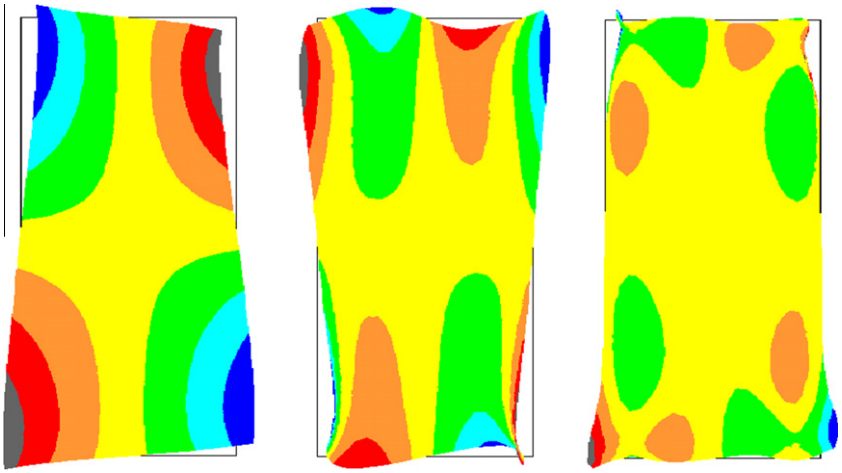

Fig. A.3. 3 first warping modes of torsion.

Appendix B

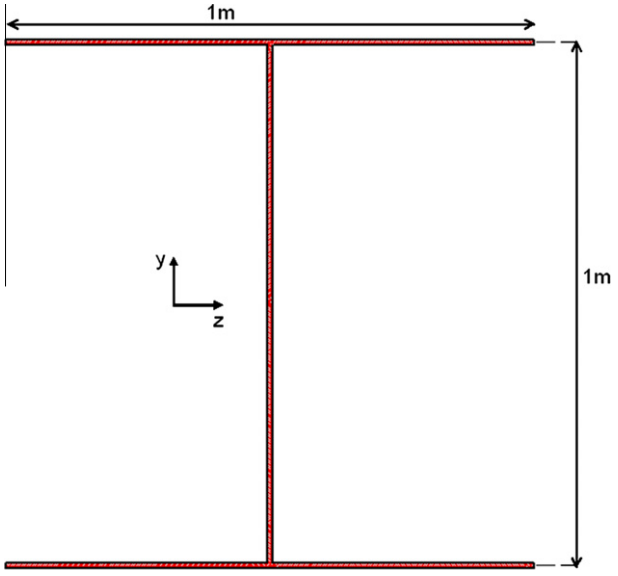

Fig. A.4. Section mesh, 2384 triangular elements and 1788 nodes.

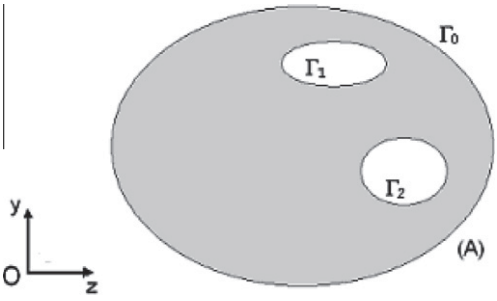

We will detail in this section a method detailed in [11] to solve the partial derivative problem, that we name SF, of the type:

$$\Delta\Omega_{n+1} = \Omega_n \text{ on } A \tag{a.1}$$

$$\frac{\partial\Omega_{n+1}}{\partial n} = t_n \quad \text{on } \Gamma \tag{a.2}$$

$$\Omega_{n+1} = 0 \text{ in a section point} \tag{a.3}$$

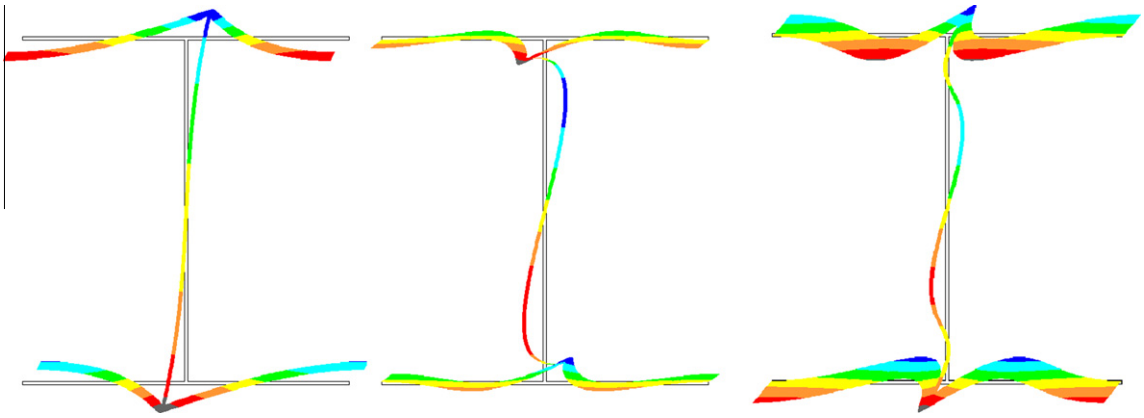

Fig. A.5. 3 first warping modes of shear along *y*.

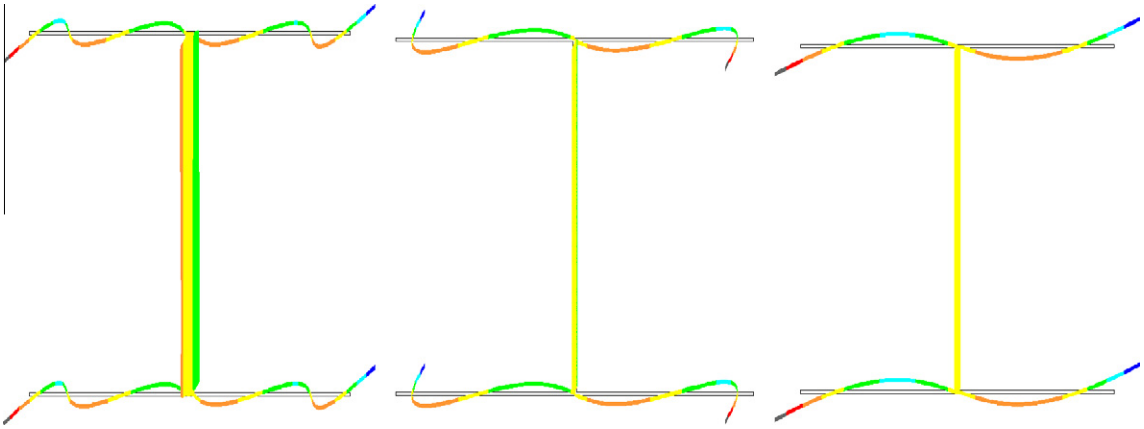

Fig. A.6. 3 first warping modes of shear along *z*.

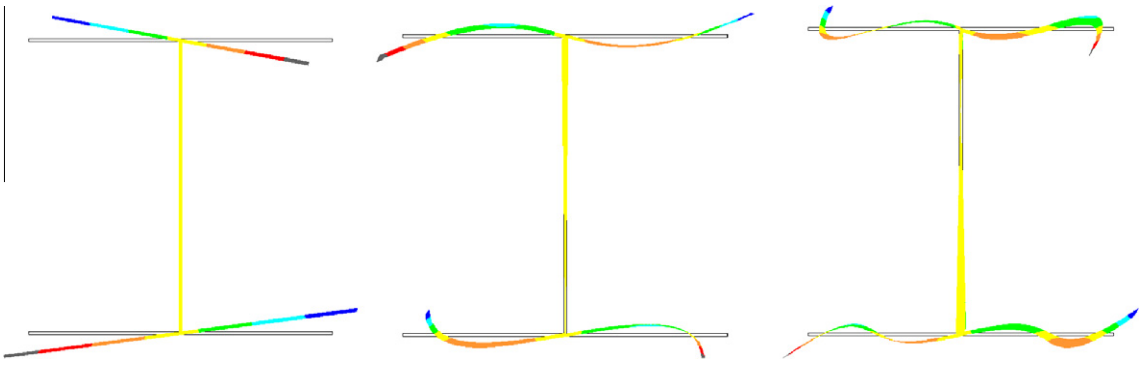

Fig. A.7. 3 first warping modes of torsion.

Let Ω_{n+1} be a solution of SF, and $f \in C^1$ a continious and a derivable real function. We can write then:

$$\int_A (\Delta\Omega_{n+1} - \Omega_n) f \, dA = 0 \tag{a.4}$$

We use the Green identity to obtain:

$$\int_A (\Delta\Omega_{n+1} - \Omega_n) f \, dA = -\int_A \Omega_n f dA - \int_A \nabla\Omega_{n+1} \cdot \nabla f \, dA + \int_\Gamma f \nabla\Omega \cdot n \, d\Gamma = 0 \tag{a.5}$$

Where n is the normal vector at a boundary point, ∇ the gradient operator, and $\cdot$ the dot product.

Using the boundary condition (a.2), we can write the weak form, WF, of the problem SF:

$$\int_A \nabla\Omega_{n+1} \cdot \nabla f \, dA = -\int_A \Omega_n f \, dA - \int_\Gamma f t_n \, d\Gamma \tag{a.6}$$

Thus we have demonstrated that if Ω_{n+1} is a solution of SF, then (a.6) is verified for every $f \in C^1$. We can easily demonstrate the inverse implication.

To solve the weak form WF of the problem, our cross section will be discretized into triangular element, where we suppose that Ω_{n+1} vary linearly. In a triangular element, the warping Ω^p_{n+1} in a point p, will be written in function of the warping Ω^i_{n+1} at the triangle vertices, by using linear shape functions N^p_i :

$$\Omega^p_{n+1} \approx \sum_{i=1}^{3} N^p_i \Omega^i_{n+1} \tag{a.7}$$

We note for the following $a(f,g) = \int_A \nabla f \cdot \nabla g \, dA$ and $(f,g) = \int_A fg \, dA$, two symmetric and bilinear forms. We replace (a.7) into (a.6) to obtain:

$$\begin{aligned} &a(\Omega_{n+1}, f) = -(\Omega_n, f) \\ &a\left(\sum N_i \Omega^i_{n+1}, \sum N_i f_i\right) = -(\Omega_n, \sum N_i f_i) \\ &\sum_i \left(\sum_j a(N_i, N_j)\Omega^j_{n+1}\right) f_i = -\sum_i (\Omega_n, N_i) f_i \end{aligned} \tag{a.8}$$

The relation (a.8) is verified for every f, thus:

$$\sum_j a(N_i, N_j)\Omega^j_{n+1} = -(\Omega_n, N_i) \quad \text{for } 1 \leqslant i \leqslant 3 \tag{a.9}$$

This equations can be written in a matrix form:

$$\begin{bmatrix} a(N_1,N_1) & a(N_1,N_2) & a(N_1,N_3) \\ & a(N_2,N_2) & a(N_2,N_3) \\ sym & & a(N_3,N_3) \end{bmatrix} \begin{Bmatrix} \Omega^1_{n+1} \\ \Omega^2_{n+1} \\ \Omega^3_{n+1} \end{Bmatrix} = -\begin{Bmatrix} (N_1,\Omega_n) \\ (N_2,\Omega_n) \\ (N_3,\Omega_n) \end{Bmatrix}$$

For a linear element Γ_i in the border of the section:

$$\begin{aligned} &f \approx M_1 f_1 + M_2 f_2 \\ &\int_{\Gamma_i} f t_n \, d\Gamma_i \approx \int_{\Gamma_i} t_n (M_1 f_1 + M_2 f_2) d\Gamma_i = [M_1, t_n] f_1 + [M_2, t_n] f_2 \end{aligned} \tag{a.10}$$

where $[f,g] = \int_\Gamma fg \, d\Gamma$.

To calculate the integrals $a(N_i,N_j)$, (N_i,Ω_n) and $[M_i,t_n]$, we can use a numerical integration method, such as the gaussian quadrature. After assembling Eqs. (a.9) and (a.10) for all the triangular elements and the border of the section mesh, we obtain an equation system, which solution gives the warping value at each node. This warping map is not yet the one desired, we have to perform the Gram–Schmidt orthogonalization process, to finally obtain the $n+1$th warping mode.

References

[1] Bauchau OA. A beam theory for anisotropic materials. J Appl Mech 1985;52:416–22.
[2] Sapountzakis EJ, Mokos VG. Warping shear stresses in nonuniform torsion by BEM. Comput Mech 2003;30:131–42.
[3] Sapountzakis EJ, Mokos VG. 3-D beam element of variable composite cross section including warping effect. ECCOMAS, 2004.
[4] Calgaro JA. Projet et construction des ponts : Analyse structurale des tabliers de ponts. Presses de l'Ecole Nationale des Ponts et Chaussées, 1994.
[5] Frey F. Analyse des structures et milieux continus: Mécanique des solides. Editions de l'Ecole Polytechnique de Lausanne, 1998.
[6] Saadé K. Finite element modelling of shear in thin walled beams with a single warping functions. Ph.D thesis of Université Libre de Bruxelles, 2004.
[7] Vlassov VZ. Pieces longues en voiles minces. Paris: Eyrolles; 1962.
[8] Fauchart J. Exemples d'étude de tabliers de ponts courants en béton précontraint, coulés sur cintre. Annales de l'Institut Technique du Bâtiment et des Travaux Publics, no. 245, 1968.
[9] El Fatmi R. Non-uniform warping including the effects of torsion and shear forces. Part I: A general beam theory. Int J Solids Struct 2007;44:5912–29.
[10] Bathe K-J. Finite element procedures. Englewood Cliffs (NJ): Prentice-Hall; 1996.
[11] Hughes TJR. The finite element method: linear static and dynamic finite element analysis. Dover Publications; 2000.

Computers and Structures 131 (2014) 12–33

Contents lists available at ScienceDirect

Computers and Structures

journal homepage: www.elsevier.com/locate/compstruc

A new beam element with transversal and warping eigenmodes

Mohammed Khalil Ferradi *, Xavier Cespedes

Pythagore R&D, SETEC-TPI, 42-52 Quai de la Rapée, 75012 Paris, France

ARTICLE INFO

Article history:
Received 11 March 2013
Accepted 2 October 2013

Keywords:
Distortion
Warping
Higher order beam element
Mesh-free element
Gyroscopic system

ABSTRACT

In this work, we present a new formulation of a 3D beam element, with a new method to describe the transversal deformation of the beam cross section and its warping. With this new method we use an enriched kinematics, allowing us to overcome the classical assumptions in beam theory, which states that the plane section remains plane after deformation and the cross section is infinitely rigid in its own plane. The transversal deformation modes are determined by decomposing the cross section into 1D elements for thin walled profiles and triangular elements for arbitrary sections, and assembling its rigidity matrix from which we extracts the Eigen-pairs. For each transversal deformation mode, we determine the corresponding warping modes by using an iterative equilibrium scheme. The additional degree of freedom in the enriched kinematics will give rise to new equilibrium equations, these have the same form as for a gyroscopic system in an unstable state, these equations will be solved exactly, leading to the formulation of a mesh free element. The results obtained from this new beam finite element are compared with the ones obtained with a shell model of the beam.

1. Introduction

The classical beam theories are all based on some hypothesis that are sufficient in most cases for structure analysis, but fail in more complex cases to give accurate results and can lead to non-negligible errors. For Timoshenko beam theory, widely used by structural engineers, two assumptions are made, the cross section remains plane after deformation and every section is infinitely rigid in its own plane, this means that the effects of warping shear lag and transversal deformation are neglected, these phenomenon are important in bridge study, especially when dealing with bridge with small width/span ratio, and with thin walled cross section.

The problem of introducing the warping effect into beam theory has been widely treated. The most classical approach is to introduce extra generalized coordinates, associated with the warping functions calculated from the Saint–Venant solution, which is exact for the uniform warping of a beam, but gives poor results in the inverse case, especially near the perturbation where the warping is restrained. Bauchau [1], proposes an approach that consists in improving the Saint–Venant solution, that considers only the warping modes for a uniform warping, by adding new eigenwarping modes, derived from the principle of minimum potential energy. Sapountzakis and Mokos [2,3] calculate a secondary shear stress, due to a non-uniform torsion warping, this can be considered as the derivation of the second torsion warping mode in the work of Ferradi et al. [4], where a more general formulation is given, based on a kinematics with multiple warping eigenmodes, obtained by considering an iterative equilibrium scheme, where at each iteration, equilibrating the residual warping normal stress will lead to the determination of the next mode, this method has given very accurate results, even in the vicinity of a fixed end where the condition of no warping is imposed.

The aim of this paper is to propose a new formulation, which not only takes into account the warping of the cross section, but also its transversal deformation, an element of this type falls in the category of GBT (generalized beam theory), which is essentially used to study elastic buckling of thin walled beam and cold formed steel members [5,6], this is done by enriching the beam's kinematics with transversal deformation modes, and then determining the contribution of every modes to the vibration of the beam. In the formulation developed by Ferradi et al. [4], a series of warping functions are determined, associated to the three rigid body motions of horizontal and vertical displacements and torsion, which can be considered as the three first transversal deformation modes. The main idea of this article is to go beyond these three first modes, and determine a series of new transversal deformation modes, calculated for an arbitrary cross section, by modeling this section with triangular or/and 1D element, assembling its rigidity matrix and extracting the eigenvalues and the corresponding eigenvectors, for a desired number of modes. Then, for each determined mode, we will derive a series of warping functions, noting that we will need at least one to represent exactly the case of uniform warping in the beam. With all these additional transversal and warping modes, we will obtain

* Corresponding author.
E-mail address: mohammed-khalil.ferradi@tpi.setec.fr (M.K. Ferradi).

0045-7949/$ - see front matter © 2013 Elsevier Ltd. All rights reserved.
http://dx.doi.org/10.1016/j.compstruc.2013.10.001

an enhanced kinematics, capable of describing accurately, arbitrary displacement and stress distribution in the beam. Using the principal of virtual work we will derive the new equilibrium equations, which appear to have the same form as the dynamical equations of a gyroscopic system in an unstable state. Unlike classical finite element formulation, where interpolation functions are used for the generalized coordinates, we will perform for this formulation, as in [4], an exact solution for the arising differential equations system, leading to the formulation of a completely mesh free element.

The results obtained from the beam element will be compared to those obtained from a shell (MITC-4) and a brick (SOLID186 in Ansys™) model of the beam. Different examples are presented to illustrate the efficiency and the accuracy of this formulation.

2. Determination of transversal deformation modes

For an arbitrary beam cross section, composed of multiple contours and thin walled profiles, to calculate the transversal deformation mode, we use a mesh with triangular elements for the 2D domain delimited by some contours and beam element for the thin walled profiles. As for a classical structure with beam and shell elements, we assemble the rigidity matrix $\boldsymbol{K_s}$ for the section, by associating to each triangular and beam element a rigidity matrix (see Appendix A.1) calculated for a given thickness. We calculate the eigenvalues and their associated eigenvectors of the assembled rigidity matrix of the section, by solving the standard eigenvalue problem (SEP):

$$\boldsymbol{K}_s\boldsymbol{v} = \lambda\boldsymbol{v} \tag{1a}$$

We note that for all that will follow, if it's written in bold, a lowercase letter means a vector and an uppercase letter means a matrix.

The strain energy associated to a transversal mode represented by its Eigen-pair (λ,$\boldsymbol{v}$) will be given by:

$$U = \frac{1}{2}\boldsymbol{v}^T\boldsymbol{K}_s\boldsymbol{v} = \frac{1}{2}\lambda\boldsymbol{v}^T\boldsymbol{v} = \frac{1}{2}\lambda \tag{1b}$$

Thus, the modes with the lowest eigenvalues mobilize less energy and then have more chances to occur. From the resolution of the SEP, in Eq. (1a) we obtain a set of vectors that we note $\boldsymbol{\psi}^i = \left(\psi_y^i, \psi_z^i\right)$, where ψ_y^i and ψ_z^i are the vertical and horizontal displacement, respectively, for the ith transversal deformation mode (Figs. 1 and 2). We note that the three first modes with a zero eigenvalue, corresponds to the classical modes of a rigid body motion:

$$\boldsymbol{\psi}^1 = (1,0), \quad \boldsymbol{\psi}^2 = (0,1), \quad \boldsymbol{\psi}^3 = (-(z-z_0), y-y_0) \tag{2}$$

where (y_0,z_0) are the coordinates of the torsion center of the section.

In our formulation, the only conditions that needs to be satisfied by the set of transversal modes functions, is that they are linearly independent, not necessarily orthogonal. Thus, an important feature of our formulation is that any linearly independent set of functions can be used to enrich our kinematics, the resolution of the differential equation system, performed later, being completely independent from the choice of the transversal and warping modes functions. In our case, the condition of linear independency is satisfied by construction, from the solution of the SEP by the well-known Arnoldi iteration algorithm, implemented in ARPACK routines.

In [7] the same method is used to determine the transversal mode for a thin walled profile, with the difference that they use a 3D Timoshenko beam for their section discretization, thus from the resolution of the SEP they derive the transversal modes and also their corresponding warping mode. We use here a different approach for the determination of the first warping mode for each transversal mode, based on the equilibrium of the beam element in the case of uniform warping; the higher order warping modes will be derived by using an iterative equilibrium scheme.

3. Determination of warping functions modes for a given transversal mode

3.1. The first warping mode determination

We consider the kinematics of a beam element, where we include only one transversal deformation mode. We then write the displacement vector **d** of an arbitrary point P of the section:

$$\boldsymbol{d} = \begin{Bmatrix} u_p \\ v_p \\ w_p \end{Bmatrix} = \begin{Bmatrix} u_p \\ \zeta\psi_y \\ \zeta\psi_z \end{Bmatrix} \tag{3}$$

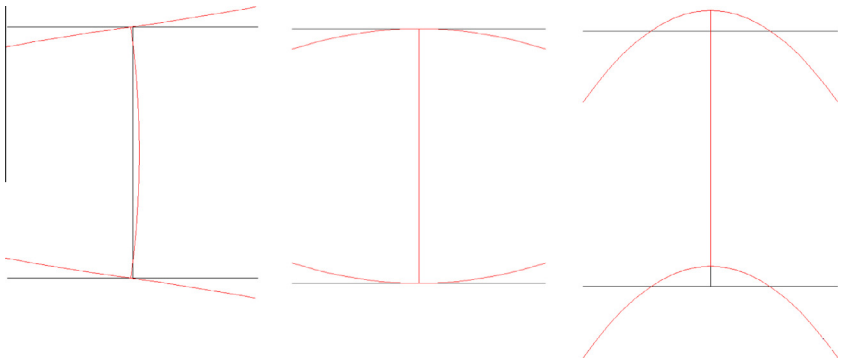

Fig. 1. Examples of transversal deformation modes for a thin walled profile I-section with 1D elements.

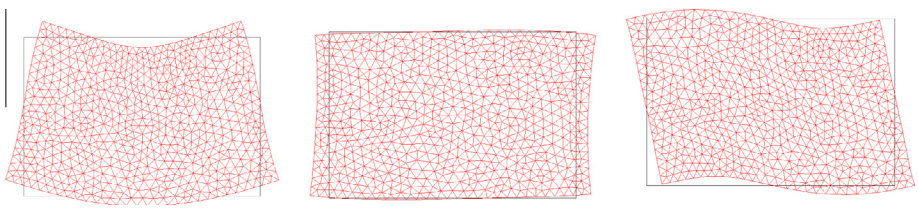

Fig. 2. Examples of transversal deformation modes for a rectangular section with triangular elements.

u_p Represents the longitudinal displacement due to the warping induced by the transversal mode and $\boldsymbol{\psi} = (\psi_y, \psi_z)$ the displacement vector of the transversal deformation mode at the point P.

From the condition of uniform warping in every section (all the beam's cross section will deform in the same manner), we can write:

$$\varepsilon_{xx} = \frac{\partial u_p}{\partial x} = 0 \tag{4}$$

This relation expresses the fact that uniform warping doesn't induce any change in the length of all the beam's fibers.

From the displacement vector, we deduce the strain field:

$$\begin{aligned} &\varepsilon_{xx} = \frac{\partial u_p}{\partial x} = 0, \quad \varepsilon_{yy} = \frac{\partial \psi_y}{\partial y}\zeta \\ &2\varepsilon_{xy} = \frac{\partial u_p}{\partial y} + \psi_y \frac{d\zeta}{dx}, \quad \varepsilon_{zz} = \frac{\partial \psi_z}{\partial z}\zeta \\ &2\varepsilon_{xz} = \frac{\partial u_p}{\partial z} + \psi_z \frac{d\zeta}{dx}, \quad 2\varepsilon_{yz} = \zeta\left(\frac{\partial \psi_y}{\partial z} + \frac{\partial \psi_z}{\partial y}\right) \end{aligned} \tag{5}$$

And the stress field:

$$\begin{aligned} &\sigma_{xx} = \lambda\zeta \operatorname{div}\boldsymbol{\psi}, \quad \sigma_{yy} = \left(2\mu\frac{\partial \psi_y}{\partial y} + \lambda \operatorname{div}\boldsymbol{\psi}\right)\zeta \\ &\sigma_{xy} = \mu\left(\frac{\partial u_p}{\partial y} + \psi_y \frac{d\zeta}{dx}\right), \quad \sigma_{zz} = \left(2\mu\frac{\partial \psi_z}{\partial z} + \lambda \operatorname{div}\boldsymbol{\psi}\right)\zeta \\ &\sigma_{xz} = \mu\left(\frac{\partial u_p}{\partial z} + \psi_z \frac{d\zeta}{dx}\right), \quad \sigma_{yz} = \mu\left(\frac{\partial \psi_y}{\partial z} + \frac{\partial \psi_z}{\partial y}\right)\zeta \end{aligned} \tag{6}$$

where $\lambda = \frac{\upsilon E}{(1+\upsilon)(1-2\upsilon)}$ and $\mu = \frac{E}{2(1+\upsilon)}$ are the Lamé coefficients, E the elasticity modulus and υ the Poisson coefficient, and div is the divergence operator: $\operatorname{div}\boldsymbol{\psi} = \frac{\partial \psi_y}{\partial y} + \frac{\partial \psi_z}{\partial z}$

We note the stress vector: $\boldsymbol{\tau} = (\sigma_{xy}, \sigma_{xz})$, that will be expressed by:

$$\boldsymbol{\tau} = \mu\left(\nabla u_p + \frac{d\zeta}{dx}\boldsymbol{\psi}\right) \tag{7}$$

where $\nabla = \left(\frac{\partial}{\partial y}, \frac{\partial}{\partial z}\right)$ is the gradient operator.

We write the equilibrium equation of the beam:

$$\frac{\partial \sigma_{xx}}{\partial x} + \operatorname{div}\boldsymbol{\tau} = 0 \tag{8}$$

$$\lambda \operatorname{div}\boldsymbol{\psi}\frac{d\zeta}{dx} + \mu(\Delta u_p + \frac{d\zeta}{dx}\operatorname{div}\boldsymbol{\psi}) = 0 \tag{9}$$

$$\Delta u_p = -\left(1 + \frac{\lambda}{\mu}\right)\operatorname{div}\boldsymbol{\psi}\frac{d\zeta}{dx} \tag{10}$$

where $\Delta = \frac{\partial^2}{\partial y^2} + \frac{\partial^2}{\partial z^2}$ is the Laplace operator.

From the last equation, we can see that the displacement u_p can be written in the following form $u_p = -\Omega\frac{d\zeta}{dx}$, where Ω is the warping function, verifying the relation:

$$\Delta\Omega = \left(1 + \frac{\lambda}{\mu}\right)\operatorname{div}\boldsymbol{\psi} \tag{11}$$

The normal component of the stress vector $\boldsymbol{\tau}$ has to be null on the border of the cross section, this condition is expressed by:

$$\boldsymbol{\tau}\cdot\boldsymbol{n} = 0 \tag{12}$$

$$\mu\frac{d\zeta}{dx}(-\nabla\Omega + \boldsymbol{\psi})\cdot\boldsymbol{n} = 0 \tag{13}$$

$$\frac{\partial\Omega}{\partial n} = \boldsymbol{\psi}\cdot\boldsymbol{n} \tag{14}$$

where $\boldsymbol{n}$ is the normal vector to the border of the section and $\frac{\partial\Omega}{\partial n} = \nabla\Omega\cdot\boldsymbol{n}$.

We resume here the equations of the partial derivatives problem, leading to the determination of the warping function Ω:

$$\begin{aligned} &\Delta\Omega = \left(1 + \tfrac{\lambda}{\mu}\right)\operatorname{div}\boldsymbol{\psi} \quad \text{on } S \\ &\tfrac{\partial\Omega}{\partial n} = \boldsymbol{\psi}\cdot\boldsymbol{n} \quad \text{on } \Gamma \\ &\textstyle\int_S \Omega\, dS = 0 \end{aligned} \tag{15}$$

where S is the cross section area.

The last relation was added to derive Ω uniquely. This relation corresponds to the condition that warping doesn't induce any uniform displacement.

The resolution of this problem can be performed by using one of the many numerical methods available, such as finite element method (FEM), finite difference method (FDM) or boundary element method (BEM), see [4] for more details.

If we consider the rigid body motion of the beam section, corresponding to the displacements v and w in the two directions of the principle axes and the rotation around the normal axis to the section θ_x, we will obtain the flexural modes and the Vlassov torsion warping [8], by solving the problem above, this shows the analogy between rigid body motion modes and the other transversal deformation modes.

Details about the derivation of the first warping mode, for a thin walled profile section, are given in Appendix A.2.

3.2. Determination of higher modes warping functions

In the case of non-uniform warping, the condition of $\varepsilon_{xx} = 0$ is no longer verified, thus we cannot state that the longitudinal displacement is of the form $u_p = -\Omega\frac{d\zeta}{dx}$, but instead we make the assumption that u_p can be written in the following form:

$$u_p = \Omega\delta = \Omega\left(\xi - \frac{d\zeta}{dx}\right) \tag{16}$$

where δ is the new rate function of the corresponding warping mode.

Thus the new normal stress is:

$$\sigma_{xx} = \underbrace{\lambda\zeta\operatorname{div}\boldsymbol{\psi}}_{\sigma^1} + \underbrace{2\mu\Omega\frac{d\xi}{dx}}_{\sigma^2} \tag{17}$$

The warping function Ω has been calculated in such a way that the normal stress σ^1 is equilibrated and the condition $\boldsymbol{\tau}\cdot\boldsymbol{n} = 0$ verified, thus in the case of a non-uniform warping the total normal stress will not be equilibrated due to the presence of the residual normal stress σ^2. Restoring equilibrium leads to the determination of a secondary shear stress associated to a second warping mode. This reasoning can be considered as the first step of an iterative equilibrium scheme, converging to the exact shape of the warping due to the considered transversal deformation mode.

We assume that we have determined the nth warping mode, and we wish to determine the $(n+1)$th warping mode. The nth warping normal stress σ^n will be then equilibrated by the $(n+1)$th warping shear stress:

$$\frac{\partial\sigma^n}{\partial x} + \operatorname{div}\boldsymbol{\tau}^{n+1} = 0 \tag{18}$$

where $\sigma^n = 2\mu\Omega_n\frac{d\xi_n}{dx}$, $\boldsymbol{\tau}^{n+1} = \mu\xi_{n+1}\nabla\Omega_{n+1}$.

Thus:

$$2\mu\Omega_n\frac{d^2\xi_n}{dx^2} + \mu\xi_{n+1}\Delta\Omega_{n+1} = 0 \tag{19}$$

The functions Ω_{n+1} and Ω_n depends only of the geometry of the cross section, whereas ξ_{n+1} and ξ_n depends of the abscissa x, so it implies that there exists necessarily two constants α_{n+1} and β_{n+1}, related to the equilibrium of the beam, verifying: $\Delta\Omega_{n+1} = \alpha_{n+1}\Omega_n$, $\xi_{n+1} = \beta_{n+1}\frac{d^2\xi_n}{dx^2}$.

Our goal is to construct a base of warping functions, where any section warping can be decomposed linearly with the aid of the generalized coordinates ξ_i that can be seen as a participation rate for the corresponding warping mode. In practice we need only to determine the warping functions to a multiplicative constant, and the participation rate for each mode will be obtained by writing the equilibrium of the beam. Thus, at the cross section level, only the problem $\Delta\Omega_{n+1} = \Omega_n$ has to be solved. For this problem, we need to define the Neumann and Dirichlet conditions to solve the problem uniquely. The Neumann condition, which specify the value of the derivative of Ω_{n+1} on the border of the section, will have the same form of the 1st warping function ($\frac{\partial\Omega_1}{\partial n} = \boldsymbol{\psi}\cdot\boldsymbol{n}$), in practice we can use the condition $\frac{\partial\Omega_{n+1}}{\partial n} = 0$ to solve the problem, and the uniqueness will be assured by the orthogonalization with the lower modes, to this aim the modified Gram-Schmidt orthogonalization process can be used. For the Dirichlet condition, we impose $\Omega_{n+1} = 0$ at an arbitrary point to solve the problem, and the condition $\int_S \Omega_{n+1} dS = 0$ will assure the uniqueness.

4. Equilibrium equations and the stiffness matrix

4.1. Kinematic, strain and stress fields

In this part we will consider general beam kinematics, with n transversal deformation modes and m warping modes, we note as mentioned before, that in this section the transversal deformation and warping modes can be completely independent and can be chosen arbitrarily from the set of continuous functions, on the unique condition that the family of warping functions and the family of transversal functions are linearly independent. We write the enriched kinematics:

$$\boldsymbol{d}_p = \begin{Bmatrix} u_p \\ v_p \\ w_p \end{Bmatrix} = \begin{Bmatrix} u + \sum_{j=1}^{m} \Omega_j \xi_j \\ \sum_{i=1}^{n} \psi_y^i \zeta^i \\ \sum_{i=1}^{n} \psi_z^i \zeta^i \end{Bmatrix} \tag{20}$$

We note that the first transversal deformation modes will correspond to the rigid body motion, and the first warping modes will correspond to the beam flexion in the direction of the two principal axes.

The strain field obtained from this kinematics will be expressed by:

$$\begin{aligned} &\varepsilon_{xx} = \frac{du}{dx} + \Omega_j \frac{d\xi_j}{dx}, \quad \varepsilon_{yy} = \frac{\partial \psi_y^i}{\partial y}\zeta^i \\ &2\varepsilon_{xy} = \frac{\partial \Omega_j}{\partial y}\xi_j + \psi_y^i \frac{d\zeta^i}{dx}, \quad \varepsilon_{zz} = \frac{\partial \psi_z^i}{\partial z}\zeta^i \\ &2\varepsilon_{xz} = \frac{\partial \Omega_j}{\partial z}\xi_j + \psi_z^i \frac{d\zeta^i}{dx}, \quad 2\varepsilon_{yz} = \left(\frac{\partial \psi_y^i}{\partial z} + \frac{\partial \psi_z^i}{\partial y}\right)\zeta^i \end{aligned} \tag{21}$$

We have used above and in all that will follow, the Einstein summation convention, to simplify as much as possible the equations expressions.

To determine the stress field from the strain field, we have to make use of the constitutive relation:

$$\boldsymbol{\sigma} = \begin{Bmatrix} \sigma_{xx} \\ \sigma_{yy} \\ \sigma_{zz}\sigma_{xy} \\ \sigma_{xz} \\ \sigma_{yz} \end{Bmatrix} = \begin{bmatrix} 2\mu+\lambda & \lambda & \lambda & & \\ & 2\mu+\lambda & \lambda & 0 & \\ & & 2\mu+\lambda & & \\ & & & \mu & \\ & sym & & & \mu \\ & & & & & \mu \end{bmatrix} \begin{Bmatrix} \varepsilon_{xx} \\ \varepsilon_{yy} \\ \varepsilon_{zz} \\ 2\varepsilon_{xy} \\ 2\varepsilon_{xz} \\ 2\varepsilon_{yz} \end{Bmatrix} \tag{22}$$

Thus:

$$\begin{aligned} &\sigma_{xx} = 2\mu\left(\frac{du}{dx} + \Omega_j \frac{d\xi_j}{dx}\right) + \sigma_r, \quad \sigma_{yy} = 2\mu \frac{\partial \psi_y^i}{\partial y}\zeta^i + \sigma_r \\ &\sigma_{xy} = \mu\left(\frac{\partial \Omega_j}{\partial y}\xi_j + \psi_y^i \frac{d\zeta^i}{dx}\right), \quad \sigma_{zz} = 2\mu \frac{\partial \psi_z^i}{\partial z}\zeta^i + \sigma_r \\ &\sigma_{xz} = \mu\left(\frac{\partial \Omega_j}{\partial z}\xi_j + \psi_z^i \frac{d\zeta^i}{dx}\right), \quad \sigma_{yz} = \mu\left(\frac{\partial \psi_y^i}{\partial z} + \frac{\partial \psi_z^i}{\partial y}\right)\zeta^i \end{aligned} \tag{23}$$

where: $\sigma_r = \lambda tr(\boldsymbol{\varepsilon}) = \lambda(\varepsilon_{xx} + \varepsilon_{yy} + \varepsilon_{zz}) = \lambda\left(\frac{du}{dx} + \zeta^i div\boldsymbol{\psi}^i + \Omega_j \frac{d\xi_j}{dx}\right)$.

4.2. The principle of virtual work and the equilibrium equations

We write the expression of the internal virtual work:

$$\delta W_{int} = \int_V \boldsymbol{\sigma}^{\boldsymbol{T}} \delta\boldsymbol{\varepsilon}\, dV \tag{24}$$

$$\begin{aligned} \delta W_{int} = \int_V &\left(\sigma_{xx}\left(\frac{d\delta u}{dx} + \Omega_j \frac{d\delta\xi_j}{dx}\right) + \left(\sigma_{xy}\frac{\partial\Omega_j}{\partial y} + \sigma_{xz}\frac{\partial\Omega_j}{\partial z}\right)\delta\xi_j \right. \\ &+ \left(\sigma_{xy}\psi_y^i + \sigma_{xz}\psi_z^i\right)\frac{d\delta\zeta^i}{dx} \\ &\left. + \left(\sigma_{yy}\frac{\partial\psi_y^i}{\partial y} + \sigma_{zz}\frac{\partial\psi_z^i}{\partial z} + \sigma_{zy}\left(\frac{\partial\psi_y^i}{\partial z} + \frac{\partial\psi_z^i}{\partial y}\right)\right)\delta\zeta^i\right) dV \end{aligned} \tag{25}$$

We integrate over the whole section to obtain:

$$\delta W_{int} = \int_0^L \left(N\frac{d\delta u}{dx} + M_j\frac{d\delta\xi_j}{dx} + T_j\delta\xi_j + \Lambda^i\frac{d\delta\zeta^i}{dx} + \Phi^i\delta\zeta^i\right) dx \tag{26}$$

Where the expressions of the generalized efforts are:

$$N = \int_S \sigma_{xx} dS = (2\mu+\lambda)S\frac{du}{dx} + \lambda P^i\zeta^i \tag{27}$$

$$M_j = \int_S \Omega_j\sigma_{xx} dS = (2\mu+\lambda)K_{jk}\frac{d\xi_k}{dx} + \lambda Q_j^i\zeta^i \tag{28}$$

$$T_j = \int_S \left(\sigma_{xy}\frac{\partial\Omega_j}{\partial y} + \sigma_{xz}\frac{\partial\Omega_j}{\partial z}\right) dS = \mu\left(J_{jk}\xi_k + D_j^l\frac{d\zeta^l}{dx}\right) \tag{29}$$

$$\Lambda^i = \int_S \left(\sigma_{xy}\psi_y^i + \sigma_{xz}\psi_z^i\right) dS = \mu\left(D_k^i\xi_k + C^{il}\frac{d\zeta^l}{dx}\right) \tag{30}$$

$$\begin{aligned} \Phi^i &= \int_S \left(\frac{\partial\psi_z^i}{\partial z}\sigma_{zz} + \frac{\partial\psi_y^i}{\partial y}\sigma_{yy} + \left(\frac{\partial\psi_y^i}{\partial z} + \frac{\partial\psi_z^i}{\partial y}\right)\sigma_{yz}\right) dS \\ &= (\mu H^{il} + \lambda F^{il})\zeta^l + \lambda\left(P^i\frac{du}{dx} + Q_j^i\frac{d\xi_j}{dx}\right) \end{aligned} \tag{31}$$

And of the coefficients:

$$\begin{aligned} &K_{jk} = \int_S \Omega_j\Omega_k dS, \quad D_j^l = \int_S \boldsymbol{\psi}^l\cdot\boldsymbol{\nabla}\Omega_j dS, \\ &C^{il} = \int_S \boldsymbol{\psi}^l\cdot\boldsymbol{\psi}^i dS, \quad J_{jk} = \int_S \boldsymbol{\nabla}\Omega_j\cdot\boldsymbol{\nabla}\Omega_k dS \\ &F^{il} = \int_S div\boldsymbol{\psi}^i div\boldsymbol{\psi}^l dS, \quad Q_j^i = \int_S \Omega_j div\boldsymbol{\psi}^i dS, \\ &P^i = \int_S div\boldsymbol{\psi}^i dS, \quad H^{il} = \int_S \Delta(\boldsymbol{\psi}^i, \boldsymbol{\psi}^l) dS \end{aligned}$$

where the operator Δ is defined by: $\Delta(\boldsymbol{\psi}^i, \boldsymbol{\psi}^l) = 2\left(\boldsymbol{\nabla}\psi_y^i\cdot\boldsymbol{\nabla}\psi_y^l + \boldsymbol{\nabla}\psi_z^i\cdot\boldsymbol{\nabla}\psi_z^l\right) - curl\boldsymbol{\psi}^i curl\boldsymbol{\psi}^l$ And: $curl\boldsymbol{\psi} = \frac{\partial\psi_y}{\partial z} - \frac{\partial\psi_z}{\partial y}$.

After integration by parts of the internal virtual work in Eq. (26), we obtain:

$$\begin{aligned} \delta W_{int} = &\int_0^L \left(-\frac{dN}{dx}\delta u - \left(\frac{dM_j}{dx} - T_j\right)\delta\xi_j - \left(\frac{d\Lambda^i}{dx} - \Phi^i\right)\delta\zeta^i\right) dx \\ &+ \underbrace{\left[N\delta u + M_j\delta\xi_j + \Lambda^i\delta\zeta^i\right]_0^L}_{\delta W_{ext}} \end{aligned} \tag{32}$$

From the principal of virtual work we have $\delta W_{int} = \delta W_{ext}$, thus we obtain:

$$\int_0^L \left(\frac{dN}{dx}\delta u + \left(\frac{dM_j}{dx} - T_j\right)\delta\xi_j + \left(\frac{d\Lambda^i}{dx} - \Phi^i\right)\delta\zeta^i\right)dx = 0 \tag{33}$$

This relation is valid for any admissible virtual displacements, it imply that the expressions between brackets have to be null, which represents the equilibrium equations of the beam:

$$\frac{dN}{dx} = 0,\ \frac{dM_j}{dx} - T_j = 0 \text{ for } 1 \leqslant j \leqslant m,\ \frac{d\Lambda^i}{dx} - \Phi^i = 0 \text{ for } 1 \leqslant i \leqslant n \tag{34}$$

We develop the two last equations from the right in Eq. (34):

$$\begin{cases} (2\mu+\lambda)K_{jk}\frac{d^2\xi_k}{dx^2} + \lambda Q_j^l\frac{d\zeta^l}{dx} - \mu\left(J_{jk}\xi_k + D_j^l\frac{d\zeta^l}{dx}\right) = 0 \\ \mu\left(D_k^i\frac{d\xi_k}{dx} + C^{il}\frac{d^2\zeta^l}{dx^2}\right) - (\mu H^{il} + \lambda F^{il})\zeta^l - \lambda\left(P^i\frac{du}{dx} + Q_k^i\frac{d\xi_k}{dx}\right) = 0 \end{cases} \tag{35}$$

$$\Rightarrow \begin{cases} (2\mu+\lambda)K_{jk}\frac{d^2\xi_k}{dx^2} - \mu B_j^l\frac{d\zeta^l}{dx} - \mu J_{jk}\xi_k = 0 \\ \mu C^{il}\frac{d^2\zeta^l}{dx^2} + \mu B_k^i\frac{d\xi_k}{dx} - (\mu H^{il} + \lambda F^{il})\zeta^l = \lambda P^i\frac{du}{dx} \end{cases} \tag{36}$$

From the expression of the normal force in Eq. (27) we have the following relation:

$$\frac{du}{dx} = \frac{1}{(2\mu+\lambda)S}(N - \lambda P^l\zeta^l) \tag{37}$$

Thus, if we replace it in the second equation in (36) we obtain:

$$\mu C^{il}\frac{d^2\zeta^l}{dx^2} + \mu B_k^i\frac{d\xi_k}{dx} - \left(\mu H^{il} + \lambda F^{il} - \frac{\lambda^2 P^i P^l}{(2\mu+\lambda)S}\right)\zeta^l = \frac{\lambda P^i}{(2\mu+\lambda)S}N \tag{38}$$

At this stage we introduce some matricial notations:

$$\boldsymbol{K} = (2\mu+\lambda)\int_S \begin{bmatrix} \Omega_1\Omega_1 & \dots & \Omega_1\Omega_m \\ & \ddots & \vdots \\ sym & & \Omega_m\Omega_m \end{bmatrix} dS,$$

$$\boldsymbol{C} = \mu\int_S \begin{bmatrix} \boldsymbol{\psi}^1\cdot\boldsymbol{\psi}^1 & \dots & \boldsymbol{\psi}^1\cdot\boldsymbol{\psi}^n \\ & \ddots & \vdots \\ sym & & \boldsymbol{\psi}^n\cdot\boldsymbol{\psi}^n \end{bmatrix} dS$$

$$\boldsymbol{J} = \mu\int_S \begin{bmatrix} \nabla\Omega_1\cdot\nabla\Omega_m & \dots & \nabla\Omega_1\cdot\nabla\Omega_m \\ & \ddots & \vdots \\ sym & & \nabla\Omega_m\cdot\nabla\Omega_m \end{bmatrix} dS, \quad \boldsymbol{p} = \frac{\lambda}{(2\mu+\lambda)S}\begin{Bmatrix} P^1 \\ \vdots \\ P^n \end{Bmatrix}$$

$$\boldsymbol{D} = \mu\int_S \begin{bmatrix} \boldsymbol{\psi}^1\cdot\nabla\Omega_1 & \dots & \boldsymbol{\psi}^n\cdot\nabla\Omega_1 \\ \vdots & \ddots & \vdots \\ \boldsymbol{\psi}^1\cdot\nabla\Omega_m & \dots & \boldsymbol{\psi}^n\cdot\nabla\Omega_m \end{bmatrix} dS,$$

$$\boldsymbol{Q} = \lambda\int_S \begin{bmatrix} \Omega_1\mathrm{div}\boldsymbol{\psi}^1 & \dots & \Omega_1\mathrm{div}\boldsymbol{\psi}^n \\ \vdots & \ddots & \vdots \\ \Omega_m\mathrm{div}\boldsymbol{\psi}^1 & \dots & \Omega_m\mathrm{div}\boldsymbol{\psi}^n \end{bmatrix} dS$$

$$\boldsymbol{F} = \lambda\int_S \begin{bmatrix} \mathrm{div}\boldsymbol{\psi}^1\mathrm{div}\boldsymbol{\psi}^1 & \dots & \mathrm{div}\boldsymbol{\psi}^1\mathrm{div}\boldsymbol{\psi}^n \\ & \ddots & \vdots \\ sym & & \mathrm{div}\boldsymbol{\psi}^n\mathrm{div}\boldsymbol{\psi}^n \end{bmatrix} dS,$$

$$\boldsymbol{H} = \mu\int_S \begin{bmatrix} \Delta(\boldsymbol{\psi}^1,\boldsymbol{\psi}^1) & \dots & \Delta(\boldsymbol{\psi}^1,\boldsymbol{\psi}^n) \\ & \ddots & \vdots \\ sym & & \Delta(\boldsymbol{\psi}^n,\boldsymbol{\psi}^n) \end{bmatrix} dS$$

and $\boldsymbol{A} = \boldsymbol{H} + \boldsymbol{F} - (2\mu+\lambda)S\boldsymbol{p}\otimes\boldsymbol{p}$, $\boldsymbol{B} = \boldsymbol{D} - \boldsymbol{Q}$.

With these notations, the system of differential equations in the first equation in (36) and in (38), can be written now in the following matrix form:

$$\boldsymbol{K}\boldsymbol{\xi}'' - \boldsymbol{B}\boldsymbol{\zeta}' - \boldsymbol{J}\boldsymbol{\xi} = 0 \tag{39}$$

$$\boldsymbol{C}\boldsymbol{\zeta}'' + \boldsymbol{B}^T\boldsymbol{\xi}' - \boldsymbol{A}\boldsymbol{\zeta} = \boldsymbol{p}N \tag{40}$$

where $\boldsymbol{\xi} = \begin{Bmatrix} \xi_1 \\ \vdots \\ \xi_m \end{Bmatrix}$, $\boldsymbol{\zeta} = \begin{Bmatrix} \zeta_1 \\ \vdots \\ \zeta_n \end{Bmatrix}$.

We note that the matrix $\boldsymbol{C}$ will be diagonal, but not necessarily the matrix $\boldsymbol{K}$, since the warping functions from different transversal modes are not necessarily orthogonal. We note also that the differential equation system obtained in (39) and (40), is analogical to a dynamical equilibrium equation system for a gyroscopic system in an unstable state. In the next part, we will solve this system exactly to assemble the rigidity matrix; the general solution will prove to be a little exhaustive because we need to separate in our system the rigid body motion and flexural modes from the others, and this is done by making two variable changes, one for the transversal modes and another for the warping modes.

4.3. Resolution of the equilibrium equations and derivation of the stiffness matrix

In order to solve the differential equation system written in (39) and (40), we first need to extract the rigid body motion modes, to this aim we will start by solving the generalized eigenvalue problem (GEP) $\boldsymbol{A}\boldsymbol{z} = \alpha\boldsymbol{C}\boldsymbol{z}$. The matrix $\boldsymbol{C}$ is the gramian matrix attached to the basis formed by the transversal deformation mode vectors, it will be then a definite positive matrix, and by noticing that $\boldsymbol{A}$ is a symmetric matrix, we can say then that the eigenvalues of our problem will be positive $\alpha \geqslant 0$, and the number of zero eigenvalues will in fact be equal to the number of rigid body motion modes, that can be superior to three for some cases, for example for a global cross section formed by n disjoints sections, then the number of rigid body modes will be equal to $3n$.

After solving the GEP, we obtain the eigenvectors matrix $\boldsymbol{P}$ verifying:

$$\boldsymbol{P}^T\boldsymbol{A}\boldsymbol{P} = \begin{bmatrix} \boldsymbol{0}_{q\times q} & \\ & \boldsymbol{G} \end{bmatrix}, \quad \boldsymbol{P}^T\boldsymbol{C}\boldsymbol{P} = \boldsymbol{I} \tag{41}$$

where $\boldsymbol{G}$ is the diagonal matrix containing the non-zero eigenvalues and q the number of rigid body modes.

We proceed with a variable change in the eigenvectors base: $\boldsymbol{\zeta} = \boldsymbol{P}\boldsymbol{\vartheta}_t = \boldsymbol{P}\begin{Bmatrix} \vartheta_q \\ \vartheta \end{Bmatrix}$.

And we note: $\boldsymbol{P} = [\boldsymbol{P}_1 \quad \boldsymbol{P}_2]$, $\boldsymbol{B}_i = \boldsymbol{B}\boldsymbol{P}_i$, $\boldsymbol{p}_i = \boldsymbol{P}_i^T\boldsymbol{p}$ for $i = 1, 2$.

We substitute this in Eq. (40) to obtain:

$$\boldsymbol{P}^T\boldsymbol{C}\boldsymbol{P}\vartheta_t'' + \boldsymbol{P}^T\boldsymbol{B}^T\boldsymbol{\xi}' - \boldsymbol{P}^T\boldsymbol{A}\boldsymbol{P}\vartheta_t = \boldsymbol{P}^T\boldsymbol{p}N$$

$$\vartheta_q'' + \boldsymbol{B}_1^T\boldsymbol{\xi}' = \boldsymbol{p}_1 N \tag{42}$$

$$\vartheta'' - \boldsymbol{G}\vartheta + \boldsymbol{B}_2^T\boldsymbol{\xi}' = \boldsymbol{p}_2 N \tag{43}$$

We make also the variable change into the Eq. (39) to fully transform our system with the new variables:

$$\boldsymbol{K}\boldsymbol{\xi}'' - \boldsymbol{J}\boldsymbol{\xi} - \boldsymbol{B}_1\vartheta_q' - \boldsymbol{B}_2\vartheta' = 0 \tag{44}$$

We integrate the Eq. (42) between 0 and x:

$$\vartheta_q' = \vartheta_{q0}' - \boldsymbol{B}_1^T(\boldsymbol{\xi} - \boldsymbol{\xi}_0) + \boldsymbol{p}_1 Nx \tag{45}$$

We also transform the generalized effort vector $\boldsymbol{\gamma} = \{\Lambda^i\}_{1\leqslant i\leqslant n}$ associated to $\boldsymbol{\zeta}$:

$$\Gamma_t = \begin{Bmatrix} \Gamma_q \\ \Gamma \end{Bmatrix} = \boldsymbol{P}^T\boldsymbol{\gamma} = \vartheta_t' + \boldsymbol{P}^T\boldsymbol{D}^T\xi \tag{46}$$

$$\Rightarrow \begin{cases} \vartheta'_{q0} = \Gamma_{q0} - \boldsymbol{D}_1^T\xi_0 \\ \Gamma = \vartheta' + \boldsymbol{D}_2^T\xi \end{cases} \Rightarrow \begin{cases} \vartheta'_q = \Gamma_{q0} - \boldsymbol{Q}_1^T\xi_0 + \boldsymbol{p}_1 Nx - \boldsymbol{B}_1^T\xi \\ \Gamma = \vartheta' + \boldsymbol{D}_2^T\xi \end{cases} \tag{47}$$

where $\boldsymbol{Q}_1 = \boldsymbol{Q}\,\boldsymbol{P}_1 = (\boldsymbol{D} - \boldsymbol{B})\boldsymbol{P}_1 = \boldsymbol{D}_1 - \boldsymbol{B}_1$.

If we substitute the expression of ϑ'_q obtained in (47) into the Eq. (44) we obtain:

$$\boldsymbol{K}\xi'' - \left(\boldsymbol{J} - \boldsymbol{B}_1\boldsymbol{B}_1^T\right)\xi - \boldsymbol{B}_2\vartheta' = \boldsymbol{B}_1\left(\Gamma_{q0} - \boldsymbol{Q}_1^T\xi_0 + \boldsymbol{p}_1 Nx\right) \tag{48}$$

Thus, the system to solve is transformed into a new equivalent one:

$$\boldsymbol{K}\xi'' - \boldsymbol{B}_2\vartheta' - \boldsymbol{J}_q\xi = \boldsymbol{B}_1(\Gamma_{q0} - \boldsymbol{Q}_1^T\xi_0 + \boldsymbol{p}_1 Nx) \tag{49}$$

$$\vartheta'' + \boldsymbol{B}_2^T\xi' - \boldsymbol{G}\vartheta = \boldsymbol{p}_2 N \tag{50}$$

where $\boldsymbol{J}_q = \boldsymbol{J} - \boldsymbol{B}_1\boldsymbol{B}_1^T$.

As for the matrix $\boldsymbol{A}$, the symmetric matrix $\boldsymbol{J}_q$ will contain some zero eigenvalues that correspond this time to the flexural modes, and in order to solve our system we also need to extract these modes and separate them from the other warping modes, thus we have to solve the GEP $\boldsymbol{J}_q\boldsymbol{z} = \alpha\boldsymbol{K}\mathrm{z}$, with $\boldsymbol{K}$ the gramian matrix attached to the warping functions base, thus it's a definite positive matrix, and as previously stated, this means that $\alpha \geqslant 0$.

After solving the eigenvalue problem, we obtain the eigenvectors matrix $\boldsymbol{R}$ verifying:

$$\boldsymbol{R}^T\boldsymbol{J}_q\boldsymbol{R} = \begin{bmatrix} \boldsymbol{0}_{l\times l} & \\ & \boldsymbol{S} \end{bmatrix}, \quad \boldsymbol{R}^T\boldsymbol{K}\boldsymbol{R} = \boldsymbol{I} \tag{51}$$

where $\boldsymbol{S}$ is the diagonal matrix containing the non-zero eigenvalues and l the number of the flexural modes, that will be equal in general to $l = 2q/3$.

We proceed to a second variable change: $\xi = \boldsymbol{R}\varphi_t = \boldsymbol{R}\begin{Bmatrix} \varphi_l \\ \varphi \end{Bmatrix}$.

And we note: $\boldsymbol{R} = [\boldsymbol{R}_1 \quad \boldsymbol{R}_2]$, $\boldsymbol{B}_{ij} = \boldsymbol{R}_j^T\boldsymbol{B}_i$, $\boldsymbol{Q}_{ij} = \boldsymbol{R}_j^T\boldsymbol{Q}_i$ for $i = 1,2$ and $j = 1,2$.

We replace in the Eq. (49) to obtain:

$$\boldsymbol{R}^T\boldsymbol{K}\boldsymbol{R}\varphi_t'' - \boldsymbol{R}^T\boldsymbol{J}_q\boldsymbol{R}\varphi_t - \boldsymbol{R}^T\boldsymbol{B}_2\vartheta' = \boldsymbol{R}^T\boldsymbol{B}_1\left(\Gamma_{q0} - \boldsymbol{Q}_1^T\xi_0 + \boldsymbol{p}_1 Nx\right) \tag{52}$$

$$\varphi_l'' - \boldsymbol{B}_{21}\vartheta' = \boldsymbol{B}_{11}\left(\Gamma_{q0} - \boldsymbol{Q}_1^T\xi_0 + \boldsymbol{p}_1 Nx\right) \tag{53}$$

$$\varphi'' - \boldsymbol{S}\varphi - \boldsymbol{B}_{22}\vartheta' = \boldsymbol{B}_{12}\left(\Gamma_{q0} - \boldsymbol{Q}_1^T\xi_0 + \boldsymbol{p}_1 Nx\right) \tag{54}$$

We integrate the Eq. (53) from 0 to x:

$$\varphi_l' = \boldsymbol{B}_{21}\vartheta + \boldsymbol{h}_x \tag{55}$$

where $\boldsymbol{h}_x = \varphi'_{l0} - \boldsymbol{B}_{21}\vartheta_0 + \boldsymbol{B}_{11}\left(\left(\Gamma_{q0} - \boldsymbol{Q}_{11}^T\varphi_{l0} - \boldsymbol{Q}_{12}^T\varphi_0\right)x + \boldsymbol{p}_1 N\frac{x^2}{2}\right)$.

By replacing (55) in the Eq. (50) after making the variable change, we have:

$$\vartheta'' - \boldsymbol{G}\vartheta + \boldsymbol{B}_{22}^T\varphi' + \boldsymbol{B}_{21}^T\varphi_l' = \boldsymbol{p}_2 N \tag{56}$$

$$\vartheta'' - \left(\boldsymbol{G} - \boldsymbol{B}_{21}^T\boldsymbol{B}_{21}\right)\vartheta + \boldsymbol{B}_{22}^T\varphi' = \boldsymbol{p}_2 N - \boldsymbol{B}_{21}^T\boldsymbol{h}_x \tag{57}$$

We transform the generalized effort vector $\boldsymbol{m} = \{M_j\}_{1\leqslant j\leqslant m}$ associated to ξ:

$$\Upsilon_t = \begin{Bmatrix} \Upsilon_l \\ \Upsilon \end{Bmatrix} = \boldsymbol{R}^T\boldsymbol{m} = \boldsymbol{R}^T(\boldsymbol{K}\xi' + \boldsymbol{Q}\zeta) = \varphi_t' + \boldsymbol{R}^T\boldsymbol{Q}\zeta = \varphi_t' + \boldsymbol{R}^T\boldsymbol{Q}_1\vartheta_q + \boldsymbol{R}^T\boldsymbol{Q}_2\vartheta \tag{58}$$

$$\Rightarrow \begin{cases} \varphi'_{l0} = \Upsilon_{l0} - \boldsymbol{Q}_{11}\vartheta_{q0} - \boldsymbol{Q}_{21}\vartheta_0 \\ \Upsilon = \varphi' + \boldsymbol{Q}_{12}\vartheta_q + \boldsymbol{Q}_{22}\vartheta \end{cases} \Rightarrow \begin{cases} \varphi_l' = \boldsymbol{B}_{21}\vartheta + \boldsymbol{h}_x \\ \Upsilon = \varphi' + \boldsymbol{Q}_{12}\vartheta_q + \boldsymbol{Q}_{22}\vartheta \end{cases} \tag{59}$$

where $\boldsymbol{h}_x$ becomes: $\boldsymbol{h}_x = \Upsilon_{l0} - \boldsymbol{D}_{21}\vartheta_0 - \boldsymbol{Q}_{11}\vartheta_{q0} + \boldsymbol{B}_{11}\left(\left(\Gamma_{q0} - \boldsymbol{Q}_{11}^T\varphi_{l0} - \boldsymbol{Q}_{12}^T\varphi_0\right)x + \boldsymbol{p}_1 N\frac{x^2}{2}\right)$.

We note:

$$\boldsymbol{G}_* = \boldsymbol{G} - \boldsymbol{B}_{21}^T\boldsymbol{B}_{21},$$

$$\boldsymbol{f}_x = \begin{Bmatrix} \boldsymbol{f}_1 \\ \boldsymbol{f}_2 \end{Bmatrix} = \begin{Bmatrix} \boldsymbol{B}_{12}\left(\Gamma_{q0} - \boldsymbol{Q}_{11}^T\varphi_{l0} - \boldsymbol{Q}_{12}^T\varphi_0 + \boldsymbol{p}_1 Nx\right) \\ \boldsymbol{p}_2 N - \boldsymbol{B}_{21}^T\boldsymbol{h}_x \end{Bmatrix}$$

$$\phi = \begin{Bmatrix} \varphi \\ \vartheta \end{Bmatrix}, \quad \boldsymbol{T} = \begin{bmatrix} \boldsymbol{I} & \boldsymbol{0} \\ \boldsymbol{0} & \boldsymbol{I} \end{bmatrix}, \quad \boldsymbol{U} = \begin{bmatrix} \boldsymbol{0} & -\boldsymbol{B}_{22} \\ \boldsymbol{B}_{22}^T & \boldsymbol{0} \end{bmatrix}, \quad \boldsymbol{V} = \begin{bmatrix} \boldsymbol{S} & \boldsymbol{0} \\ \boldsymbol{0} & \boldsymbol{G}_* \end{bmatrix}$$

Thus, from (54) and (57) we can write the final system to solve:

$$\begin{cases} \varphi'' - \boldsymbol{B}_{22}\vartheta' - \boldsymbol{S}\varphi = \boldsymbol{f}_1 \\ \vartheta'' + \boldsymbol{B}_{22}^T\varphi' - \boldsymbol{G}_*\vartheta = \boldsymbol{f}_2 \end{cases} \Rightarrow \boldsymbol{T}\phi'' + \boldsymbol{U}\phi' - \boldsymbol{V}\phi = \boldsymbol{f}_x \tag{60}$$

We resume here all the equations that form our new system, that we will solve exactly, equivalent to the initial system in (39) and (40):

$$\begin{cases} u' = \frac{N}{(2\mu+\lambda)S} - \boldsymbol{p}_1\cdot\vartheta_q - \boldsymbol{p}_2\cdot\vartheta \\ \vartheta'_q = \Gamma_{q0} - \boldsymbol{Q}_{11}^T\varphi_{l0} - \boldsymbol{Q}_{12}^T\varphi_0 - \boldsymbol{B}_{11}^T\varphi_l - \boldsymbol{B}_{12}^T\varphi + \boldsymbol{p}_1 Nx \\ \varphi_l' = \boldsymbol{B}_{21}\vartheta + \boldsymbol{h}_x \\ \boldsymbol{T}\phi'' + \boldsymbol{U}\phi' - \boldsymbol{V}\phi = \boldsymbol{f}_x \end{cases} \tag{61}$$

We note $k = m + n - q - l$ the dimension of the last second order differential equation system in Eq. (61).

Now that we have uncoupled the rigid body motion and flexural modes from the other modes, we detail the solution of the differential equation system (62) without the second member:

$$\boldsymbol{T}\phi'' + \boldsymbol{U}\phi' - \boldsymbol{V}\phi = \boldsymbol{0} \tag{62}$$

$$\boldsymbol{T}\partial_x^2\phi + \boldsymbol{U}\partial_x\phi - \boldsymbol{V}\phi = \boldsymbol{0} \Rightarrow (\boldsymbol{T}\partial_x^2 + \boldsymbol{U}\partial_x - \boldsymbol{V})\phi = \boldsymbol{0} \tag{63}$$

where ∂_x is the derivate about x operator.

To solve the system we will need then to solve its characteristic equation:

$$\det(\boldsymbol{T}\omega^2 + \boldsymbol{U}\omega - \boldsymbol{V}) = \det(\boldsymbol{T})\omega^{2k} + \textit{lower order term} = 0 \tag{64}$$

$\boldsymbol{T}$is a positive definite matrix, thus det $(\boldsymbol{T}) > 0$, this implies that the roots of the Eq. (64) with their multiplicity will be equal to 2 k. Solving this equation corresponds in fact to solving a special class of eigenvalue problem called the quadratic eigenvalue problem QEP, see [9], where we need to find $(\omega, \boldsymbol{z}) \in \mathbb{C}^{k+1}$ verifying:

$$\boldsymbol{G}(\omega) = (\boldsymbol{T}\omega^2 + \boldsymbol{U}\omega - \boldsymbol{V})\boldsymbol{z} = 0$$

Proposition 1. *If T and V are definite positive matrices, then the eigenvalues of the QEP G(ω)z = 0 will be finite and non-null.*

Proof. We introduce some notations: $t(z) = z^*Tz$, $u(z) = z^*Uz$, $v(z) = z^*Vz$, where $*$ define the conjugate transpose of a matrix. For (ω, z) an Eigen-pair, we can write:

$$\boldsymbol{G}(\omega)\boldsymbol{z} = \boldsymbol{0} \Rightarrow \boldsymbol{z}^*\boldsymbol{G}(\omega)\boldsymbol{z} = t(\boldsymbol{z})\omega^2 + u(\boldsymbol{z})\omega - v(\boldsymbol{z}) = 0 \tag{65}$$

The solution of the second order equation $z^*G(\omega)z = 0$ will be written in the following form:

$$\omega = \frac{-u(\boldsymbol{z}) \pm \sqrt{u(\boldsymbol{z})^2 + 4t(\boldsymbol{z})\,v(\boldsymbol{z})}}{2t(\boldsymbol{z})} \tag{66}$$

$T$is a definite positive matrix thus $t(z) > 0$, it implies that ω will have finite values. V is also a definite positive matrix then $t(z)v(z) > 0$, thus $\sqrt{u(\boldsymbol{z})^2 + 4t(\boldsymbol{z})\,v(\boldsymbol{z})} \neq |u(\boldsymbol{z})| \Rightarrow \omega \neq 0$. □

Proposition 2. *For T and U real symmetric matrices and V a real skew-symmetric matrix, then the eigenvalues of the QEP will have Hamiltonian properties, which mean that they are symmetric about the real and imaginary axis of the complex plane.*

Proof. Gverifies the following relations:

$$\boldsymbol{G}(\omega)^{*} = \overline{\boldsymbol{G}(\omega)^{\boldsymbol{T}}} = \boldsymbol{T}\bar{\omega}^2 - \boldsymbol{U}\bar{\omega} - \boldsymbol{V} = \boldsymbol{G}(-\bar{\omega}) \tag{67}$$

T, U and V are real matrices, thus from Eq. (67): $G(\omega)^T = G(-\omega)$.

From these two relations verified by G we can deduce that if ω is an eigenvalue then $\bar{\omega}$, $-\bar{\omega}$ and $-\omega$ are also eigenvalues of the problem. □

The solution of a QEP is performed with the aid of a linearization, which transforms the problem to a classical generalized eigenvalue problem:

$$\begin{bmatrix} \boldsymbol{0} & \boldsymbol{I} \\ \boldsymbol{V} & -\boldsymbol{U} \end{bmatrix} \begin{Bmatrix} \boldsymbol{w} \\ \boldsymbol{y} \end{Bmatrix} = \omega \begin{bmatrix} \boldsymbol{I} & \boldsymbol{0} \\ \boldsymbol{0} & \boldsymbol{T} \end{bmatrix} \begin{Bmatrix} \boldsymbol{w} \\ \boldsymbol{y} \end{Bmatrix} \tag{68}$$

where $\boldsymbol{w} = \boldsymbol{z}$, $\boldsymbol{y} = \omega \boldsymbol{z}$.

After the resolution of this problem we obtain $2k$ eigenvalues verifying the properties of propostion 1 and 2, assembled in the diagonal matrix $\boldsymbol{S}$, and $\boldsymbol{R}_{k\times 2k}$ there corresponding eigenvectors matrix. Thus the solution of the system can be written in the following form:

$$\phi_x = \boldsymbol{R}e^{\boldsymbol{S}x}\boldsymbol{a} \tag{69}$$

where $\boldsymbol{a} \in \mathbb{R}^{2k}$ is a vector of arbitrary constants that will be expressed later in function of the boundary conditions.

Knowing that the eigenvalues verify Hamiltonian properties, we can re-arrange the matrix $\boldsymbol{S}$ and $\boldsymbol{R}$ in the following way:

$$\boldsymbol{S} = \begin{bmatrix} \boldsymbol{S}_1 & & & \\ & -\boldsymbol{S}_1 & & \boldsymbol{0} \\ & & \boldsymbol{S}_2 & \\ & \boldsymbol{0} & & \overline{\boldsymbol{S}_2} \end{bmatrix} = \begin{bmatrix} \boldsymbol{S}_1 & & & \\ & -\boldsymbol{S}_1 & & \boldsymbol{0} \\ & & \boldsymbol{S}_{2r} & \\ & \boldsymbol{0} & & \boldsymbol{S}_{2r} \end{bmatrix} + i \begin{bmatrix} \boldsymbol{0} & & & \\ & \boldsymbol{0} & & \boldsymbol{0} \\ & & \boldsymbol{S}_{2i} & \\ & \boldsymbol{0} & & -\boldsymbol{S}_{2i} \end{bmatrix} = \boldsymbol{S}_r + i\boldsymbol{S}_i \tag{70}$$

$$\boldsymbol{R} = \begin{bmatrix} \boldsymbol{\Phi}_1 & -\boldsymbol{\Phi}_1 & \boldsymbol{\Phi}_2 & \overline{\boldsymbol{\Phi}}_2 \end{bmatrix} = \boldsymbol{R}_r + i\boldsymbol{R}_i \tag{71}$$

where $\boldsymbol{S}_r$, $\boldsymbol{S}_i$, $\boldsymbol{R}_r$ and $\boldsymbol{R}_i$ are real matrices, and i is the complex number verifying $i^2 = -1$.

Proposition 3. *The solution of the differential equation system in (62) can be written in a real form as follows:*

$$\phi_x = (\boldsymbol{R}_r\boldsymbol{Y}_x + \boldsymbol{R}_i\boldsymbol{Z}_x)e^{\boldsymbol{S}_r x}\boldsymbol{a} \tag{72}$$

where

$$\boldsymbol{Y}_x = \begin{bmatrix} \boldsymbol{I} & & & \\ & \boldsymbol{I} & & \boldsymbol{0} \\ & & \boldsymbol{X}_{sx} & \\ & \boldsymbol{0} & & \boldsymbol{X}_{cx} \end{bmatrix}, \quad \boldsymbol{Z}_x = \begin{bmatrix} \boldsymbol{I} & & & \\ & \boldsymbol{I} & & \boldsymbol{0} \\ & & \boldsymbol{X}_{cx} & \\ & \boldsymbol{0} & & \boldsymbol{X}_{sx} \end{bmatrix},$$

$$\boldsymbol{X}_{cx} = cos(\boldsymbol{S}_{2i}x), \quad \boldsymbol{X}_{sx} = sin(\boldsymbol{S}_{2i}x) \tag{73}$$

Proof. See Appendix A.3. □

To complete the solution of our system, we write its particular solution:

$$\phi_{px} = \int_0^x \boldsymbol{R}e^{\boldsymbol{S}(x-t)}\boldsymbol{L}f_t dt = \boldsymbol{R}e^{\boldsymbol{S}x}\int_0^x e^{-\boldsymbol{S}t}\boldsymbol{L}f_t dt \tag{74}$$

where $\boldsymbol{R}$ and $\boldsymbol{L}$ are respectively the right and left eigenvectors, verifying the following relations:

$$\boldsymbol{RL} = \boldsymbol{0}, \quad \boldsymbol{TRSL} = \boldsymbol{I} \tag{75}$$

And:

$$\boldsymbol{f}_x = \begin{Bmatrix} \boldsymbol{f}_1 \\ \boldsymbol{f}_2 \end{Bmatrix} = \begin{Bmatrix} \boldsymbol{B}_{12}\left(\boldsymbol{\Gamma}_{q0} - \boldsymbol{Q}_{11}^{\boldsymbol{T}}\boldsymbol{\varphi}_{l0} - \boldsymbol{Q}_{12}^{\boldsymbol{T}}\boldsymbol{\varphi}_0 + \boldsymbol{p}_1 N x\right) \\ \boldsymbol{p}_2 N - \boldsymbol{B}_{21}^{\boldsymbol{T}}\left(\boldsymbol{\Upsilon}_{l0} - \boldsymbol{D}_{21}\vartheta_0 - \boldsymbol{Q}_{11}\vartheta_{q0} + \boldsymbol{B}_{11}\left(\left(\boldsymbol{\Gamma}_{q0} - \boldsymbol{Q}_{11}^{\boldsymbol{T}}\boldsymbol{\varphi}_{l0} - \boldsymbol{Q}_{12}^{\boldsymbol{T}}\boldsymbol{\varphi}_0\right)x + \boldsymbol{p}_1 N\frac{x^2}{2}\right)\right) \end{Bmatrix} \tag{76}$$

$$\boldsymbol{f}_x = \underbrace{\begin{Bmatrix} \boldsymbol{B}_{12}\left(\boldsymbol{\Gamma}_{q0} - \boldsymbol{Q}_{11}^{\boldsymbol{T}}\boldsymbol{\varphi}_{l0} - \boldsymbol{Q}_{12}^{\boldsymbol{T}}\boldsymbol{\varphi}_0\right) \\ \boldsymbol{p}_2 N - \boldsymbol{B}_{21}^{\boldsymbol{T}}(\boldsymbol{\Upsilon}_{l0} - \boldsymbol{D}_{21}\vartheta_0 - \boldsymbol{Q}_{11}\vartheta_{q0}) \end{Bmatrix}}_{\boldsymbol{g}_1} + \underbrace{\begin{Bmatrix} \boldsymbol{B}_{12}\boldsymbol{p}_1 N \\ -\boldsymbol{B}_{21}^{\boldsymbol{T}}\boldsymbol{B}_{11}\left(\boldsymbol{\Gamma}_{q0} - \boldsymbol{Q}_{11}^{\boldsymbol{T}}\boldsymbol{\varphi}_{l0} - \boldsymbol{Q}_{12}^{\boldsymbol{T}}\boldsymbol{\varphi}_0\right) \end{Bmatrix}}_{\boldsymbol{g}_2} x - \underbrace{\frac{1}{2}\begin{Bmatrix} \boldsymbol{0} \\ \boldsymbol{B}_{21}^{\boldsymbol{T}}\boldsymbol{B}_{11}\boldsymbol{p}_1 N \end{Bmatrix}}_{\boldsymbol{g}_3} x^2 \tag{77}$$

$$\boldsymbol{f}_x = \boldsymbol{g}_1 + \boldsymbol{g}_2 x - \boldsymbol{g}_3 x^2$$

Proposition 4. *For a differential equation system: $\boldsymbol{T}\phi'' + \boldsymbol{U}\phi' - \boldsymbol{V}\phi = \boldsymbol{f}_x$, if the second member $\boldsymbol{f}_x$ has the following form: $\boldsymbol{f}_x = \sum_{i=0}^{n}\boldsymbol{f}_i x^i$, then the particular solution ϕ_p of the system can be written as follows:*

$$\phi_p = -\sum_{i=0}^{n}\boldsymbol{R}\boldsymbol{S}^{-i-1}\boldsymbol{L}f_x^{(i)} \tag{78}$$

where $\boldsymbol{f}_x^{(i)}$ denote the ith derivate of $\boldsymbol{f}_x$ about x.

Proof. See Appendix A.4. □

Thus, the particular solution of our system is:

$$\phi_{px} = -\boldsymbol{V}^{-1}\boldsymbol{f}_x - \boldsymbol{V}^{-1}\boldsymbol{U}\boldsymbol{V}^{-1}(\boldsymbol{g}_2 - 2\boldsymbol{g}_3 x) + 2(\boldsymbol{V}^{-1}\boldsymbol{T}\boldsymbol{V}^{-1} + \boldsymbol{V}^{-1}(\boldsymbol{U}\boldsymbol{V}^{-1})^2)\boldsymbol{g}_3 \tag{79}$$

We can write the total solution of the system:

$$\phi_x = \boldsymbol{W}_x\boldsymbol{a} + \boldsymbol{G}_1\vartheta_{q0} + \boldsymbol{G}_2\vartheta_0 + (\boldsymbol{G}_3 + \boldsymbol{G}_4 x)\left(\boldsymbol{\Gamma}_{q0} - \boldsymbol{Q}_{11}^{\boldsymbol{T}}\boldsymbol{\varphi}_{l0} - \boldsymbol{Q}_{12}^{\boldsymbol{T}}\boldsymbol{\varphi}_0\right) + \boldsymbol{G}_5\boldsymbol{\Upsilon}_{l0} + (\boldsymbol{G}_6 + \boldsymbol{G}_7 x + \boldsymbol{G}_8 x^2)N \tag{80}$$

where

$$\boldsymbol{W}_x = (\boldsymbol{R}_r\boldsymbol{Y}_x + \boldsymbol{R}_i\boldsymbol{Z}_x)e^{\boldsymbol{S}_r x}$$

$$\boldsymbol{G}_1 = -\boldsymbol{V}^{-1}\begin{bmatrix} \boldsymbol{0} \\ \boldsymbol{B}_{21}^{\boldsymbol{T}}\boldsymbol{Q}_{11} \end{bmatrix}, \quad \boldsymbol{G}_2 = -\boldsymbol{V}^{-1}\begin{bmatrix} \boldsymbol{0} \\ \boldsymbol{B}_{21}^{\boldsymbol{T}}\boldsymbol{D}_{21} \end{bmatrix},$$

$$\boldsymbol{G}_3 = \boldsymbol{V}^{-1}\left(\boldsymbol{U}\boldsymbol{V}^{-1}\begin{bmatrix} \boldsymbol{0} \\ \boldsymbol{B}_{21}^{\boldsymbol{T}}\boldsymbol{B}_{11} \end{bmatrix} - \begin{bmatrix} \boldsymbol{B}_{12} \\ \boldsymbol{0} \end{bmatrix}\right), \quad \boldsymbol{G}_4 = \boldsymbol{V}^{-1}\begin{bmatrix} \boldsymbol{0} \\ \boldsymbol{B}_{21}^{\boldsymbol{T}}\boldsymbol{B}_{11} \end{bmatrix}$$

$$\boldsymbol{G}_5 = \boldsymbol{V}^{-1}\begin{bmatrix}\boldsymbol{0}\\ \boldsymbol{B}_{21}^T\end{bmatrix},$$

$$\boldsymbol{G}_6 = \boldsymbol{V}^{-1}\left((\boldsymbol{T}\boldsymbol{V}^{-1} + (\boldsymbol{U}\boldsymbol{V}^{-1})^2)\begin{bmatrix}\boldsymbol{0}\\ \boldsymbol{B}_{21}^T\boldsymbol{B}_{11}\boldsymbol{p}_1\end{bmatrix} - \boldsymbol{U}\boldsymbol{V}^{-1}\begin{bmatrix}\boldsymbol{B}_{12}\boldsymbol{p}_1\\ \boldsymbol{0}\end{bmatrix} - \begin{bmatrix}\boldsymbol{0}\\ \boldsymbol{p}_2\end{bmatrix}\right)$$

$$\boldsymbol{G}_7 = \boldsymbol{V}^{-1}\left(\boldsymbol{U}\boldsymbol{V}^{-1}\begin{bmatrix}\boldsymbol{0}\\ \boldsymbol{B}_{21}^T\boldsymbol{B}_{11}\boldsymbol{p}_1\end{bmatrix} - \begin{bmatrix}\boldsymbol{B}_{12}\boldsymbol{p}_1\\ \boldsymbol{0}\end{bmatrix}\right), \boldsymbol{G}_8 = \frac{1}{2}\boldsymbol{V}^{-1}\begin{bmatrix}\boldsymbol{0}\\ \boldsymbol{B}_{21}^T\boldsymbol{B}_{11}\boldsymbol{p}_1\end{bmatrix}$$

We express the limit conditions at the two extremities of the beam, in $x = 0$ and L:

$$\boldsymbol{\phi}_0 - \boldsymbol{G}_1\vartheta_{q0} - \boldsymbol{G}_2\vartheta_0 - \boldsymbol{G}_3\left(\boldsymbol{\Gamma}_{q0} - \boldsymbol{Q}_{11}^T\boldsymbol{\varphi}_{l0} - \boldsymbol{Q}_{12}^T\boldsymbol{\varphi}_0\right) - \boldsymbol{G}_5\boldsymbol{\Upsilon}_{l0} - \boldsymbol{G}_6 N = \boldsymbol{W}_0\boldsymbol{a} \tag{81}$$

$$\boldsymbol{\phi}_L - \boldsymbol{G}_1\vartheta_{q0} - \boldsymbol{G}_2\vartheta_0 - (\boldsymbol{G}_3 + \boldsymbol{G}_4 L)\left(\boldsymbol{\Gamma}_{q0} - \boldsymbol{Q}_{11}^T\boldsymbol{\varphi}_{l0} - \boldsymbol{Q}_{12}^T\boldsymbol{\varphi}_0\right) - \boldsymbol{G}_5\boldsymbol{\Upsilon}_{l0} - (\boldsymbol{G}_6 + \boldsymbol{G}_7 L + \boldsymbol{G}_8 L^2)N = \boldsymbol{W}_L\boldsymbol{a} \tag{82}$$

We assemble (81) and (82) to obtain the expression of the vector $\boldsymbol{a}$:

$$\boldsymbol{a} = \begin{bmatrix}\boldsymbol{W}_0\\ \boldsymbol{W}_L\end{bmatrix}^{-1} \begin{bmatrix}\boldsymbol{I} & \boldsymbol{0} & -\boldsymbol{G}_1 & -\boldsymbol{G}_2 & -\boldsymbol{G}_3 & -\boldsymbol{G}_5 & -\boldsymbol{G}_6\\ \boldsymbol{0} & \boldsymbol{I} & -\boldsymbol{G}_1 & -\boldsymbol{G}_2 & -(\boldsymbol{G}_3 + \boldsymbol{G}_4 L) & -\boldsymbol{G}_5 & -(\boldsymbol{G}_6 + \boldsymbol{G}_7 L + \boldsymbol{G}_8 L^2)\end{bmatrix} \begin{Bmatrix}\boldsymbol{\phi}_0\\ \boldsymbol{\phi}_L\\ \vartheta_{q0}\\ \vartheta_0\\ \boldsymbol{\Gamma}_{q0} - \boldsymbol{Q}_{11}^T\boldsymbol{\varphi}_{l0} - \boldsymbol{Q}_{12}^T\boldsymbol{\varphi}_0\\ \boldsymbol{\Upsilon}_{l0}\\ N\end{Bmatrix}$$

Thus, we can express the vector $\boldsymbol{a}$ in function of the boundary values:

$$\boldsymbol{a} = \boldsymbol{H}_0\boldsymbol{\phi}_0 + \boldsymbol{H}_L\boldsymbol{\phi}_L + \boldsymbol{H}_1\vartheta_{q0} + \boldsymbol{H}_2\vartheta_0 + \boldsymbol{H}_3\left(\boldsymbol{\Gamma}_{q0} - \boldsymbol{Q}_{11}^T\boldsymbol{\varphi}_{l0} - \boldsymbol{Q}_{12}^T\boldsymbol{\varphi}_0\right) + \boldsymbol{H}_4\boldsymbol{\Upsilon}_{l0} + \boldsymbol{H}_5 N \tag{83}$$

And by noting: $\boldsymbol{H}_{2\phi}\boldsymbol{\phi}_0 = [\boldsymbol{0}\quad \boldsymbol{H}_2]\begin{Bmatrix}\boldsymbol{\varphi}_0\\ \vartheta_0\end{Bmatrix}$, $\boldsymbol{G}_{2\phi} = [\boldsymbol{0}\quad \boldsymbol{G}_2]$, $\boldsymbol{H}_{3\phi} = [\boldsymbol{H}_3\boldsymbol{Q}_{12}^T\quad \boldsymbol{0}]$, $\boldsymbol{G}_{i\phi} = [\boldsymbol{G}_i\boldsymbol{Q}_{12}^T\quad \boldsymbol{0}]$, $i = 3,4$ We can re-express our solution in the following form:

$$\boldsymbol{\phi}_x = (\boldsymbol{G}_{2\phi} + \boldsymbol{G}_{3\phi} + \boldsymbol{G}_{4\phi}x + \boldsymbol{W}_x(\boldsymbol{H}_0 + \boldsymbol{H}_{2\phi} + \boldsymbol{H}_{3\phi}))\boldsymbol{\phi}_0 + \boldsymbol{W}_x\boldsymbol{H}_L\boldsymbol{\phi}_L + (\boldsymbol{G}_1 + \boldsymbol{W}_x\boldsymbol{H}_1)\vartheta_{q0} + (\boldsymbol{G}_3 + \boldsymbol{G}_4 x + \boldsymbol{W}_x\boldsymbol{H}_3)\left(\boldsymbol{\Gamma}_{q0} - \boldsymbol{Q}_{11}^T\boldsymbol{\varphi}_{l0}\right) + (\boldsymbol{G}_5 + \boldsymbol{W}_x\boldsymbol{H}_4)\boldsymbol{\Upsilon}_{l0} + (\boldsymbol{G}_6 + \boldsymbol{G}_7 x + \boldsymbol{G}_8 x^2 + \boldsymbol{W}_x\boldsymbol{H}_5)N \tag{84}$$

$$\boldsymbol{\phi}_x = \boldsymbol{E}_{\eta x}\boldsymbol{\eta}_{0L} + \boldsymbol{E}_{\Xi x}\boldsymbol{\Xi}_{0L} \tag{85}$$

where: $\boldsymbol{\eta}_x = \begin{Bmatrix}u\\ \vartheta_q\\ \boldsymbol{\varphi}_l\\ \boldsymbol{\phi}\end{Bmatrix}$, $\boldsymbol{\eta}_{0L} = \begin{Bmatrix}\boldsymbol{\eta}_0\\ \boldsymbol{\eta}_L\end{Bmatrix}$, $\boldsymbol{\Xi}_x = \begin{Bmatrix}N\\ \boldsymbol{\Gamma}_q\\ \boldsymbol{\Upsilon}_l\\ \boldsymbol{\Upsilon}\\ \boldsymbol{\Gamma}\end{Bmatrix}$, $\boldsymbol{\Xi}_{0L} = \begin{Bmatrix}\boldsymbol{\Xi}_0\\ \boldsymbol{\Xi}_L\end{Bmatrix}$

$$\boldsymbol{E}_{\eta x} = [\boldsymbol{0}\quad \boldsymbol{G}_1 + \boldsymbol{W}_x\boldsymbol{H}_1\quad -(\boldsymbol{G}_3 + \boldsymbol{G}_4 x + \boldsymbol{W}_x\boldsymbol{H}_3)\boldsymbol{Q}_{11}^T\quad \boldsymbol{G}_{23} + \boldsymbol{G}_{4\phi}x + \boldsymbol{W}_x\boldsymbol{H}_{023}\quad \boldsymbol{0}\ \boldsymbol{0}\ \boldsymbol{0}\quad \boldsymbol{W}_x\boldsymbol{H}_L] \tag{86}$$

$$\boldsymbol{E}_{\Xi x} = [(\boldsymbol{G}_6 + \boldsymbol{G}_7 x + \boldsymbol{G}_8 x^2 + \boldsymbol{W}_x\boldsymbol{H}_5)\quad \boldsymbol{G}_3 + \boldsymbol{G}_4 x + \boldsymbol{W}_x\boldsymbol{H}_3\quad \boldsymbol{G}_5 + \boldsymbol{W}_x\boldsymbol{H}_4\quad \boldsymbol{0}\ \boldsymbol{0}\ \boldsymbol{0}\ \boldsymbol{0}\ \boldsymbol{0}] \tag{87}$$

And: $\boldsymbol{H}_{023} = \boldsymbol{H}_0 + \boldsymbol{H}_{2\phi} + \boldsymbol{H}_{3\phi}$, $\boldsymbol{G}_{23} = \boldsymbol{G}_{2\phi} + \boldsymbol{G}_{3\phi}$

We note:

$$\boldsymbol{\phi}_{-1x} = \int_0^x \boldsymbol{\phi}_t dt = \boldsymbol{E}_{-1,\eta x}\boldsymbol{\eta}_{0L} + \boldsymbol{E}_{-1,\Xi x}\boldsymbol{\Xi}_{0L},\ \boldsymbol{E}_{-1,\eta x} = \int_0^x \boldsymbol{E}_{\eta t}dt,\ \boldsymbol{E}_{-1,\Xi x} = \int_0^x \boldsymbol{E}_{\Xi t}dt \tag{88}$$

$$\boldsymbol{\phi}_{-2x} = \int_0^x \boldsymbol{\phi}_{-1t}dt = \boldsymbol{E}_{-2,\eta x}\boldsymbol{\eta}_{0L} + \boldsymbol{E}_{-2,\Xi x}\boldsymbol{\Xi}_{0L},\ \boldsymbol{E}_{-2,\eta x} = \int_0^x \boldsymbol{E}_{-1,\eta t}dt,\ \boldsymbol{E}_{-2,\Xi x} = \int_0^x \boldsymbol{E}_{-1,\Xi t}dt \tag{89}$$

$$\boldsymbol{\phi}_{1x} = \boldsymbol{\phi}_x' = \boldsymbol{E}_{1,\eta x}\boldsymbol{\eta}_{0L} + \boldsymbol{E}_{1,\Xi x}\boldsymbol{\Xi}_{0L},\ \boldsymbol{E}_{1,\eta x} = \frac{d\boldsymbol{E}_{\eta x}}{dx},\ \boldsymbol{E}_{1,\Xi x} = \frac{d\boldsymbol{E}_{\Xi x}}{dx} \tag{90}$$

For the calculation of the integrals and derivative of $\boldsymbol{\phi}_x$, see Appendix A.5.

By using the solution of the system, we obtain ϑ that we can replace in the third equation of (61) to obtain $\boldsymbol{\varphi}_l'$ and by integrating we obtain $\boldsymbol{\varphi}_l$ in function of the boundary conditions:

$$\begin{aligned}&\boldsymbol{\varphi}_l' = \boldsymbol{B}_{21}\vartheta + \boldsymbol{h}_x\\ &\boldsymbol{\varphi}_l = \boldsymbol{\varphi}_{l0} + \boldsymbol{h}_{-1x} + \boldsymbol{B}_{21}\int_0^x \vartheta dt\\ &\boldsymbol{\varphi}_l = \boldsymbol{\varphi}_{l0} + \boldsymbol{h}_{-1x} + \boldsymbol{B}_{21}\boldsymbol{A}_\vartheta(\boldsymbol{E}_{-1,\eta x}\boldsymbol{\eta}_{0L} + \boldsymbol{E}_{-1,\Xi x}\boldsymbol{\Xi}_{0L})\\ &\Rightarrow\ \boldsymbol{\varphi}_l = \boldsymbol{F}_{\eta x}\boldsymbol{\eta}_{0L} + \boldsymbol{F}_{\Xi x}\boldsymbol{\Xi}_{0L}\end{aligned} \tag{91}$$

where $\boldsymbol{A}_\vartheta = [\boldsymbol{0}\quad \boldsymbol{I}]$, $\boldsymbol{h}_{-1x} = \int_0^x \boldsymbol{h}_t dt = (\boldsymbol{\Upsilon}_{l0} - \boldsymbol{D}_{21}\vartheta_0 - \boldsymbol{Q}_{11}\vartheta_{q0})x + \boldsymbol{B}_{11}\left(\left(\boldsymbol{\Gamma}_{q0} - \boldsymbol{Q}_{11}^T\boldsymbol{\varphi}_{l0} - \boldsymbol{Q}_{12}^T\boldsymbol{\varphi}_0\right)\frac{x^2}{2} + \boldsymbol{p}_1 N\frac{x^3}{6}\right)$.

With $\boldsymbol{\varphi}$ and $\boldsymbol{\varphi}_l$ obtained, we can replace then in the second equation of (61) to obtain ϑ_q' and by integrating we obtain ϑ_q in function of the boundary conditions:

$$\begin{aligned}&\vartheta_q' = \boldsymbol{\Gamma}_{q0} - \boldsymbol{Q}_{11}^T\boldsymbol{\varphi}_{l0} - \boldsymbol{Q}_{12}^T\boldsymbol{\varphi}_0 - \boldsymbol{B}_{11}^T\boldsymbol{\varphi}_l - \boldsymbol{B}_{12}^T\boldsymbol{\varphi}\\ &\vartheta_q' = \boldsymbol{\Gamma}_{q0} - \boldsymbol{Q}_{11}^T\boldsymbol{\varphi}_{l0} - \boldsymbol{Q}_{12}^T\boldsymbol{\varphi}_0 - \boldsymbol{B}_{11}^T(\boldsymbol{\varphi}_{l0} + \boldsymbol{h}_{-1x} + \boldsymbol{B}_{21}\boldsymbol{A}_\vartheta\boldsymbol{\phi}_{-1x}) - \boldsymbol{B}_{12}^T\boldsymbol{A}_\varphi\boldsymbol{\phi}_x\\ &\vartheta_q = \vartheta_{q0} + \left(\boldsymbol{\Gamma}_{q0} - \boldsymbol{Q}_{11}^T\boldsymbol{\varphi}_{l0} - \boldsymbol{Q}_{12}^T\boldsymbol{\varphi}_0\right)x - \boldsymbol{B}_{11}^T(\boldsymbol{\varphi}_{l0}x + \boldsymbol{h}_{-2x} + \boldsymbol{B}_{21}^T\boldsymbol{A}_\vartheta(\boldsymbol{E}_{-2,\eta x}\boldsymbol{\eta}_{0L} + \boldsymbol{E}_{-2,\Xi x}\boldsymbol{\Xi}_{0L})) - \boldsymbol{B}_{12}A_\varphi(\boldsymbol{E}_{-1,\eta x}\boldsymbol{\eta}_{0L} + \boldsymbol{E}_{-1,\Xi x}\boldsymbol{\Xi}_{0L})\\ &\Rightarrow \vartheta_q = \boldsymbol{H}_{\eta x}\boldsymbol{\eta}_{0L} + \boldsymbol{H}_{\Xi x}\boldsymbol{\Xi}_{0L}\end{aligned} \tag{92}$$

where $\boldsymbol{A}_\varphi = [\boldsymbol{I}\quad \boldsymbol{0}]$, $\boldsymbol{h}_{-2x} = \int_0^x \boldsymbol{h}_{-1t}dt = (\boldsymbol{\Upsilon}_{l0} - \boldsymbol{D}_{21}\vartheta_0 - \boldsymbol{Q}_{11}\vartheta_{q0})\frac{x^2}{2} + \boldsymbol{B}_{11}\left(\left(\boldsymbol{\Gamma}_{q0} - \boldsymbol{Q}_{11}^T\boldsymbol{\varphi}_{l0} - \boldsymbol{Q}_{12}^T\boldsymbol{\varphi}_0\right)\frac{x^3}{6} + \boldsymbol{p}_1 N\frac{x^4}{24}\right)$.

The resolution is completed by performing a simple variable change to obtain the original vectors ξ and ζ. To derive the rigidity matrix, we will as in Ferradi et al. [4], assemble all the equilibrium equations that we will express at the two extremities of the beam, in $x = 0$ and $x = L$.

From (47) and (59) we have:

$$\begin{cases}\boldsymbol{\Upsilon} = \boldsymbol{\varphi}' + \boldsymbol{Q}_{12}\vartheta_q + \boldsymbol{Q}_{22}\vartheta\\ \boldsymbol{\Gamma} = \vartheta' + \boldsymbol{D}_{21}^T\boldsymbol{\varphi}_l + \boldsymbol{D}_{22}^T\boldsymbol{\varphi}\end{cases} \Rightarrow \begin{Bmatrix}\boldsymbol{\Upsilon}\\ \boldsymbol{\Gamma}\end{Bmatrix} = \boldsymbol{E}_{1,\eta x}\boldsymbol{\eta}_{0L} + \boldsymbol{E}_{1,\Xi x}\boldsymbol{\Xi}_{0L} + \begin{bmatrix}\boldsymbol{0} & \boldsymbol{Q}_{12} & \boldsymbol{0} & \boldsymbol{0} & \boldsymbol{Q}_{22}\\ \boldsymbol{0} & \boldsymbol{0} & \boldsymbol{D}_{21}^T & \boldsymbol{D}_{22}^T & \boldsymbol{0}\end{bmatrix}\boldsymbol{\eta}_x \tag{93}$$

This system is expressed at the two extremities of the beam, at $x = 0$ and $x = L$, so we obtain $2k$ equations:

$$\begin{Bmatrix}\boldsymbol{\Upsilon}_0\\ \boldsymbol{\Gamma}_0\boldsymbol{\Upsilon}_L\\ \boldsymbol{\Gamma}_L\end{Bmatrix} - \begin{bmatrix}\boldsymbol{E}_{1,\Xi 0}\\ \boldsymbol{E}_{1,\Xi L}\end{bmatrix}\boldsymbol{\Xi}_{0L} = \left(\begin{bmatrix}\boldsymbol{E}_{1,\eta 0}\\ \boldsymbol{E}_{1,\eta L}\end{bmatrix} + \begin{bmatrix}\boldsymbol{0} & \boldsymbol{Q}_{12} & \boldsymbol{0} & \boldsymbol{0} & \boldsymbol{Q}_{22} & & & & & \\ \boldsymbol{0} & \boldsymbol{0} & \boldsymbol{D}_{21}^T & \boldsymbol{D}_{22}^T & \boldsymbol{0} & & & & & \\ & & & & & \boldsymbol{0} & \boldsymbol{Q}_{12} & \boldsymbol{0} & \boldsymbol{0} & \boldsymbol{Q}_{22}\\ & & & & & \boldsymbol{0} & \boldsymbol{0} & \boldsymbol{D}_{21}^T & \boldsymbol{D}_{22}^T & \boldsymbol{0}\end{bmatrix}\right)\boldsymbol{\eta}_{0L}$$

Table 1
The transversal modes with their corresponding warping modes for the beam models used in the listed figures.

	Beam model (type of cross section)	Transversal modes	Corresponding warping modes
Fig. 5	A (1D)	1	5
		2–3	1
Fig. 6	A (2D)	1	4
		2–3	1
	B (2D)	1	2
		2–3	1
Fig. 7	A (2D)	1	2
		2–10	1
	B (2D)	1	2
		2–12	1
	C (2D)	1	2
		2–20	1
	D (2D)	1	2
		2–3	1
Fig. 8	A (2D)	1	2
		2–3	1
	B (2D)	1	2
		2–20	1
Fig. 12	A (2D)	1	2
		2–3	1
	B (2D)	1	2
		2–6	1
	C (2D)	1	2
		2–10	1
Fig. 14	A (2D); B (1D)	1	5
		2	1
		3	4
Fig. 15	A (2D)	1	5
		2	1
		3	4
		4–6	1
	B (2D)	1	2
		2–3	1

Table 2
The transversal modes with their corresponding warping modes for the beam models used in the listed figures.

	Beam model (type of cross section)	Transversal modes	Corresponding warping modes
Fig. 18	A (1D)	1	2
		2–3	1
	B (1D)	1	2
		2–6	1
	C (1D)	1	2
		2–10	1
	D (2D)	1	2
		2–10	1
Fig. 19	A (1D)	1	4
		2	1
		3	4
	B (2D)	1	4
		2	1
		3	4
Fig. 20	A (1D)	1	4
		2	1
		3	4
	B (2D)	1	4
		2	1
		3	4

We also have from (47) and (59) the expression of the generalized efforts vectors $\boldsymbol{\Gamma}_q$ and $\boldsymbol{\Upsilon}_l$, that we will express in function of the boundary values:

$$\begin{cases} \boldsymbol{\Gamma}_q = \boldsymbol{\vartheta}_q' + \boldsymbol{D}_{11}^T\boldsymbol{\varphi}_l + \boldsymbol{D}_{12}^T\boldsymbol{\varphi} \\ \boldsymbol{\Upsilon}_l = \boldsymbol{\varphi}_l' + \boldsymbol{Q}_{11}\boldsymbol{\vartheta}_q + \boldsymbol{Q}_{21}\boldsymbol{\vartheta} \end{cases} \Rightarrow \begin{Bmatrix} \boldsymbol{\Gamma}_q \\ \boldsymbol{\Upsilon}_l \end{Bmatrix} = \begin{bmatrix} \boldsymbol{H}_{1,\eta x} \\ F_{1,\eta x} \end{bmatrix}\boldsymbol{\eta}_{0L} + \begin{bmatrix} \boldsymbol{H}_{1,\Xi x} \\ F_{1,\Xi x} \end{bmatrix}\boldsymbol{\Xi}_{0L} + \begin{bmatrix} \boldsymbol{0} & \boldsymbol{0} & \boldsymbol{D}_{11}^T & \boldsymbol{D}_{12}^T & \boldsymbol{0} \\ \boldsymbol{0} & \boldsymbol{Q}_{11} & \boldsymbol{0} & \boldsymbol{0} & \boldsymbol{Q}_{21} \end{bmatrix}\boldsymbol{\eta}_x \tag{95}$$

where $\boldsymbol{F}_{1,\eta x} = \frac{d\boldsymbol{F}_{\eta x}}{dx}$, $\boldsymbol{F}_{1,\Xi x} = \frac{d\boldsymbol{F}_{\Xi x}}{dx}$, $\boldsymbol{H}_{1,\eta x} = \frac{d\boldsymbol{H}_{\eta x}}{dx}$, $\boldsymbol{H}_{1,\Xi x} = \frac{d\boldsymbol{H}_{\Xi x}}{dx}$.

We express (95) only at $x = L$, to obtain $q + l$ equations:

$$\begin{Bmatrix} \boldsymbol{\Gamma}_{qL} \\ \boldsymbol{\Upsilon}_{lL} \end{Bmatrix} - \begin{bmatrix} \boldsymbol{H}_{1,\Xi L} \\ \boldsymbol{F}_{1,\Xi L} \end{bmatrix}\boldsymbol{\Xi}_{0L} = \begin{bmatrix} \boldsymbol{H}_{1,\eta L} \\ \boldsymbol{F}_{1,\eta L} \end{bmatrix}\boldsymbol{\eta}_{0L} + \begin{bmatrix} \boldsymbol{0} & \boldsymbol{0} & \boldsymbol{D}_{11}^T & \boldsymbol{D}_{12}^T & \boldsymbol{0} \\ \boldsymbol{0} & \boldsymbol{Q}_{11} & \boldsymbol{0} & \boldsymbol{0} & \boldsymbol{Q}_{21} \end{bmatrix}\boldsymbol{\eta}_L \tag{96}$$

By expressing $\boldsymbol{\vartheta}_q$ and $\boldsymbol{\varphi}_l$ at $x = L$, we obtain the remaining $q + l$ equations:

$$\begin{bmatrix} \boldsymbol{H}_{\Xi L} \\ \boldsymbol{F}_{\Xi L} \end{bmatrix}\boldsymbol{\Xi}_{0L} = \left(\begin{bmatrix} \boldsymbol{H}_{\eta L} \\ \boldsymbol{F}_{\eta L} \end{bmatrix} - \begin{bmatrix} \boldsymbol{0} & \boldsymbol{0} & \boldsymbol{0} & \boldsymbol{0} & \boldsymbol{0} & \boldsymbol{0} & \boldsymbol{I} & \boldsymbol{0} & \boldsymbol{0} & \boldsymbol{0} \\ \boldsymbol{0} & \boldsymbol{0} & \boldsymbol{0} & \boldsymbol{0} & \boldsymbol{0} & \boldsymbol{0} & \boldsymbol{0} & \boldsymbol{I} & \boldsymbol{0} & \boldsymbol{0} \end{bmatrix}\right)\boldsymbol{\eta}_{0L} \tag{97}$$

And finally from the integration of the first equation in (61) and the equilibrium equation $\frac{dN}{dx} = 0$, we add the two following Eqs. (98) and (99):

$$\begin{aligned} u_L - u_0 &= \frac{N_0 L}{(2\mu+\lambda)S} - \boldsymbol{p}_1 \cdot \int_0^L \vartheta_q dx - \boldsymbol{p}_2 \cdot \int_0^L \vartheta dx \\ u_L - u_0 &= \frac{N_0 L}{(2\mu+\lambda)S} - \boldsymbol{p}_1 \cdot (\boldsymbol{H}_{-1,\eta x}\boldsymbol{\eta}_{0L} + \boldsymbol{H}_{-1,\Xi x}\boldsymbol{\Xi}_{0L}) \\ &\quad - \boldsymbol{p}_2 \cdot \boldsymbol{A}_\vartheta(\boldsymbol{E}_{-1,\eta x}\boldsymbol{\eta}_{0L} + \boldsymbol{E}_{-1,\Xi x}\boldsymbol{\Xi}_{0L}) \\ \Rightarrow u_L - u_0 &+ (\boldsymbol{H}_{-1,\eta x}^T\boldsymbol{p}_1 + \boldsymbol{E}_{-1,\eta x}^T\boldsymbol{A}_\vartheta^T\boldsymbol{p}_2)\cdot\boldsymbol{\eta}_{0L} \\ &= \frac{N_0 L}{(2\mu+\lambda)S} - \left(\boldsymbol{H}_{-1,\Xi x}^T\boldsymbol{p}_1 + \boldsymbol{E}_{-1,\Xi x}^T\boldsymbol{A}_\vartheta^T\boldsymbol{p}_2\right)\cdot\boldsymbol{\Xi}_{0L} \end{aligned} \tag{98}$$

$$N_L - N_0 = 0 \tag{99}$$

where $\boldsymbol{F}_{-1,\eta x} = \int_0^x \boldsymbol{F}_{\eta t} dt$, $\boldsymbol{F}_{-1,\Xi x} = \int_0^x \boldsymbol{F}_{\Xi t} dt$, $\boldsymbol{H}_{-1,\eta x} = \int_0^x \boldsymbol{H}_{\eta t} dt$, $\boldsymbol{H}_{-1,\Xi x} = \int_0^x \boldsymbol{H}_{\Xi t} dt$.

Thus, by assembling all these equations we obtain a system of 2(m + n+1) equations, written in the following form:

$$\boldsymbol{K}_\Xi\boldsymbol{\Xi}_{0L} = \boldsymbol{K}_\eta\boldsymbol{\eta}_{0L} \Rightarrow \boldsymbol{\Xi}_{0L} = \underbrace{\boldsymbol{K}_\Xi^{-1}\boldsymbol{K}_\eta}_{\boldsymbol{K}_r}\boldsymbol{\eta}_{0L} \tag{100}$$

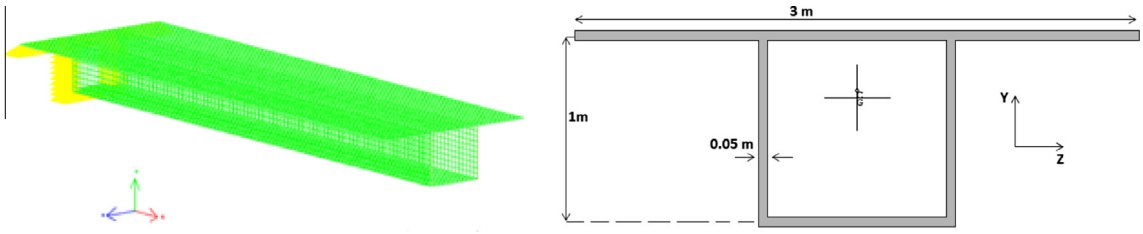

Fig. 3. A view of the shell model of the beam andits cross section.

$\boldsymbol{K}_r$ is then the rigidity matrix of the beam element, derived from the exact solution of the equilibrium equation. This matrix was implemented in Pythagore™ software.

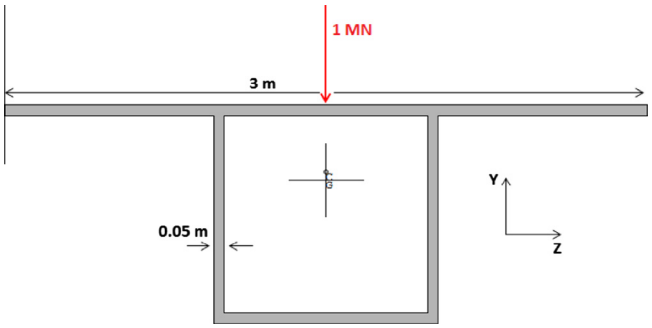

Fig. 4. Beam cross section with the centred applied load.

An important remark concern the case of quasi-incompressible materials ($\upsilon \mapsto 0.5 \Rightarrow \lambda \mapsto +\infty$), where a special attention must be given to the transversal modes we are using in our kinematics to avoid incompressible locking. In the expression of the stress tensor in Eq. (23), we have the apparition of the stress $\sigma_r = \lambda \operatorname{tr}(\boldsymbol{\varepsilon}) = \lambda\left(\frac{du}{dx} + \zeta^i \operatorname{div}\boldsymbol{\psi}^i + \Omega_j \frac{d\xi_j}{dx}\right)$, thus when $\lambda \mapsto +\infty$ we need to be able represent $\operatorname{tr}(\boldsymbol{\varepsilon}) = 0$, and this can be assured by associating to every warping mode Ω_j, a transversal deformation mode $\boldsymbol{\psi}^{j*}$, constructed in a way to compensate the warping mode, and thus to satisfy $\operatorname{tr}(\boldsymbol{\varepsilon}) = 0$ when it's needed. These newly determined transversal modes will be called 'incompressible deformation modes' and will verify the relation $\operatorname{div}\boldsymbol{\psi}^{j*} = \Omega_j$. We have also noticed that even for $0 < \upsilon < 0.5$ (for example $\upsilon = 0.3$ for steel) the error in the results cannot be negligible if we do not consider the 'incompressible deformation modes', thus we have chosen in all our examples to take $\upsilon = 0$ to avoid any discrepancy, noting that this subject will be treated in detail in upcoming work.

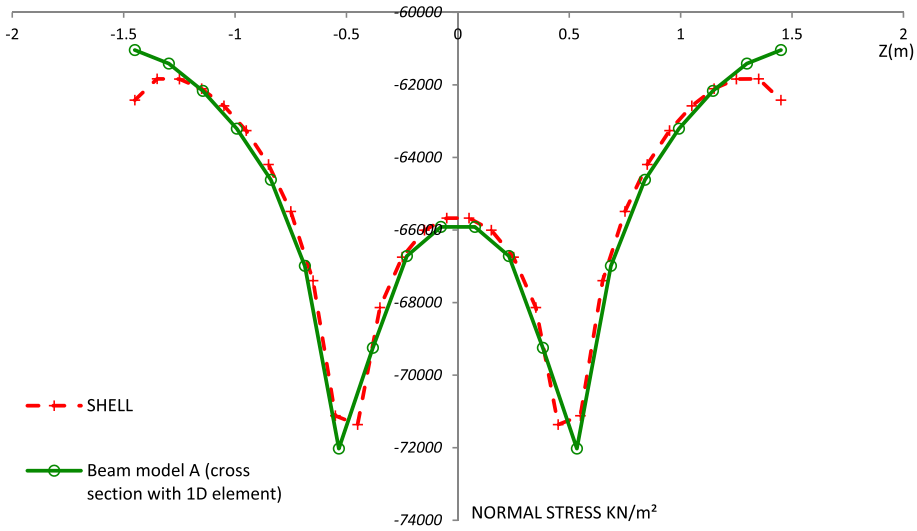

Fig. 5. Comparison of the normal stresses between the shell and the beam model, at $x = 0.05$ m and at mid-depth of the upper slab (Ty = −1 MN).

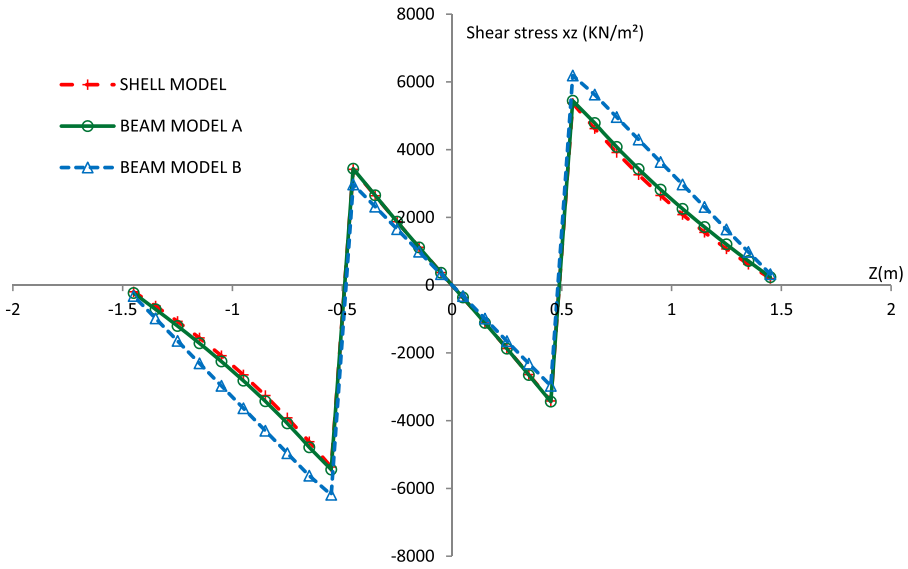

Fig. 6. Comparison of the shear stress xz between the shell and the beam models, at $x = 0.95$ m and at mid-depth of the upper slab (Ty = −1 MN).

5. The generalized effort vector

We have the displacement vector of an arbitrary point P of the section:

$$\boldsymbol{d}_p=\begin{Bmatrix}u_p\\ v_p\\ w_p\end{Bmatrix}=\begin{Bmatrix}u+\sum_{j=1}^{m}\Omega_j\xi_j\\ \sum_{i=1}^{n}\psi_y^i\zeta^i\\ \sum_{i=1}^{n}\psi_z^i\zeta^i\end{Bmatrix}\Rightarrow \boldsymbol{d}_p=\underbrace{\begin{bmatrix}1 & 0 & \dots & 0 & \Omega_1 & \dots & \Omega_m\\ 0 & \psi_y^1 & \dots & \psi_y^n & 0 & \dots & 0\\ 0 & \psi_z^1 & \dots & \psi_z^n & 0 & \dots & 0\end{bmatrix}}_{\boldsymbol{F}}\underbrace{\begin{Bmatrix}u\\ \zeta^1\\ \vdots\\ \zeta^n\\ \xi_1\\ \vdots\\ \xi_m\end{Bmatrix}}_{\boldsymbol{d}} \tag{101}$$

where **d** is the vector representing the generalized coordinates.

If we apply at the point P a force represented by its vector $\boldsymbol{f}_p$, we will have the following equivalent generalized stress resultants:

$$\boldsymbol{f}_p=\begin{Bmatrix}N\\ T_y\\ T_z\end{Bmatrix}\Rightarrow \boldsymbol{f}=\boldsymbol{F}^T\boldsymbol{f}_p\Rightarrow \boldsymbol{f}=\begin{Bmatrix}N\\ \psi_y^1T_y+\psi_z^1T_z\\ \vdots\\ \psi_y^nT_y+\psi_z^nT_z\\ \Omega_1N\\ \vdots\\ \Omega_mN\end{Bmatrix} \tag{102}$$

6. Numerical examples

In all the examples presented in this section, we will perform three types of comparisons, one concerns the comparison of the displacement at the section where the load is applied and where the effect of the higher transversal modes will be important, the second concerns the normal stress at $x = 0.05$ m the vicinity of the fixed end, where the effect of restrained warping is the most

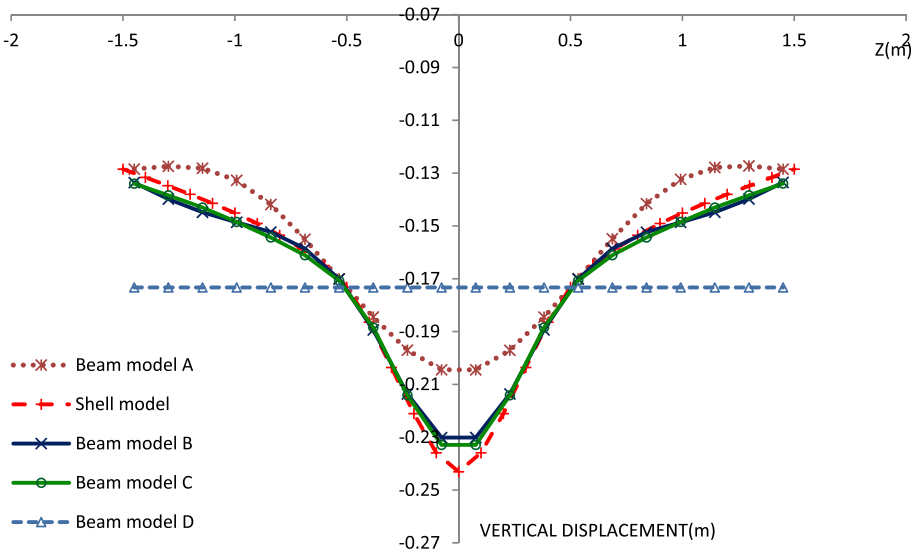

Fig. 7. Comparison of the displacement between the shell and the beam models, at $x = 10$ m and at mid-depth of the upper slab (Ty = −1 MN).

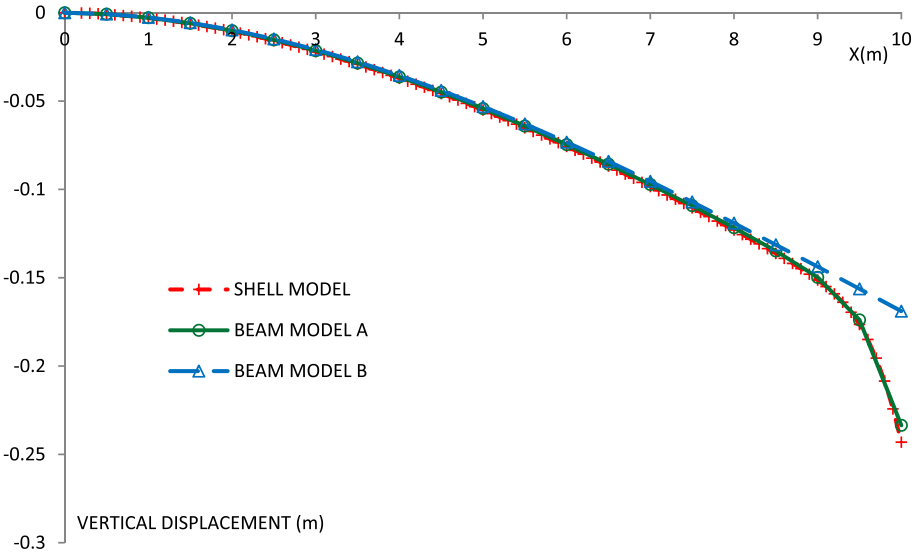

Fig. 8. Comparison of the vertical displacement along the beam length between the shell and the beam models.

important and the effect of the higher warping modes are non-negligible and the third concerns the shear stress in the upper slab at $x = 0.95$ m.

For all the figures representing the numerical results, the Tables 1 and 2 give the transversal modes used for each beam model in the figure and the number of corresponding warping modes used for each transversal mode and gives also the type of cross section used in the beam models, 1D if the cross section is discretized with 1D (or beam) element and 2D if it's discretized with triangular element.

6.1. Box girder

We consider in the following examples a 10 m length cantilever beam, with $E = 40$ GPa and $\upsilon = 0$, loaded at its free end. The comparisons will be performed between a shell model of the cantilever beam using the well-known MITC- 4 shell element described in [10], and a model with just *one element* of the new beam finite element, using different numbers of transversal modes. All comparisons have been performed with Pythagore™ Software.

The boundary conditions of the considered example are:

- No displacement at the beam's bearing: $u = 0$, $\xi_j = 0$, $\zeta^i = 0$ for all warping and transversal modes.
- At the free end: $\frac{d\xi_j}{dx} = 0$, $\frac{d\zeta^i}{dx} = 0$.

For the beam cross section we choose a box girder represented in Fig. 3. Some numerical values for the matrices in p. 12 are given in Appendix A.7.

The beam cross section will be discretized in two manners, the first one with 7024 2D triangular elements, and the second one as a thin walled section with 6 1D elements. For the representation of the warping and transversal modes see Appendix A.6.

For the shell model of the beam, to obtain accurate results we use a refined meshing, where the dimension of the small square element is 0.1 m, the model will then comport 6000 shell element, 6060 nodes and 36 360 degree of freedom. To measure the effect of

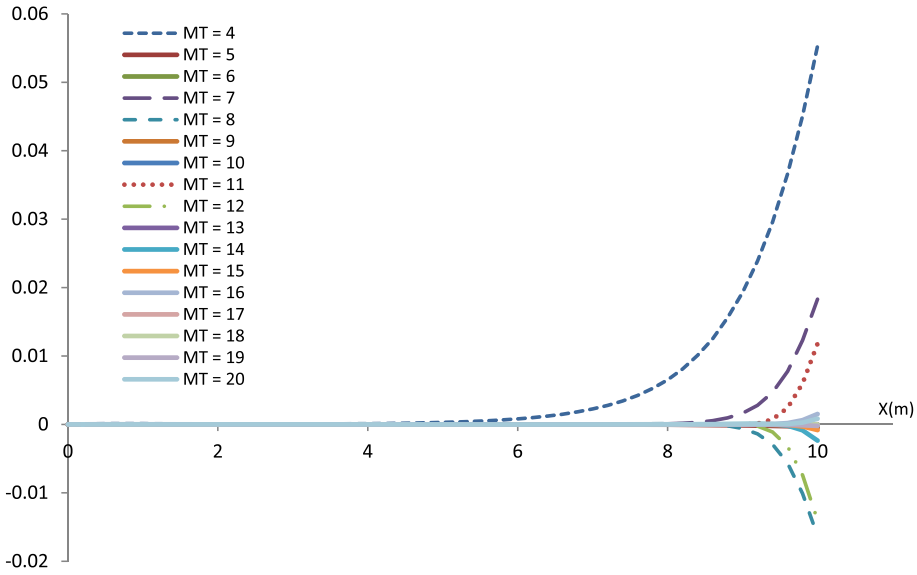

Fig. 9. representation of the generalized coordinates associated with the higher transversal modes (4–20) along the beam's length, for the beam model C in Fig. 7.

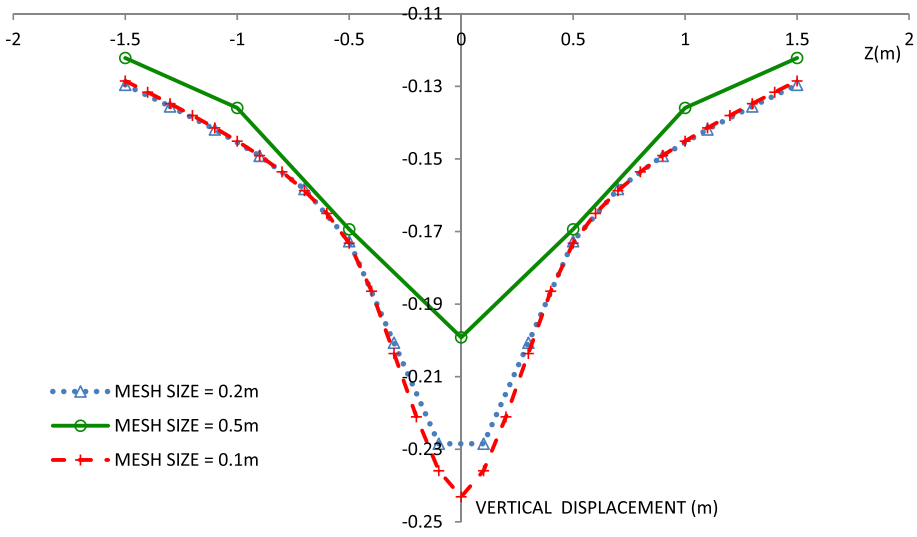

Fig. 10. Comparison of the results obtained from the shell model with different mesh size.

the meshing refinement and its necessity for the shell model of the beam, we will compare the different results obtained from shell models with different meshing.

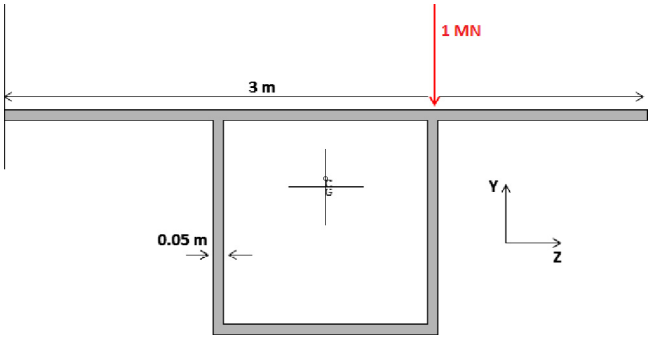

Fig. 11. Beam cross section with the excentred applied load.

We consider as a first load case a centred force $T_y = -1$ MN at the upper slab of the box cross section and at the free end of the cantilever beam, see Fig. 4.

The Fig. 5 illustrate the fact that in this example the shear lag effect near the fixed end is correctly predicted by using five warping modes for the vertical displacement mode. Fig. 6 shows that we have a precise representation of shear stress distribution with only three transversal modes (rigid body motion) and four warping modes associated to the vertical displacement mode.

In Fig. 7, we can see that the beam model B (12 transversal modes) gives satisfactory results that still can be refined by using more transversal modes, and this is performed with the beam model C (20 transversal modes). We can see also from Fig. 7 that at the connections between the upper slab and the two webs ($z = -0.5$ m and $z = 0.5$ m), the vertical displacement is exactly the one corresponding to a rigid body motion, and this is valid for the shell and all the beam models. Figs. 8 and 9 shows that the effect of the higher order transversal modes become more and more important when we approach the loading zone, Fig. 8 shows also that we obtain a precise description of the vertical

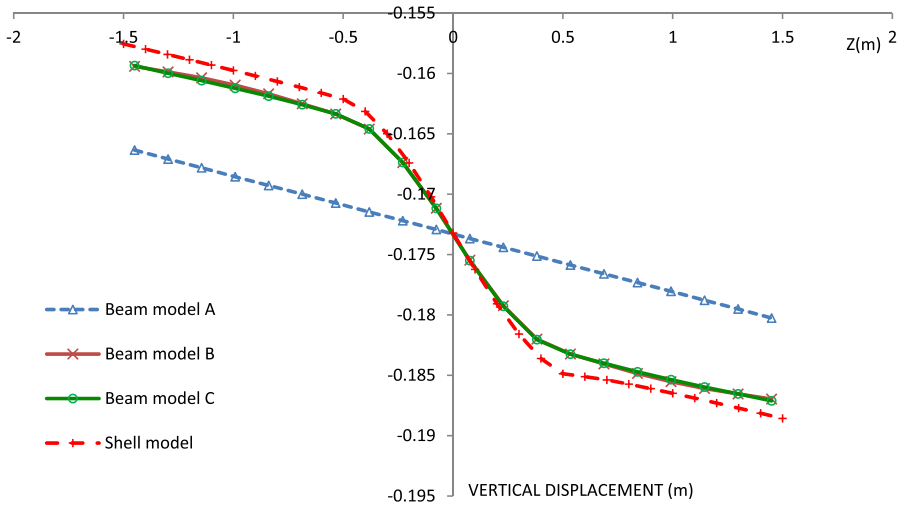

Fig. 12. Comparison of the displacement between the shell and the beam models, at $x = 10$ m and at mid-depth of the upper slab (Ty = −1 MN).

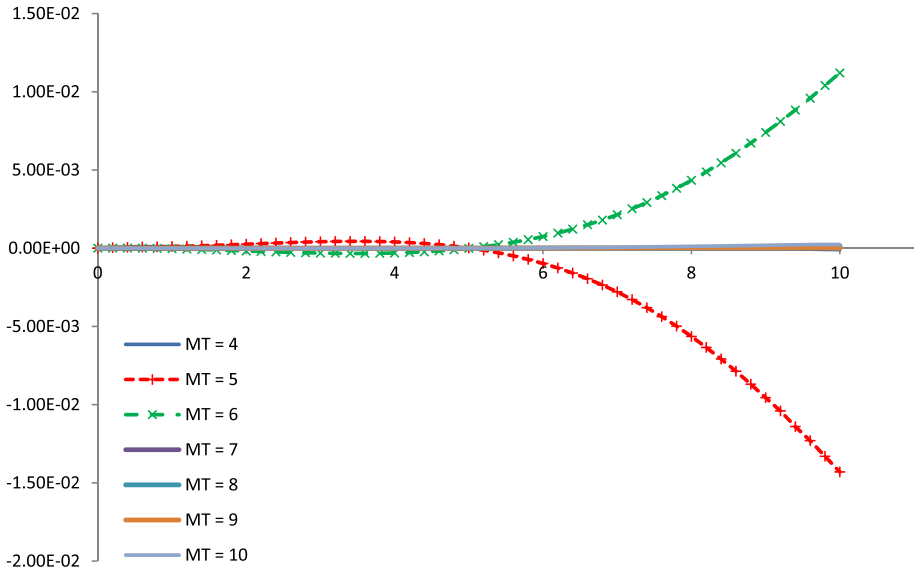

Fig. 13. representation of the generalized coordinates associated to the higher transversal modes (4–10) along the beam's length, for the beam model B in Fig. 12.

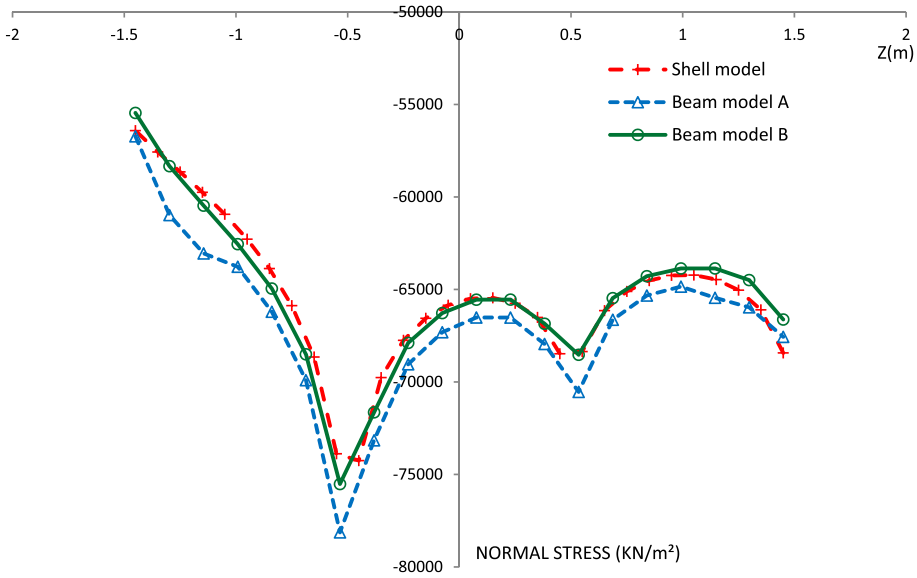

Fig. 14. Comparison of the normal stresses between the shell and the beam model, at $x = 0.05$ m and at mid-depth of the upper slab (Ty = −1 MN).

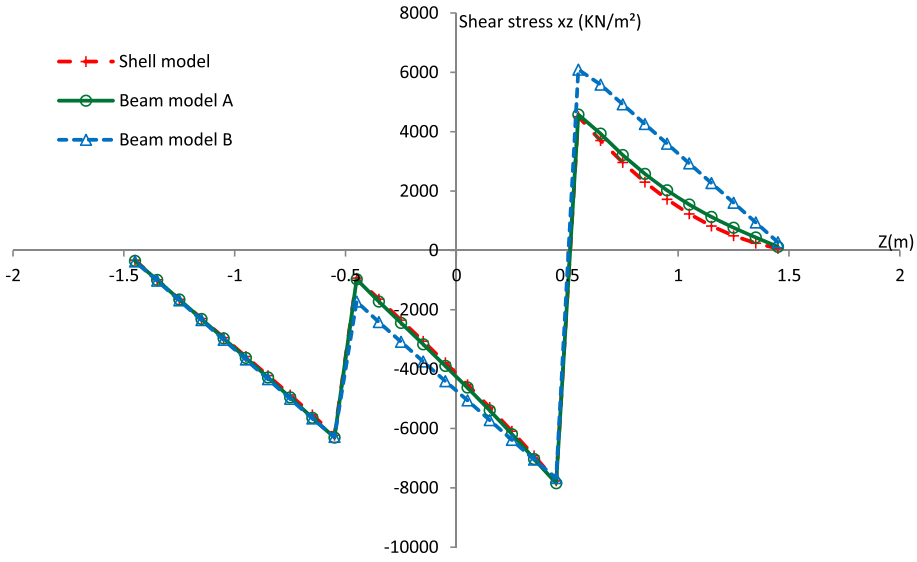

Fig. 15. Comparison of the shear stress *xz* between the shell and the beam models, at $x = 0.95$ m and at mid-depth of the upper slab (Ty = −1 MN).

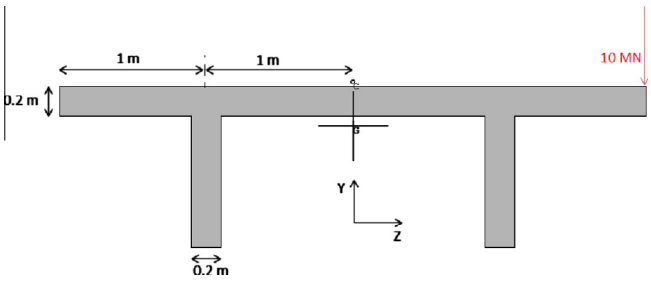

Fig. 16. A view of the beam cross section.

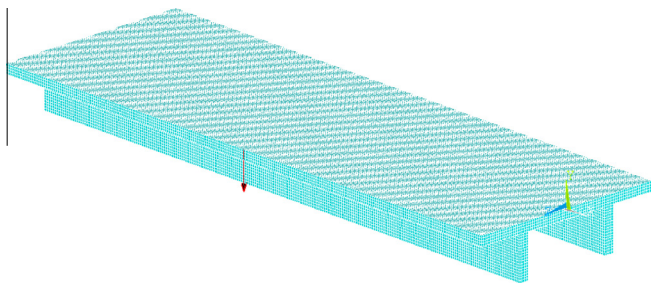

Fig. 17. A view of the brick model of the beam.

displacement distribution along the beam, especially near the loading zone.

From Fig. 10, we deduce that the refined shell model of the beam, with a mesh size equal to 0.1 m, is necessary to obtain accurate prediction of the vertical displacement at the loading cross section. This model has 6000 shell elements, 6060 nodes, with a total of 36360 d.o.f., and compared to the beam model B with *one beam element* and twelve transversal modes, with a total of 50 d.o.f., it shows the advantage of using such enriched beam

element, even if it necessitate some preliminary cross section treatment to obtain the transversal and warping modes characteristics, because this step will be done only once and we can after perform as many calculation as we want with different loadings and configurations with the same reduced number of degree of freedom. We can see also that solving the equilibrium equations exactly, allows us to obtain accurate results without using a refined meshing of our beam element, and this is showed in the numerical examples where only one beam element is needed.

As a second load case, we apply the same vertical force $T_y = -1$MN at the upper slab but eccentric from the centre of gravity and torsion ($z = 0.5$ m), see Fig. 11.

From Fig. 12, we obtain satisfactory result with only six transversal modes, and always with just *one beam element*, which corresponds to a model with a total of 28 d.o.f. Fig. 13 shows that only the fifth and the sixth transversal modes give a substantial contribution to represent the beam behaviour; this is in accordance with the results of Fig. 12, where there is no difference in the displacement distribution obtained with a beam model enriched with 6 or 10 transversal modes.

Figs. 14 and 15 compare the stress distribution between shell and beam models, the results clearly show the effectiveness of the enriched beam model.

6.2. Double T cross section

In this example we consider a 12 m beam clamped at its both end and loaded with an eccentric ($z = 2$ m) vertical force of 10MN in its middle ($x = 6$ m), see Figs. 16 and 17, the material characteristics will be the same as the previous example. We will use *two beam finite elements* to discretize the whole beam. To test the performance of our beam element, we will perform a comparison with

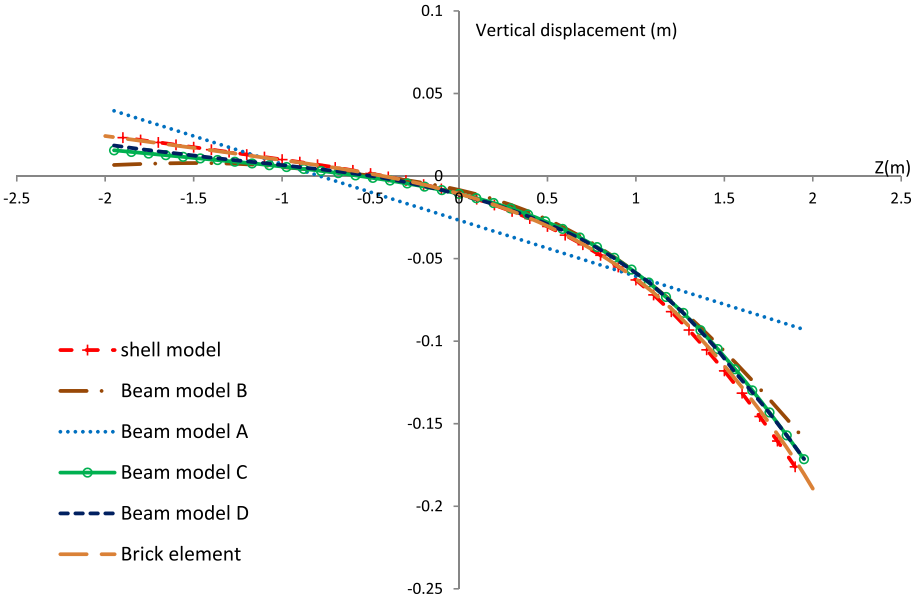

Fig. 18. Comparison of the displacement between the brick, shell and the beam models, at $x = 6$ m and at mid-depth of the upper slab (Ty = −10 MN).

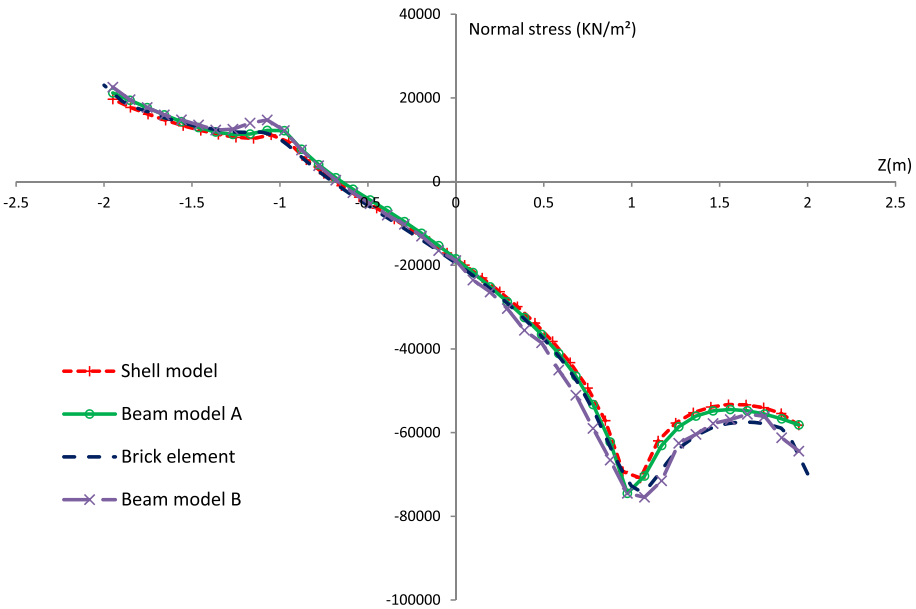

Fig. 19. Comparison of the normal stresses between the brick, shell and beam model, at $x = 0.05$ m and at mid-depth of the upper slab (Ty = −10 MN).

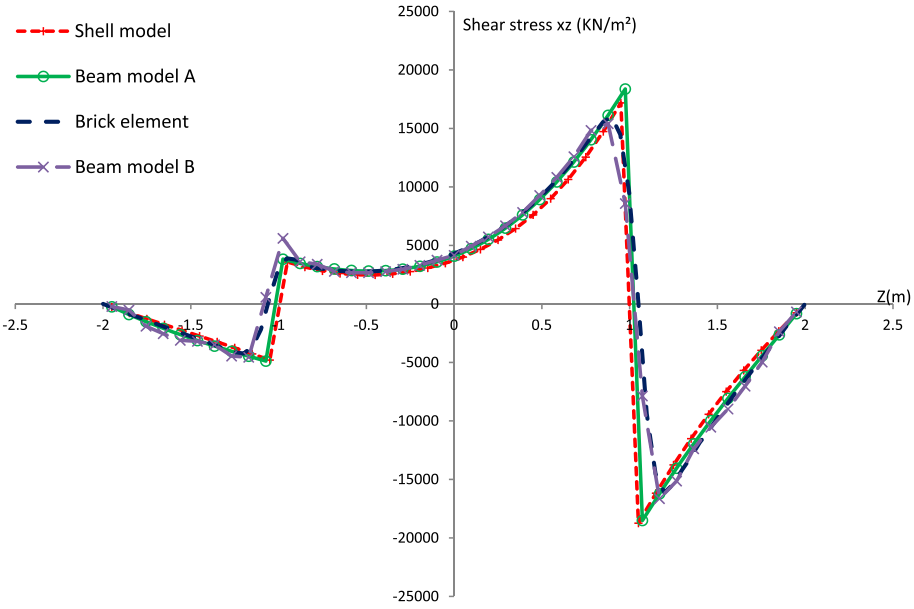

Fig. 20. Comparison of the shear stress *xz* between the brick shell and beam models, at $x = 0.95$ m and at mid-depth of the upper slab (Ty = −10 MN).

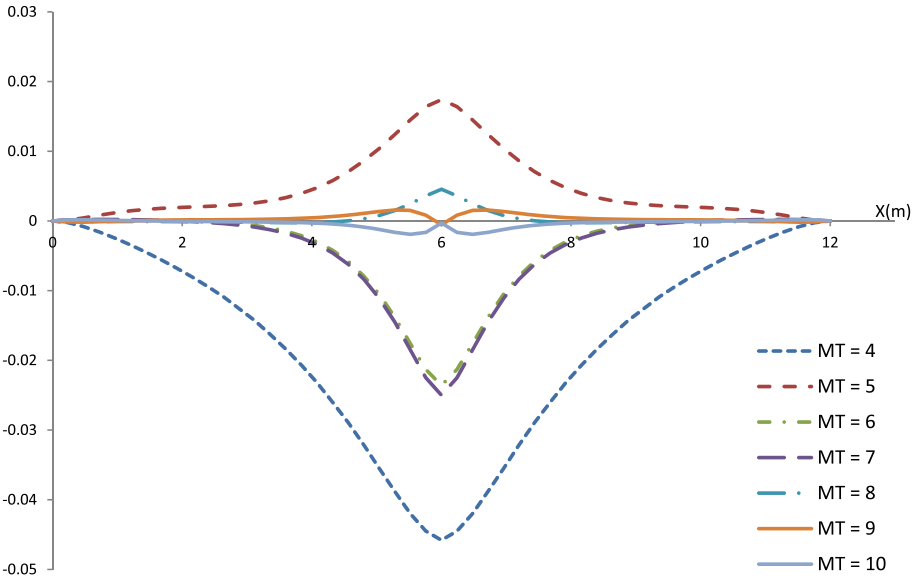

Fig. 21. representation of the generalized coordinates associated to the higher transversal modes (4–10) along the beam's length, for the beam model C in Fig. 18.

a shell (MITC-4 element) and a brick (SOLID186 in Ansys™) model of the beam (Fig. 17).

Figs. 18–20 illustrate the comparison between a brick & shell models of the beam with our beam finite element models, showing the efficiency and the accuracy of our formulation. We note from Figs. 19 and 20 that the beam models B, with a cross section meshed with 2D triangular element is more close to the brick model. The beam models A, with a cross section meshed with 1D elements can be more closely compared to the shell model. In Fig. 21 we have the distribution in the beam length of the higher transversal modes coordinates.

7. Conclusion

In this work, we have presented a new beam finite element based on a new enhanced kinematics, enriched with transversal and warping eigenmodes, capable of representing the deformation and the displacement field of the beam in a very accurate way. A complete description of the method to derive these modes for an arbitrary section form is given. Theoretically we can determine as many warping modes as we want to enrich our kinematics, but we have observed that the number of modes that we can derive accurately is limited, due to the numerical errors accumulated in every new iteration of the iterative equilibrium process.

The additional transversal and warping modes give rise to new equilibrium equations associated with the newly introduced d.o.f. corresponding to each mode, forming a system of differential equations that can be assimilated to a one obtained from a gyroscopic system in an unstable state. An exact solution of these equations is performed, leading to the formulation of the rigidity matrix of a mesh free element. However we must note a limitation to this formulation: we need to calculate the exponential of a scalar

(corresponding to an eigenvalue of the equation system) multiplied by the beam's length, if this product is great enough, its exponential cannot be calculated in the range of a classical machine precision, a solution would be to discretize sufficiently the beam to reduce the length of the beam elements, or to eliminate the corresponding mode associated to this eigenvalue.

Appendix A

A.1. Stiffness matrices for the triangular and the 1D element

For the 1D element, we use the stiffness matrix of a planar Euler–Bernoulli element, expressed by:

$$\boldsymbol{K}_b = \begin{bmatrix} \frac{ES}{l} & 0 & 0 & -\frac{ES}{l} & 0 & 0 \\ & \frac{12EI}{l^3} & \frac{6EI}{l^2} & 0 & -\frac{12EI}{l^3} & \frac{6EI}{l^2} \\ & & \frac{4EI}{l} & 0 & -\frac{6EI}{l^2} & \frac{2EI}{l} \\ & & & \frac{ES}{l} & 0 & 0 \\ & sym & & & \frac{12EI}{l^3} & -\frac{6EI}{l^2} \\ & & & & & \frac{4EI}{l} \end{bmatrix} \tag{a.1}$$

where $S = t^2$ is the surface, t the thin walled profile thickness, 1 its length and $I = t^4/12$ its inertia.

For the triangular element, we use the rigidity matrix in planar stress, expressed by:

$$\boldsymbol{K}_t = \frac{Et}{4\Delta(1-\upsilon)} = \begin{bmatrix} a_1^2+\alpha b_1^2 & (\alpha+\upsilon)a_1b_1 & a_1a_2+\alpha b_1b_2 & \upsilon a_1b_2+\alpha a_2b_1 & a_1a_3+\alpha b_1b_3 & \upsilon a_1b_3+\alpha a_3b_1 \\ & b_1^2+\alpha a_1^2 & \upsilon a_2b_1+\lambda a_1b_2 & b_1b_2+\alpha a_1a_2 & \upsilon a_3b_1+\alpha a_1b_3 & a_1a_3+\alpha b_1b_3 \\ & & a_2^2+\alpha b_2^2 & (\upsilon+\alpha)a_2b_2 & a_2a_3+\alpha b_2b_3 & \upsilon a_2b_3+\alpha a_3b_2 \\ & & & b_2^2+\alpha a_2^2 & \upsilon a_3b_2+\alpha a_2b_3 & a_2a_3+\alpha b_2b_3 \\ & sym & & & a_3^2+\alpha b_3^2 & (\upsilon+\alpha)a_3b_3 \\ & & & & & b_3^2+\alpha a_3^2 \end{bmatrix}$$

where Δ is the triangular element surface, t its thickness and $\alpha = (1-\upsilon)/2$.

And for (x_1,y_1), (x_2,y_2), (x_3,y_3) the triangular element nodes coordinate we have:

$$a_1 = y_2 - y_3, \quad a_2 = y_3 - y_1, \quad a_3 = y_1 - y_2$$
$$b_1 = x_3 - x_2, \quad b_2 = x_1 - x_3, \quad b_3 = x_2 - x_1$$

A.2. Derivation of the warping functions for thin walled profiles

For thin walled profiles we make two approximations:

- The tangential shear stress in the cross section is tangential to the thin walled profile.
- The tangential shear stress is constant in the thin walled profile thickness.

The expression of the tangential shear stress vector is given by:

$$\boldsymbol{\tau} = \mu(\boldsymbol{\psi} - \nabla\Omega)\frac{d\zeta}{dx}$$

$$\tau_s = \boldsymbol{\tau}\cdot\boldsymbol{t}$$

$$\tau_s = \mu(\boldsymbol{\psi}\cdot\boldsymbol{t} - \nabla\Omega\cdot\boldsymbol{t})\frac{d\zeta}{dx} \Rightarrow \frac{\partial\Omega}{\partial s} = \boldsymbol{\psi}\Rightarrow \boldsymbol{t} - \frac{\tau_s}{\mu\frac{d\zeta}{dx}} \tag{a.3}$$

where $\boldsymbol{t}$ is the tangential vector to the thin walled profile, and $\nabla\Omega\cdot\boldsymbol{t} = \frac{\partial\Omega}{\partial s}$.

For a section free to warp, we have as already written:

$$\frac{\partial u_p}{\partial x} = 0 \Rightarrow \Omega\frac{d^2\zeta}{dx^2} = 0 \Rightarrow \frac{d\zeta}{dx} = cst$$

We consider then that $\mu\frac{d\zeta}{dx} = \frac{1}{J}$, with J a constant. We can then write:

$$\frac{\partial\Omega}{\partial s} = \boldsymbol{\psi}\cdot\boldsymbol{t} - J\tau_s \Rightarrow \frac{\partial^2\Omega}{\partial s^2} = \frac{\partial}{\partial s}(\boldsymbol{\psi}\cdot\boldsymbol{t}) - J\frac{\partial\tau_s}{\partial s} \tag{a.4}$$

We write the equilibrium equation of the beam:

$$\frac{\partial\sigma_{xx}}{\partial x} + \operatorname{div}\boldsymbol{\tau} = \frac{\partial\sigma_{xx}}{\partial x} + \frac{\partial\tau_s}{\partial s} = 0$$
$$J\frac{\partial\tau_s}{\partial s} = -\frac{\lambda}{\mu}\operatorname{div}\boldsymbol{\psi} \tag{a.5}$$

After replacing this in the Eq. (a.2), we obtain:

$$\frac{\partial^2\Omega}{\partial s^2} = \frac{\partial}{\partial s}(\boldsymbol{\psi}\cdot\boldsymbol{t}) + \frac{\lambda}{\mu}\operatorname{div}\boldsymbol{\psi} \tag{a.6}$$

By integrating this equation twice, we obtain Ω as a function of its limit values in the extremities of the thin walled profile. After assembling the equations expressing Ω for each thin profile constituting the section, we obtain a system of equations that can be solved to an additive constant, thus to solve the problem uniquely we add the condition $\int_A \Omega dA = 0$.

A.3. Proof of Proposition 3

We replace the obtained solution $\boldsymbol{R}e^{\boldsymbol{S}x}\boldsymbol{a}$ in the equation system:

$$(\boldsymbol{TRS}^2 + \boldsymbol{URS} - \boldsymbol{VR})e^{\boldsymbol{S}x}\boldsymbol{a} = \boldsymbol{0} \tag{a.7}$$

This relation is valid for an arbitrary vector $\boldsymbol{a}$, thus:

$$\boldsymbol{TRS}^2 + \boldsymbol{URS} - \boldsymbol{VR} = \boldsymbol{0} \tag{a.8}$$

By developing this relation we obtain:

$$\begin{aligned} &\left(\boldsymbol{T}\left(\boldsymbol{R}_r\left(\boldsymbol{S}_r^2 - \boldsymbol{S}_i^2\right) - 2\boldsymbol{R}_i\boldsymbol{S}_i\boldsymbol{S}_r\right) + \boldsymbol{U}(\boldsymbol{R}_r\boldsymbol{S}_r - \boldsymbol{R}_i\boldsymbol{S}_i) - \boldsymbol{VR}_r\right) \\ &\quad + i\left(\boldsymbol{T}\left(\boldsymbol{R}_i\left(\boldsymbol{S}_r^2 - \boldsymbol{S}_i^2\right) + 2\boldsymbol{R}_r\boldsymbol{S}_i\boldsymbol{S}_r\right)\right. \\ &\quad \left.+\boldsymbol{U}(\boldsymbol{R}_r\boldsymbol{S}_i + \boldsymbol{R}_i\boldsymbol{S}_r) - \boldsymbol{VR}_i\right) = \boldsymbol{0} \end{aligned} \tag{a.9}$$

Thus, we have the following two formulas:

$$\boldsymbol{T}\left(\boldsymbol{R}_r\left(\boldsymbol{S}_r^2 - \boldsymbol{S}_i^2\right) - 2\boldsymbol{R}_i\boldsymbol{S}_i\boldsymbol{S}_r\right) + \boldsymbol{U}(\boldsymbol{R}_r\boldsymbol{S}_r - \boldsymbol{R}_i\boldsymbol{S}_i) - \boldsymbol{VR}_r = \boldsymbol{0} \tag{a.10}$$

$$\boldsymbol{T}\left(\boldsymbol{R}_i\left(\boldsymbol{S}_r^2 - \boldsymbol{S}_i^2\right) + 2\boldsymbol{R}_r\boldsymbol{S}_i\boldsymbol{S}_r\right) + \boldsymbol{U}(\boldsymbol{R}_r\boldsymbol{S}_i + \boldsymbol{R}_i\boldsymbol{S}_r) - \boldsymbol{VR}_i = \boldsymbol{0} \tag{a.11}$$

We calculate now the first and second derivate of $\phi_x = (\boldsymbol{R}_r\boldsymbol{Y} + \boldsymbol{R}_i\boldsymbol{Z})e^{\boldsymbol{S}_r x}\boldsymbol{a}$:

$$\phi_x' = (\boldsymbol{R}_r\boldsymbol{S}_r\boldsymbol{Y} + \boldsymbol{R}_r\boldsymbol{S}_i\boldsymbol{Z} + \boldsymbol{R}_i\boldsymbol{S}_r\boldsymbol{Z} - \boldsymbol{R}_i\boldsymbol{S}_i\boldsymbol{Y})e^{\boldsymbol{S}_r x}\boldsymbol{a}$$
$$\phi_x'' = \left(\boldsymbol{R}_r\left(\boldsymbol{S}_r^2 - \boldsymbol{S}_i^2\right)\boldsymbol{Y} + 2\boldsymbol{R}_r\boldsymbol{S}_i\boldsymbol{S}_r\boldsymbol{Z} + \boldsymbol{R}_i\left(\boldsymbol{S}_r^2 - \boldsymbol{S}_i^2\right)\boldsymbol{Z} - 2\boldsymbol{R}_i\boldsymbol{S}_i\boldsymbol{S}_r\boldsymbol{Y}\right)e^{\boldsymbol{S}_r x}\boldsymbol{a}$$

We replace the expressions of the derivatives in the equation system (62) to obtain:

$$\begin{aligned} \boldsymbol{T}\phi_x'' + \boldsymbol{U}\phi_x' - \boldsymbol{V}\phi_x = &\left(\boldsymbol{T}\left(\boldsymbol{R}_r\left(\boldsymbol{S}_r^2 - \boldsymbol{S}_i^2\right) - 2\boldsymbol{R}_i\boldsymbol{S}_i\boldsymbol{S}_r\right)\right. \\ &+\boldsymbol{U}(\boldsymbol{R}_r\boldsymbol{S}_r - \boldsymbol{R}_i\boldsymbol{S}_i) - \boldsymbol{VR}_r)e^{\boldsymbol{S}_r x}\boldsymbol{Ya} \\ &+\left(\boldsymbol{T}\left(\boldsymbol{R}_i\left(\boldsymbol{S}_r^2 - \boldsymbol{S}_i^2\right) + 2\boldsymbol{R}_r\boldsymbol{S}_i\boldsymbol{S}_r\right)\right. \\ &\left.+\boldsymbol{U}(\boldsymbol{R}_r\boldsymbol{S}_i + \boldsymbol{R}_i\boldsymbol{S}_r) - \boldsymbol{VR}_i)e^{\boldsymbol{S}_r x}\boldsymbol{Za}\right. \end{aligned} \tag{a.12}$$

Thus, from the Eqs. (a.10) and (a.11) that we replace in (a.12), we obtain $\boldsymbol{T}\phi_x'' + \boldsymbol{U}\phi_x' - \boldsymbol{V}\phi_x = \boldsymbol{0}$, which verify that $\phi_x = (\boldsymbol{R}_r\boldsymbol{Y} + \boldsymbol{R}_i\boldsymbol{Z})e^{\boldsymbol{S}_r x}\boldsymbol{a}$ is a solution of the system.

A.4. Proof of Proposition 4

We suppose that the second member $\boldsymbol{f}$ is of the form $\boldsymbol{f}_x = \boldsymbol{f}_n \boldsymbol{x}^n$, we suppose then that the particular solution will be given by:

$$\boldsymbol{\phi}_p = -\sum_{i=0}^{n} \boldsymbol{R}\boldsymbol{S}^{-i-1}\boldsymbol{L}\boldsymbol{f}_x^{(i)} = -\sum_{i=0}^{n} \boldsymbol{R}\boldsymbol{S}^{-i-1}\boldsymbol{L}\boldsymbol{f}_n x^{n-i}\frac{n!}{(n-i)!} \tag{a.13}$$

We calculate the expression of $\boldsymbol{V}\boldsymbol{\phi}_p, \boldsymbol{U}\boldsymbol{\phi}'_p$ and $\boldsymbol{T}\boldsymbol{\phi}''_p$:

$$\begin{aligned}
\boldsymbol{V}\boldsymbol{\phi}_p &= -\sum_{i=0}^{n} \boldsymbol{V}\boldsymbol{R}\boldsymbol{S}^{-i-1}\boldsymbol{L}\boldsymbol{f}_n x^{n-i}\frac{n!}{(n-i)!} \\
&= -\boldsymbol{V}\boldsymbol{R}\boldsymbol{S}^{-1}\boldsymbol{L}\boldsymbol{f}_n x^n - \boldsymbol{V}\boldsymbol{R}\boldsymbol{S}^{-2}\boldsymbol{L}\boldsymbol{f}_n n x^{n-1} - \sum_{i=2}^{n} \boldsymbol{V}\boldsymbol{R}\boldsymbol{S}^{-i-1}\boldsymbol{L}\boldsymbol{f}_n x^{n-i}\frac{n!}{(n-i)!} \\
\boldsymbol{U}\boldsymbol{\phi}'_p &= -\sum_{i=0}^{n-1} \boldsymbol{U}\boldsymbol{R}\boldsymbol{S}^{-i-1}\boldsymbol{L}\boldsymbol{f}_n x^{n-i-1}\frac{n!}{(n-i-1)!} \\
&= -\boldsymbol{U}\boldsymbol{R}\boldsymbol{S}^{-1}\boldsymbol{L}\boldsymbol{f}_n n x^{n-1} - \sum_{i=2}^{n} \boldsymbol{U}\boldsymbol{R}\boldsymbol{S}^{-i}\boldsymbol{L}\boldsymbol{f}_n x^{n-i}\frac{n!}{(n-i)!} \\
\boldsymbol{T}\boldsymbol{\phi}''_p &= -\sum_{i=0}^{n-2} \boldsymbol{T}RS^{-i-1}\boldsymbol{L}\boldsymbol{f}_n x^{n-i-2}\frac{n!}{(n-i-2)!} \\
&= -\sum_{i=2}^{n} \boldsymbol{T}RS^{-i+1}\boldsymbol{L}\boldsymbol{f}_n x^{n-i}\frac{n!}{(n-i)!}
\end{aligned}$$

Thus:

$$\begin{aligned}
\boldsymbol{T}\boldsymbol{\phi}''_p + \boldsymbol{U}\boldsymbol{\phi}'_p - \boldsymbol{V}\boldsymbol{\phi}_p &= \boldsymbol{V}\boldsymbol{R}\boldsymbol{S}^{-1}\boldsymbol{L}\boldsymbol{f}_n x^n - (\boldsymbol{U}\boldsymbol{R}\boldsymbol{S} - \boldsymbol{V}\boldsymbol{R})\boldsymbol{S}^{-2}\boldsymbol{L}\boldsymbol{f}_n n x^{n-1} \\
&\quad -\sum_{i=2}^{n} (\boldsymbol{T}RS^2 + \boldsymbol{U}\boldsymbol{R}\boldsymbol{S} - \boldsymbol{V}\boldsymbol{R})\boldsymbol{S}^{-i-1}\boldsymbol{L}\boldsymbol{f}_n x^{n-i}\frac{n!}{(n-i)!}
\end{aligned} \tag{a.14}$$

By using the following relations deduced from the Eq. (75):

$$\boldsymbol{T}\boldsymbol{R}\boldsymbol{S}^2 + \boldsymbol{U}\boldsymbol{R}\boldsymbol{S} - \boldsymbol{V}\boldsymbol{R} = \boldsymbol{0}, (\boldsymbol{U}\boldsymbol{R}\boldsymbol{S} - \boldsymbol{V}\boldsymbol{R})\boldsymbol{S}^{-2}\boldsymbol{L} = \boldsymbol{T}\boldsymbol{R}\boldsymbol{L} = \boldsymbol{0}, \boldsymbol{R}\boldsymbol{S}^{-1}\boldsymbol{L} = \boldsymbol{V}^{-1}$$

We verify that: $\boldsymbol{T}\boldsymbol{\phi}''_p + \boldsymbol{U}\boldsymbol{\phi}'_p - \boldsymbol{V}\boldsymbol{\phi}_p = \boldsymbol{f}_n x^n$, thus $\boldsymbol{\phi}_p$ is a particular solution system, and by the superposition principle, its straightforward that for a second member in the differential equation system of the form $\boldsymbol{f}_x = \sum_{i=0}^{n} \boldsymbol{f}_i x^i$ the particular solution is $\boldsymbol{\phi}_p = -\sum_{i=0}^{n} \boldsymbol{R}\boldsymbol{S}^{-i-1}\boldsymbol{L}\boldsymbol{f}_x^{(i)}$.

A.5

In the calculation of the integrals and the derivative of $\boldsymbol{\phi}_x$ expressed in the relations (85)–(87), the only difficulty is the calculation of the integrals and derivative of $\boldsymbol{W}_x = (\boldsymbol{R}_r\boldsymbol{Y}_x + \boldsymbol{R}_i\boldsymbol{Z}_x)\boldsymbol{e}^{\boldsymbol{S}_r x}$ used in its expression. Thus, we want to calculate the expression of $\boldsymbol{W}_{-1x}$, $\boldsymbol{W}_{-2x}$, $\boldsymbol{W}_{-3x}$ and $\boldsymbol{W}_{1x}$:

$$\begin{aligned}
\boldsymbol{W}_{-1x} &= \int_0^x \boldsymbol{W}_t dt, \quad \boldsymbol{W}_{-2x} = \int_0^x \boldsymbol{W}_{-1t} dt, \quad \boldsymbol{W}_{-3x} \\
&= \int_0^x \boldsymbol{W}_{-2t} dt, \quad \boldsymbol{W}_{1x} = \boldsymbol{W}'_x
\end{aligned} \tag{a.15}$$

We have the expression of $\boldsymbol{W}_x$:

$$\begin{aligned}
\boldsymbol{W}_x &= (\boldsymbol{R}_r\boldsymbol{Y}_x + \boldsymbol{R}_i\boldsymbol{Z}_x)\boldsymbol{e}^{\boldsymbol{S}_r x} \\
&= \left(\boldsymbol{R}_r \begin{bmatrix} e^{\boldsymbol{S}_1 x} & & & \\ & e^{-\boldsymbol{S}_1 x} & & 0 \\ & & \boldsymbol{X}_{sx} e^{\boldsymbol{S}_{2r} x} & \\ & 0 & & \boldsymbol{X}_{cx} e^{\boldsymbol{S}_{2r} x} \end{bmatrix} + \boldsymbol{R}_i \begin{bmatrix} e^{\boldsymbol{S}_1 x} & & & \\ & e^{-\boldsymbol{S}_1 x} & & 0 \\ & & \boldsymbol{X}_{cx} e^{\boldsymbol{S}_{2r} x} & \\ & 0 & & \boldsymbol{X}_{sx} e^{\boldsymbol{S}_{2r} x} \end{bmatrix} \right)
\end{aligned} \tag{a.16}$$

If we note $\boldsymbol{Q} = \begin{bmatrix} \boldsymbol{0} & & & \boldsymbol{0} \\ & \boldsymbol{0} & & \\ & & \boldsymbol{0} & \boldsymbol{I} \\ \boldsymbol{0} & & \boldsymbol{I} & \boldsymbol{0} \end{bmatrix}$ and $\boldsymbol{R}_{ri} = \boldsymbol{R}_r + \boldsymbol{R}_i\boldsymbol{Q}$ then we can express $\boldsymbol{W}_x$ in the following form:

$$\boldsymbol{W}_x = \boldsymbol{R}_{ri} \begin{bmatrix} e^{\boldsymbol{S}_1 x} & & & \\ & e^{-\boldsymbol{S}_1 x} & & 0 \\ & & \boldsymbol{X}_{sx} e^{\boldsymbol{S}_{2r} x} & \\ & 0 & & \boldsymbol{X}_{cx} e^{\boldsymbol{S}_{2r} x} \end{bmatrix} \tag{a.17}$$

The first integral of $\boldsymbol{W}_x$ will be expressed by:

$$\boldsymbol{W}_{-1x} = \boldsymbol{R}_{ri} \begin{bmatrix} \int_0^x e^{\boldsymbol{S}_1 t} dt & & & \\ & \int_0^x e^{-\boldsymbol{S}_1 t} dt & & 0 \\ & & \int_0^x \boldsymbol{X}_{st} e^{\boldsymbol{S}_{2r} t} dt & \\ & 0 & & \int_0^x \boldsymbol{X}_{ct} e^{\boldsymbol{S}_{2r} t} dt \end{bmatrix} \tag{a.18}$$

We need to calculate: $\int_0^x \boldsymbol{X}_{ct} e^{\boldsymbol{S}_{2r} t} dt$ and $\int_0^x \boldsymbol{X}_{st} e^{\boldsymbol{S}_{2r} t} dt$. This is performed easily by using the complex number:

$$\begin{aligned}
\int_0^x \boldsymbol{X}_{ct} e^{\boldsymbol{S}_{2r} t} dt + i \int_0^x \boldsymbol{X}_{st} e^{\boldsymbol{S}_{2r} t} dt &= \int_0^x e^{(\boldsymbol{S}_{2r} + i\boldsymbol{S}_{2i})t} dt \\
&= (\boldsymbol{S}_{2r} + i\boldsymbol{S}_{2i})^{-1} (e^{(\boldsymbol{S}_{2r} + i\boldsymbol{S}_{2i})x} - \boldsymbol{I}) \\
&= \left(\boldsymbol{S}_{2r}^2 + \boldsymbol{S}_{2i}^2\right)^{-1} (\boldsymbol{S}_{2r} - i\boldsymbol{S}_{2i})((\boldsymbol{X}_{cx} \\
&\quad + i\boldsymbol{X}_{sx}) e^{\boldsymbol{S}_{2r} x} - \boldsymbol{I}) \\
&= (((\boldsymbol{A}_{2r}\boldsymbol{X}_{cx} + \boldsymbol{A}_{2i}\boldsymbol{X}_{sx}) e^{\boldsymbol{S}_{2r} x} - \boldsymbol{A}_{2r}) \\
&\quad + i((\boldsymbol{A}_{2r}\boldsymbol{X}_{sx} - \boldsymbol{A}_{2i}\boldsymbol{X}_{cx}) e^{\boldsymbol{S}_{2r} x} + \boldsymbol{A}_{2i}))
\end{aligned}$$

where $\boldsymbol{A}_{2r} = \left(\boldsymbol{S}_{2r}^2 + \boldsymbol{S}_{2i}^2\right)^{-1} \boldsymbol{S}_{2r}, \boldsymbol{A}_{2r} = \left(\boldsymbol{S}_{2r}^2 + \boldsymbol{S}_{2i}^2\right)^{-1} \boldsymbol{S}_{2i}$.

Thus:

$$\int_0^x \boldsymbol{X}_{ct} e^{\boldsymbol{S}_{2r} t} dt = (\boldsymbol{A}_{2r}\boldsymbol{X}_{cx} + \boldsymbol{A}_{2i}\boldsymbol{X}_{sx}) e^{\boldsymbol{S}_{2r} x} - \boldsymbol{A}_{2r} \tag{a.19}$$

$$\int_0^x \boldsymbol{X}_{st} e^{\boldsymbol{S}_{2r} t} dt = (\boldsymbol{A}_{2r}\boldsymbol{X}_{sx} - \boldsymbol{A}_{2i}\boldsymbol{X}_{cx}) e^{\boldsymbol{S}_{2r} x} + \boldsymbol{A}_{2i} \tag{a.20}$$

With (a.19) and (a.20) we can then determine $\boldsymbol{W}_{-1x}$ easily.

In the same way, for the calculation of $\boldsymbol{W}_{-2x}$ we will need to calculate $\int_0^x ((\boldsymbol{A}_{2r}\boldsymbol{X}_{ct} + \boldsymbol{A}_{2i}\boldsymbol{X}_{st}) e^{\boldsymbol{S}_{2r} t} - \boldsymbol{A}_{2r}) dt$ and $\int_0^x ((\boldsymbol{A}_{2r}\boldsymbol{X}_{sx} - \boldsymbol{A}_{2i}\boldsymbol{X}_{cx}) e^{\boldsymbol{S}_{2r} x} + \boldsymbol{A}_{2i}) dt$, this can be done by using the expressions in (a.19) and (a.20). Thus:

$$\begin{aligned}
&\int_0^x ((\boldsymbol{A}_{2r}\boldsymbol{X}_{ct} + \boldsymbol{A}_{2i}\boldsymbol{X}_{st}) e^{\boldsymbol{S}_{2r} t} - \boldsymbol{A}_{2r}) dt \\
&= \boldsymbol{A}_{2r}((\boldsymbol{A}_{2r}\boldsymbol{X}_{cx} + \boldsymbol{A}_{2i}\boldsymbol{X}_{sx}) e^{\boldsymbol{S}_{2r} x} - \boldsymbol{A}_{2r}) + \boldsymbol{A}_{2i}((\boldsymbol{A}_{2r}\boldsymbol{X}_{sx} \\
&\quad - \boldsymbol{A}_{2i}\boldsymbol{X}_{cx}) e^{\boldsymbol{S}_{2r} x} + \boldsymbol{A}_{2i}) - \boldsymbol{A}_{2r} x \\
&= \left(\left(\boldsymbol{A}_{2r}^2 - \boldsymbol{A}_{2i}^2\right)\boldsymbol{X}_{cx} + 2\boldsymbol{A}_{2r}\boldsymbol{A}_{2i}\boldsymbol{X}_{sx}\right) e^{\boldsymbol{S}_{2r} x} - \boldsymbol{A}_{2r} x + \boldsymbol{A}_{2i}^2 - \boldsymbol{A}_{2r}^2
\end{aligned} \tag{a.21}$$

$$\begin{aligned}
&\int_0^x \left[(\boldsymbol{A}_{2r}\boldsymbol{X}_{st} - \boldsymbol{A}_{2i}\boldsymbol{X}_{ct}) e^{\boldsymbol{S}_{2r} t} + \boldsymbol{A}_{2i}\right] dt \\
&= \boldsymbol{A}_{2r}((\boldsymbol{A}_{2r}\boldsymbol{X}_{sx} - \boldsymbol{A}_{2i}\boldsymbol{X}_{cx}) e^{\boldsymbol{S}_{2r} x} + \boldsymbol{A}_{2i}) - \boldsymbol{A}_{2i}((\boldsymbol{A}_{2r}\boldsymbol{X}_{cx} \\
&\quad + \boldsymbol{A}_{2i}\boldsymbol{X}_{sx}) e^{\boldsymbol{S}_{2r} x} - \boldsymbol{A}_{2r}) + \boldsymbol{A}_{2i} x \\
&= \left(\left(\boldsymbol{A}_{2r}^2 - \boldsymbol{A}_{2i}^2\right)\boldsymbol{X}_{sx} - 2\boldsymbol{A}_{2i}\boldsymbol{A}_{2r}\boldsymbol{X}_{cx}\right) e^{\boldsymbol{S}_{2r} x} + \boldsymbol{A}_{2i} x + 2\boldsymbol{A}_{2i}\boldsymbol{A}_{2r}
\end{aligned} \tag{a.22}$$

Finally for the third integral, it will be expressed with the aid of the two following integrals:

$$\begin{aligned}
&\int_0^x \left(\left(\left(\boldsymbol{A}_{2r}^2 - \boldsymbol{A}_{2i}^2\right)\boldsymbol{X}_{ct} + 2\boldsymbol{A}_{2r}\boldsymbol{A}_{2i}\boldsymbol{X}_{st}\right) e^{\boldsymbol{S}_{2r} t} - \boldsymbol{A}_{2r} t + \boldsymbol{A}_{2i}^2 - \boldsymbol{A}_{2r}^2\right) dt \\
&= \left(\left(\boldsymbol{A}_{2r}^3 + \boldsymbol{A}_{2i}^2\boldsymbol{A}_{2r}\right)\boldsymbol{X}_{cx} - \left(\boldsymbol{A}_{2i}^3 + \boldsymbol{A}_{2i}\boldsymbol{A}_{2r}^2\right)\boldsymbol{X}_{sx}\right) e^{\boldsymbol{S}_{2r} x} - \boldsymbol{A}_{2r}\frac{x^2}{2} \\
&\quad + \left(\boldsymbol{A}_{2i}^2 - \boldsymbol{A}_{2r}^2\right) x - \left(\boldsymbol{A}_{2r}^3 - \boldsymbol{A}_{2i}^2\boldsymbol{A}_{2r}\right)
\end{aligned} \tag{a.23}$$

$$\int_0^x \left(\left(\left(\boldsymbol{A}_{2r}^2 - \boldsymbol{A}_{2i}^2\right)\boldsymbol{X}_{st} - 2\boldsymbol{A}_{2i}\boldsymbol{A}_{2r}\boldsymbol{X}_{ct}\right)e^{\boldsymbol{s}_{2r}t} + \boldsymbol{A}_{2i}t + 2\boldsymbol{A}_{2i}\boldsymbol{A}_{2r}\right)dt$$
$$= \left(\left(\boldsymbol{A}_{2r}^3 - 3\boldsymbol{A}_{2i}^2\boldsymbol{A}_{2r}\right)\boldsymbol{X}_{sx} + \left(\boldsymbol{A}_{2i}^3 - 3\boldsymbol{A}_{2i}\boldsymbol{A}_{2r}^2\right)\boldsymbol{X}_{cx}\right)e^{\boldsymbol{s}_{2r}x} + \boldsymbol{A}_{2i}$$
$$\times \frac{x^2}{2} + 2\boldsymbol{A}_{2i}\boldsymbol{A}_{2r}x + 3\boldsymbol{A}_{2i}\boldsymbol{A}_{2r}^2 - \boldsymbol{A}_{2i}^3 \qquad \text{(a.24)}$$

A.6

Rigid body motion modes:

Transversal modes	1st warping mode	2nd warping mode	3rd warping mode
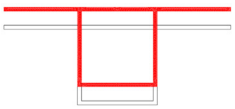	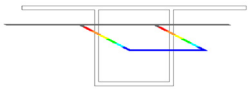	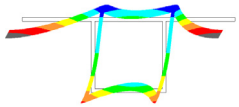	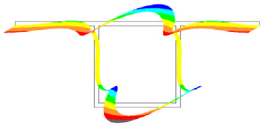
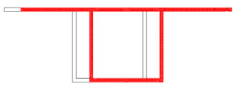	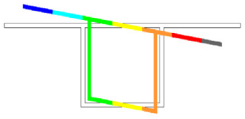	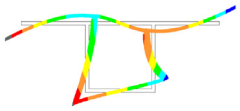	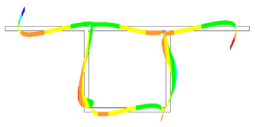
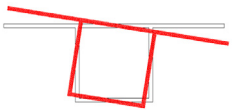	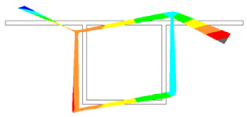	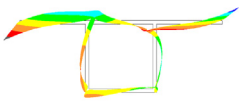	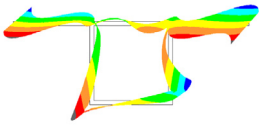

Transversal modes	1st warping mode	2nd warping mode	3rd warping mode
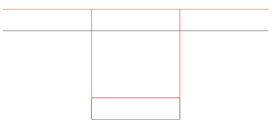			
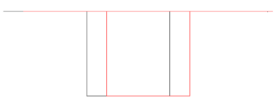	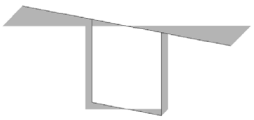		
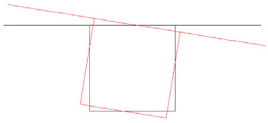	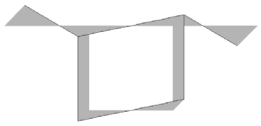		

Higher transversal modes:

Transversal mode	Corresponding 1st warping mode	Transversal mode	Corresponding 1st warping mode
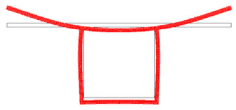	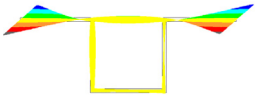	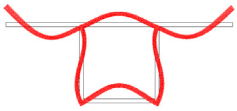	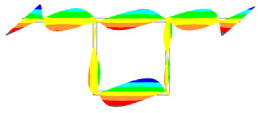
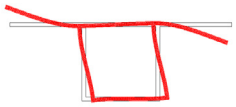	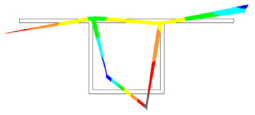	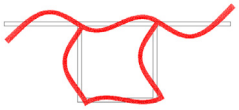	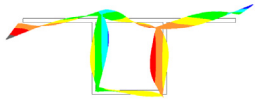
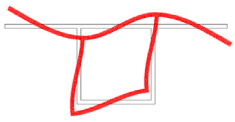	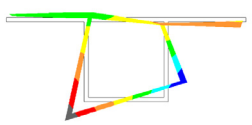	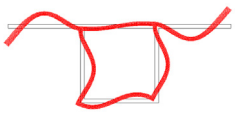	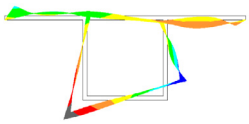
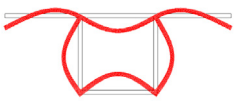	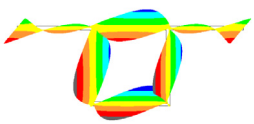		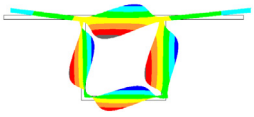

A.7

For the box girder section, we consider 10 transversal modes, with one warping mode associated to each one of them. We give the numerical values of the matrices introduced in page 12. The authors are also disposed to provide to the interested reader, more numerical values for different cross section form and for any number of distortion modes with their associated warping modes.

$$\boldsymbol{C} = 10^{-5}\mu \begin{vmatrix} 29750 & & & & & & & & & \\ & 29750 & & & & & & & & \\ & & 19090 & & & & & \mathbf{0} & & \\ & & & 3070 & & & & & & \\ & & & & 5170 & & & & & \\ & & & & & 10410 & & & & \\ & & & & & & 9090 & & & \\ & & & & & & & 5650 & & \\ & & \mathbf{0} & & & & & & 6600 & \\ & & & & & & & & & 4930 \end{vmatrix}, \quad \boldsymbol{p} = \frac{\lambda 10^{-5}}{(2\mu+\lambda)S} \begin{Bmatrix} 0 \\ 0 \\ 0 \\ 3.43 \\ 0 \\ -0.27 \\ 3.21 \\ -73.75 \\ -2.10 \\ 3.75 \end{Bmatrix}$$

$$\boldsymbol{H} = 10^{-5}\mu \begin{vmatrix} 0 & 0 & 0 & 0 & 0 & 0 & 0 & 0 & 0 & 0 \\ 0 & 0 & 0 & 0 & 0 & 0 & 0 & 0 & 0 & 0 \\ 0 & 0 & 0 & 0 & 0 & 0 & 0 & 0 & 0 & 0 \\ 0 & 0 & 0 & 5.70 & 0.05 & 0.04 & -0.06 & 0.11 & -0.05 & -0.05 \\ 0 & 0 & 0 & 0.05 & 16.49 & 0.22 & -0.05 & 0.08 & -0.25 & -0.09 \\ 0 & 0 & 0 & 0.04 & 0.22 & 64.68 & -0.11 & 0.16 & -0.43 & -0.38 \\ 0 & 0 & 0 & -0.06 & -0.05 & -0.11 & 227.39 & -0.68 & 0.41 & 0.47 \\ 0 & 0 & 0 & 0.11 & 0.08 & 0.16 & -0.68 & 320.32 & -1.45 & -1.56 \\ 0 & 0 & 0 & -0.05 & -0.25 & -0.43 & 0.41 & -1.45 & 432.29 & 3.93 \\ 0 & 0 & 0 & -0.05 & -0.09 & -0.38 & 0.47 & -1.56 & 3.93 & 529.50 \end{vmatrix}$$

$$\boldsymbol{F} = 10^{-5}\lambda \begin{vmatrix} 0 & 0 & 0 & 0 & 0 & 0 & 0 & 0 & 0 & 0 \\ 0 & 0 & 0 & 0 & 0 & 0 & 0 & 0 & 0 & 0 \\ 0 & 0 & 0 & 0 & 0 & 0 & 0 & 0 & 0 & 0 \\ 0 & 0 & 0 & 12.13 & 0.10 & 0.09 & -0.10 & 0.11 & -0.10 & -0.11 \\ 0 & 0 & 0 & 0.10 & 35.13 & 0.25 & -0.11 & 0.19 & -0.37 & -0.19 \\ 0 & 0 & 0 & 0.09 & 0.25 & 138.22 & -0.24 & 0.32 & -0.54 & -0.79 \\ 0 & 0 & 0 & -0.10 & -0.11 & -0.24 & 484.53 & -0.99 & 0.89 & 0.99 \\ 0 & 0 & 0 & 0.11 & 0.19 & 0.32 & -0.99 & 685.20 & -3.01 & -3.28 \\ 0 & 0 & 0 & -0.10 & -0.37 & -0.54 & 0.89 & -3.01 & 924.40 & 5.97 \\ 0 & 0 & 0 & -0.11 & -0.19 & -0.79 & 0.99 & -3.28 & 5.97 & 1133.80 \end{vmatrix}$$

$$\boldsymbol{K} = 10^{-5}(2\mu + \lambda) \begin{vmatrix} 14109.70 & 0 & 0 & 0 & 0 & 0 & 0 & 0 & 0 & 0 \\ 0 & 4982.74 & 0 & 0 & 0 & 0 & 0 & 0 & 0 & 0 \\ 0 & 0 & 228.73 & -1.18 & -204.43 & 231.24 & -0.04 & 0.89 & -43.12 & 52.20 \\ 0 & 0 & -1.18 & 0.85 & 1.28 & -1.84 & 0.06 & 0.14 & 0.21 & -0.41 \\ 0 & 0 & -204.43 & 1.28 & 237.41 & -362.59 & -0.05 & -0.53 & 34.59 & -80.86 \\ 0 & 0 & 231.24 & -1.84 & -362.59 & 701.44 & 0.23 & 0.06 & -30.16 & 154.81 \\ 0 & 0 & -0.04 & 0.06 & -0.05 & 0.23 & 2.12 & 0.07 & 0.02 & 0.05 \\ 0 & 0 & 0.89 & 0.14 & -0.53 & 0.06 & 0.07 & 1.37 & -0.20 & 0.03 \\ 0 & 0 & -43.12 & 0.21 & 34.59 & -30.16 & 0.02 & -0.20 & 10.44 & -7.12 \\ 0 & 0 & 52.20 & -0.41 & -80.86 & 154.81 & 0.05 & 0.03 & -7.12 & 35.50 \end{vmatrix}$$

$$\boldsymbol{J} = 10^{-5}\mu \begin{vmatrix} 29750.00 & 0 & -1186.52 & 9.85 & 2136.78 & -6082.40 & -8.81 & 132.19 & -6168.80 & 3112.52 \\ 0 & 29750.00 & -0.63 & -4725.72 & 56.02 & 16.07 & -1543.38 & -4272.53 & -151.85 & -139.75 \\ -1186.52 & -0.63 & 13997.50 & 17.58 & 2227.67 & 2076.11 & 4.42 & -37.87 & 1495.99 & 209.45 \\ 9.85 & -4725.72 & 17.58 & 3811.80 & -16.23 & -10.50 & 248.05 & 664.51 & 17.18 & 22.32 \\ 2136.78 & 56.02 & 2227.67 & -16.23 & 4263.84 & -1285.47 & -5.28 & 15.71 & -990.77 & 96.36 \\ -6082.40 & 16.07 & 2076.11 & -10.50 & -1285.47 & 10945.70 & -1.36 & -16.49 & 832.41 & -732.00 \\ -8.81 & -1543.38 & 4.42 & 248.05 & -5.28 & -1.36 & 9083.50 & 238.16 & 9.36 & 5.56 \\ 132.19 & -4272.53 & -37.87 & 664.51 & 15.71 & -16.49 & 238.16 & 6166.33 & 2.10 & 37.52 \\ -6168.80 & -151.85 & 1495.99 & 17.18 & -990.77 & 832.41 & 9.36 & 2.10 & 7455.76 & -753.63 \\ 3112.52 & -139.75 & 209.45 & 22.32 & 96.36 & -732.00 & 5.56 & 37.52 & -753.63 & 5127.14 \end{vmatrix}$$

$$\boldsymbol{D} = 10^{-5}\mu \begin{vmatrix} 0.00 & 29750.00 & 0 & 0 & 0 & 0 & 0 & 0 & 0 & 0 \\ -29750.00 & 0 & 0 & 0 & 0 & 0 & 0 & 0 & 0 & 0 \\ 0.63 & -1186.52 & 13950.30 & 17.67 & 2313.21 & 1834.02 & 4.38 & -33.31 & 1249.04 & 333.72 \\ 4725.72 & 9.85 & 17.83 & 3060.96 & -8.11 & -6.03 & 2.97 & -14.11 & -4.71 & -0.70 \\ -56.02 & 2136.78 & 2312.94 & -7.90 & 4110.37 & -848.01 & -2.01 & 14.77 & -548.58 & -128.97 \\ -16.07 & -6082.40 & 1833.55 & -6.37 & -848.81 & 9700.45 & -1.56 & 11.41 & -427.51 & -94.34 \\ 1543.38 & -8.81 & 4.06 & 2.68 & -1.69 & -2.26 & 9002.08 & 16.18 & -0.47 & -0.90 \\ 4272.53 & 132.19 & -32.73 & -14.41 & 14.21 & 12.77 & 16.88 & 5550.64 & 7.83 & 3.80 \\ 151.85 & -6168.80 & 1249.90 & -4.69 & -547.69 & -429.27 & -0.69 & 8.31 & 6176.07 & -107.71 \\ 139.75 & 3112.52 & 333.54 & -1.05 & -126.75 & -95.57 & -0.51 & 3.19 & -109.54 & 4799.30 \end{vmatrix}$$

$$\boldsymbol{Q} = 10^{-5}\mu \begin{vmatrix} 0 & 0 & 0 & -0.06 & -10.67 & 0.85 & -0.12 & 1.07 & -24.94 & -85.70 \\ 0 & 0 & 0 & 5.20 & -0.05 & -0.05 & -17.64 & -29.83 & -0.53 & -1.68 \\ 0 & 0 & 0 & -0.02 & -1.71 & -3.49 & 0.06 & -0.74 & 25.44 & 16.90 \\ 0 & 0 & 0 & -0.29 & -0.01 & -0.02 & 4.13 & -6.25 & -0.17 & 0.16 \\ 0 & 0 & 0 & 0.00 & -0.94 & -1.99 & -0.06 & 0.27 & -9.77 & 4.16 \\ 0 & 0 & 0 & 0.02 & 2.13 & 6.07 & 0.02 & -0.59 & 24.04 & 1.99 \\ 0 & 0 & 0 & 1.02 & -0.02 & -0.01 & 18.41 & 0.97 & 0.03 & -0.01 \\ 0 & 0 & 0 & 0.28 & 0.01 & 0.01 & 0.65 & 13.51 & -0.01 & 0.15 \\ 0 & 0 & 0 & 0 & -0.39 & -0.28 & 0.03 & -0.01 & 17.33 & -3.08 \\ 0 & 0 & 0 & -0.03 & -1.06 & -0.98 & 0.05 & -0.11 & 3.46 & 15.21 \end{vmatrix}$$

References

[1] Bauchau OA. A beam theory for anisotropic materials. J Appl Mech 1985;52:416–22.
[2] Sapountzakis EJ, Mokos VG. Warping shear stresses in nonuniform torsion by BEM. Comput Mech 2003;30:131–42.
[3] Sapountzakis EJ, Mokos VG. 3-D beam element of variable composite cross section including warping effect. ECCOMAS, 2004.
[4] Ferradi MK, Cespedes X, Arquier M. A higher order beam finite element with warping eigenmodes. Eng Struct 2013;46:748–62.
[5] Silvestre N, Camotim D. Nonlinear generalized beam theory for cold-formed steel members. Int J Struct Stab Dyn 2003;3(04):461–90.
[6] Bebiano R, Silvestre N, Camotim D. GBTUL-a code for the buckling analysis of cold-formed steel members. In: Proceedings of 19th international specialty conference on recent research and developments in cold-formed steel design and construction, 2008. p. 14–5.
[7] Jang GW, Kim MJ, Kim YY. Analysis of Thin-Walled Straight Beams with Generally-Shaped Closed Sections Using Numerically-Determined Sectional Deformation Functions. J Struct Eng 2012;1:438.
[8] Vlassov VZ. Pieces longues en voiles minces. Paris: Eyrolles; 1962.
[9] Tisseur F, Meerbergen K. The quadratic eigenvalue problem. SIAM Rev 2001;43(2):235–86.
[10] Bathe K-J. Finite Element Procedures. Englewood Cliffs, NJ: Prentice-Hall; 1996.

A model reduction technique for beam analysis with the asymptotic expansion method

Mohammed Khalil Ferradi[1,2], Arthur Lebée[2], Agnès Fliscounakis[1], Xavier Cespedes[1], Karam Sab[2]

[1] Strains engineering, 9 rue Dareau, 75014, Paris, France

[2] Université Paris-Est, Laboratoire Navier, Ecole des Ponts ParisTech, IFSTTAR, CNRS UMR 8205, 6 et 8 avenue Blaise Pascal, 77455 Marne-la-Vallée Cedex 2, France

E-mail: mohammed-khalil.ferradi@strains.fr

Abstract:

In this paper, we apply the asymptotic expansion method to the mechanical problem of beam equilibrium, to derive a new beam model. The asymptotic procedure will lead to a series of mechanical problems at different orders, solved successively. For each order, new transverse (in-plane) deformation and warping (out of plane) deformation modes are determined, in function of the applied loads and the limits conditions of the problem. The presented method can be seen as a more simple and efficient alternative to beam model reduction techniques such as POD or PGD methods. At the end of the asymptotic expansion procedure, an enriched kinematic describing the displacement of the beam is obtained, and will be used for the formulation of an exact beam element by solving exactly the arising new equilibrium equations. A surprising result of this work, is that even for concentrated forces (Dirac delta function), we obtain, with only few additional modes, a very good representation of the beam's deformation.

1. Introduction:

The development of higher order beam model that are able to represent accurately the transverse deformation and the warping of the cross section, is of great interest for bridge and structural engineers. These kind of elements have the advantage to contain in a single beam model, the global and local response of the structure, instead of multiple models with different type of elements. Thus, using higher order beam elements will result in a major time reduction and work simplification for their users. In practice however, there are very few engineering offices and software editors for bridge analysis that uses these kind of elements, mainly because the many necessary aspects for bridge analysis, such as shrinkage, creep, skewed curved slab …, are not yet completely treated for these elements, and still the subject of an intense research work.

Many higher order beam element has been developed using different approach [9-17], for example the GBT (generalized beam theory) theory, developed mainly for thin walled profiles, the VABS (variational asymptotic beam sectional analysis) method, all giving very good results in comparison with reference models made with shell or 3D finite elements. In all the aforementioned methods, the beam model is derived in two step as in [1-2]. First, a cross section analysis to determine an appropriate kinematics (or a basis in which the model is reduced) and then to solve the equilibrium equations, generally by using one of the available numerical method (FEM, BEM…).

In a previous work [1-2], a new beam model was presented and its derivation was performed in two independent steps. The first one is the construction of an enriched kinematic of the beam, with the aid of transverse deformation modes, obtained from an eigenvalue analysis of the cross section, and their associated warping modes, obtained from an iterative equilibrium schemes. Once the kinematic is obtained, the second step consists in using the principle of virtual work to obtain the new equilibrium equations associated to the newly introduced degrees of freedom. These equations were solved exactly in order to assemble the stiffness matrix of the element. The advantages of the beam model in

[1], in comparison to other higher order beam element present in the literature, is its validity for thick and thin-walled profile and its stiffness matrix derived from the exact solution of the equilibrium equations. Nevertheless, the main weakness of the element is that the transverse deformation and warping modes representing its kinematic, aren't specific to the applied loadings, and thus may or may not have an effect on the beam's response, which may results only in adding unnecessary degrees of freedom to the system. From here originate the idea of instead of using arbitrary modes from an eigenvalue analysis, to determine specific modes to the loading that will have by definition an effect on the beam's response under the considered loading. These modes will allow us to obtain the same accurate results in [1], but with much less additional degrees of freedom in the kinematics.

The asymptotic expansion method (AEM) can be seen as more simple and efficient alternative to the model reduction techniques such as POD and PGD, for which a complete 3D pre-analysis of the beam needs to be performed, whereas only a cross section pre-analysis is necessary for the AEM, to determine the prominent modes into the beam's response, under a definite loading. An implicit hypothesis is used in all beam's theory, which is a separation of the longitudinal variation with the transversal one, into the kinematics description. It can be seen from the asymptotic expansion method that this hypothesis is valid if a variable separation is verified by the external forces.

In section 2 of this work, we give a summary of the previous work developed in [1], then in section 3 the objective of this paper is stated. In section 4, the asymptotic expansion method (see [3-8]) is developed in details, to derive the enriched kinematic of the beam in function of the applied external forces and limits conditions. Finally in section 5, the principle of virtual work is used to derive the new equilibrium equations, which will be solved exactly as in [1], to obtain the stiffness matrix of the beam.

In all the numerical results obtained from the developed beam model, and compared to reference models with shell or brick elements, the AEM has proven to be a very efficient method to determine the minimum basis representing the deformation of the beam.

Notations:

We set the notations used in this paper:

- The letters written in bold will designate tensors or vectors.

- The coordinates system attached to the beam will be expressed by $\boldsymbol{X} = (x_1, x_2, x_3)$ or $\boldsymbol{Y} = (y_1, y_2, y_3)$, where the longitudinal component is represented by x_3 or y_3 and the transversal components by $\boldsymbol{x} = (x_1, x_2)$ or $\boldsymbol{y} = (y_1, y_2)$.

- The repeated index summation convention will always be used (unless the contrary is explicitly specified), where the latin letters indices takes the values from 1 to 3 and the greek letters indices the values 1 and 2 :

$$a_i b_i \coloneqq \sum_{i=1}^{3} a_i b_i \quad , \quad a_\alpha b_\alpha \coloneqq \sum_{\alpha=1}^{2} a_\alpha b_\alpha$$

- For the derivation we use the following notations:

$$a_{,1} = \partial_1 a = \frac{\partial a}{\partial y_1} \quad , \quad a_{,2} = \partial_2 a = \frac{\partial a}{\partial y_2} \quad , \quad a_{,\alpha} = \partial_\alpha a = \frac{\partial a}{\partial y_\alpha}$$

$$a_{,ij} = \partial_i \partial_j a = \frac{\partial^2 a}{\partial y_i \partial y_j} \quad , \quad a^{(n)} = \frac{\partial^n a}{\partial {y_3}^n}$$

2. Summary of previous work:

Before developing the asymptotic expansion method for a beam element, we explain in this section the general philosophy of the paper. Our goal is to develop a beam element capable of representing accurately the transverse deformation (in-plane deformation) and the warping (out of plane deformation) of the cross sections under arbitrary loadings, and thus to obtain with the beam model, equivalent results to those of a shell or brick models. The starting point for the development of a beam element is not the equilibrium equations, but its kinematic, which is the key element of every beam model. For example in the well-known Euler-Bernoulli beam theory, the model fails to give the shear strains because of the choice made on the kinematic, which is that the rotation of the cross section is equal to the deflection derivate. Another example concerns the torsion in both Timoshenko and Euler-Bernoulli beam theory. In those two models the torsion inertia is equal to the polar inertia, which is wrong in most cases. Thus, the accuracy of the beam model will depend crucially on its adopted kinematic.

In [1], a kinematic was proposed to describe the arbitrary transverse deformation and warping of the cross section. To determine first the transverse deformation modes, the section surface is discretized with 2D triangular elements, to which a stiffness matrix is associated, then the global stiffness matrix $\boldsymbol{K}_s$ of the section is assembled, for which an eigenvalue analysis is performed by solving the following standard eigenvalue problem:

$$\text{find } (\lambda, \boldsymbol{v}) \quad / \ \boldsymbol{K}_s \boldsymbol{v} = \lambda \boldsymbol{v} \tag{1}$$

The eigenvectors will form a basis of transverse deformation modes that will be used to enrich the kinematic', and where an arbitrary transverse deformation will be decomposed. We note that by construction of this basis, the modes are linearly independent, and that the strain energy U associated to a mode is given by:

$$2U = \boldsymbol{v}^T \boldsymbol{K}_s \boldsymbol{v} = \lambda \boldsymbol{v}^T \boldsymbol{v} = \lambda \tag{2}$$

From Eq.2, it can be deduced that the modes with the lowest eigenvalues mobilizes less energy, and thus have more chances to occur. From this argument, if we want to determine a basis of n transverse deformation functions to enrich our kinematic, we will use then the n eigenvectors with the lowest eigenvalues. But the main drawback of this procedure, is that the selected modes may not participate to the beam's response, depending on the applied loads and boundary conditions.

For the determination of the warping mode basis in [1], we start by deriving for each transverse deformation mode, an associated warping mode of the first order, by making the assumption of uniform warping. To develop the procedure, let us consider the following kinematic:

$$\boldsymbol{d} \coloneqq \begin{Bmatrix} \psi_1 \zeta \\ \psi_2 \zeta \\ u \end{Bmatrix} \tag{3}$$

Where $\boldsymbol{\psi}(\boldsymbol{x}) = \big(\psi_1(\boldsymbol{x}) \,,\ \psi_2(\boldsymbol{x})\big)$ is a known arbitrary transverse deformation mode, $\zeta(x_3)$ its associated degree of freedom, and $u(x_1, x_2, x_3)$ the longitudinal displacement that has an unknown form for the moment that need to be defined.

In order to determine the form of u, we make the assumption of uniform warping along the beam, which means that the length of the beam's fiber does not change. This condition is expressed with the following equation:

$$\varepsilon_{33} = 0 \tag{4}$$

Where $\varepsilon_{33} \coloneqq \frac{\partial u}{\partial x_3}$ is the longitudinal strain component.
We use now the following equilibrium equation:

$$\frac{\partial \sigma_{33}}{\partial x_3} + \mathrm{div}_{\boldsymbol{x}} \boldsymbol{\tau} = 0 \tag{5}$$

Where $\boldsymbol{\tau} \coloneqq (\sigma_{13}, \sigma_{23}) = \boldsymbol{\nabla_x} u + \boldsymbol{\psi}\, \zeta_{,3}$ is the shear stress vector, $\mathrm{div}_{\boldsymbol{x}}(\cdot) \coloneqq \frac{\partial \cdot}{\partial x_1} + \frac{\partial \cdot}{\partial x_2}$ the divergence operator, and $\boldsymbol{\nabla_x}(\cdot) \coloneqq \left(\frac{\partial \cdot}{\partial x_1}, \frac{\partial \cdot}{\partial x_2}\right)$ the gradient operator on the cross section.

By replacing the stresses with their expression in Eq.5, and using the condition in Eq.4 (in the case of a null Poisson coefficient $\nu = 0$), Eq.5 becomes:

$$\Delta_{\boldsymbol{x}} u = -\frac{d\zeta}{dx_3} \mathrm{div}_{\boldsymbol{x}}\, \boldsymbol{\psi} \tag{6}$$

Where $\Delta_{\boldsymbol{x}}(\cdot) \coloneqq \frac{\partial^2 \cdot}{\partial x_1^2} + \frac{\partial^2 \cdot}{\partial x_2^2}$ is the Laplace operator on the cross section.

From Eq.6 we can deduce that the longitudinal displacement can be expressed in the following way:

$$u = -\,\zeta_{,3}\, \Omega \tag{7}$$

Where $\Omega(\boldsymbol{x})$ is a warping (out of plane) deformation, depending only on the cross section geometry and verifying the following relation:

$$\Delta_{\boldsymbol{x}} \Omega = \mathrm{div}_{\boldsymbol{x}}\, \boldsymbol{\psi} \tag{8}$$

To solve the equation in Eq.8, we need to define its boundaries conditions. We use then the condition expressing the fact that the normal component of the shear stress vector $\boldsymbol{\tau}$ on the section border has to be null:

$$\boldsymbol{\tau} \cdot \boldsymbol{n} = 0 \tag{9}$$

$$\boldsymbol{\nabla_x} \Omega \cdot \boldsymbol{n} = \boldsymbol{\psi} \cdot \boldsymbol{n} \tag{10}$$

Where $\boldsymbol{n} = (n_1, n_2)$ is the normal vector to the border of the cross section.

The relations in Eq.8 and 10 defines a partial derivative problem that can be solved uniquely up to an additive uniform displacement:

$$\begin{cases} \Delta_{\boldsymbol{x}} \Omega = \mathrm{div}_{\boldsymbol{x}}\, \boldsymbol{\psi} & \text{in S} \\ \boldsymbol{\nabla_x} \Omega \cdot \boldsymbol{n} = \boldsymbol{\psi} \cdot \boldsymbol{n} & \text{in } \Gamma_s \end{cases} \tag{11}$$

Where Γ_s is the cross section border.

Thus, we can determine for each transverse deformation mode, the first warping mode Ω associated to it. For the general case of non-uniform warping, the warping mode derived from Eq.11 will generate a normal stress that will not be equilibrated. By restoring equilibrium with shear stresses generated by a new mode, we can define an iterative equilibrium scheme, based on the following relation:

$$\sigma_{33,3}^{n} + \mathrm{div}_{\boldsymbol{x}}\, \boldsymbol{\tau}^{n+1} = 0 \tag{12}$$

Where $\sigma_{33}^{n} = E \xi_{,3}^{n} \Omega^{n}$ is the non-equilibrated normal stress of the n$^{\text{th}}$ warping mode.
And $\boldsymbol{\tau}^{n+1} = G \xi^{n+1} \boldsymbol{\nabla_x} \Omega^{n+1}$ the shear stress vector of the n+1$^{\text{th}}$ warping mode. We note that Eq.12 was stated in [1] based on a physical intuition, where the normal stress of the old warping mode is equilibrated by the shear stress of the new warping mode. A rigorous justification will be instead obtained in this paper, by using the AEM.

By replacing with the expressions of the stresses, Eq.12 becomes:

$$E\xi^{n}_{,33}\,\Omega^{n} + G\xi^{n+1}\,\Delta_{\boldsymbol{x}}\Omega^{n+1} = 0 \tag{13}$$

Since the functions Ω^{n+1} and Ω^{n} depends only of the geometry of the cross section, we can deduce from Eq.13 that these functions verifies:

$$\Delta_{\boldsymbol{x}}\Omega^{n+1} = a\,\Omega^{n} \tag{14}$$

Where *a* is a constant.

Our goal here is to form a basis for the description of the section warping. Since the participation rate of each mode will be obtained from the equilibrium of the beam, we need only the form of the warping modes on the cross section. Thus, the constant *a* will be dropped from Eq.14, and by using the boundary condition $\boldsymbol{\tau}^{n+1}\cdot\boldsymbol{n} = 0$, we obtain the partial derivative problem leading to the derivation of the new warping mode Ω^{n+1}:

$$\begin{cases}\Delta_{\boldsymbol{x}}\Omega^{n+1} = \Omega^{n}\\ \boldsymbol{\nabla}_{\boldsymbol{x}}\Omega^{n+1}\cdot\boldsymbol{n} = 0\end{cases} \tag{15}$$

The problem above can be solved uniquely up to an additive uniform constant. The n+1th warping mode is then deduced, which in turn give arise to a non-equilibrated normal stress that will be equilibrated by the n+2th warping mode. This iterative equilibrium procedure can be developed until the desired precision is reached.

3. Objective of this paper:

We summarized in the last section the method used in [1] to obtain the enriched kinematic for the description of the beam's deformation. We can imagine using an infinitely great number of warping and transverse deformation functions to enrich our model, allowing us to represent accurately any arbitrary deformations. The difficulty then, is not mainly in enriching the beams kinematic, but in finding the minimum functions that describes the deformation of the beam while minimizing the error. To achieve this goal, the AEM has proven to be a powerful tool, since from the applied forces, we will determine an associated transverse deformation and warping modes basis, which means that by construction, these modes will participate to the beam's response under the considered forces.

Our objective in this work is to use the AEM only to determine the transverse deformation and warping modes basis for the enrichment of the beam's kinematic. The general equilibrium equations are obtained in section 5 from the principle of virtual work. Their exact solution, will follow exactly the same method described in [1], and therefore will not be detailed in this work.

To illustrate the advantage of using the AEM instead of the method in [1] to enrich the beam's kinematic, we consider the example of the 10m cantilever beam with a box girder cross section (Fig.1), treated in [1]. The material characteristics are E=40 GPa and υ=0. We apply a concentrated vertical force of 1MN at the center of the beam's free end. The comparison will be performed between the results of a shell (MITC- 4) model of the cantilever beam, the results of the beam model in [1] and the results of the present beam model, with no meshing used, since the equilibrium equations are solved exactly as in [1].

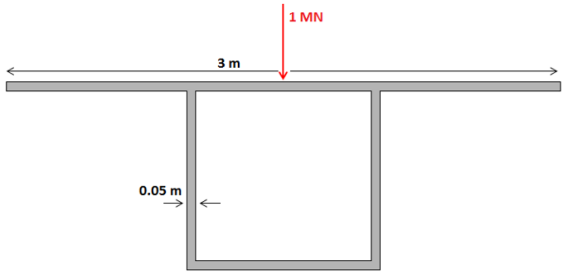

Figure 1: beam cross section with a centered vertical load.

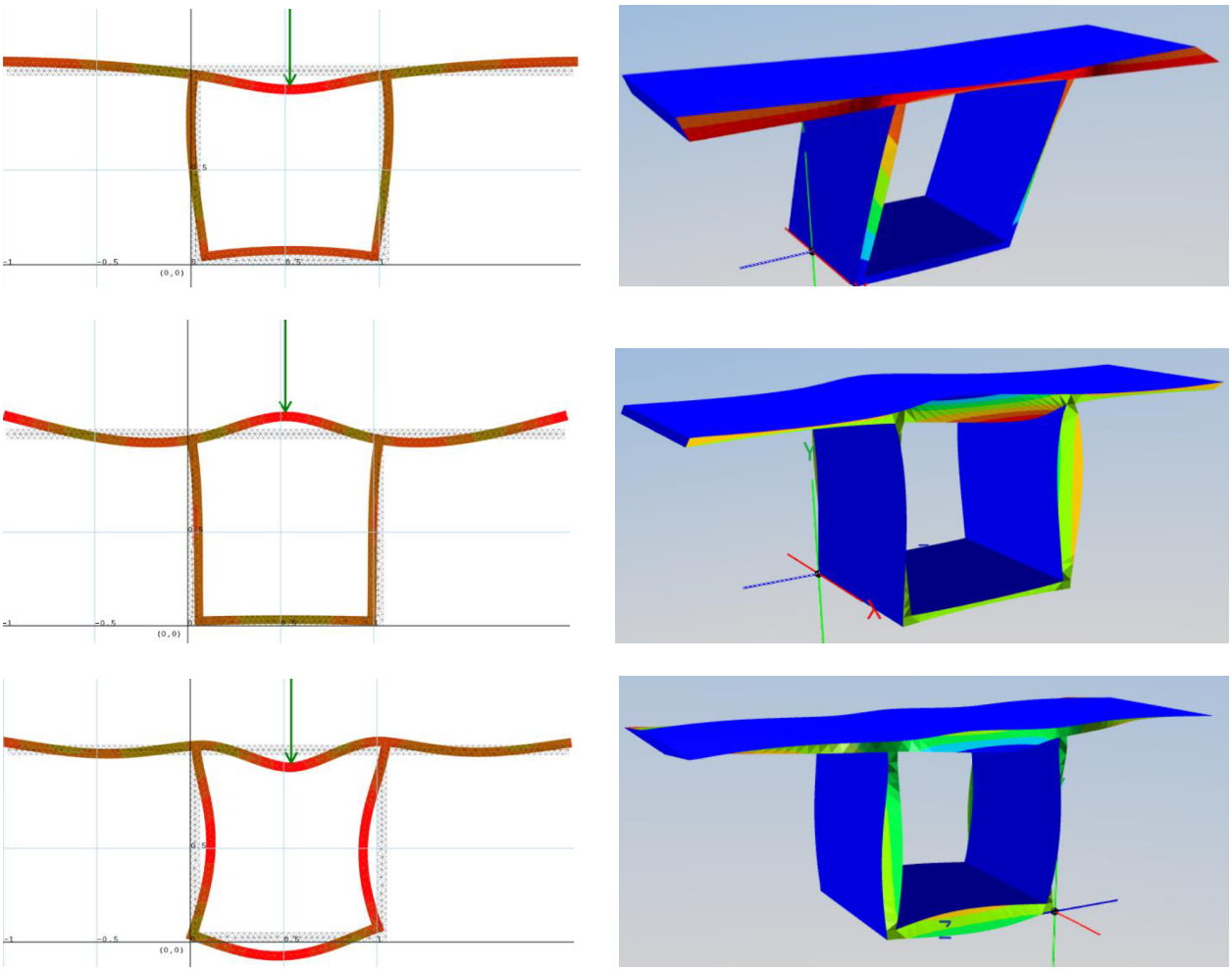

Figure 2: the transverse deformation and warping modes due to the vertical force from the AEM.

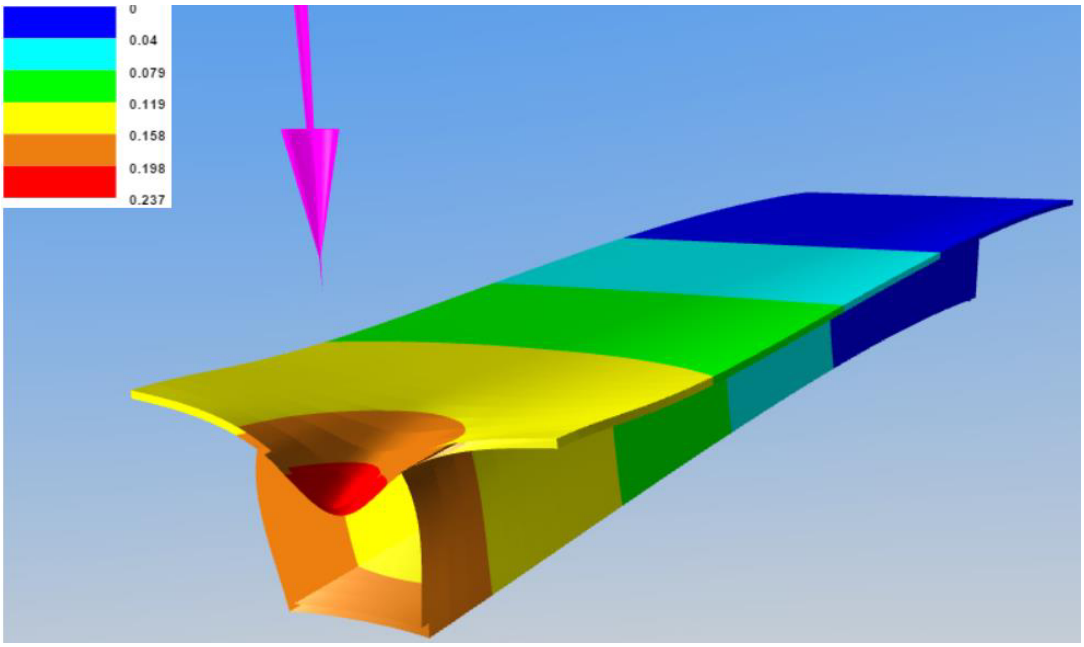

Figure 3: A view of the amplified deformation of the beam with only one element.

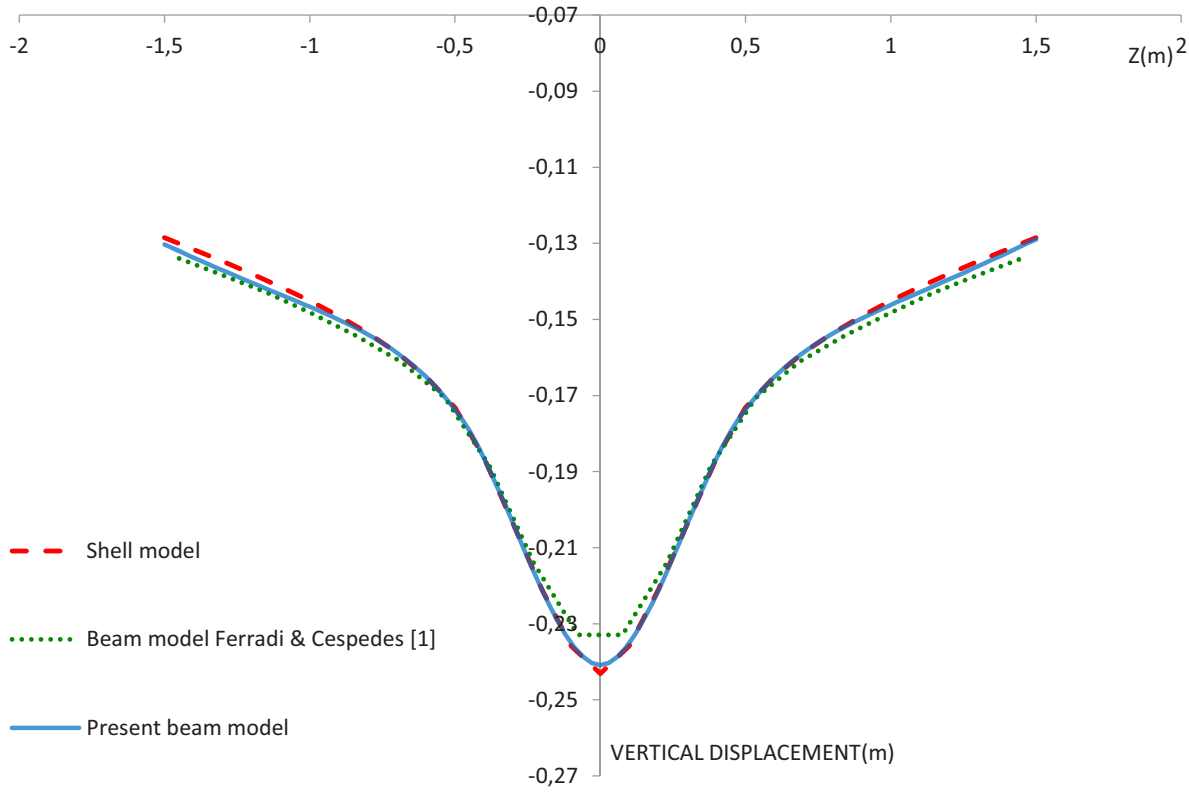

Figure 4: Comparison of the displacement between the shell and the beam models, at x= 10m and at mid-depth of the upper slab.

For the result obtained in this study and represented in Fig.4 with the blue curve, the AEM was used to enrich the kinematic, leading to the derivation of the transverse deformation and warping modes associated to the external force (Fig.2), plus the mode corresponding to the Saint-Venant solution, obtained also from the AEM. Thus, a total of nine warping modes and nine transverse deformation modes were used to enrich the present beam model. This result is compared to the one from [1], where we have used twenty transverse deformation modes and twenty-two warping modes, obtained from

the procedure summarized above. Clearly, the results represented in Fig.3-4 shows that the same accurate displacement is obtained but with much less modes, even for this extreme comparison case, where the external force is concentrated (a Dirac delta function).

4. The asymptotic expansion method:

4.1 The 3D elastic beam problem:

The starting point of the AEM is the general 3D equilibrium equations. For a prismatic beam element with a length L, occupying a volume $V = [0, L] \times S$, where S is the beam's cross section. The standard strong form of the equilibrium equations, for an elastic mechanical problem, can be written in the following form:

$$\begin{cases} \mathrm{div}_{\boldsymbol{X}}(\boldsymbol{\sigma}) + \bar{\boldsymbol{b}} = \boldsymbol{0} & \text{in } V \\ \boldsymbol{\varepsilon} = \boldsymbol{\nabla}^s_{\boldsymbol{X}} \boldsymbol{d} & \\ \boldsymbol{\sigma} = \boldsymbol{C} : \boldsymbol{\varepsilon} & \\ \boldsymbol{\sigma} \cdot \boldsymbol{n} = \bar{\boldsymbol{t}} & \text{in } \Gamma \\ \boldsymbol{d} = \bar{\boldsymbol{d}} & \text{in } \Gamma_d \end{cases} \tag{16}$$

Where $\bar{\boldsymbol{b}}$ is the applied body force, **n** the normal vector to the surface Γ, $\bar{\boldsymbol{t}}$ the applied surfacic force vector, $\bar{\boldsymbol{d}}$ the imposed displacements on the surface Γ_d and $\boldsymbol{X} = (x_1, x_2, x_3)$ the global coordinate of an arbitrary point of the volume. The unknowns of this system are the displacement vector, the deformation and the stress tensors fields $\boldsymbol{d}$, $\boldsymbol{\varepsilon}$ and $\boldsymbol{\sigma}$ respectively (in the elastic case, the only unknown is the displacement, from which the deformation and the stress fields are deduced).

4.2 Change of coordinates, scaling and statement of the problems to solve :

The starting point of the asymptotic expansion method is a variable change on the global coordinates:

$$(x_1, x_2, x_3) \coloneqq (hy_1, hy_2, Ly_3) \tag{17}$$

Where h is the dimension of the beam's cross section.

This variable change is applied to the differential operators used in Eq.16, to re-express them into the new coordinates system:

$$\begin{cases} \boldsymbol{\nabla}^s_{\boldsymbol{X}} = \dfrac{1}{L}\left(\boldsymbol{\nabla}^s_{y_3} + \dfrac{1}{\eta}\boldsymbol{\nabla}^s_{\boldsymbol{y}}\right) \\ \mathrm{div}_{\boldsymbol{X}} = \dfrac{1}{L}\left(\mathrm{div}_{y_3} + \dfrac{1}{\eta}\mathrm{div}_{\boldsymbol{y}}\right) \end{cases} \tag{18}$$

Where $\eta \coloneqq \frac{h}{L}$ is the scaling parameter and $\boldsymbol{y} \coloneqq (y_1, y_2)$.

The asymptotic expansion method is based on the assumption that the unknowns and the entries of the mechanical problem are written as power series of the scaling parameter η. We write then the displacement, stress and strain fields in the following forms:

$$\boldsymbol{d} \coloneqq L\left(\frac{1}{\eta}\boldsymbol{d}^{-1} + \boldsymbol{d}^0 + \eta\,\boldsymbol{d}^1 + \eta^2\boldsymbol{d}^2 + \cdots\right) \tag{19}$$

$$\boldsymbol{\sigma} \coloneqq \boldsymbol{\sigma}^0 + \eta\,\boldsymbol{\sigma}^1 + \eta^2\boldsymbol{\sigma}^2 + \cdots \tag{20}$$

$$\boldsymbol{\varepsilon} \coloneqq \boldsymbol{\varepsilon}^0 + \eta\,\boldsymbol{\varepsilon}^1 + \eta^2\boldsymbol{\varepsilon}^2 + \cdots \tag{21}$$

We assume for the applied forces a variable separation and that they vary longitudinally according to the function *f(y₃)*. The forces are introduced at definite powers of η:

$$\overline{b_\alpha} \coloneqq \frac{1}{h}\,\eta^2\, b_\alpha(\boldsymbol{y})\, f(y_3) \quad , \quad \overline{b_3} \coloneqq \frac{1}{h}\,\eta\, b_3(\boldsymbol{y})\, f(y_3) \tag{22}$$

$$\overline{t_\alpha} \coloneqq \eta^2\, t_\alpha(\boldsymbol{y})\, f(y_3) \quad , \quad \overline{t_3} \coloneqq \eta\, t_3(\boldsymbol{y})\, f(y_3) \tag{23}$$

We assume for the AEM that the function *f(y₃)* is infinitely differentiable (class C^∞). But it can be seen from all the examples presented in this paper, that the applied forces can be punctual, representing a case where *f* is a Dirac delta function that is clearly not differentiable. Still, we see that for these extreme comparison case, using the kinematic obtained from the AEM will give very good results.

Replacing now all the asymptotic expressions above (Eq.19-23) into the general equilibrium equations in Eq.16, leads to a set of problems for each power of η.

By using the expression of the displacement vector in Eq.19 and of the symmetric gradient operator in Eq.18 into the compatibility equation in Eq.16, the following equation is obtained:

$$\boldsymbol{\varepsilon} = \boldsymbol{\nabla}_{\boldsymbol{X}}^s \boldsymbol{d} = \eta^{-2}\boldsymbol{\nabla}_{\boldsymbol{y}}^s \boldsymbol{d}^{-1} + \eta^{-1}\left(\boldsymbol{\nabla}_{\boldsymbol{y}}^s \boldsymbol{d}^0 + \boldsymbol{\nabla}_{y_3}^s \boldsymbol{d}^{-1}\right) + \left(\boldsymbol{\nabla}_{\boldsymbol{y}}^s \boldsymbol{d}^1 + \boldsymbol{\nabla}_{y_3}^s \boldsymbol{d}^0\right) + \cdots \tag{24}$$

By identifying the terms corresponding to the same power of the scaling parameter between Eq.21 and Eq.24, the following set of equations is obtained (written also in a simpler indicial form):

$$\boldsymbol{\varepsilon}^{-2} = \boldsymbol{\nabla}_{\boldsymbol{y}}^s \boldsymbol{d}^{-1} = \boldsymbol{0} \quad \Leftrightarrow \quad d_{\alpha,\beta}^{-1} + d_{\beta,\alpha}^{-1} = 0 \quad , \quad d_{3,\alpha}^{-1} = 0 \tag{25}$$

$$\boldsymbol{\varepsilon}^{-1} = \boldsymbol{\nabla}_{\boldsymbol{y}}^s \boldsymbol{d}^0 + \boldsymbol{\nabla}_{y_3}^s \boldsymbol{d}^{-1} = \boldsymbol{0} \quad \Leftrightarrow \quad d_{3,3}^{-1} = 0 \quad , \quad d_{\alpha,\beta}^0 + d_{\beta,\alpha}^0 = 0 \quad , \quad d_{3,\alpha}^0 + d_{\alpha,3}^{-1} = 0 \tag{26}$$

$$\boldsymbol{\varepsilon}^p = \boldsymbol{\nabla}_{\boldsymbol{y}}^s \boldsymbol{d}^{p+1} + \boldsymbol{\nabla}_{y_3}^s \boldsymbol{d}^p \;\Leftrightarrow\; \varepsilon_{\alpha\beta}^p = \frac{1}{2}\left(d_{\alpha,\beta}^{p+1} + d_{\beta,\alpha}^{p+1}\right) ,\; \varepsilon_{\alpha 3}^p = \frac{1}{2}\left(d_{3,\alpha}^{p+1} + d_{\alpha,3}^p\right) ,\; \varepsilon_{33}^p = d_{3,3}^p \;\text{ for } p \in \mathbb{N} \tag{27}$$

Using the same procedure, the expression of the stress tensor in Eq.20 is used into the equilibrium equation in Eq.16 to obtain:

$$\mathrm{div}_{\boldsymbol{X}}(\boldsymbol{\sigma}) + \overline{\boldsymbol{b}} = \boldsymbol{0} \;\Longrightarrow\; \frac{1}{L}\left(\mathrm{div}_{y_3} + \frac{1}{\eta}\mathrm{div}_{\boldsymbol{y}}\right)(\boldsymbol{\sigma}^0 + \eta\,\boldsymbol{\sigma}^1 + \eta^2\boldsymbol{\sigma}^2 + \cdots) + \overline{\boldsymbol{b}} = \boldsymbol{0} \tag{28}$$

$$\mathrm{div}_{\boldsymbol{y}}(\boldsymbol{\sigma}^0) + \eta\left(\mathrm{div}_{y_3}(\boldsymbol{\sigma}^0) + \mathrm{div}_{\boldsymbol{y}}(\boldsymbol{\sigma}^1)\right) + \eta^2\left(\mathrm{div}_{y_3}(\boldsymbol{\sigma}^1) + \mathrm{div}_{\boldsymbol{y}}(\boldsymbol{\sigma}^2)\right) + \cdots = -L\overline{\boldsymbol{b}} \tag{29}$$

By replacing $\overline{\boldsymbol{b}}$ in the equation above by its asymptotic expression in Eq.22 and identifying the terms corresponding to the same power of η, the set of the following equations is obtained:

$$\sigma_{i\alpha,\alpha}^0 = 0 \tag{30}$$

$$\begin{cases} \sigma_{\alpha\beta,\beta}^1 + \sigma_{\alpha 3,3}^0 = 0 \\ \sigma_{3\beta,\beta}^1 + \sigma_{33,3}^0 + b_3 f = 0 \end{cases} \tag{31}$$

$$\begin{cases} \sigma_{\alpha\beta,\beta}^2 + \sigma_{\alpha 3,3}^1 + b_\alpha f = 0 \\ \sigma_{3\beta,\beta}^2 + \sigma_{33,3}^1 = 0 \end{cases} \tag{32}$$

$$\sigma_{i\beta,\beta}^p + \sigma_{i3,3}^{p-1} = 0 \quad \text{for} \quad p \geq 3 \tag{33}$$

To finish re-expressing the mechanical problem according to the new variables from the asymptotic expression, the constitutive equation is considered:

$$\boldsymbol{\sigma} = \boldsymbol{C} : \boldsymbol{\varepsilon} \quad \Longrightarrow \quad \boldsymbol{\sigma} = \boldsymbol{C} : (\boldsymbol{\varepsilon}^0 + \eta\, \boldsymbol{\varepsilon}^1 + \eta^2 \boldsymbol{\varepsilon}^2 + \cdots) \tag{34}$$

$$\Longrightarrow \quad \boldsymbol{\sigma}^p = \boldsymbol{C} : \boldsymbol{\varepsilon}^p \quad , \quad p \in \mathbb{N} \tag{35}$$

And the boundary condition on the stress field:

$$\boldsymbol{\sigma} \cdot \boldsymbol{n} = \bar{\boldsymbol{t}} \quad \Longrightarrow \quad \begin{cases} (\boldsymbol{\sigma}_\alpha^0 + \eta\, \boldsymbol{\sigma}_\alpha^1 + \cdots) \cdot \boldsymbol{n} = \eta^2 t_\alpha f \\ (\boldsymbol{\sigma}_3^0 + \eta\, \boldsymbol{\sigma}_3^1 + \cdots) \cdot \boldsymbol{n} = \eta\, t_3\, f \end{cases} \tag{36}$$

Thus:

$$\boldsymbol{\sigma}^0 \cdot \boldsymbol{n} = \boldsymbol{0} \tag{37}$$

$$\begin{cases} \boldsymbol{\sigma}_\alpha^1 \cdot \boldsymbol{n} = 0 \\ \boldsymbol{\sigma}_3^1 \cdot \boldsymbol{n} = t_3\, f \end{cases} \tag{38}$$

$$\begin{cases} \boldsymbol{\sigma}_\alpha^2 \cdot \boldsymbol{n} = t_\alpha\, f \\ \boldsymbol{\sigma}_3^2 \cdot \boldsymbol{n} = 0 \end{cases} \tag{39}$$

$$\boldsymbol{\sigma}^p \cdot \boldsymbol{n} = 0 \quad \text{for} \quad p \geq 3 \tag{40}$$

Summary of the problems to solve:

For each order (or power of η), the corresponding equations are assembled, leading to a series of hierarchal problems to solve:

- The problem P^0 constituted from Eq.25-26 :

$$d_{\alpha,\beta}^{-1} + d_{\beta,\alpha}^{-1} = 0 \quad , \quad d_{3,\alpha}^{-1} = 0$$
$$d_{3,3}^{-1} = 0 \quad , \quad d_{\alpha,\beta}^{0} + d_{\beta,\alpha}^{0} = 0 \quad , \quad d_{3,\alpha}^{0} + d_{\alpha,3}^{-1} = 0 \tag{41}$$

- The problem P^1 constituted from Eq.27,30,35 and 37 :

$$\begin{cases} \sigma_{\alpha\beta,\beta}^0 = 0 & (a) \\ \sigma_{3\beta,\beta}^0 = 0 & (b) \\ \varepsilon_{\alpha\beta}^0 = \dfrac{1}{2}\left(d_{\alpha,\beta}^1 + d_{\beta,\alpha}^1\right) \quad , \quad \varepsilon_{\alpha 3}^0 = \dfrac{1}{2}\left(d_{3,\alpha}^1 + d_{\alpha,3}^0\right) \quad , \quad \varepsilon_{33}^0 = d_{3,3}^0 & \\ \sigma_{ij}^0 = 2\mu\varepsilon_{ij}^0 + \lambda\varepsilon_{kk}^0\delta_{ij} & \\ \sigma_{ij}^0 n_j = 0 & \end{cases} \tag{42}$$

Where : $\mu \coloneqq \frac{E}{2(1+\nu)}$, $\lambda \coloneqq \frac{\nu E}{2(1+\nu)(1-2\nu)}$ are the Lamé coefficients.

- The problem P^2 constituted from Eq.27,31,35 and 38 :

$$\begin{cases} \sigma^1_{\alpha\beta,\beta} + \sigma^0_{\alpha 3,3} = 0 & (a) \\ \sigma^1_{3\beta,\beta} + \sigma^0_{33,3} + b_3 f = 0 & (b) \\ \varepsilon^1_{\alpha\beta} = \frac{1}{2}\left(d^2_{\alpha,\beta} + d^2_{\beta,\alpha}\right) \quad , \quad \varepsilon^1_{\alpha 3} = \frac{1}{2}\left(d^2_{3,\alpha} + d^1_{\alpha,3}\right) \quad , \quad \varepsilon^1_{33} = d^1_{3,3} & \\ \sigma^1_{ij} = 2\mu\varepsilon^1_{ij} + \lambda\varepsilon^1_{kk}\delta_{ij} & \\ \sigma^1_{\alpha j} n_j = 0 & \\ \sigma^1_{3j} n_j = t_3 f & \end{cases} \tag{43}$$

- The problem P³ constituted from Eq.27,32,35 and 39 :

$$\begin{cases} \sigma^2_{\alpha\beta,\beta} + \sigma^1_{\alpha 3,3} + b_\alpha f = 0 & (a) \\ \sigma^2_{3\beta,\beta} + \sigma^1_{33,3} = 0 & (b) \\ \varepsilon^2_{\alpha\beta} = \frac{1}{2}\left(d^3_{\alpha,\beta} + d^3_{\beta,\alpha}\right) \quad , \quad \varepsilon^2_{\alpha 3} = \frac{1}{2}\left(d^3_{3,\alpha} + d^2_{\alpha,3}\right) \quad , \quad \varepsilon^2_{33} = d^3_{3,3} & \\ \sigma^2_{ij} = 2\mu\varepsilon^2_{ij} + \lambda\varepsilon^2_{kk}\delta_{ij} & \\ \sigma^2_{\alpha j} n_j = t_\alpha f & \\ \sigma^2_{3j} n_j = 0 & \end{cases} \tag{44}$$

- And the problem Pᵖ for $p \geq 3$, constituted from Eq.27,33,35 and 40 :

$$\begin{cases} \sigma^p_{i\beta,\beta} + \sigma^{p-1}_{i3,3} = 0 & (a) \\ \varepsilon^p_{\alpha\beta} = \frac{1}{2}\left(d^{p+1}_{\alpha,\beta} + d^{p+1}_{\beta,\alpha}\right) \quad , \quad \varepsilon^p_{\alpha 3} = \frac{1}{2}\left(d^{p+1}_{3,\alpha} + d^p_{\alpha,3}\right) \quad , \quad \varepsilon^p_{33} = d^p_{3,3} & \\ \sigma^p_{ij} = 2\mu\varepsilon^p_{ij} + \lambda\varepsilon^p_{kk}\delta_{ij} & \\ \sigma^p_{ij} n_j = 0 & \end{cases} \tag{45}$$

The solution of the problems:

We give here directly the solution of the problems established from the AEM for a homogeneous material. The general case of a composite material will be given in the next section, along with the details of the solution derivation.

From the problems in Eq.41-45 we can deduce the expressions of the displacements vectors $\boldsymbol{d}^p$ for $p \geq -1$, and by replacing them into Eq.19, we obtain the form of the displacement vector $\boldsymbol{d}$:

$$d_\alpha = U_\alpha + \psi^{\text{tor}}_\alpha \theta + \eta\, \psi^{1.3}_\alpha U_{3,3} + \eta^2 \psi^{1.\beta}_\alpha U_{\beta,33} + \sum_{odd\ p \geq 3} \eta^p \left(\psi^{p.1}_\alpha f^{(p-3)} + \psi^{p.2}_\alpha f^{(p-2)}\right) \tag{46}$$

$$d_3 = U_3 + \eta\left(-y_\alpha U_{\alpha,3} + \Omega^{1.1}\theta_{,3}\right) + \eta^3 \Omega^{2.\alpha} T_\alpha + \eta^2 \Omega^{2.3} f + \sum_{even\ p \geq 4} \eta^p \left(\Omega^{p.1} f^{(p-3)} + \Omega^{p.2} f^{(p-2)}\right) \tag{47}$$

Where $f^{(p)} \coloneqq \frac{d^p f}{dx_3^p}$ is the pᵗʰ derivate of f with respect to the longitudinal variable x_3. $U_i(x_3)$ and $\theta(x_3)$ are the components of the rigid body motion, $\boldsymbol{\psi}^{\text{tor}} \coloneqq (-y_2, y_1)$ represents the torsion mode expressed in a vector form, and T_α the shear efforts. In this article, all the warping modes (cross section out of plane deformation) will be designated with the greek letter $\Omega(\boldsymbol{y})$ and the transverse deformation modes (cross section in-plane deformation) with the letter $\boldsymbol{\psi}(\boldsymbol{y}) = \left(\psi_1(\boldsymbol{y}), \psi_2(\boldsymbol{y})\right)$. The notation *'p.i'* into the exponents of the warping and transverse deformation modes means: 'p' the order to which they correspond and 'i' simply represents the number of the mode in the considered order.

We note that $\Omega^{1.1}, \Omega^{2.\alpha}$ and $\boldsymbol{\psi}^{1.i}$, are the particular warping and transverse deformation modes corresponding to the well-known Saint-Venant solution, and are determined independently of the external loading. The higher order modes of warping ($\Omega^{p.\alpha}$) and transverse deformation $\left(\boldsymbol{\psi}^{p.\alpha} = \left(\psi_1^{p.\alpha}, \psi_2^{p.\alpha}\right)\right)$ associated to f or one of its derivative, depends by construction of the applied loads. We note that if the form of the variation of the external force is polynomial, $f(y_3) = \sum_{i=1}^{n} a_i y_3^i$, the infinite sums in Eq.46-47 will be truncated at the order of the polynomial, since $f^{(n+1)} = 0$.

Remark: From Eq.46-47, we note that for the case of no external forces applied to the beam ($f = 0$), the displacement obtained from the AEM will take exactly the form of the classical Saint-Venant solution.

The transverse deformation modes $\boldsymbol{\psi}^{1.i}(\boldsymbol{y})$ can be written explicitly in the case of a homogeneous material, in the following way:

$$\begin{cases} \psi_1^{1.1} = \dfrac{\nu}{2}(y_1^2 - y_2^2) \\ \psi_2^{1.1} = \nu\, y_1 y_2 \end{cases} \quad , \quad \begin{cases} \psi_1^{1.2} = \nu\, y_1 y_2 \\ \psi_2^{1.2} = \dfrac{\nu}{2}(y_2^2 - y_1^2) \end{cases} \quad , \quad \begin{cases} \psi_1^{1.3} = -\nu\, y_1 \\ \psi_2^{1.3} = -\nu\, y_2 \end{cases} \tag{48}$$

Where $\nu = \frac{\lambda}{2(\lambda+\mu)}$ is the Poisson's coefficient.

The warping modes $\left(\Omega^{1.1}(\boldsymbol{y}), \Omega^{2.\alpha}(\boldsymbol{y})\right)$ are obtained from the solution of the following partial derivatives problems, expressed on the beam's cross section in the following manner:

$$\begin{cases} \Delta_{\boldsymbol{y}} \Omega^{1.1} = 0 & \text{in } S \\ \dfrac{\partial \Omega^{1.1}}{\partial n} = -y_2 n_1 + y_1 n_2 & \text{in } \Gamma_s \end{cases} \tag{49}$$

$$\begin{cases} \Delta_{\boldsymbol{y}} \Omega^{2.1} = -2y_1 & \text{in } S \\ \dfrac{\partial \Omega^{2.1}}{\partial n} = \dfrac{\nu}{2}(y_1^2 - y_2^2) n_1 + \nu\, y_1 y_2 n_2 & \text{in } \Gamma_s \end{cases} \tag{50}$$

$$\begin{cases} \Delta_{\boldsymbol{y}} \Omega^{2.2} = -2y_2 & \text{in } S \\ \dfrac{\partial \Omega^{2.2}}{\partial n} = \nu\, y_1 y_2 n_1 + \dfrac{\nu}{2}(y_2^2 - y_1^2) n_2 & \text{in } \Gamma_s \end{cases} \tag{51}$$

Where we remind that $\boldsymbol{n} = (n_1, n_2)$ is the normal vector to the cross section border Γ_s, and $\Delta_{\boldsymbol{y}} = \frac{\partial^2}{\partial y_1^2} + \frac{\partial^2}{\partial y_2^2}$ is the Laplace operator.

For the higher order warping and transverse deformation modes associated to the external forces, we obtain a recurrence relation from the AEM. If we want to determine the warping mode Ω^p, while we know the modes of the last order $\boldsymbol{\psi}^{p-1}$ and Ω^{p-2}, the recurrence relation is written by:

$$\begin{cases} \mu \Delta_{\boldsymbol{y}} \Omega^p = (\mu + \lambda) \mathrm{div}_{\boldsymbol{y}}(\boldsymbol{\psi}^{p-1} - \boldsymbol{\Phi}^p) + (2\mu + \lambda)(\Omega^{p-2} - \vartheta^p) & \text{in S} \\ \dfrac{\partial \Omega^p}{\partial n} = (\boldsymbol{\psi}^{p-1} - \boldsymbol{\Phi}^p) \cdot \boldsymbol{n} & \text{in } \Gamma_s \end{cases} \tag{52}$$

Where :

$$\Phi_\alpha^p \coloneqq \frac{P^p}{ES}\psi_\alpha^{1.3} + \frac{Q_1^p}{EI_1}\psi_\alpha^{1.1} + \frac{Q_2^p}{EI_2}\psi_\alpha^{1.2} \quad , \quad \vartheta^p \coloneqq \frac{P^p}{ES} - \frac{Q_1^p}{EI_1} y_1 - \frac{Q_2^p}{EI_2} y_2 \tag{53}$$

$$P^p \coloneqq \int_S \left((2\mu + \lambda)\Omega^{p-2} + \lambda\, \psi_{\beta,\beta}^{p-1}\right) dS \quad , \quad Q_\alpha^p \coloneqq \int_S y_\alpha \left((2\mu + \lambda)\Omega^{p-2} + \lambda\, \psi_{\beta,\beta}^{p-1}\right) dS \tag{54}$$

We note that P^p and Q_α^p can be assimilated to a normal effort and bending moments, respectively, obtained from the transverse deformation and warping modes of the last orders.

The problem in Eq.52 represents a Poisson equation with a Neumann boundary condition. The problem is solved up to an additive uniform displacement. Generally, to assure the uniqueness, we add the condition $\int_S \Omega^p dS = 0$. But in order to obtain a solution independent of the choice of the condition to add, the problem needs to be self-equilibrated. We mean by self-equilibrated that the "source functions" charging the Poisson problem, do not generate any normal force or bending moments, which in terms of equations is expressed in the following way:

$$\int_S g\, dS + \int_{\Gamma_s} q\, d\Gamma_s = 0 \quad , \quad \int_S y_\alpha\, g\, dS + \int_{\Gamma_s} y_\alpha\, q\, d\Gamma_s = 0 \tag{55}$$

Where $g(\boldsymbol{y})$ and $q(\boldsymbol{y})$ are the "source functions" charging the Poisson problem in Eq.52:

$$g = (\mu+\lambda)\mathrm{div}_{\boldsymbol{y}}(\boldsymbol{\psi}^{p-1} - \boldsymbol{\Phi}^p) + (2\mu+\lambda)(\Omega^{p-2} - \vartheta^p) \quad , \quad q = \mu(\boldsymbol{\psi}^{p-1} - \boldsymbol{\Phi}^p)\cdot \boldsymbol{n} \tag{56}$$

We can see that, by construction of the functions $\boldsymbol{\Phi}^p$ and ϑ^p, g and q will verify the relations in Eq.55. Thus, we can say that the problem in Eq.52 is self-equilibrated.

To determine the transverse deformation mode $\boldsymbol{\psi}^p$, we have the following recurrence relation obtained from the AEM:

$$\text{find } \boldsymbol{\psi}^p/\forall \boldsymbol{w},\ W\left(\psi_\alpha^p, w_\alpha\right) = \int_S \mu\left(\Omega_{,\alpha}^{p-1} + \psi_\alpha^{p-2} - \frac{Z^p}{\mu J}\left(\Omega_{,\alpha}^{1.1} + \psi_\alpha^{\mathrm{tor}}\right)\right) w_\alpha\, dS - \int_S \lambda\left(\Omega^{p-1} - \frac{Z^p}{\mu J}\Omega^{1.1}\right) w_{\alpha,\alpha} dS \tag{57}$$

Where W is a symmetric bilinear form expressed by:

$$W(u_\alpha, w_\alpha) \coloneqq \int_S \mu\left(u_{\alpha,\beta} + u_{\beta,\alpha}\right) w_{\alpha,\beta}\, dS + \int_S \lambda u_{\beta,\beta} w_{\alpha,\alpha}\, dS \tag{58}$$

And:

$$Z^p \coloneqq \int_S \mu\psi_\alpha^{\mathrm{tor}}\left(\Omega_{,\alpha}^{p-1} + \psi_\alpha^{p-2}\right) dS \tag{59}$$

We can see that Z^p corresponds to the torsion moment created by the shear strains due the last orders modes. Being present in Eq.57, it assures the problem to be torsion free, and can be solved uniquely on the cross section, up to a rigid body motion.

We will detail now the derivation of the solution of the problems stated in Eq.41-45. At the exception of the problem P^0 and P^1, the procedure needs to be performed, for each order, in two levels. A macroscopic level where the macroscopic equilibrium equations are determined, and a microscopic level where the form of the displacement vector is obtained from the solution of local problems, which are expressed on the beam's cross section and that are self-equilibrated by using the macroscopic equilibrium equations.

4.3 Solution of the problem P^n for an arbitrary order n :

Problem P^0 :

From Eq.25, the following form of the displacements vector $\boldsymbol{d}^{-1}$ can be easily deduced:

$$d_{\alpha,\beta}^{-1} + d_{\beta,\alpha}^{-1} = 0 \quad , \quad d_{3,\alpha}^{-1} = 0 \qquad \Longrightarrow \qquad \boldsymbol{d}^{-1} = \begin{Bmatrix} U_1^{-1}(y_3) - y_2\theta^{-1}(y_3) \\ U_2^{-1}(y_3) + y_1\theta^{-1}(y_3) \\ U_3^{-1}(y_3) \end{Bmatrix} \tag{60}$$

From Eq.26, the form of the displacements vector $\boldsymbol{d}^0$ is obtained along with a condition on d_3^{-1}:

$$d_{3,3}^{-1} = 0 \quad \Longrightarrow \quad U_3^{-1} = cte = 0 \tag{61}$$

$$d_{\alpha,\beta}^{0} + d_{\beta,\alpha}^{0} = 0 \quad , \quad d_{3,\alpha}^{0} + d_{\alpha,3}^{-1} = 0 \quad \Longrightarrow \quad \boldsymbol{d}^{0} = \begin{Bmatrix} U_1^{0}(y_3) - y_2\theta^{0}(y_3) \\ U_2^{0}(y_3) + y_1\theta^{0}(y_3) \\ U_3^{0}(y_3) - y_\alpha U_{\alpha,3}^{-1}(y_3) \end{Bmatrix} \quad , \quad \theta^{-1} = 0 \tag{62}$$

If we stop the asymptotic expansion at this order and we sum the two displacements vectors obtained above, we obtain a kinematic to the Timoshenko beam theory. We note that the transversal rigid body motion due to U_α^{-1} in $\boldsymbol{d}^{-1}$, has led, in the next order, to the flexural longitudinal motion $\left(-y_\alpha U_{\alpha,3}^{-1}\right)$ in $\boldsymbol{d}^0$.

Problem P¹ :

Our goal for this order is to solve the local equilibrium problem P¹ in Eq.42 and determine the form, in the beam's cross section, of the displacement vector $\boldsymbol{d}^1$. The derivation of the transversal components (d_1^1, d_2^1) will lead to the determination of transversal deformation modes and the derivation of the longitudinal component d_3^1 will lead to the determination of warping modes. For an isotropic material, the two problems are completely independent and will be solved by using a variational formulation in the cross section S.

The problem leading to the derivation of the transversal deformation modes at this order, is obtained by writing the weak form of Eq.42a :

$$\int_S \sigma_{\alpha\beta,\beta}^0 w_\alpha dS = 0 \tag{63}$$

After an integration by parts:

$$-\int_S \sigma_{\alpha\beta}^0 w_{\alpha,\beta}\, dS + \int_{\Gamma_S} \underbrace{\sigma_{\alpha\beta}^0 n_\beta}_{=0} w_\alpha\, d\Gamma_S = 0 \tag{64}$$

Using the constitutive relation, Eq.64 becomes:

$$\int_S \left(2\mu\varepsilon_{\alpha\beta}^0 + \lambda\varepsilon_{kk}^0\delta_{\alpha\beta}\right) w_{\alpha,\beta}\, dS = 0 \tag{65}$$

Replacing the strains in Eq.65 with their expressions in function of the displacements, we obtain:

$$\int_S \mu\left(d_{\alpha,\beta}^1 + d_{\beta,\alpha}^1\right) w_{\alpha,\beta}\, dS + \int_S \lambda d_{\beta,\beta}^1 w_{\alpha,\alpha}\, dS + \int_S \lambda d_{3,3}^0 w_{\alpha,\alpha}\, dS = 0 \tag{66}$$

$$W(d_\alpha^1, w_\alpha) + \int_S \lambda d_{3,3}^0 w_{\alpha,\alpha}\, dS = 0 \tag{67}$$

$$W(d_\alpha^1, w_\alpha) = U_{\beta,33}^{-1} \int_S \lambda y_\beta w_{\alpha,\alpha}\, dS - U_{3,3}^0 \int_S \lambda w_{\alpha,\alpha}\, dS \tag{68}$$

Where W is a symmetric bilinear form (already defined in Eq.58), representing an elastic energy and from which the stiffness matrix of the cross section will be deduced.

The vector d_α^1 in Eq.68 will be obtained up to a rigid body motion and by noticing that the problem is linear, the form of d_α^1 is stated to be written in the following form:

$$\begin{Bmatrix} d_1^1 \\ d_2^1 \end{Bmatrix} = \begin{Bmatrix} U_1^1 - y_2\theta^1 \\ U_2^1 + y_1\theta^1 \end{Bmatrix} + \begin{Bmatrix} \psi_1^{1.\beta} U_{\beta,33}^{-1} + \psi_1^{1.3} U_{3,3}^0 \\ \psi_2^{1.\beta} U_{\beta,33}^{-1} + \psi_2^{1.3} U_{3,3}^0 \end{Bmatrix} \tag{69}$$

Where $\psi_\alpha^{1.i}(y_1, y_2)$ designate the transversal deformation modes for this order.

From Eq.68, we deduce the variational equations leading to $\psi_\alpha^{1.i}$:

$$\text{find } \boldsymbol{\psi}^{1.\beta} \,/\, \forall \boldsymbol{w}, \qquad W\left(\psi_\alpha^{1.\beta}, w_\alpha\right) = \int_S \lambda y_\beta w_{\alpha,\alpha}\, dS \tag{70}$$

$$\text{find } \boldsymbol{\psi}^{1.3} \,/\, \forall \boldsymbol{w}, \qquad W(\psi_\alpha^{1.3}, w_\alpha) = -\int_S \lambda w_{\alpha,\alpha}\, dS \tag{71}$$

The three independent problems expressed in Eq.70-71 are solved in the beam's cross section by using a finite element discretization (triangular elements). The left part of the equations will gives arise to a stiffness matrix, and the right parts to three different effort vectors. Finding the values of the modes $\psi_\alpha^{1.i}$ on the cross section, is then reduced to solving a linear system of equations. For the special case of homogeneous material, it is possible to write the functions $\psi_\alpha^{1.i}$ explicitly (Eq.48).

For the derivation of the form of the longitudinal displacement, Eq.42b is considered:

$$\sigma_{3\alpha,\alpha}^0 = 0 \quad \Longrightarrow \quad \mu\varepsilon_{3\alpha,\alpha}^0 + \mu_{,\alpha}\varepsilon_{3\alpha}^0 = 0 \tag{72}$$

$$\mu\left(d_{3,\alpha\alpha}^1 + d_{\alpha,3\alpha}^0\right) + \mu_{,\alpha}\left(d_{3,\alpha}^1 + d_{\alpha,3}^0\right) = 0 \tag{73}$$

$$\mu\Delta_{\boldsymbol{y}} d_3^1 + \boldsymbol{\nabla}_{\boldsymbol{y}}\mu \cdot \boldsymbol{\nabla}_{\boldsymbol{y}} d_3^1 = -\mu_{,\alpha} d_{\alpha,3}^0 \tag{74}$$

$$\mu\Delta_{\boldsymbol{y}} d_3^1 + \boldsymbol{\nabla}_{\boldsymbol{y}}\mu \cdot \boldsymbol{\nabla}_{\boldsymbol{y}} d_3^1 = -\mu_{,\alpha}\left(U_{\alpha,3}^0 + \psi_\alpha^{\mathrm{tor}}\theta_{,3}^0\right) \tag{75}$$

Where we remind that $\boldsymbol{\psi}^{\mathrm{tor}} \coloneqq (-y_2, y_1)$ represents the rigid body mode of torsion.

And from the boundary condition:

$$\sigma_{3j}^0 n_j = 0 \quad \Longrightarrow \quad d_{3,\alpha}^1 n_\alpha = -d_{\alpha,3}^0 n_\alpha \tag{76}$$

$$\frac{\partial d_3^1}{\partial n} = -\left(U_{\alpha,3}^0 + \psi_\alpha^{\mathrm{tor}}\theta_{,3}^0\right) n_\alpha \tag{77}$$

Where $\frac{\partial d_3^1}{\partial n} \coloneqq d_{3,\alpha}^1 n_\alpha$

The terms associated to $U_{\alpha,3}^0$ will only give the flexural modes already introduced at the last order for d_3^0. The new warping mode at this order is the one associated to $\theta_{,3}^0$, that corresponds to the well-known warping mode of torsion (in Vlassov or Saint-Venant theory), obtained from the solution of the following partial derivatives problem:

$$\begin{cases} \mu\Delta_{\boldsymbol{y}}\Omega^{1.1} + \boldsymbol{\nabla}_{\boldsymbol{y}}\mu \cdot \boldsymbol{\nabla}_{\boldsymbol{y}}\Omega^{1.1} = -\boldsymbol{\nabla}_{\boldsymbol{y}}\mu \cdot \boldsymbol{\psi}^{\mathrm{tor}} & \text{in } S \\ \dfrac{\partial\Omega^{1.1}}{\partial n} = -\boldsymbol{\psi}^{\mathrm{tor}} \cdot \boldsymbol{n} & \text{in } \Gamma_s \end{cases} \tag{78}$$

Since it is only needed to determine $\Omega^{1.1}$ up to an additive constant, we can add the condition $\int_S \Omega^{1.1} dS = 0$ to determine $\Omega^{1.1}$ uniquely. The equivalent weak form of Eq.78 is given in appendix A.1.

The complete form of the displacement vector $\boldsymbol{d}^1$ can know be written:

$$\boldsymbol{d}^1 = \underbrace{\begin{Bmatrix} U_1^1 - y_2\theta^1 \\ U_2^1 + y_1\theta^1 \\ U_3^1 - y_\alpha U_{\alpha,3}^0 \end{Bmatrix}}_{P^{-1}} + \underbrace{\begin{Bmatrix} \psi_1^{1.\beta} U_{\beta,33}^{-1} + \psi_1^{1.3} U_{3,3}^0 \\ \psi_2^{1.\beta} U_{\beta,33}^{-1} + \psi_2^{1.3} U_{3,3}^0 \\ \Omega^{1.1}\theta_{,3}^0 \end{Bmatrix}}_{P^0} \tag{79}$$

Remark: the longitudinal variation of the rotation θ^0 at the last order is not necessarily null $\left(\theta_{,3}^0 \neq 0\right)$. This non null variation has led, in the next order problem P¹, to the derivation of a warping mode $\Omega^{1.1}$ weighted by $\theta_{,3}^0$. This allow us to introduce a general and important feature about the asymptotic expansion method in this work: the longitudinal variation of a transverse deformation mode, will give arise, at the next order, to a warping mode and vice versa.

Problem P²:

At this order the external longitudinal forces appears and will naturally give arise to a corresponding new warping mode. But before starting to solve the problem P² to find the form of the displacement vector $\boldsymbol{d}^2$, we need to determine the macroscopic equilibrium equations for this order that will be used to obtain self-equilibrated problems. We take then the mean values of Eq.43a and 43b:

$$\langle \sigma_{\alpha\beta,\beta}^1 + \sigma_{\alpha 3,3}^0 \rangle = 0 \quad , \quad \langle \psi_\alpha^{\text{tor}} \left(\sigma_{\alpha\beta,\beta}^1 + \sigma_{\alpha 3,3}^0 \right) \rangle = 0 \tag{80}$$

$$\langle \sigma_{3\beta,\beta}^1 + \sigma_{33,3}^0 + b_3 f \rangle = 0 \quad , \quad \langle y_\alpha \left(\sigma_{3\beta,\beta}^1 + \sigma_{33,3}^0 + b_3 f \right) \rangle = 0 \tag{81}$$

Where: $\langle \cdot \rangle \coloneqq \int_S \cdot \, dS$

By replacing with the expression of the stresses and using the boundaries conditions, we obtain from Eq.80-81 six macroscopic equilibrium equations:

$$T_{\alpha,3}^0 = 0 \quad , \quad M_{3,3}^0 = 0 \tag{82}$$

$$N_{,3}^0 + r_3 f = 0 \quad , \quad M_{\alpha,3}^0 + T_\alpha^1 + m_\alpha f = 0 \tag{83}$$

Where r_3 and m_α are the resultants of the external longitudinal force on the cross section:

$$r_3 \coloneqq \int_S b_3 dS + \int_{\Gamma_s} t_3 d\Gamma_s \quad , \quad m_\alpha \coloneqq \int_S y_\alpha b_3 dS + \int_{\Gamma_s} y_\alpha t_3 d\Gamma_s \tag{84}$$

And the expression of the generalized internal efforts are given by:

$$T_\alpha^0 \coloneqq \int_S \sigma_{\alpha 3}^0 \, dS = \int_S \mu \left(d_{3,\alpha}^1 + d_{\alpha,3}^0 \right) dS = \mu J_\alpha \theta_{,3}^0 \tag{85}$$

$$M_3^0 \coloneqq \int_S \psi_\alpha^{\text{tor}} \sigma_{\alpha 3}^0 \, dS = \mu J \theta_{,3}^0 \tag{86}$$

$$N^0 \coloneqq \int_S \sigma_{33}^0 \, dS = \int_S \left((2\mu + \lambda) d_{3,3}^0 + \lambda d_{\alpha,\alpha}^1 \right) dS = A_{33} U_{3,3}^0 + A_{3\alpha} U_{\alpha,33}^{-1} \tag{87}$$

$$M_\alpha^0 \coloneqq -\int_S y_\alpha \sigma_{33}^0 \, dS = A_{\alpha 3} U_{3,3}^0 + A_{\alpha\beta} U_{\beta,33}^{-1} \tag{88}$$

And the coefficients:

$$\mu J \coloneqq \int_S \mu\psi_\alpha^{\mathrm{tor}}\left(\Omega_{,\alpha}^{1.1} + \psi_\alpha^{\mathrm{tor}}\right)dS \tag{89}$$

$$\mu J_\alpha \coloneqq \int_S \mu\left(\Omega_{,\alpha}^{1.1} + \psi_\alpha^{\mathrm{tor}}\right)dS \tag{90}$$

$$A_{33} \coloneqq \int_S \left(2\mu + \lambda + \lambda \mathrm{div}_{\boldsymbol{y}}(\boldsymbol{\psi}^{1.3})\right)dS = \int_S \mu\left(2 - \mathrm{div}_{\boldsymbol{y}}(\boldsymbol{\psi}^{1.3})\right)dS \tag{91}$$

$$A_{3\alpha} \coloneqq \int_S \left(\lambda \mathrm{div}_{\boldsymbol{y}}(\boldsymbol{\psi}^{1.\alpha}) - (2\mu + \lambda)y_\alpha\right)dS = -\int_S \mu\left(2y_\alpha + \mathrm{div}_{\boldsymbol{y}}(\boldsymbol{\psi}^{1.\alpha})\right)dS \tag{92}$$

$$A_{\alpha 3} \coloneqq -\int_S \left(2\mu + \lambda + \lambda \mathrm{div}_{\boldsymbol{y}}(\boldsymbol{\psi}^{1.3})\right)y_\alpha dS = -\int_S \mu\left(2 - \mathrm{div}_{\boldsymbol{y}}(\boldsymbol{\psi}^{1.3})\right)y_\alpha dS \tag{93}$$

$$A_{\alpha\beta} \coloneqq \int_S \left((2\mu + \lambda)y_\alpha - \lambda \mathrm{div}_{\boldsymbol{y}}\left(\boldsymbol{\psi}^{1.\beta}\right)\right)y_\beta dS = \int_S \mu\left(2y_\alpha + \mathrm{div}_{\boldsymbol{y}}(\boldsymbol{\psi}^{1.\alpha})\right)y_\beta dS \tag{94}$$

The constant J corresponds to the torsion inertia as obtained in the Saint-Venant or Vlassov beam theory. It can easily be proven that by construction of the function $\Omega^{1.1}$, the constants J_α are equal to zero and that by construction of the functions $\boldsymbol{\psi}^{1.i}$, the matrix A_{ij} is symmetric definite positive.

For a homogeneous material, we can use the expressions of the functions $\boldsymbol{\psi}^{1.i}$ in Eq.48 to obtain a simplified form of the coefficients expressed in Eq.91-94:

$$A_{33} = ES \quad , \quad A_{3\alpha} = A_{\alpha 3} = -E\int_S y_\alpha dS \quad , \quad A_{\alpha\beta} = E\int_S y_\alpha y_\beta dS \tag{95}$$

Where $E = \frac{\mu(2\mu+3\lambda)}{\mu+\lambda}$ is the Young modulus.

We define the gravity center and the principal axis orientation of the cross section by the following equations:

$$A_{\alpha 3} = 0 \quad , \quad A_{12} = 0 \tag{96}$$

From Eq.95-96, we note that the definition of the principal axis for a homogeneous material, corresponds to the classical definition that is commonly used. In the case of an arbitrary composite material, the expressions of the functions $\boldsymbol{\psi}^{1.i}$ in Eq.48 are no longer valid, and thus the relations in Eq.95 will also be no longer valid. In order then to find the principal axis of the cross section in accordance to the conditions defined in Eq.96, it is necessary, in a first step, to determine the functions $\boldsymbol{\psi}^{1.i}$ for an arbitrary set of orthogonal axis in the section, and then, in a second step, find the position and the orientation of the axis that verifies Eq.96.

By replacing the expressions of the internal efforts in Eq.85-88 into the macro equilibrium equation in Eq.82-83, the following relations are obtained:

$$\theta_{,33}^0 = 0 \quad , \quad U_{3,33}^0 = -\frac{r_3}{ES}f \quad , \quad U_{\alpha,333}^{-1} = -\frac{1}{EI_\alpha}(T_\alpha^1 + m_\alpha f) \text{ (no sum on α)} \tag{97}$$

These relations are important for what follows. For example we can deduce that the warping mode due to torsion $\Omega^{1.1}$, determined for $\boldsymbol{d}^1$ and weighted by $\theta_{,3}^0$, will not induce any transverse deformation mode at the next order, since its longitudinal variation is equal to zero ($\theta_{,33}^0 = 0$). We can say the same thing for $U_{3,33}^0$ if $f = 0$, but what import most is that these equations will allow us to obtain self-equilibrated microscopic problems for the determination of the warping modes of this order.

Let us now solve the microscopic problem at the cross section level to obtain the form of the displacement vector $\boldsymbol{d}^2$. Since at this order no new transversal modes are determined, we consider only the equation Eq.43b in which the stresses are replaced by their expression in function of the displacements to obtain:

$$\partial_\alpha\left(\mu d^2_{3,\alpha}\right) = -\partial_\alpha\left(\mu d^1_{\alpha,3}\right) - \lambda d^1_{\alpha,\alpha 3} - (2\mu+\lambda) d^0_{3,33} - b_3 f \tag{98}$$

The equation above will have the same form for any arbitrary order, only the exponents' needs to be incremented for each order.

The expressions of the displacements components d^1_α and d^0_3 are substituted in Eq.98 to obtain:

$$\partial_\alpha\left(\mu d^2_{3,\alpha}\right) = -\left(\partial_\alpha(\mu\psi^{1.3}_\alpha) + \lambda\psi^{1.3}_{\alpha,\alpha} + 2\mu + \lambda\right)U^0_{3,33} - \left(\partial_\gamma\left(\mu\psi^{1.\alpha}_\gamma\right) + \lambda\psi^{1.\alpha}_{\gamma,\gamma} - (2\mu+\lambda)y_\alpha\right)U^{-1}_{\alpha,333} - b_3 f \tag{99}$$

And by using the expressions of $U^0_{3,33}$ and $U^{-1}_{\alpha,333}$ in Eq.97, the equation above becomes:

$$\begin{aligned}\partial_\alpha\left(\mu d^2_{3,\alpha}\right) = {} & \left(\partial_\alpha(\mu\psi^{1.1}_\alpha) + \lambda\psi^{1.1}_{\alpha,\alpha} - (2\mu+\lambda)y_1\right)\frac{T^1_1}{EI_1} + \left(\partial_\alpha(\mu\psi^{1.2}_\alpha) + \lambda\psi^{1.2}_{\alpha,\alpha} - (2\mu+\lambda)y_2\right)\frac{T^1_2}{EI_2} \\ & + \left(\partial_\alpha(\mu\phi^2_\alpha) + \lambda\phi^2_{\alpha,\alpha} + (2\mu+\lambda)\vartheta^2 - b_3\right)f\end{aligned} \tag{100}$$

Where :

$$\phi^2_\alpha \coloneqq \frac{r_3}{ES}\psi^{1.3}_\alpha + \frac{m_1}{EI_1}\psi^{1.1}_\alpha + \frac{m_2}{EI_2}\psi^{1.2}_\alpha \quad , \quad \vartheta^2 \coloneqq \frac{r_3}{ES} - \frac{m_1}{EI_1}y_1 - \frac{m_2}{EI_2}y_2 \tag{101}$$

We develop now the boundary condition for this order:

$$\sigma^1_{3j}n_j = t_3 f_0 \quad \Longrightarrow \quad \mu d^2_{3,\alpha}n_\alpha = -\mu d^1_{\alpha,3}n_\alpha \tag{102}$$

$$\mu\frac{\partial d^2_3}{\partial n} = -\mu\left(\psi^{1.3}_\gamma U^0_{3,33} + \psi^{1.\alpha}_\gamma U^{-1}_{\alpha,333}\right)n_\gamma + t_3 f \tag{103}$$

$$\mu\frac{\partial d^2_3}{\partial n} = \mu\left(\frac{T^1_1}{EI_1}\psi^{1.1}_\alpha n_\alpha + \frac{T^1_2}{EI_2}\psi^{1.2}_\alpha n_\alpha\right) + \left(\mu\phi^2_{\alpha,\alpha}n_\alpha + t_3\right)f \tag{104}$$

The longitudinal component d^2_3 has the same form as in Eq.79 for d^1_3 with the addition of the new warping modes that will be derived from Eq.100 and Eq.104:

$$d^2_3 = U^2_3 - y_\alpha U^1_{\alpha,3} + \Omega^{1.1}\theta^1_{,3} + \Omega^{2.\beta}T^1_\beta + \Omega^{2.3}f \tag{105}$$

The problem formed by the relations in Eq.100 and Eq.104 can then be decomposed into three separate independent problems:

$$\begin{cases}\partial_\alpha\left(\mu\Omega^{2.\beta}_{,\alpha}\right) = \dfrac{1}{EI_\beta}\left(\partial_\alpha\left(\mu\psi^{1.\beta}_\alpha\right) + \lambda\psi^{1.\beta}_{\alpha,\alpha} - (2\mu+\lambda)y_\beta\right) & \text{in } S \\ \dfrac{\partial\Omega^{2.\beta}}{\partial n} = \dfrac{1}{EI_\beta}\psi^{1.\beta}_\alpha n_\alpha & \text{in } \Gamma_s\end{cases} \quad \text{(no sum on β)} \tag{106}$$

$$\begin{cases}\partial_\alpha\left(\mu\Omega^{2.3}_{,\alpha}\right) = \partial_\alpha(\mu\phi^2_\alpha) + \lambda\phi^2_{\alpha,\alpha} + (2\mu+\lambda)\vartheta^2 - b_3 & \text{in } S \\ \mu\dfrac{\partial\Omega^{2.3}}{\partial n} = \mu\phi^2_{\alpha,\alpha}n_\alpha + t_3 & \text{in } \Gamma_s\end{cases} \tag{107}$$

We note that the functions $\Omega^{2.\beta}$ determined in Eq.106, corresponds to the classical warping modes, for shear efforts, in the Saint-Venant solution of beam elements.

We can write now the complete form of the displacement vector $\boldsymbol{d}^2$:

$$\boldsymbol{d}^2 = \underbrace{\begin{Bmatrix} U_1^2 - y_2\theta^2 + \psi_1^{1.\beta}U_{\beta,33}^0 + \psi_1^{1.3}U_{3,3}^1 \\ U_2^2 + y_1\theta^2 + \psi_1^{1.\beta}U_{\beta,33}^0 + \psi_1^{1.3}U_{3,3}^1 \\ U_3^2 - y_\alpha U_{\alpha,3}^1 + \Omega^{1.1}\theta_{,3}^1 + \Omega^{2.\beta}T_\beta^1 \end{Bmatrix}}_{\text{St-Venant kinematic}} + \begin{Bmatrix} 0 \\ 0 \\ \Omega^{2.3}f \end{Bmatrix} \tag{108}$$

Problem P³:

At this order the transversal forces appears, leading to the determination of a corresponding transversal deformation mode. We note that since no new transversal modes have been determined at the last order, no new warping modes will appears for this order. Thus, only the relation in Eq.44a is used to obtain the new transversal modes, but, as for the last mode, we determine first the macroscopic equilibrium equations. From the integration of Eq.44a we obtain:

$$\langle \sigma_{\alpha\beta,\beta}^2 + \sigma_{\alpha 3,3}^1 + b_\alpha f \rangle = 0 \qquad , \quad \langle \psi_\alpha^{\text{tor}} \left(\sigma_{\alpha\beta,\beta}^2 + \sigma_{\alpha 3,3}^1 + b_\alpha f \right) \rangle = 0 \tag{109}$$

$$\Longrightarrow \qquad T_{\alpha,3}^1 + r_\alpha f = 0 \qquad , \qquad M_{3,3}^1 + m_3 f = 0 \tag{110}$$

Where r_α and m_3 are the shear and torsion resultants, respectively, of the external transverse forces acting on the cross section:

$$r_\alpha \coloneqq \int_S b_\alpha dS + \int_{\Gamma_s} t_\alpha d\Gamma_s \qquad , \qquad m_3 \coloneqq \int_S \psi_\alpha^{\text{tor}} b_\alpha dS + \int_{\Gamma_s} \psi_\alpha^{\text{tor}} t_\alpha d\Gamma_s \tag{111}$$

And the expression of the generalized internal efforts:

$$T_\alpha^1 \coloneqq \int_S \sigma_{\alpha 3}^1 \, dS \qquad , \qquad M_3^1 \coloneqq \int_S \psi_\alpha^{\text{tor}} \sigma_{\alpha 3}^1 \, dS \tag{112}$$

By developing the expression of the internal torsion moment and replacing it into the torsion macro equilibrium equation in Eq.110, we obtain the following relation:

$$\theta_{,33}^1 = -\frac{1}{\mu J}\left((m_3 + Z^{3.\alpha} r_\alpha) f + Z^{3.3} f_{,3} \right) \tag{113}$$

Where the constants $Z^{3.i}$ can be assimilated to the torsion moment created by the shear stresses of the last order modes, and expressed by:

$$Z^{3.i} \coloneqq \int_S \mu \, \psi_\alpha^{\text{tor}} \left(\Omega_{,\alpha}^{2.i} + \psi_\alpha^{1.i} \right) dS \tag{114}$$

The weak form of Eq.43a is now considered, and after using the same operations for P¹ that led to Eq.66, we obtain for this order:

$$W(d_\alpha^3, w_\alpha) = -\int_S \lambda d_{3,3}^2 w_{\alpha,\alpha} dS + \int_S \sigma_{\alpha 3,3}^1 w_\alpha \, dS + f\left(\int_S b_\alpha w_\alpha \, dS + \int_{\Gamma_s} t_\alpha w_\alpha \, d\Gamma_s \right) \tag{115}$$

From the expressions of the displacements vectors $\boldsymbol{d}^1$ and $\boldsymbol{d}^2$ in Eq.79 and 108, $d_{3,3}^2$ and $\sigma_{\alpha 3,3}^1$ are expressed by:

$$d^2_{3,3} = \Omega^{1.1}\theta^1_{,33} + \Omega^{2.\beta}T^1_{\beta,3} + \Omega^{2.3}f_{,3} = \left(\Omega^{2.3} - \frac{Z^{3.3}}{\mu J}\Omega^{1.1}\right)f_{,3} - \left(\Omega^{2.\beta}r_\beta + \frac{1}{\mu J}\left(m_3 + Z^{3.\beta}r_\beta\right)\Omega^{1.1}\right)f \tag{116}$$

$$\begin{aligned}\sigma^1_{\alpha 3,3} &= \mu\left(d^2_{3,\alpha 3} + d^1_{\alpha,33}\right)\\ &= \mu\left(\Omega^{2.3}_{,\alpha} - \phi^2_\alpha - \frac{Z^{3.3}}{\mu J}\left(\Omega^{1.1}_{,\alpha} + \psi^{\mathrm{tor}}_\alpha\right)\right)f_{,3}\\ &\quad - \mu\left(\Omega^{2.\beta}_{,\alpha}r_\beta + \frac{r_1}{EI_1}\psi^{1.1}_\alpha + \frac{r_2}{EI_2}\psi^{1.2}_\alpha + \frac{1}{\mu J}\left(m_3 + Z^{3.\beta}r_\beta\right)\left(\Omega^{1.1}_{,\alpha} + \psi^{\mathrm{tor}}_\alpha\right)\right)f\end{aligned} \tag{117}$$

We use the following notations:

$$\Upsilon := \Omega^{2.\beta}r_\beta + \frac{1}{\mu J}\left(m_3 + Z^{3.\beta}r_\beta\right)\Omega^{1.1} \quad , \quad \varphi_\alpha := \frac{r_1}{EI_1}\psi^{1.1}_\alpha + \frac{r_2}{EI_2}\psi^{1.2}_\alpha + \frac{1}{\mu J}\left(m_3 + Z^{3.\beta}r_\beta\right)\psi^{\mathrm{tor}}_\alpha \tag{118}$$

Thus Eq.116-117 can be re-written in the following form:

$$d^2_{3,3} = \Omega^{1.1}\theta^1_{,33} + \Omega^{2.\beta}T^1_{\beta,3} + \Omega^{2.3}f_{,3} = \left(\Omega^{2.3} - \frac{Z^{3.3}}{\mu J}\Omega^{1.1}\right)f_{,3} - \Upsilon f \tag{119}$$

$$\sigma^1_{\alpha 3,3} = \mu\left(d^2_{3,\alpha 3} + d^1_{\alpha,33}\right) = \mu\left(\Omega^{2.3}_{,\alpha} - \phi^2_\alpha - \frac{Z^{3.3}}{\mu J}\left(\Omega^{1.1}_{,\alpha} + \psi^{\mathrm{tor}}_\alpha\right)\right)f_{,3} - \mu\left(\Upsilon_{,\alpha} + \varphi_\alpha\right)f \tag{120}$$

By replacing these relations above into Eq.115, we can deduce the form of the transversal components of the displacements vector $\boldsymbol{d}^3$, corresponding to the same form in Eq.108 for $\boldsymbol{d}^2$ plus the contribution of the two new transverse deformations modes $\boldsymbol{\psi}^{3.1}$ and $\boldsymbol{\psi}^{3.2}$, associated to f and $f_{,3}$ respectively.

These modes are obtained from the solutions of the following variational problems:

$$W(\psi^{3.1}_\alpha, w_\alpha) = \int_S b_\alpha w_\alpha \, dS + \int_{\Gamma_s} t_\alpha w_\alpha \, d\Gamma_s + \int_S \lambda\Upsilon w_{\alpha,\alpha} dS - \int_S \mu\left(\Upsilon_{,\alpha} + \varphi_\alpha\right)w_\alpha \, dS \tag{121}$$

$$W(\psi^{3.2}_\alpha, w_\alpha) = -\int_S \lambda\left(\Omega^{2.3} - \frac{Z^{3.3}}{\mu J}\Omega^{1.1}\right)w_{\alpha,\alpha} dS + \int_S \mu\left(\Omega^{2.3}_{,\alpha} - \phi_\alpha - \frac{Z^{3.3}}{\mu J}\left(\Omega^{1.1}_{,\alpha} + \psi^{\mathrm{tor}}_\alpha\right)\right)w_\alpha \, dS \tag{122}$$

In Eq.121 a new transversal mode associated to the transversal forces is obtained. We note that the two first integrals will be equilibrated by the two last integrals, so that the variational problem is self-equilibrated on the cross section. The problem will be then solved uniquely up to a rigid body motion. From Eq.122, a new transversal mode is obtained, due to the variation of the longitudinal external forces $\left(f_{,3} \neq 0\right)$.

We write now the displacement vector for this order:

$$\boldsymbol{d}^3 = \underbrace{\begin{Bmatrix} U^3_1 - y_2\theta^3 + \psi^{1.\beta}_1 U^1_{\beta,33} + \psi^{1.3}_1 U^2_{3,3} \\ U^3_2 + y_1\theta^3 + \psi^{1.\beta}_2 U^1_{\beta,33} + \psi^{1.3}_2 U^2_{3,3} \\ U^3_3 - y_\alpha U^2_{\alpha,3} + \Omega^{1.1}\theta^2_{,3} + \Omega^{2.\beta}T^2_\beta \end{Bmatrix}}_{\text{St}-\text{Venant kinematic}} + \begin{Bmatrix} \psi^{3.1}_1 f + \psi^{3.2}_1 f_{,3} \\ \psi^{3.1}_2 f + \psi^{3.2}_2 f_{,3} \\ 0 \end{Bmatrix} \tag{123}$$

We note that in all the following orders, the even number order will give arise to two new warping modes and the odd number order will, instead, give arise to two new transversal modes. Both problems are solved in the cross section and are self-equilibrated by construction by using the macro

equilibrium equations. In the next parts we will derive the formulations for the determination of the new modes, for the odd and even order problem types.

Problem P^k ($k>2$) for k even:

For the problem P^k when k is even, we determine a new warping mode. Thus, to define the iterative procedure from the asymptotic expansion method, leading to the derivation of this new warping mode, we suppose known the form of the displacement, for the two last orders P^{k-2} and P^{k-1}:

$$\boldsymbol{d}^{k-2} = \begin{Bmatrix} U_1^{k-2} - y_2\theta^{k-2} + \psi_1^{1.\beta}U_{\beta,33}^{k-4} + \psi_1^{1.3}U_{3,3}^{k-3} \\ U_2^{k-2} + y_1\theta^{k-2} + \psi_2^{1.\beta}U_{\beta,33}^{k-4} + \psi_2^{1.3}U_{3,3}^{k-3} \\ U_3^{k-2} - y_\alpha U_{\alpha,3}^{k-3} + \Omega^{1.1}\theta_{,3}^{k-3} + \Omega^{2.\beta}T_\beta^{k-3} \end{Bmatrix} + \begin{Bmatrix} 0 \\ 0 \\ \Omega^{k-2}f^{(k-4)} \end{Bmatrix} \tag{124}$$

$$\boldsymbol{d}^{k-1} = \begin{Bmatrix} U_1^{k-1} - y_2\theta^{k-1} + \psi_1^{1.\beta}U_{\beta,33}^{k-3} + \psi_1^{1.3}U_{3,3}^{k-2} \\ U_2^{k-1} + y_1\theta^{k-1} + \psi_2^{1.\beta}U_{\beta,33}^{k-3} + \psi_2^{1.3}U_{3,3}^{k-2} \\ U_3^{k-1} - y_\alpha U_{\alpha,3}^{k-2} + \Omega^{1.1}\theta_{,3}^{k-2} + \Omega^{2.\beta}T_\beta^{k-2} \end{Bmatrix} + \begin{Bmatrix} \psi_1^{k-1}f^{(k-3)} \\ \psi_2^{k-1}f^{(k-3)} \\ 0 \end{Bmatrix} \tag{125}$$

Our goal is to determine the form of the displacement vector $\boldsymbol{d}^k$, which will contain the Saint-Venant kinematic plus the new warping mode Ω^k:

$$\boldsymbol{d}^k = \underbrace{\begin{Bmatrix} \cdots \\ \cdots \\ \cdots \end{Bmatrix}}_{\text{St-Venant kinematic}} + \begin{Bmatrix} 0 \\ 0 \\ \Omega^k f^{(k-2)} \end{Bmatrix} \tag{126}$$

We re-write the relation in Eq.98 for this order by incrementing the exponents to the order k:

$$\partial_\alpha\left(\mu d_{3,\alpha}^k\right) = -\partial_\alpha\left(\mu d_{\alpha,3}^{k-1}\right) - \lambda d_{\alpha,\alpha 3}^{k-1} - (2\mu+\lambda)d_{3,33}^{k-2} \tag{127}$$

$$\begin{aligned}\partial_\alpha\left(\mu d_{3,\alpha}^k\right) = -\partial_\alpha\left(\mu\left(\psi_\alpha^{1.\beta}U_{\beta,333}^{k-3} + \psi_\alpha^{1.3}U_{3,33}^{k-2} + \psi_\alpha^{k-1}f^{(k-2)}\right)\right) - \lambda\left(\psi_{\alpha,\alpha}^{1.\beta}U_{\beta,333}^{k-3} + \psi_{\alpha,\alpha}^{1.3}U_{3,33}^{k-2} + \psi_{\alpha,\alpha}^{k-1}f^{(k-2)}\right) \\ - (2\mu+\lambda)\left(U_{3,33}^{k-2} - y_\alpha U_{\alpha,333}^{k-3} + \Omega^{k-2}f^{(k-2)}\right)\end{aligned} \tag{128}$$

From the boundary condition, we obtain:

$$\sigma_{3j}^{k-1}n_j = 0 \quad \Longrightarrow \quad \mu d_{3,\alpha}^k n_\alpha = -\mu d_{\alpha,3}^{k-1}n_\alpha \tag{129}$$

By using the expression of $d_{\alpha,3}^{k-1}$ in Eq.125 into the relation above, Eq.129 becomes:

$$\mu\frac{\partial d_3^k}{\partial n} = -\left(\psi_\alpha^{k-1}f^{(k-2)} + \psi_\alpha^{1.\beta}U_{\beta,33}^{k-3} + \psi_\alpha^{1.3}U_{3,3}^{k-2}\right)n_\alpha \tag{130}$$

At this stage, we must note that the problem defined with Eq.128, 130 is not necessarily self-equilibrated, since we haven't used yet the macro equilibrium equations. Let us now determine the expressions of the normal force and flexion moments for the last even order k-2:

$$N^{k-2} = \int_S \sigma_{33}^{k-2}\,dS = \int_S \left((2\mu+\lambda)d_{3,3}^{k-2} + \lambda d_{\alpha,\alpha}^{k-1}\right)dS = ESU_{3,3}^{k-2} + P^k f^{(k-3)} \tag{131}$$

$$M_\alpha^{k-2} = -\int_S y_\alpha\sigma_{33}^{k-2}\,dS = EI_\alpha U_{\alpha,33}^{k-3} + Q_\alpha^k\,f^{(k-3)} \quad \text{(no sum on α)} \tag{132}$$

Where:

$$P^k \coloneqq \int_S \left((2\mu+\lambda)\Omega^{k-2} + \lambda\,\psi_{\beta,\beta}^{k-1}\right) dS \tag{133}$$

$$Q_\alpha^k \coloneqq \int_S y_\alpha \left((2\mu+\lambda)\Omega^{k-2} + \lambda\,\psi_{\beta,\beta}^{k-1}\right) dS \tag{134}$$

We use the macroscopic equilibrium equations for this order to obtain:

$$\begin{cases} N_{,3}^{k-2} = 0 \\ M_{\alpha,3}^{k-2} + T_\alpha^{k-1} = 0 \end{cases} \quad \Longrightarrow \quad \begin{cases} U_{3,33}^{k-2} = -\dfrac{P^k}{ES}\, f^{(k-2)} \\ U_{\alpha,333}^{k-3} = -\dfrac{1}{EI_\alpha}\left(T_\alpha^{k-1} + Q_\alpha^k\, f^{(k-2)}\right) \quad \text{(no sum on α)} \end{cases} \tag{135}$$

By replacing $U_{3,33}^{k-2}$ and $U_{\beta,333}^{k-3}$ in Eq.128, 130 with their expressions in Eq.135 and identifying the terms associated to $f^{(k-2)}$, we obtain a self-equilibrated partial derivative problem, leading to the derivation of the new warping mode for this order:

$$\begin{cases} \partial_\alpha\left(\mu\Omega_{,\alpha}^k\right) = -\partial_\alpha\left(\mu(\psi_\alpha^{k-1} - \Phi_\alpha^k)\right) - \lambda\left(\psi_{\alpha,\alpha}^{k-1} - \Phi_{\alpha,\alpha}^k\right) - (2\mu+\lambda)(\Omega^{k-2} - \vartheta^k) & \text{in S} \\ \dfrac{\partial\Omega^k}{\partial n} = -(\psi_\alpha^{2k-1} - \Phi_\alpha^k)n_\alpha & \text{in } \Gamma_s \end{cases} \tag{136}$$

Where :

$$\Phi_\alpha^k \coloneqq \frac{P^k}{ES}\psi_\alpha^{1.3} + \frac{Q_1^k}{EI_1}\psi_\alpha^{1.1} + \frac{Q_2^k}{EI_2}\psi_\alpha^{1.2} \qquad , \qquad \vartheta^k \coloneqq \frac{P^k}{ES} - \frac{Q_1^k}{EI_1}y_1 - \frac{Q_2^k}{EI_2}y_2 \tag{137}$$

It can be easily verified that the problem in Eq.136 is self-equilibrated, and thus can be solved uniquely, up to an additive uniform displacement.

Problem P^k (k>3) for k odd:

For this category of problems (k an odd number), a new transversal mode has to be determined. As for the P^k problem (with k an even number), we suppose given the form of the displacement for the two last orders $\boldsymbol{d}^{k-2}$ and $\boldsymbol{d}^{k-1}$, expressed in the following form:

$$\boldsymbol{d}^{k-2} = \begin{Bmatrix} U_1^{k-2} - y_2\theta^{k-2} + \psi_1^{1.\beta}U_{\beta,33}^{k-4} + \psi_1^{1.3}U_{3,3}^{k-3} \\ U_2^{k-2} + y_1\theta^{k-2} + \psi_2^{1.\beta}U_{\beta,33}^{k-4} + \psi_2^{1.3}U_{3,3}^{k-3} \\ U_3^{k-2} - y_\alpha U_{\alpha,3}^{k-3} + \Omega^{1.1}\theta_{,3}^{k-3} + \Omega^{2.\beta}T_\beta^{k-3} \end{Bmatrix} + \begin{Bmatrix} \psi_1^{k-2}\, f^{(k-5)} \\ \psi_2^{k-2}\, f^{(k-5)} \\ 0 \end{Bmatrix} \tag{138}$$

$$\boldsymbol{d}^{k-1} = \begin{Bmatrix} U_1^{k-1} - y_2\theta^{k-1} + \psi_1^{1.\beta}U_{\beta,33}^{k-3} + \psi_1^{1.3}U_{3,3}^{k-2} \\ U_2^{k-1} + y_1\theta^{k-1} + \psi_2^{1.\beta}U_{\beta,33}^{k-3} + \psi_2^{1.3}U_{3,3}^{k-2} \\ U_3^{k-1} - y_\alpha U_{\alpha,3}^{k-2} + \Omega^{1.1}\theta_{,3}^{k-2} + \Omega^{2.\beta}T_\beta^{k-2} \end{Bmatrix} + \begin{Bmatrix} 0 \\ 0 \\ \Omega^{k-1}\, f^{(k-4)} \end{Bmatrix} \tag{139}$$

And that we want to determine the form of the displacement vector for the problem P^k (k odd), which will contain the Saint-Venant kinematic plus the new transversal mode $\boldsymbol{\psi}^k$:

$$\boldsymbol{d}^k = \underbrace{\begin{Bmatrix} \cdots \\ \cdots \\ \cdots \end{Bmatrix}}_{\text{St-Venant kinematic}} + \begin{Bmatrix} \psi_1^k\, f^{(k-3)} \\ \psi_2^k\, f^{(k-3)} \\ 0 \end{Bmatrix} \tag{140}$$

The relation in Eq.115 is re-written for this order by incrementing the variables exponents:

$$W(d_\alpha^k, w_\alpha) = -\int_S \lambda d_{3,3}^{k-1} w_{\alpha,\alpha} dS + \int_S \sigma_{\alpha 3,3}^{k-2} w_\alpha \, dS \tag{141}$$

The expression of $d_{3,3}^{k-1}$ and $\sigma_{\alpha 3,3}^{k-2}$ are deduced from the expressions of the displacements vectors in Eq.138-139:

$$d_{3,3}^{k-1} = \Omega^{1.1}\theta_{,33}^{k-2} + \Omega^{k-1} f^{(k-3)} \tag{142}$$

$$\sigma_{\alpha 3,3}^{k-2} = \mu\left(d_{3,\alpha 3}^{k-1} + d_{\alpha,33}^{k-2}\right) = \mu\left(\left(\Omega_{,\alpha}^{1.1} + \psi_\alpha^{0.3}\right)\theta_{,33}^{k-2} + \left(\Omega_{,\alpha}^{k-1} + \psi_\alpha^{k-2}\right) f^{(k-3)}\right) \tag{143}$$

We need to eliminate the terms associated to θ^{k-2} in the expressions above, to this aim the torsion macroscopic equilibrium equation is used. Let us determine the expression of the torsion for the last odd order *k-2*:

$$M_3^{k-2} = \int_S \psi_\alpha^{\mathrm{tor}} \sigma_{\alpha 3}^{k-2} dS \tag{144}$$

$$M_3^{k-2} = \int_S \mu\psi_\alpha^{\mathrm{tor}} \left(\left(\Omega_{,\alpha}^{1.1} + \psi_\alpha^{\mathrm{tor}}\right)\theta_{,3}^{k-2} + \left(\Omega_{,\alpha}^{k-1} + \psi_\alpha^{k-2}\right) f^{(k-4)}\right) dS \tag{145}$$

$$M_3^{k-2} = \mu J \theta_{,3}^{k-2} + Z^k f^{(k-4)} \tag{146}$$

Where:

$$Z^k := \int_S \mu\psi_\alpha^{\mathrm{tor}}\left(\Omega_{,\alpha}^{k-1} + \psi_\alpha^{k-2}\right) dS \tag{147}$$

As previously defined in the problem P^3, the constants Z^k correspond to the torsion moment created by the shear strains of the last order modes.

From the torsion macroscopic equilibrium equation, we obtain the relation between θ^{k-2} and *f*:

$$M_{3,3}^{k-2} = 0 \quad \Longrightarrow \quad \theta_{,33}^{k-2} = -\frac{Z^k}{\mu J} f^{(k-3)} \tag{148}$$

We replace the expression of $\theta_{,33}^{k-2}$ in Eq.148 into Eq142-143 and then replace the newly obtained expressions into Eq.141. Identifying the terms associated to $f^{(k-3)}$, leads to a self-equilibrated problem for the new transversal mode $\boldsymbol{\psi}^k$:

$$W(\psi_\alpha^k, w_\alpha) = \int_S \mu\left(\Omega_{,\alpha}^{k-1} + \psi_\alpha^{k-2} - \frac{Z^k}{\mu J}\left(\Omega_{,\alpha}^{1.1} + \psi_\alpha^{\mathrm{tor}}\right)\right) w_\alpha \, dS - \int_S \lambda\left(\Omega^{k-1} - \frac{Z^k}{\mu J}\Omega^{1.1}\right) w_{\alpha,\alpha} dS \tag{149}$$

We note that we didn't equilibrate the above problem in accordance to shear efforts since by construction of the functions Ω^{k-1} and ψ_α^{k-2}, the resultants of their shear strains are equal to zero. Thus, we needed only to equilibrate the problem from the torsion resultant Z^k.

4.4 General form of the displacements:

Now that the solutions of the problems in Eq.41-45 are detailed for an arbitrary order, the resulting displacements vector $\boldsymbol{d}$ in Eq.19 is obtained by summing all the displacements vectors from the different order and expressed by:

$$d_\alpha = \left(\frac{1}{\eta}U_\alpha^{-1} + U_\alpha^0 + \eta U_\alpha^1 + \cdots\right) + \psi_\alpha^{\mathrm{tor}}(\theta^0 + \eta\theta^1 + \cdots) + \psi_\alpha^{1.\beta}\left(\eta U_{\beta,33}^{-1} + \eta^2 U_{\beta,33}^0 + \cdots\right) + \psi_\alpha^{1.3}\left(\eta U_{3,3}^0 + \eta^2 U_{3,3}^0 + \cdots\right) + \sum_{k=1}^{+\infty}\eta^{2k+1}\left(\psi_\alpha^{2k+1.1} f^{(2k-2)} + \psi_\alpha^{2k+1.2} f^{(2k-1)}\right) \tag{150}$$

$$d_3 = (U_3^0 + \eta U_3^1 + \cdots) - y_\alpha\left(U_{\alpha,3}^{-1} + \eta U_{\alpha,3}^0 + \cdots\right) + \Omega^{1.1}\left(\eta\theta_{,3}^0 + \eta^2\theta_{,3}^1 + \cdots\right) + \eta^2\Omega^{2.\alpha}T_\alpha + \eta^2\Omega^{2.3}f + \sum_{k=2}^{+\infty}\eta^{2k}\left(\Omega^{2k.1} f^{(2k-3)} + \Omega^{2k.2} f^{(2k-2)}\right) \tag{151}$$

Where: $T_\alpha = \int_S \sigma_{\alpha 3} dS$ are the components of the shear effort.

To re-write the above relations in a condensed form, we introduce the following notations:

$$U_\alpha \coloneqq \frac{1}{\eta}U_\alpha^{-1} + U_\alpha^0 + \eta U_\alpha^1 + \cdots \quad , \quad U_3 \coloneqq U_3^0 + \eta U_3^1 + \cdots \quad , \quad \theta \coloneqq \theta^0 + \eta\theta^1 + \cdots \tag{152}$$

Thus Eq.150-151 becomes:

$$d_\alpha = U_\alpha + \psi_\alpha^{\mathrm{tor}}\theta + \eta\,\psi_\alpha^{1.3}U_{3,3} + \eta^2\psi_\alpha^{1.\beta}U_{\beta,33} + \sum_{odd\ k\geq 3}\eta^k\left(\psi_\alpha^{k.1} f^{(k-3)} + \psi_\alpha^{k.2} f^{(k-2)}\right) \tag{153}$$

$$d_3 = U_3 + \eta\left(-y_\alpha U_{\alpha,3} + \Omega^{1.1}\theta_{,3}\right) + \eta^2\Omega^{2.\alpha}T_\alpha + \eta^2\Omega^{2.3}f + \sum_{even\ k\geq 4}\eta^k\left(\Omega^{k.1} f^{(k-3)} + \Omega^{k.2} f^{(k-2)}\right) \tag{154}$$

The infinite sums in the equations above, represents the contribution of the applied loading to the displacement response of the beam. If there is no applied efforts, the displacement of the beam can be written exactly in the following form:

$$d_\alpha = U_\alpha + \psi_\alpha^{\mathrm{tor}}\theta + \eta\,\psi_\alpha^{1.3}U_{3,3} + \eta^2\psi_\alpha^{1.\beta}U_{\beta,33} \tag{155}$$

$$d_3 = U_3 + \eta\left(-y_\alpha U_{\alpha,3} + \Omega^{1.1}\theta_{,3}\right) - \eta^2\Omega^{2.\alpha}T_\alpha \tag{156}$$

Where the expression of the displacement vector in Eq.155-156 correspond to the classical Saint-Venant solution.

5. The general equilibrium equations:

The asymptotic expansion method (AEM) applied to a beam element, as described in the last sections, will give arise to an enriched kinematics with pre-determined warping and transverse deformation modes, where the displacement of an arbitrary point of the beam can be given as a projection into these modes basis:

$$\boldsymbol{d} = \begin{Bmatrix} \psi_1^i \zeta^i \\ \psi_2^i \zeta^i \\ \Omega_j \xi_j \end{Bmatrix} \tag{157}$$

Where Ω_j and $\boldsymbol{\psi}^i$ are the warping and transverse deformation modes obtained from the AEM respectively, and (ξ_j, ζ^i) the generalized coordinates associated to the different modes. In this section,

we note that the latin letter indices 'i' and 'j' are no longer restricted to the values from 1 to 3, but varies from 1 to the total numbers of the transverse deformation and warping modes, that are arbitrary.

We recall that the AEM was only used to obtain the kinematic of the beam written in Eq.157, the general equilibrium was not obtained in the iterative process. Thus, the goal of this section is to follow exactly the same procedure in [1], in which the equilibrium equations of the beam were obtained and solved exactly. From the exact solution, the variation along the beam's length of the introduced degrees of freedom (ξ_j, ζ^i) is known and the stiffness matrix is assembled.

To obtain the equilibrium equations, we use, as in [1], the principle of virtual work. The expression of the internal virtual work, using the kinematic in Eq.157, is given by:

$$\delta W_{int} = \int_V \boldsymbol{\sigma} : \delta\boldsymbol{\varepsilon}\, dV \tag{158}$$

$$\delta W_{int} = \int_V \left(\sigma_{33}\, \Omega_j\, \delta\xi_{j,3} + \sigma_{3\alpha}\Omega_{j,\alpha}\delta\xi_j + \sigma_{3\alpha}\psi^i_\alpha\delta\zeta^i_{,3} + \sigma_{\alpha\beta}\psi^i_{\alpha,\beta}\delta\zeta^i\right)dV \tag{159}$$

After integrating over the cross section, Eq.159 becomes:

$$\delta W_{int} = \int_0^L \left(M_j\delta\xi_{j,3} + T_j\delta\xi_j + \Lambda^i\delta\zeta^i_{,3} + \Phi^i\delta\zeta^i\right)dx_3 \tag{160}$$

Where the expression of the generalized efforts are:

$$M_j = \int_S \sigma_{33}\Omega_j\, dS = K_{jk}\xi_{k,3} + Q^i_j\zeta^i \tag{161}$$

$$T_j = \int_S \sigma_{3\alpha}\Omega_{j,\alpha} dS = J_{jk}\xi_k + D^i_j\zeta^i_{,3} \tag{162}$$

$$\Lambda^i = \int_S \sigma_{3\alpha}\psi^i_\alpha\, dS = D^i_j\xi_j + C^{il}\zeta^l_{,3} \tag{163}$$

$$\Phi^i = \int_S \sigma_{\alpha\beta}\psi^i_{\alpha,\beta} dS = Q^i_j\xi_{j,3} + H^{il}\zeta^l \tag{164}$$

And the coefficients:

$$K_{jk} = \int_S (2\mu+\lambda)\Omega_j\Omega_k\, dS \quad , \quad J_{jk} = \int_S \mu\, \Omega_{j,\alpha}\, \Omega_{k,\alpha}\, dS \quad , \quad D^i_j = \int_S \mu\, \psi^i_\alpha\, \Omega_{j,\alpha}\, dS \tag{165}$$

$$Q^i_j = \int_S \lambda\, \Omega_j\, \psi^i_{\alpha,\alpha} dS \quad , \quad C^{il} = \int_S \mu\, \psi^i_\alpha\, \psi^l_\alpha\, dS \quad , \quad H^{il} = \int_S \left(\mu\psi^i_{\alpha,\beta}\psi^l_{\alpha,\beta} + \lambda\psi^i_{\alpha,\alpha}\psi^l_{\beta,\beta}\right)dS \tag{166}$$

After an integration by parts Eq.160 becomes:

$$\delta W_{int} = -\int_0^L \left(\left(M_{j,3} - T_j\right)\delta\xi_j + \left(\Lambda^i_{,3} - \Phi^i\right)\delta\zeta^i\right) dx_3 + \underbrace{\left[M_j\delta\xi_j + \Lambda^i\delta\zeta^i\right]_0^L}_{\delta W_{ext}} \tag{167}$$

$$\Longrightarrow \quad \int_0^L \left(\left(M_{j,3} - T_j\right)\delta\xi_j + \left(\Lambda^i_{,3} - \Phi^i\right)\delta\zeta^i\right) dx_3 = 0 \tag{168}$$

The relation in Eq.168 is valid for an arbitrary virtual displacement $(\delta\xi_j, \delta\zeta^i)$, thus the expressions between brackets have to be null, representing the equilibrium equations :

$$M_{j,3} - T_j = 0 \qquad , \qquad \Lambda^i_{,3} - \Phi^i = 0 \tag{169}$$

By replacing in the equations of Eq.169 with the expressions of the generalized efforts in Eq.161-164, the following system of differential equations is obtained:

$$\begin{cases} K_{jk}\xi_{k,33} + \left(Q^i_j - D^i_j\right)\zeta^i_{,3} - J_{jk}\xi_k = 0 \\ C^{il}\zeta^l_{,33} - \left(Q^i_j - D^i_j\right)\xi_{j,3} - H^{il}\zeta^l = 0 \end{cases} \tag{170}$$

This system is solved exactly. All details of the solution can be found in [1].

In [1] we discussed that for $\nu \mapsto 0.5$ incompressible locking occurs, and can be overcome by introducing specific transverse deformation or warping modes. By using the asymptotic expansion method, these 'incompressible deformation modes' are automatically obtained in the iterative process.

6. Examples:

We will use the same examples in [1], to demonstrate that with fewer modes, derived from the asymptotic expansion method, we can obtain the same accurate results. The comparisons are performed with Qantara software, in which the present beam model is implemented. We note that in all the following examples 'p' will denote the order where the asymptotic expansion of the displacement is stopped.

Box girder:

We consider here the same example of the 10m cantilever beam presented in the beginning of the article in section 2 (Fig. 1-4). For this case, the applied load will be changed to the middle of the beam, at the abscissa x = 5m.

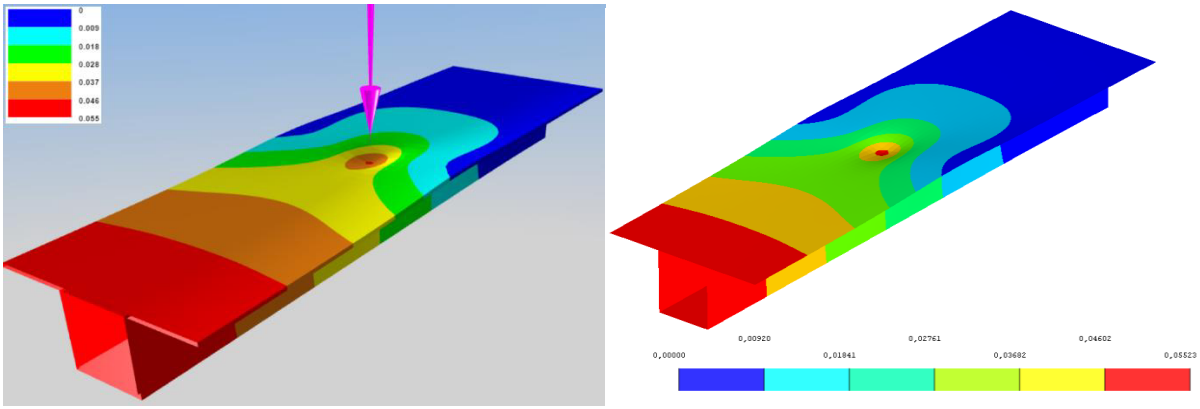

(a) (b)

Figure 5: the deformation of the cantilever beam: (a) present beam model with one element (b) shell model

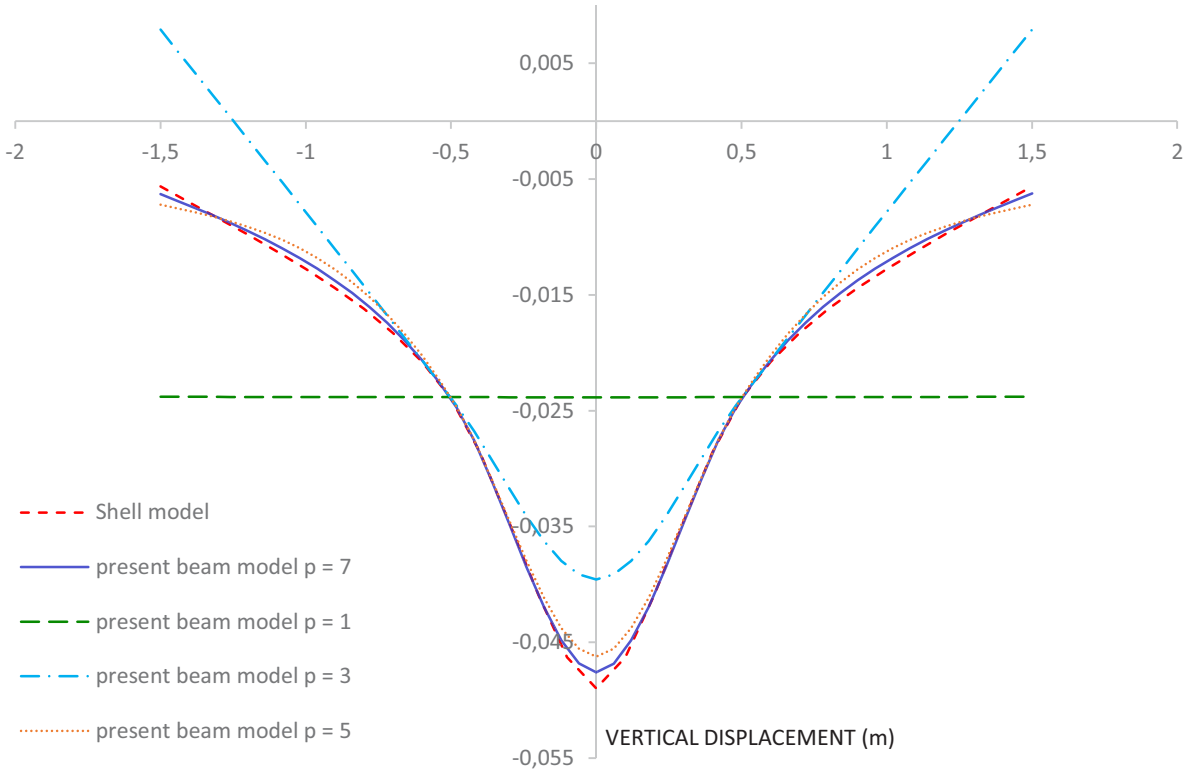

Figure 6: comparison of the vertical displacement at the cross section where the external force is applied.

For this example we stopped the asymptotic expansion at the seventh order (p = 7), thus the kinematic obtained for this order is formed by the Saint-Venant modes, plus the warping and transverse deformation modes associated to the applied force, which are the same as those represented in Fig.2. The present beam model contain only *one beam*, and has then a total of 36 degrees of freedom. For the shell model, we used 6000 MITC-4 shell elements (6060 nodes), representing a total of 36360 degrees of freedom.

In this example, a concentrated vertical force was applied, thus the function representing its variation longitudinally is a Dirac delta function. We remind that the AEM is developed for smooth functions along the beam length, thus using a Dirac delta function is the most extreme case of comparison to test the efficiency of the AEM. We observe indeed in Fig.6, where we have compared the vertical displacement at x = 5m (applied force section) and at the mid-depth of the upper slab, a very good agreement between the result of the present beam model ($p \geq 5$) and the shell model, when we needed to go in the asymptotic expansion up to the seventh order.

In Fig.5, we drew the global deformation of the cantilever beam obtained from the present beam and the shell model. We observe also a very good accordance between the iso-deformation lines of the two models.

Double T cross section:

In this example we consider a 12m beam clamped at its both end and loaded with an eccentric (z=2m) vertical force of 10MN in its middle(x=6m), see Fig.7, the material characteristics will be the same as the previous example. We will use as usual only *one beam finite element*. The results will be compared to a brick model of the beam.

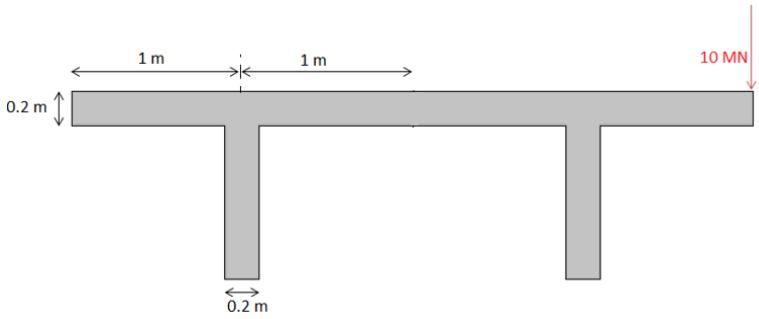

Figure 7: A view of the beam cross section.

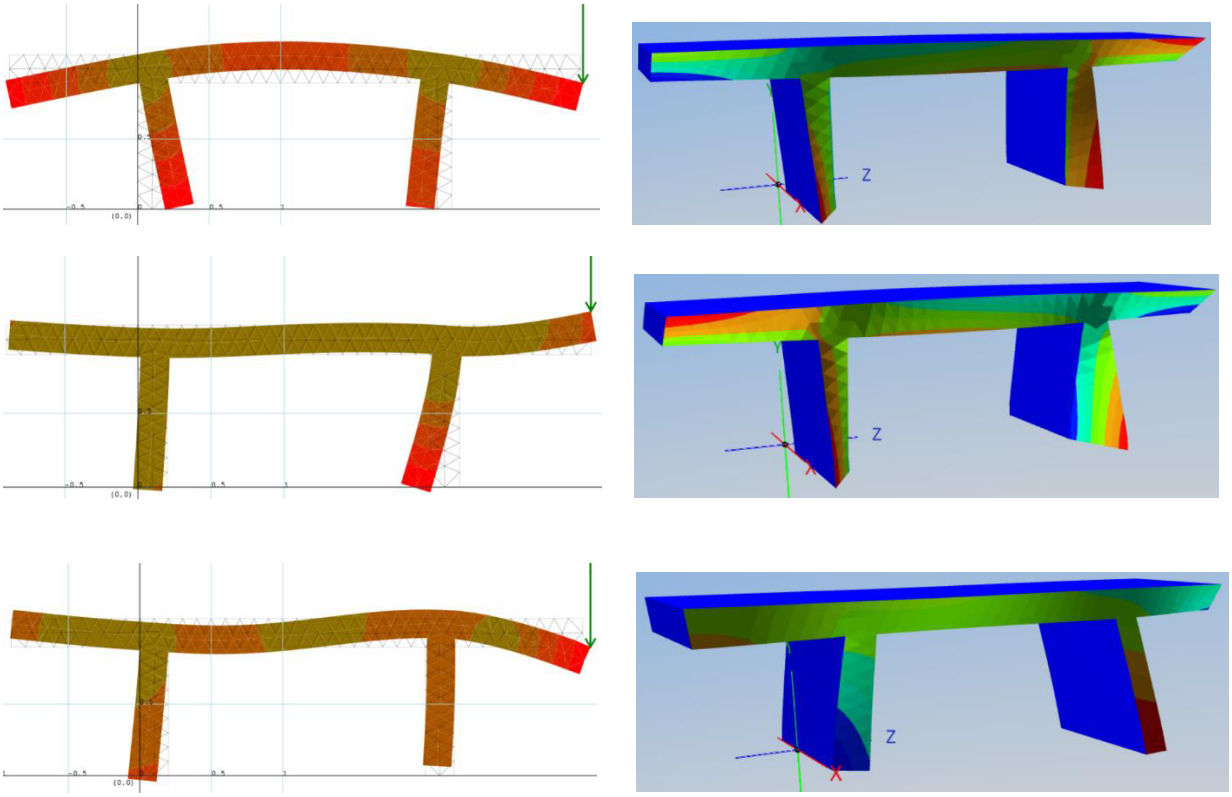

Figure 8: the transverse deformation and warping modes due for the vertical force applied to on the section.

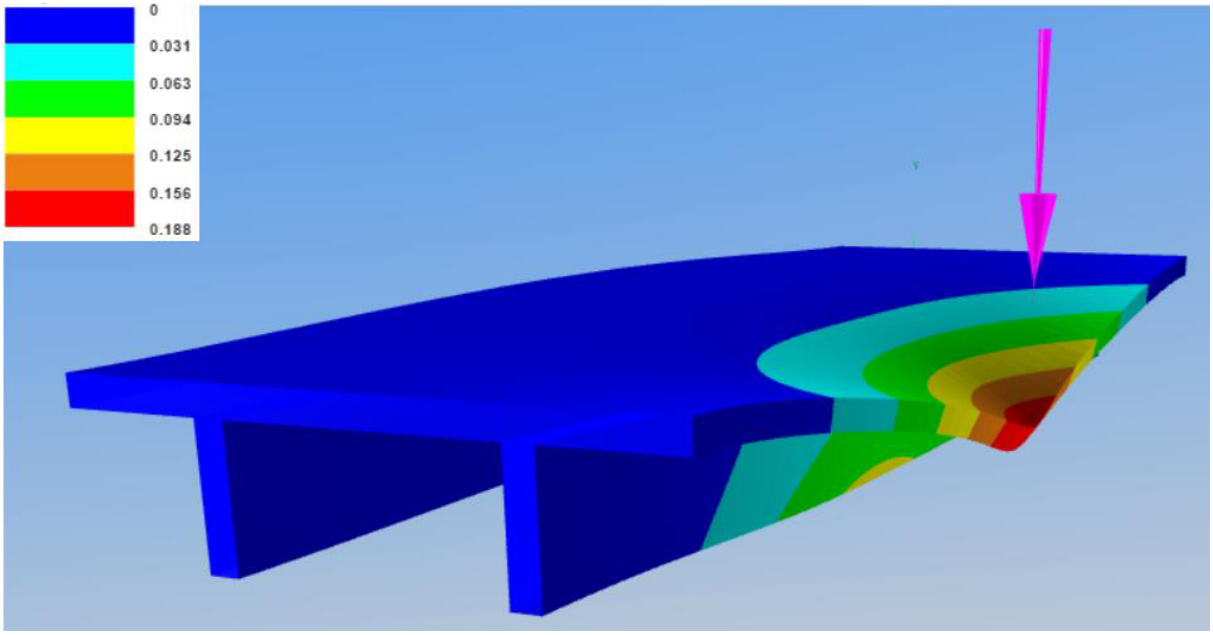

Figure 9: A view of the amplified deformation of the beam model with only one element.

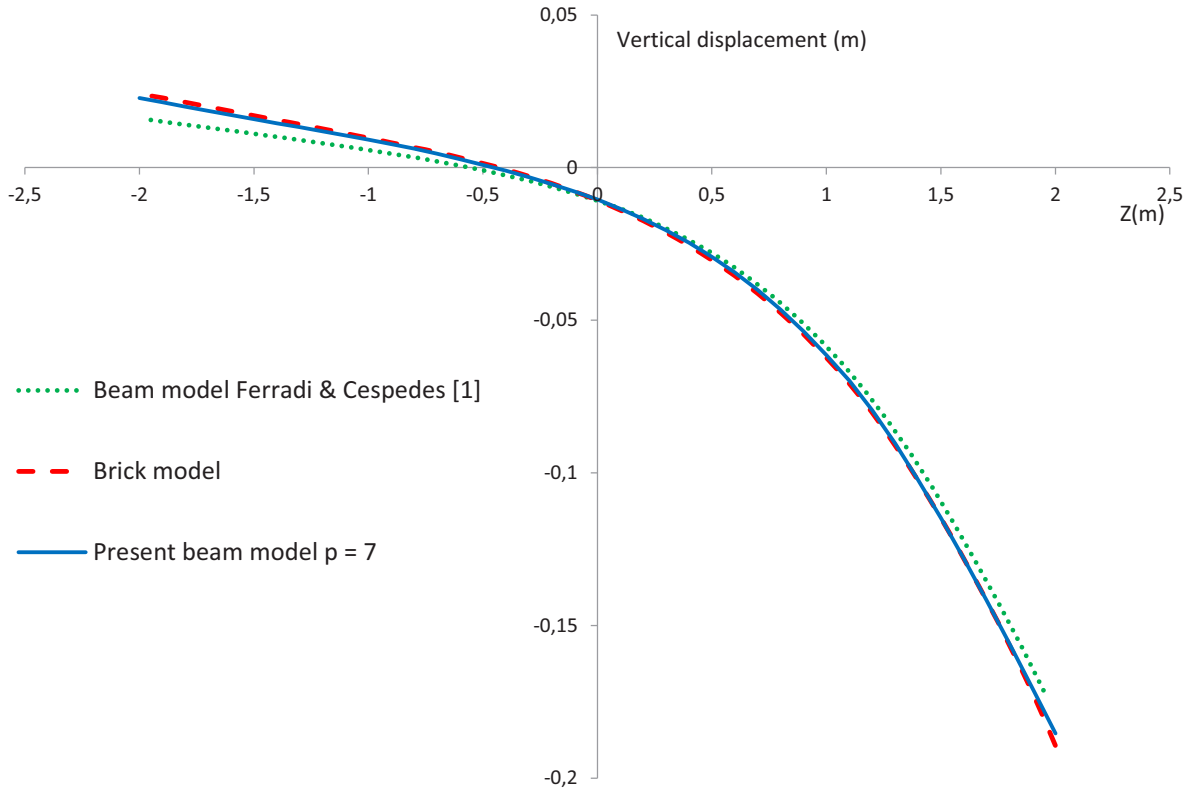

Figure 10: Comparison of the displacement between the brick, shell and the beam models, at x= 6m and at mid-depth of the upper slab (Ty = -10 MN)

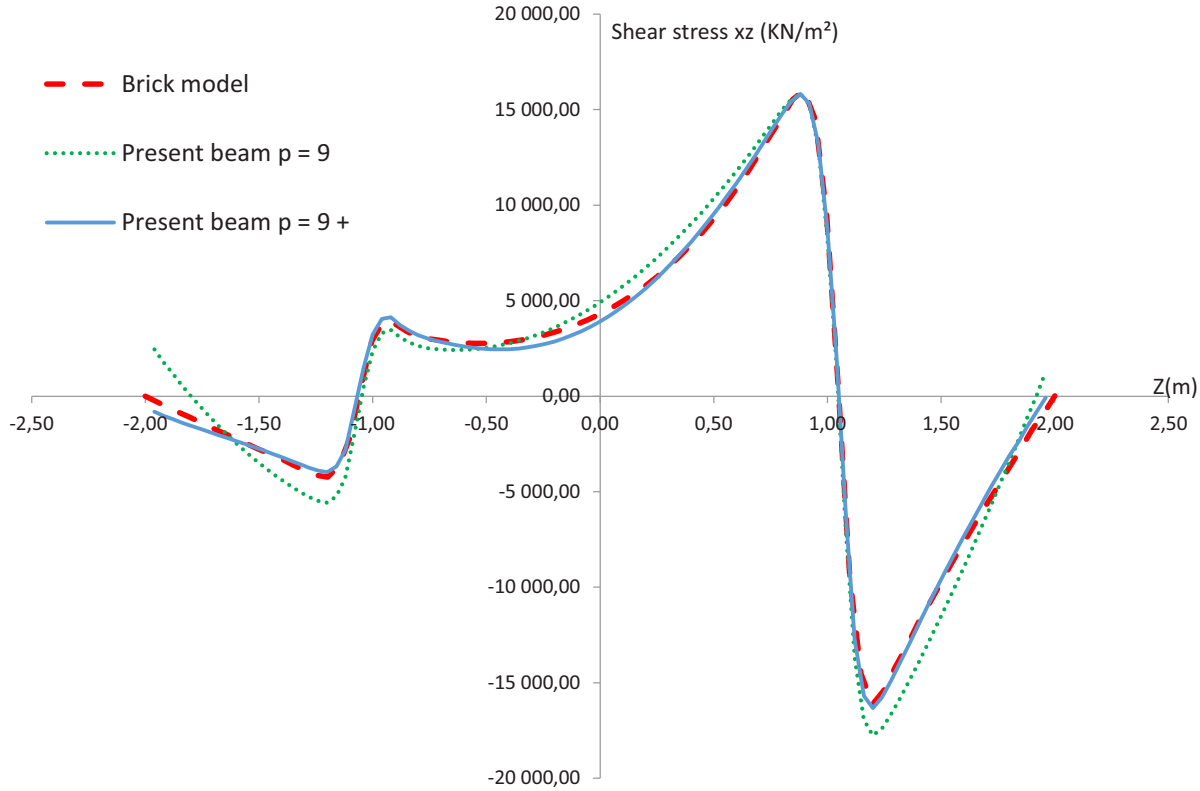

Figure 11: Comparison of the shear stress xz between the brick and beam models, at x= 0.95m and at mid-depth of the upper slab (Ty = -10 MN)

For this example we stopped the asymptotic expansion at the ninth order (p = 9), giving a beam model with seven transverse deformation modes and ten warping modes, where the modes associated to the applied force are in Fig.8. The results of the present beam model are compared to the one obtained in [1], where we have chosen a total of ten transversal deformation modes and eleven warping modes. Fig.10 shows a very good agreement between the results of the brick model, the present beam model and the beam model in [1]. In Fig.9 we have the global deformation of the beam, obtained with *one beam*.

The comparison of the horizontal shear stresses in Fig.11 is interesting, it shows that near the clamping, considering only the modes from the asymptotic expansion method (doted green line), do not give very accurate result in comparison to the one from the brick model of the beam, but by adding some warping modes corresponding to the higher warping modes of horizontal shear (see [1] and [2]), that cannot be obtained from a rigorous application of the asymptotic expansion method, we observe a clear amelioration in the result (continuous blue line). The result in Fig.11 shows one of the drawback of the AEM, it does not give good results near the region where the limits conditions on the displacements are applied.

7. Conclusion and future research direction:

The asymptotic expansion method (AEM) was used successfully to obtain an enriched kinematic for the beam, capable of describing the local deformations shapes due to the applied forces in a very accurate, and with using a minimum number of modes. This is done with the aid of transverse deformation and warping modes that are specifically determined for the applied loading, and thus, will have by construction a non-null contribution to the deformation of the beam.

The AEM gives also an original approach for the justification of the Saint-Venant solution, which corresponds to the exact kinematic of an infinite beam, in absence of external forces. An exact kinematic can also be obtained in the case of an external force varying in accordance to a polynomial.

The kinematic obtained from the AEM was combined with an exact solution of the general equilibrium equations of the beam, allowing us to use only one beam element, to obtain the exact variation along the beam's length of the introduced degrees of freedom. The obtained results in the proposed examples, shows a very good accordance with the one from reference models of the beam with brick or shell elements. However, the kinematic obtained from the AEM fails to give good results in the vicinity of the clamping. Finding a method to solve this drawback can be a subject for future investigation to ameliorate the method, along with taking into account material and geometric non linearities within the AEM framework.

Appendix A.1:

The general strong form, for an arbitrary order p, of the problem leading to the determination of a new warping mode, is written in the following way:

$$\begin{cases} \partial_\alpha\left(\mu\Omega^p_{,\alpha}\right) = -\partial_\alpha\left(\mu\psi^{p-1}_\alpha\right) - \lambda\psi^{p-1}_{\alpha,\alpha} - (2\mu+\lambda)\Omega^{p-2} & \text{for S} \\ \dfrac{\partial\Omega^p}{\partial n} = -\psi^{p-1}_\alpha n_\alpha & \text{for } \Gamma_s \end{cases} \tag{171}$$

Where Ω^p is the unknown warping mode of the problem, and $\boldsymbol{\psi}^{p-1}$, Ω^{p-2} represents the entries (or the loading) of the problem.

The problem in Eq.171 can be re-written differently, in a more convenient way to obtain the weak form:

$$\begin{cases} \mathrm{div}_{\boldsymbol{y}}\left(\mu\left(\boldsymbol{\nabla}_{\boldsymbol{y}}\Omega^p + \boldsymbol{\psi}^{p-1}\right)\right) = -\lambda\mathrm{div}_{\boldsymbol{y}}(\boldsymbol{\psi}^{p-1}) - (2\mu+\lambda)\Omega^{p-2} & \text{for } S \\ \left(\boldsymbol{\nabla}_{\boldsymbol{y}}\Omega^p + \boldsymbol{\psi}^{p-1}\right)\cdot\boldsymbol{n} = 0 & \text{for } \Gamma_s \end{cases} \tag{172}$$

We write the equivalent weak form of this problem:

$$\int_S \left(\mathrm{div}_{\boldsymbol{y}}\left(\mu\left(\boldsymbol{\nabla}_{\boldsymbol{y}}\Omega^p + \boldsymbol{\psi}^{p-1}\right)\right) + \lambda\mathrm{div}_{\boldsymbol{y}}(\boldsymbol{\psi}^{p-1}) + (2\mu+\lambda)\Omega^{p-2}\right) u\, dS = 0 \tag{173}$$

Where u is an arbitrary (virtual) longitudinal displacement.

After integrating by parts and replacing with the boundary condition, Eq.173 becomes:

$$\int_{\Gamma_s} \mu\left(\boldsymbol{\nabla}_{\boldsymbol{y}}\Omega^p + \boldsymbol{\psi}^{p-1}\right)\cdot\boldsymbol{n}\, u\, d\Gamma_s - \int_S \mu\left(\boldsymbol{\nabla}_{\boldsymbol{y}}\Omega^p + \boldsymbol{\psi}^{p-1}\right)\cdot\boldsymbol{\nabla}u\, dS + \int_S \left(\lambda\mathrm{div}_{\boldsymbol{y}}(\boldsymbol{\psi}^{p-1}) + (2\mu+\lambda)\Omega^{p-2}\right)u\, dS = 0 \tag{174}$$

$$\int_S \mu\boldsymbol{\nabla}_{\boldsymbol{y}}\Omega^p\cdot\boldsymbol{\nabla}_{\boldsymbol{y}}u\, dS = -\int_S \mu\boldsymbol{\psi}^{p-1}\cdot\boldsymbol{\nabla}_{\boldsymbol{y}}u\, dS + \int_S \lambda\mathrm{div}_{\boldsymbol{y}}(\boldsymbol{\psi}^{p-1})u\, dS + \int_S (2\mu+\lambda)\Omega^{p-2}u\, dS \tag{175}$$

From the above equations, the problem can be solved by discretizing the cross section with finite elements, and choosing adequate interpolation functions, as it is done in a classical way with the FEM.

References:

[1] Ferradi, M. K., & Cespedes, X. (2014). A new beam element with transversal and warping eigenmodes. *Computers & Structures*, *131*, 12-33.

[2]. Ferradi, M. K., Cespedes, X., & Arquier, M. (2013). A higher order beam finite element with warping eigenmodes. *Engineering Structures*, *46*, 748-762.

[3] Buannic, N., & Cartraud, P. (2001). Higher-order effective modeling of periodic heterogeneous beams. I. Asymptotic expansion method. *International Journal of Solids and Structures*, *38*(40), 7139-7161.

[4] Cimetière, A., Geymonat, G., Le Dret, H., Raoult, A., & Tutek, Z. (1988). Asymptotic theory and analysis for displacements and stress distribution in nonlinear elastic straight slender rods. *Journal of elasticity*, *19*(2), 111-161.

[5] Trabucho, L., & Viaño, J. M. (1990). A new approach of Timoshenko's beam theory by asymptotic expansion method. *ESAIM: Mathematical Modelling and Numerical Analysis-Modélisation Mathématique et Analyse Numérique*, *24*(5), 651-680.

[6] Karwowski, A. J. (1990). Asymptotic models for a long, elastic cylinder. *Journal of Elasticity*, *24*(1-3), 229-287.

[7] Lebée, A., & Sab, K. (2013). Justification of the Bending-Gradient theory through asymptotic expansions. In *Generalized Continua as Models for Materials* (pp. 217-236). Springer Berlin Heidelberg.

[8] Dallot, J., Sab, K., & Foret, G. (2009). Limit analysis of periodic beams.*European Journal of Mechanics-A/Solids*, *28*(1), 166-178.

[9] Sapountzakis, E. J., & Dikaros, I. C. (2015). Advanced 3D beam element of arbitrary composite cross section including generalized warping effects.*International Journal for Numerical Methods in Engineering*.

[10] Vieira, R. F., Virtuoso, F. B. E., & Pereira, E. B. R. (2015). Definition of warping modes within the context of a higher order thin-walled beam model. *Computers & Structures*, *147*, 68-78.

[11] Vieira, R. F., Virtuoso, F. B. E., & Pereira, E. B. R. (2015). A higher order beam model for thin-walled structures with in-plane rigid cross-sections. *Engineering Structures*, *84*, 1-18.

[12] De Miranda, S., Madeo, A., Miletta, R., & Ubertini, F. (2014). On the relationship of the shear deformable Generalized Beam Theory with classical and non-classical theories. *International Journal of Solids and Structures*, *51*(21), 3698-3709.

[13] Genoese, A., Genoese, A., Bilotta, A., & Garcea, G. (2013). A mixed beam model with non-uniform warpings derived from the Saint Venànt rod. *Computers & Structures*, *121*, 87-98.

[14]. Silvestre, N., & Camotim, D. (2003). Nonlinear generalized beam theory for cold-formed steel members. *International Journal of Structural Stability and Dynamics, 3(04), 461-490.*

[15]. Jang, G. W., Kim, M. J., & Kim, Y. Y. (2012). Analysis of Thin-Walled Straight Beams with Generally-Shaped Closed Sections Using Numerically-Determined Sectional Deformation Functions. *Journal of Structural Engineering*, *1*, 438.

[16] Yu, W., Hodges, D. H., Volovoi, V., & Cesnik, C. E. (2002). On Timoshenko-like modeling of initially curved and twisted composite beams. *International Journal of Solids and Structures*, *39*(19), 5101-5121.

[17] Yu, W., Volovoi, V. V., Hodges, D. H., & Hong, X. (2002). Validation of the variational asymptotic beam sectional analysis. *AIAA journal*, *40*(10), 2105-2112.

[18]. Tisseur, F., & Meerbergen, K. (2001). The quadratic eigenvalue problem. *Siam Review*, *43*(2), 235-286.